

REVISTA

DE PIELĂRIE ÎNCĂLTĂMINTE Leather and Footwear Journal

June / Iunie 2020
Volume / Volumul 20
No / Numărul 2

INCDTP - SUCURSALA INSTITUTUL DE CERCETĂRI PIELĂRIE ÎNCĂLTĂMINTE
INCDTP - DIVISION: LEATHER AND FOOTWEAR RESEARCH INSTITUTE



REVISTA DE PIELĂRIE INCĂLTĂMINTE

LEATHER AND FOOTWEAR JOURNAL

AIMS AND SCOPE

Revista de Pielarie Incaltaminte / Leather and Footwear Journal (Print ISSN 1583-4433) is published 4 times a year, by Leather and Footwear Research Institute (ICPI) Bucharest, Romania, Division of The National Research and Development Institute for Textiles and Leather (INCDTP), CERTEX Press. *Revista de Pielarie Incaltaminte / Leather and Footwear Journal* aims to present current science and technology developments as well as initiatives in Romania and South Eastern Europe region. The Journal publishes original research papers of experimental and theoretical nature, followed by scientific, technical, economic and statistic information, reviews of local and foreign conferences, congresses, symposia, with the purpose of stimulating the dissemination of research results.

Revista de Pielarie Incaltaminte / Leather and Footwear Journal focuses particular attention on the key areas of new systems and technologies applied in leather, footwear and rubber goods sectors; biomaterials, collagen-based medical devices, biochemistry of collagen; environment; innovation; leather and parchment cultural heritage; management and marketing, quality control; applications of IT field in these sectors, and other related fields.

OPEN ACCESS STATEMENT

Revista de Pielarie Incaltaminte / Leather and Footwear Journal is a peer reviewed, open access journal. All articles published open access will be immediately and permanently free for everyone to read, download, copy and distribute, under the provisions of a Creative Commons Attribution (CC BY) which lets others distribute and copy the article, create extracts, abstracts, and other revised versions, adaptations or derivative works of or from an article (such as a translation), include in a collective work (such as an anthology), text or data mine the article, even for commercial purposes, as long as they credit the author(s), do not represent the author as endorsing their adaptation of the article, and do not modify the article in such a way as to damage the author's honor or reputation.

PEER-REVIEW PROCEDURE

Submission of a manuscript to *Revista de Pielarie Incaltaminte* implies that the work described has not been published before (except in the form of an abstract or as part of a published lecture, review, or thesis); that it is not under consideration for publication elsewhere; that its publication has been approved by all coauthors, if any.

Submitted manuscripts are single-blind peer-reviewed by two qualified reviewers selected by the Editorial Board. The manuscript will be accepted for publication provided reviews are favorable. In case of diversified opinions of the reviewers, the Editorial board will make the final decision. If the paper is not accepted for publication, the manuscripts and the figures will not normally be returned. The authors will be notified as soon as possible of the result of the paper evaluation (to be published, to be modified, rejected).

JOURNAL SPONSORSHIP

Edited with the sponsorship from the Ministry of Education and Research. We are pleased to acknowledge support from the following: The Confederation of National Associations of Tanners and Dressers of the European Community – COTANCE, Belgium; Romanian Leather and Fur Producers Association, APPBR, Romania; SFERA FACTOR, Romania.

COPYRIGHT

The copyright for all articles published in *Revista de Pielarie Incaltaminte / Leather and Footwear Journal* shall remain the property of the author(s). The copyright on the layout and final design of the articles published in *Revista de Pielarie Incaltaminte / Leather and Footwear Journal* belongs to INCDTP – Division: Leather and Footwear Research Institute and cannot be used in other publications.

ABSTRACTING AND INDEXING

Revista de Pielarie Incaltaminte / Leather and Footwear Journal is acknowledged in Romania by the National University Research Council (CNCSIS) in B+ Category (code 565), and is indexed in Chemical Abstracts Service (CAS) Database, USA, CAB Database (CAB International, UK), Elsevier's Compendex and SCOPUS, CrossRef, EBSCO, CiteFactor, Research

Bible, Index Copernicus and listed in AcademicKeys, Environmental XPRT, MIAR, Electronic Journals Library, Cosmos Impact Factor, Science Library Index and SCIPIO.

INCDTP-ICPI is a member of The Publishers International Linking Association, Inc. (PILA), a nonprofit corporation doing business as Crossref. As a PILA member, we have the right to assign Digital Object Identifiers (DOIs) to journal content. DOIs are persistent links to an object/entity and can be used to cite and link to any article existing online, even if full citation information is not yet available. We strongly recommend that authors cite references using DOIs where possible. For details regarding citation format and examples, please visit the Instructions for Authors section on *Revista de Pielarie Incaltaminte / Leather and Footwear Journal*'s website, <http://www.revistapielarieincaltaminte.ro>

FEES AND SUBSCRIPTIONS

Revista de Pielarie Incaltaminte / Leather and Footwear Journal requires article processing charges of 200 EURO per article, for accepted manuscripts, payable by the author to cover the costs associated with publication. There are no submission charges. Hard copies of journal issues are available for purchase at subscription rates of 160 EURO for companies and 100 EURO for individual subscribers, while the rate for a single issue is 40 EURO. Subscriptions (include mailing costs) can be made at the editorial office, to the following address: INCDTP – DIVISION: LEATHER AND FOOTWEAR RESEARCH INSTITUTE, 93 Ion Minulescu Street, postal code 031215, sector 3, Bucharest, Romania, Europe.

Both article processing charges and subscription fees are to be paid in the following account:

Account holder: INCDTP – Division: Leather and Footwear Research Institute; Address of the account holder: 93 Ion Minulescu Street, postal code 031215, sector 3, Bucharest, Romania, Europe
IBAN Code: RO25 RNCBROU 0074029208380005
Bank code: 300413024
Swift bank address: RNCBROBU; Bank: BCR sector 3 (ROMANIAN COMMERCIAL BANK – SECTOR 3); Bank address: 11 Decebal Blvd., Bl. S14, sector 3, Bucharest, Romania.

CORRESPONDENCE

Editor-in-Chief – Dana Gurău

INCDTP – Division: Leather and Footwear Research Institute (ICPI), 93, Ion Minulescu Street, Bucharest, sector 3, postal code 031215, Romania, Europe; tel./fax: +40 21 323 52 80, e-mail: jlfjournal@gmail.com

CERTEX Publishing House – Bucharest, 16 Lucrețiu Pătrașcanu St., sector 3; Tel./ Fax: (0040) 21 340.55.15; certex@ns.certex.ro

Website: <http://www.revistapielarieincaltaminte.ro>

Facebook: <http://www.facebook.com/LeatherFootwearJournal>

Title DOI: <https://doi.org/10.24264/ljf>

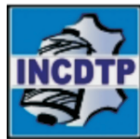


ICAMS 2020

1-3 October
Bucharest, ROMANIA

CALL FOR PAPERS

The 8th International Conference on Advanced Materials and Systems



ORGANIZED BY:



NATIONAL RESEARCH & DEVELOPMENT INSTITUTE FOR TEXTILE AND LEATHER (INCIDTP)
DIVISION LEATHER & FOOTWEAR RESEARCH INSTITUTE (ICPI), BUCHAREST, ROMANIA

SUPPORTED BY:



MINISTRY OF EDUCATION AND RESEARCH

PARTNERS:



EAST SIBERIA
STATE UNIVERSITY
OF TECHNOLOGY &
MANAGEMENT,
ULAN-UDE, RUSSIA



LEATHER ENGINEERING DEPT.,
EGE UNIVERSITY
IZMIR, TURKEY



MUSTAFA KEMAL
UNIVERSITY,
ANTAKYA-HATAY, TURKEY



CHINA LEATHER
& FOOTWEAR
RESEARCH INSTITUTE,
CHINA



"GH. ASACHI"
TECHNICAL UNIVERSITY
IASI, ROMANIA



"POLITEHNICA"
UNIVERSITY
BUCHAREST,
ROMANIA



BUCHAREST ACADEMY
OF ECONOMIC STUDIES,
ROMANIA



COTANCE,
BELGIUM



ROMANIAN LEATHER & FUR
PRODUCERS ASSOCIATION
BUCHAREST, ROMANIA



SFERA FACTOR
THE ROMANIAN
LEATHER MANUFACTURERS
ORGANIZATION



ITA TEXCONF - INNOVATION
AND TECHNOLOGICAL
TRANSFER INCUBATOR
BUCHAREST, ROMANIA

Accepted papers will be published in *ICAMS Conference Proceedings*, indexed in Web of Science Conference Proceedings, Elsevier's Scopus and Compendex, Crossref, Index Copernicus, CiteFactor, Research Bible, Cosmos Impact Factor, and Science Library Index.

IMPORTANT DATES (EXTENDED!)

July 10

July 17

August 7

August 21

October 1-3

Submission
of abstracts

Notification
of abstract
acceptance

Submission
of full papers

Notification
of full papers
acceptance

Conference
date

The 8th INTERNATIONAL CONFERENCE ON ADVANCED MATERIALS AND SYSTEMS

The 8th International Conference on Advanced Materials and Systems (ICAMS 2020) is going to be another major international conference held in the South-Eastern region of Europe, in the area of Materials Science, intending to bring together eminent scientists, technologists and young researchers from several disciplines, across the globe, to provide a common platform for discussing their achievements and newest directions of research. ICAMS 2020 conference is focused on Advanced Materials and Systems and recent developments in material science and technology, covering fields from theory and experiment to industrial practice. The scientific program will consist of plenary sessions, invited talks, oral and poster presentations.

CONFERENCE TOPICS

- | | |
|--|--|
| 1. Advanced Materials and Nanomaterials | 4. Ecological Processes for Circular and Neutral Economy |
| 2. Biomaterials and Biotechnologies | 5. Creative Industries and Cultural Heritage |
| 3. Innovative Systems, Technologies and Quality Management | 6. Education and Digitalization |

SUBMISSION OF ABSTRACTS/FULL PAPERS

The **abstracts** (ca. 200 words followed by **3 key words**) should be submitted in A4 format, one page with Times New Roman font 12 pt. Abstracts should provide a good **overview** of your full paper and cover the following headings: Introduction; Issues to be addressed; Objectives of your paper; Methods; Results; Originality; Conclusions. Please submit the **abstracts** as attachment in MS Word format no later than **July 10th** to icams.ro@gmail.com.

Notification of acceptance will be e-mailed to the contact authors by **July 17th**. The submission of **full paper** is due before **August 7th**. Papers will be blind cross-evaluated by reviewers. Further guidelines concerning the format of the full papers will be soon available on the Conference website (www.icams.ro).

Please e-mail the full paper as attachment in MS Word format to: icams.ro@gmail.com.

Authors will be notified until **August 21st**. Accepted papers will be published in **ICAMS 2020 Proceedings (Proceedings will be indexed in international databases such as Web of Science Conference Proceedings, SCOPUS, Compendex, Crossref, CiteFactor and others)**. Papers may be excluded from the Proceedings if registration fees are not received by **September 7th, 2020**.

CONFERENCE FEES

	Before 7 september	After 7 September
--	-----------------------	----------------------

Participant	300 Euro	350 Euro
Student	125 Euro	125 Euro
Accompanying person	125 Euro	125 Euro

* The conference fee includes the participation with two papers as first author and the conference materials.

SCIENTIFIC COMMITTEE

- Laurenția ALEXANDRESCU, INC DTP-ICPI, RO
Carmen GHITULEASA, INC DTP, RO
Gheorghe COARĂ, INC DTP-ICPI, RO
Alina POPESCU, INC DTP, RO
Carmen GAIDĂU, INC DTP-ICPI, RO
Lucreția MIU, INC DTP-ICPI, RO
Mădălina Georgiana ALBU KAYA, INC DTP-ICPI, RO
Ana-Maria VASILESCU, INC DTP-ICPI, RO
Elena BADEA, University of Craiova and INC DTP-ICPI, RO
Gabriel ZĂINESCU, INC DTP-ICPI, RO
Maria SÖNMEZ, INC DTP-ICPI, RO
Minodora MARIN, INC DTP-ICPI, RO
Behzat Oral BITLISLI, Ege University, Izmir, TR
Mehmet METE MUTLU, Ege University, Izmir, TR
Huseyin ATA KARAVANA, Ege University, Izmir, TR
Gurbuz GULUMSER, Ege University, Izmir, TR
Bahri BASARAN, Ege University, Izmir, TR
Arife Candan ADIGUZEL ZENGİN, Ege University, Izmir, TR
Dmitriy SHALBUEV, East Siberia State Univ. of Techn.&Manag., RU
Aura MIHAI, "Gheorghe Asachi" Technical Univ. of Iasi, RO
Stelian MAIER, "Gheorghe Asachi" Technical Univ. of Iasi, RO
Nizami DURAN, Mustafa Kemal University, Antakya, TR
Alpaslan KAYA, Mustafa Kemal University, Antakya, TR
Gustavo GONZALEZ-QUIJANO, Secretary General, COTANCE, BE
Dimosthenis PAPAKONSTANTINOU, CRE.THI.DEV, GR
Zenovia MOLDOVAN, University of Bucharest, RO
Cristina CARŞOTE, National Museum of Romanian History, RO
Margareta FLORESCU, Bucharest Academy of Economic Studies, RO
Mihaela GHICA, "Carol Davila" Univ. of Medicine&Pharmacy, RO
Alcino MARTINHO, CTIC, PT
Jeannette LUCEJKO, University of Pisa, IT
Carmen ARIAS CASTELLANO, General Secretary, CEC, BE
Keyong TANG, Zhengzhou University, CN
Georgios PANAGIARIS, Technological Education Institute, GR
Victoriya PLAVAN, Kiev Nat. Univ. of Techn&Design, UA
Irina TITORENCU, "N. Simionescu" I.C.B.P., RO
Aurelia MEGHEA, "Politehnica" University Bucharest, RO
Anton FICALI, "Politehnica" University Bucharest, RO
Paul STĂNESCU, "Politehnica" University Bucharest, RO
Maria José FERREIRA, CTCP, PT
Vera PINTO, CTCP, PT
Enrique MONTIEL PARREÑO, Vesica Piscis Footwear, ES
Anna BACARDIT, University of Lleida, ES
Karel KOLOMAZNÍK, Tomas Bata University, Zlin, CZ
Jin ZHOU, Sichuan University, CN
Jianzhong MA, Shaanxi University of Science and Technology, CN

ORGANIZING COMMITTEE

- Laurenția ALEXANDRESCU, Chair, Scientific Secretary, INC DTP - ICPI, RO
Gheorghe COARĂ, Co-Chair, Director INC DTP – Leather and Footwear Research Institute Division (ICPI), RO
Carmen GHITULEASA, Co-Chair, General Director, National Research and Development Institute for Textile and Leather, RO
Dana GURĂU, INC DTP - ICPI, RO
Ioana PIVNICERU, INC DTP - ICPI, RO
Ciprian CHELARU, INC DTP - ICPI, RO
Mihai GEORGESCU, INC DTP - ICPI, RO
Elena NINCULEANU, INC DTP - ICPI, RO
Dan VICOVAN, INC DTP - ICPI, RO

ICAMS 2020 Secretariat

Contact Person:

Ms. Dana Gurau

Address: 93 Ion Minulescu St., code 030215,
Bucharest, Romania

Tel: +4021-323.50.60

Fax: +4021-323.52.80

Email: icams.ro@gmail.com

EDITOR IN CHIEF

Dana GURAU
Dissemination
Compartiment

EDITOR

Dr. Gheorghe COARĂ
Director

EDITOR

Dr. Laurenția ALEXANDRESCU
Scientific Secretary

EDITOR

Dr. Carmen GAIDĂU
Head of Leather
Research
Department

EDITOR

Dr. Mihaela NIȚIUCĂ
Rubber Research
Department

EDITORIAL ADVISORY BOARD

Prof. Dr. Aurel ARDELEAN

Western University "Vasile Goldis" Arad
94-96 Revolutiei Blvd., 310025, Arad, Romania
Member of the Romanian Academy of Medical Sciences,
Member of Academy of Science, New York
Tel./Fax: +40 257 28 03 35
e-mail: rectorat@uvvg.ro

Emeritus Prof. Dr. Aurelia MEGHEA

Head of Projects and Grants Department, Romanian Academy
General Director of Research Centre for Environmental
Protection and Eco-Friendly Technologies, UPB
University "Politehnica" of Bucharest
1-7 Polizu, sector 1, 011061, Bucharest, Romania
Tel.: +4021 3154193
e-mail: a_meghea@gmail.com, aurelia@acad.ro

Prof. Dr. Anton FICAI

University "Politehnica" of Bucharest
Faculty of Applied Chemistry and Materials Science
1-7 Polizu, sector 1, 011061, Bucharest, Romania 35100,
Phone/Fax: 004021 402 3852
e-mail: anton.ficai@upb.ro

Prof. Dr. Behzat Oral BITLISLI

Ege University Faculty of Engineering
Head of Leather Engineering Department
35100, Bornova, Izmir, Turkey
Tel: + 90 232-311 26 44; Fax: +90 232 342 53 76
e-mail: oral.bitlisli@ege.edu.tr

Prof. Dr. Viacheslav BARSUKOV

National University of Technology & Design
2, Nemyrovych-Danchenko Str., Kiev, Ukraine
Tel./Fax: +380 (44) 290-05-12
e-mail: keeh@knutd.com.ua

Prof. Dr. Mehmet Mete MUTLU

Ege University, Faculty of Engineering
Leather Engineering Department,
35100 Bornova, Izmir, Turkey
Tel.: +90 232 3880110 – 2644; Fax: + 90 232 342 53 76
e-mail: mete.mutlu@ege.edu.tr

Prof. Dr. Todorka Gancheva VLADKOVA

University of Chemical Technology and Metallurgy,
Bld. Kliment Ohridsky 8, Sofia, 1756, Bulgaria
e-mail: tgv@uctm.edu

Prof. Dr. Margareta FLORESCU

The Bucharest Academy of Economic Studies
6 Piata Romana, 010374, Bucharest, Romania
Tel.: +40 21 319 1900; +40 21 319 1901; Fax: +40 21 319 1899
e-mail: icefaceus@yahoo.com

Assoc. Prof. Dr. Zenovia MOLDOVAN

University of Bucharest
90-92 Șos. Panduri, 050663, sector 5, Bucharest, Romania
Tel.: +40 21 4103178/125
e-mail: z_moldovan@yahoo.com

Prof. Dr. Hüseyin Ata KARAVANA

Ege University, Faculty of Engineering
Leather Engineering Department,
35100 Bornova, Izmir, Turkey
Tel.: +90 232 3880110 – 2644; Fax: + 90 232 342 53 76
e-mail: huseyin.ata.karavana@ege.edu.tr

Prof. Dr. Wuyong CHEN

National Engineering Laboratory for Clean Technology of
Leather Manufacture, Sichuan University,
Chengdu 610065, Sichuan, P. R. China
Tel: +86-(0)28-85404462; +86-28-85405840
Fax: +86-28-85405237
e-mail: wuyong.chen@163.com

Dr. Ding ZHIWEN

China Leather & Footwear Industry Research Institute
18 Jiangtaixi Road, Chaoyang District,
Beijing, P. R. China, 100015
Tel: +86-10-13701315570
e-mail: ding-zhiwen@263.net

Assoc. Prof. Dr. Alina IOVAN-DRAGOMIR

"Gh. Asachi" Technical University of Iasi
28 Dimitrie Mangeron Blvd., Iași, Romania
Tel.: +40 232 21 23 22; Fax: +40 232-21 16 67
e-mail: adragomir@tex.tuiasi.ro

Assoc. Prof. Dr. Sergiu Stelian MAIER

"Gh. Asachi" Technical University of Iasi
28 Dimitrie Mangeron Blvd., Iași, Romania
Tel.: +40 232 21 23 22; Fax: +40 232-21 16 67
e-mail: smaier@ch.tuiasi.ro

Dipl. Eng. Dorel ACSINTE

Director of S.C PIELOREX S.A.
President of Romanian Leather and Fur Producers Association,
APPBR
33 A, Prelungirea Sos. Giurgiului, Ilfov, Romania
Tel. + 40 31 425 5556; Fax + 40 21 457 1018
e-mail: pielorexa@yahoo.com, appb.ro@gmail.com

Prof. Dr. Aura MIHAI

"Gh. Asachi" Technical University of Iasi
28 Dimitrie Mangeron Blvd., Iași, Romania
Tel.: +40 232 21 23 22; Fax: +40 232-21 16 67
e-mail: amihai@tex.tuiasi.ro

Assoc. Prof. Dr. Dana Corina DESELNICU

University "Politehnica" of Bucharest
1-7 Polizu, sector 1, 011061, Bucharest, Romania
Tel.: +40 021 212 99 52
e-mail: dana.deselnicu@upb.ro

	CONTENTS	CUPRINS	SOMMAIRE
Shiya RAN Hao LIU Shiyang YAN Ruoyi LI Jitka BADUROVA Luming YANG	Comparison of Foot Morphology between Chinese and Mongolian Children	Compararea morfoloiei piciorului la copiii chinezi și mongoli	Comparaison de la morphologie du pied entre les enfants chinois et mongoliens
Nur Mutia ROSIATI Fitrilia SILVIANTI Mustafidah UDKHIYATI	Characterization of Silica/Silver-based Antibacterial Leather	Caracterizarea pielii cu proprietăți antibacteriene tratate cu silice/argint	Caractérisation du cuir antibactérien traité avec de silice/d'argent
Abdón SEGUNDO ESPADA Liliana MARRUFO SALDAÑA Julio BARRA HINOJOSA Rosa CONTRERAS PANIZO	Development of a Degreasing Process for Paiche Skins (Arapaima gigas) for Tanning Preserving the Natural Pattern and Color	Dezvoltarea unui proces de degresare pentru tăbăcirea pielii de pește paiche (Arapaima gigas) păstrând modelul și culoarea naturale ale acesteia	Développement d'un procédé de dégraissage des peaux de paiche (Arapaima gigas) pour le tannage, en préservant le motif et la couleur naturels
Mariana Daniela BERECHET Corina CHIRILĂ Demetra SIMION Olga NICULESCU Maria STANCA Cosmin-Andrei ALEXE Ciprian CHELARU Maria RÂPĂ Dana Florentina GURĂU	Antifungal Activity of Leather Treated with Anethum graveolens and Melaleuca alternifolia Essential Oils against Trichophyton interdigitale	Activitatea antifungică a pieilor tratate cu uleiuri esențiale de Anethum graveolens și Melaleuca alternifolia împotriva Trichophyton interdigitale	L'activité antifongique des cuirs traités avec des huiles essentielles d'Anethum graveolens et Melaleuca alternifolia contre Trichophyton interdigitale
Fangchuan LI Shuangjia LIU Luyu JIANG Weihua ZHANG Jin ZHOU	Novel Use of the Intel RealSense SR300 Camera for Foot 3D Reconstruction	Utilizare nouă a camerei Intel RealSense SR300 pentru reconstrucția 3D a piciorului	Une nouvelle utilisation de la caméra Intel RealSense SR300 pour la reconstruction 3D du pied
Emiliana ANGGRIYANI Laili RACHMAWATI Nais Pinta ADETYA	Development of Processes in the Use of Peroxide as an Ingredient to Reduce Free Formaldehyde Levels in the Skin	Dezvoltarea unor procese de utilizare a peroxidului ca ingredient pentru reducerea nivelului de formaldehidă liberă în piele	Développement d'un procédé d'utilisation du peroxyde comme ingrédient pour réduire les niveaux de formaldéhyde libre dans la peau
Ruoyi LI Hao LIU Xuecan CHEN Jitka BADUROVA Haojun FAN Luming YANG	Load Transference with Running Speed in Natural Rear-foot Strike Male Runners	Transferul de sarcină în funcție de viteza de alergare în cazul alergătorilor de sex masculin care ating solul cu retroriciorul	Transfert de charge en fonction de la vitesse de course pour les coureurs du sexe masculin qui touchent le sol avec l'arrière-pied
Mihaela NITUICĂ (VÎLSAN) Maria SÖNMEZ Mihai GEORGESCU Maria Daniela STELESCU Laurentia ALEXANDRESCU Dana GURĂU Carmen CURUȚIU Lia Maria DITU	Antibacterial Compound Based on Silicone Rubber and ZnO and TiO ₂ Nanoparticles for the Food and Pharmaceutical Industries. Part I – Obtaining and Characterisation	Compound antibacterian pe bază de elastomer siliconic și nanoparticule de ZnO și TiO ₂ pentru domeniul alimentar și farmaceutic. Partea I – Obținere și caracterizare	Composé antibactérien à base d'élastomère de silicone et de nanoparticules de ZnO et TiO ₂ pour le domaine alimentaire et pharmaceutique. Partie I - Obtention et caractérisation

Halyna YEFIMCHUK Vladyslava SKIDAN Mariya NAZARCHUK Eduard SELEZNOV Anzhelika YANOVETS	Multicriteria Compromise Optimization for Leather and Fur Skin Materials Tanning Technology	Optimizare multicriterială a tehnologiilor de tăbăcire a pieilor și blănurilor prin găsirea unei soluții de compromis	Optimisation multicritères des technologies de tannage du cuir et de la fourrure visant à trouver un compromis	183
Lucreția MIU Elena BADEA Claudiu ȘENDREA	Characterization of New and Artificially Aged Parchments	Caracterizarea pergamentelor noi și îmbătrânite artificial	Caractérisation des parchemins nouveaux et âgés artificiellement	197
	European Research Area	Spațiul european al cercetării	Espace Européen de la Recherche	205

COMPARISON OF FOOT MORPHOLOGY BETWEEN CHINESE AND MONGOLIAN CHILDREN

Shiya RAN¹, Hao LIU², Shiyang YAN^{1,2}, Ruoyi LI^{1,2}, Jitka BADUROVA³, Luming YANG^{1,2*}

¹National Engineering Laboratory for Clean Technology Leather Manufacture, Sichuan University, Chengdu 610065, China

²Key Laboratory of Leather Chemistry and Engineering, Ministry of Education, Sichuan University, Chengdu 610065, China

³Tomas Bata University, Zlin, 76001, Czech Republic

Received: 16.01.2020

Accepted: 03.04.2020

<https://doi.org/10.24264/lfj.20.2.1>

COMPARISON OF FOOT MORPHOLOGY BETWEEN CHINESE AND MONGOLIAN CHILDREN

ABSTRACT. Knowledge of foot morphology is fundamental to optimize children's footwear design. The aim of this study is to compare the foot morphology of Chinese and Mongolian children from 7 to 14 years old. Relative data of 339 Mongolian children and another matched 379 Chinese children were collected using 3D foot scanner. The findings of this study are as follows: i) the absolute foot length of Chinese children is significantly greater than that of Mongolian children of the same age; ii) Mongolian children show significantly greater heel width, toe thickness, lateral malleolus height, instep height and ball girth compared to Chinese children of the same age. The foot width of Chinese children is significantly greater than that of Mongolian children of the same age; iii) Chinese children have a higher risk of *hallux valgus* than Mongolian children of both sexes. Small variations in foot morphology discussed in this paper could be useful when considering the shoes design for Mongolian and Chinese children.

KEY WORDS: foot morphology, Mongolian children, Chinese children, footwear design

COMPARAREA MORFOLOGIEI PICIORULUI LA COPILII CHINEZI ȘI MONGOLI

REZUMAT. Cunoașterea morfoloiei piciorului este fundamentală pentru a optimiza proiectarea încălțămintei pentru copii. Scopul acestui studiu este de a compara morfoloia piciorului la copiii chinezi și mongoli cu vârste între 7 și 14 ani. S-au colectat date de la 339 de copii mongoli și 379 de copii chinezi folosind un scanner 3D pentru picioare. Rezultatele acestui studiu sunt următoarele: i) lungimea absolută a piciorului la copiii chinezi este semnificativ mai mare decât în cazul copiilor mongoli de aceeași vîrstă; ii) copiii mongoli prezintă lățimea călcâiului, grosimea degetelor, înălțimea maleolei exterioare, înălțimea căputei și circumferința zonei metatarsofalangiene semnificativ mai mari în comparație cu copiii chinezi de aceeași vîrstă. Lățimea piciorului la copii chinezi este semnificativ mai mare decât în cazul copiilor mongoli de aceeași vîrstă; iii) copiii chinezi au un risc mai mare de a dezvolta *hallux valgus* decât copiii mongoli de ambele sexe. Micile variații ale morfoloiei picioarelor discutate în această lucrare ar putea fi utile la proiectarea încălțămintei pentru copiii mongoli și chinezi.

CUVINTE CHEIE: morfoloia piciorului, copii mongoli, copii chinezi, proiectarea încălțămintei

COMPARAISON DE LA MORPHOLOGIE DU PIED ENTRE LES ENFANTS CHINOIS ET MONGOLIENS

RÉSUMÉ. La connaissance de la morphologie du pied est fondamentale pour optimiser la conception des chaussures pour enfants. Le but de cette étude est de comparer la morphologie du pied des enfants chinois et mongols de 7 à 14 ans. Les données relatives de 339 enfants mongols et de 379 enfants chinois ont été collectées à l'aide d'un scanner 3D pour le pied. Les résultats de cette étude sont les suivants : i) la longueur absolue du pied des enfants chinois est nettement supérieure à celle des enfants mongols du même âge ; ii) les enfants mongols présentent une largeur de talon, une épaisseur des orteils, une hauteur de malléole latérale, une hauteur de cou-de-pied et une circonférence de la région des métatarses sensiblement plus grandes que les enfants chinois du même âge. La largeur du pied des enfants chinois est nettement supérieure à celle des enfants mongols du même âge ; iii) les enfants chinois ont un risque d'*hallux valgus* plus élevé que les enfants mongols des deux sexes. Les petites variations dans la morphologie du pied discutées dans cet article pourraient être utiles lors de la conception de chaussures pour les enfants mongols et chinois.

MOTS CLÉS : morphologie du pied, enfants mongols, enfants chinois, conception de chaussures

INTRODUCTION

Knowledge of foot morphology is the most essential requirement to optimize children's footwear design [1]. The foot morphology and motor development of children are changeable with increasing age [2-4]. Studies indicated that there was high variability of foot morphology of children due to difference in region, lifestyle, ethnicity, etc. [5]. Isabel C.N. Sacco *et al.* [6] found that German children had a wider forefoot (5 to 9 years old) and narrower rear foot (4 years

old) compared to Brazilian children. Kusumoto, A. [7] showed that the protuberance of the first metatarsal phalanx joint was found in 4.5% of Filipino children, but in none of Japanese children. Mauch, M. *et al.* [8] found that German children displayed a significantly longer and flatter foot compared to Australian children. Previous literature also reported the significant differences in foot morphology of adults living in different countries [9, 10]. Therefore, the footwear industry should vary the last dimensions

* Correspondence to: Assoc. Prof. Luming YANG, Key Laboratory of Leather Chemistry and Engineering, Sichuan University, No. 24 South Section 1, Yihuan Road, Chengdu, China, 610065, phone: +86 186 2811 7800, e-mail: yml1982@126.com

on the basis of foot morphology when exporting products to different countries [11].

Most children's footwear purchased in Mongolia are designed and manufactured overseas, mainly from China [12]. As previously mentioned, differences in foot morphology may exist among different countries. It is not sure if using Chinese lasts in Mongolian footwear industries can ensure a good fit for Mongolian children shoes [13]. Ill-fitting footwear has been reported to be the major cause for discomfort, pain, and even foot problems [14]. Therefore, the purpose of this study is to investigate the foot morphology between Chinese and Mongolian children from 7 to 14 years through comparative analysis of foot dimensions. The hypothesis put forward is that there are obvious differences in foot morphology between Chinese and Mongolian children.

MATERIALS AND METHODS

Participants

Two anthropometric databases were involved. The Mongolian database consists of 339

children aged 7 to 14 years old, who were recruited from Ulan Bator, Mongolia [12]. To match the Mongolian database in terms of age, body height and body mass, 379 healthy Chinese children aged 7 to 14 years in the Chinese database were selected. These Chinese children were recruited from randomly selected primary schools and middle schools in Yantai city, Shandong Province, China. Children who demonstrated a history of neuromuscular disease, orthopedic, lower-limb injury or discomfort during walking were excluded from the study.

The participants were separated into eight age groups at an interval of one year, and every age group was classified by gender. The basic information of all participants is shown in Table 1. The descriptive values are presented as mean (standard deviation). Parents or guardians were informed of children's participation in the study in advance and signed a written informed consent. The study was approved by the Ethics Committee of the Sichuan University.

Table 1: Basic information of participants (mean (standard deviation))

Age (yrs)	China					Mongolia				
	Height	Body mass	BMI	Boys	Girls	Height	Body mass	BMI	Boys	Girls
	(cm)	(kg)	(kg/m ²)	(n)	(n)	(cm)	(kg)	(kg/m ²)	(n)	(n)
7-	126.4 (4.8)	25.1(1.8)	16.2(0.6)	19	30	124.5(2.9)	24.4(2.7)	15.2(1.1)	24	15
8-	131.7 (4.2)	30.2(2.0)	17.4(0.2)	49	63	129.7(4.6)	26.1(3.4)	15.5(1.3)	14	15
9-	137.6(4.8)	34.0(2.1)	18.0(0.5)	24	30	135.5(4.9)	29.7(3.9)	16.2(1.5)	16	15
10-	144.3(6.3)	39.4(3.8)	18.9(0.7)	15	28	143.9(6.0)	35.3(5.5)	17.0(1.9)	17	16
11-	151.3(8.1)	45.2(6.0)	19.7(1.1)	15	25	150.5(7.6)	40.6(7.3)	17.8(2.1)	34	27
12-	157.4(8.4)	48.8(5.8)	19.6(0.7)	19	24	156.4(7.4)	44.9(6.7)	18.3(2.1)	28	21
13-	163.8(5.8)	53.8(4.7)	20.0(1.0)	9	14	161.5(5.6)	49.5(6.4)	18.9(1.5)	31	14
14-	164.7(10.6)	55.6(8.1)	20.4(0.6)	5	10	160.8(9.4)	49.3(9.0)	18.9(1.6)	22	30

Procedure

Foot measurements were obtained with the Infoot foot scanner (IFU-S-01), which was developed by I-Ware Lab, Japan. Eight digital cameras were used to synchronously record the foot measurements. The foot scanner was mounted on a level and smooth ground. After familiarization, each participant was required to stand still with bipedal support and with the body weight evenly distributed on both feet.

Statistical Analysis

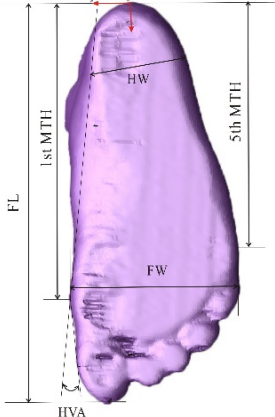
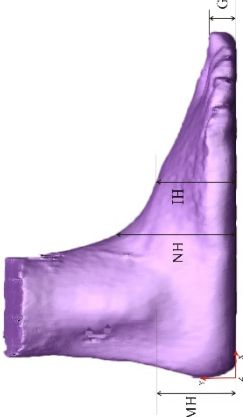
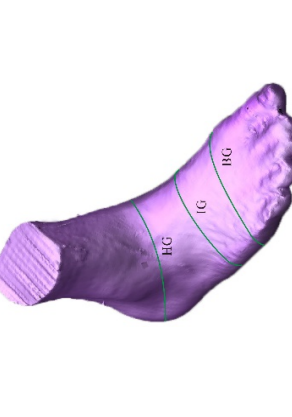
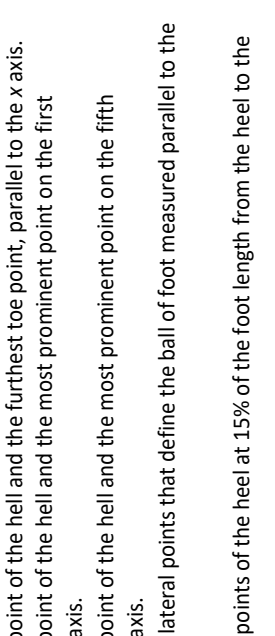
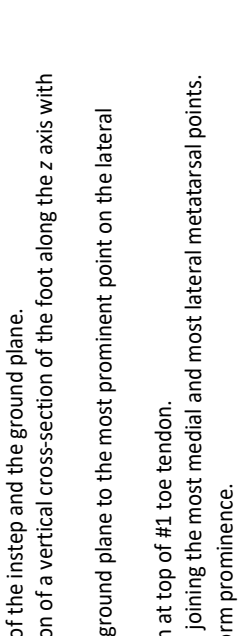
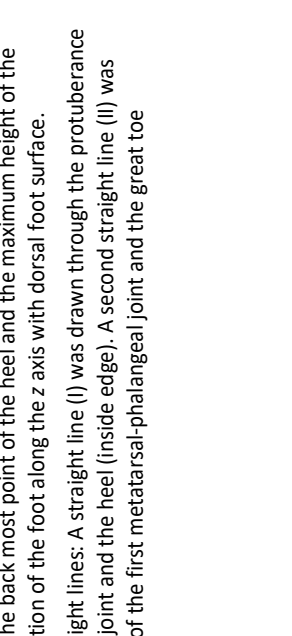
Thirteen foot parameters of foot morphology are shown in Table 2.

All analyses were performed for the right foot [15-18]. Statistical analyses were conducted with SPSS 17.0 (IBM). One-sample Kolmogorov-Smirnov test was tested for all data. Independent t-test was used to compare the significant differences of all normally distributed data between group 1 (Chinese children) and

group 2 (Mongolian children). Effect size (ES) was calculated as a tool of consistent measure using Cohen's d value. The interpretation of ES was set at trivial (0-0.2), small (0.2-0.6), moderate (0.6-1.2) and large (> 1.2) [19]. Linear regression equation and correlation coefficient

'r' were calculated. Chi-square test was used to determine the difference of the hallux valgus rate between genders and countries. The level of $p < 0.05$ was perceived as significance for statistical analyses.

Table 2: Foot dimension definitions

Foot dimension	Definition	Figure
Foot length (FL)	Distance between the back most point of the heel and the furthest toe point, parallel to the x axis.	
Heel to first metatarsal head (H-1st MTH)	Distance between the back most point of the heel and the most prominent point on the first metatarsal head, parallel to the x axis.	
Heel to fifth metatarsal head (H-5th MTH)	Distance between the back most point of the heel and the most prominent point on the fifth metatarsal head, parallel to the x axis.	
Foot width (FW)	Distance between the medial and lateral points that define the ball of foot measured parallel to the y axis.	
Heel width (HW)	Distance between the two widest points of the heel at 15% of the foot length from the heel to the toe.	
Instep height (IH)	Distance between the protrusion of the instep and the ground plane.	
Navicular height (NH)	Maximum height of the intersection of a vertical cross-section of the foot along the z axis with dorsal foot surface.	
Lateral malleolus height (LMH)	Vertical (z axis) distance from the ground plane to the most prominent point on the lateral malleolus.	
Toe #1 thickness (GT)	Height of the vertical cross-section at top of #1 toe tendon.	
Ball girth (BG)	Total perimeter of the ball section joining the most medial and most lateral metatarsal points.	
Instep girth (IG)	Smallest girth over middle cuneiform prominence.	
Heel girth (HG)	Shortest perimeter that contains the back most point of the heel and the maximum height of the intersection of a vertical cross-section of the foot along the z axis with dorsal foot surface.	
Hallux valgus angle (HVA)	The angle between these two straight lines: A straight line (I) was drawn through the protuberance of the first metatarsal-phalangeal joint and the heel (inside edge). A second straight line (II) was drawn through the protuberance of the first metatarsal-phalangeal joint and the great toe (proximal phalanx).	

RESULTS

Foot Dimension

The trend of foot length with age is shown in Figure 1. The foot length of children increased

with age in both countries. Measures of absolute foot length of Chinese children were significantly greater than that of Mongolian children at the same age ($p < 0.05$).

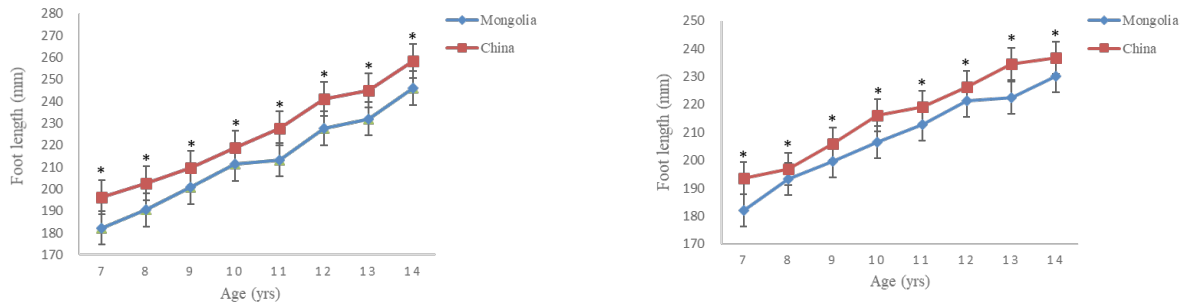


Figure 1. (a): Relationship between foot length and age of boys aged 7-14 years; (b): Relationship between foot length and age of girls aged 7-14 years

Descriptive values of H-1st MTH and H-5th MTH are shown in Table 3. Significant differences for H-1st MTH and H-5th MTH were not found between the two groups. Table 4 shows that the FW of Mongolian children was significantly smaller than that of Chinese children (8 to 10 years old). The HW of Mongolian children was significantly greater than that of Chinese children (9 to 10 years old). However, if we analyze the normalized HW, significant differences were found. It showed that the normalized HW of Mongolian children was significantly greater than that of Chinese children (7 to 10 years old).

Descriptive values of GT, IH, NH and LMH are shown in Table 5. Mongolian children showed significantly greater GT and LMH compared to Chinese children for all ages. Chinese children's feet were significantly smaller in IH than Mongolian children at the age of 7, 8, 9, 11, 12. Descriptive values of GT, IH, NH and LMH are shown in Table 6. When BG was normalized to the foot length, significant differences can be found. It showed that the normalized BG of Mongolian children was significantly greater than that of Chinese children at the age of 7, 14.

Table 3: Mean (SD) values of absolute and normalized foot length dimensions with *p* values and effect sizes for significant results for the two groups

Variables	Age (yrs)	Absolute (mm)		<i>p</i> value, ES*	Normalized (to foot length)		<i>p</i> value, ES*
		Group 1	Group 2		Group 1	Group 2	
H-1st MTH	7-	143.68(6.37)	132.63(9.12)	0.44	0.73 (0.02)	0.72 (0.01)	0.42
	8-	148.75(6.41)	139.07(11.75)	0.21	0.73 (0.02)	0.73 (0.01)	0.42
	9-	153.89(9.49)	147.38(7.01)	0.17	0.74 (0.02)	0.74 (0.02)	0.09
	10-	162.68(9.71)	153.82(11.74)	0.10	0.75 (0.02)	0.74 (0.02)	0.11
	11-	170.6(7.81)	154.62(8.52)	0.14	0.75 (0.02)	0.74 (0.01)	0.13
	12-	178.63(9.24)	167.39(10.63)	0.31	0.75 (0.01)	0.74 (0.01)	0.42
	13-	178.93(6.43)	170.03(9.79)	0.12	0.76 (0.02)	0.74 (0.01)	0.14
	14-	188.89(20.67)	177.41(9.83)	0.07	0.73 (0.02)	0.72 (0.01)	0.09
H-5th MTH	7-	126.44(6.18)	115.42(7.64)	0.45	0.64 (0.01)	0.63 (0.02)	0.42
	8-	130.41(6.45)	120.14(9.21)	0.39	0.64 (0.02)	0.63 (0.01)	0.43
	9-	136.91(6.12)	126.06(6.98)	0.12	0.65 (0.02)	0.63 (0.01)	0.09
	10-	142.65(8.5)	133.71(9.21)	0.09	0.65 (0.02)	0.63 (0.02)	0.11
	11-	148.01(8.32)	135.82(9.18)	0.07	0.65 (0.01)	0.64 (0.02)	0.09
	12-	155.69(8.42)	143.36(9.53)	0.23	0.65 (0.01)	0.64 (0.02)	0.13
	13-	156.91(7.23)	145.68(8.70)	0.47	0.65 (0.02)	0.64 (0.01)	0.42
	14-	164.16(20.6)	153.32(8.05)	0.09	0.65 (0.02)	0.64 (0.01)	0.10

Group 1: Chinese children, Group 2: Mongolian children.

Table 4: Mean (SD) values of absolute and normalized foot width dimensions with *p* values and effect sizes for significant results for the two groups

Variables	Age (yrs)	Absolute (mm)		<i>p</i> value, ES*	Normalized (to foot length)		<i>p</i> value, ES*
		Group 1	Group 2		Group 1	Group 2	
FW	7-	75.99(3.82)	67.54(5.54)	0.07	0.39 (0.02)	0.37 (0.01)	0.09
	8-	77.94(4.17)	68.64(5.96)	< 0.05, 1.80*	0.39 (0.03)	0.36 (0.02)	< 0.05, 1.17*
	9-	80.93(4.93)	72.75(4.14)	< 0.05, 1.79*	0.39 (0.02)	0.36 (0.01)	< 0.05, 1.89*
	10-	82.92(5.84)	77.29(5.08)	< 0.05, 1.03*	0.40 (0.03)	0.36 (0.01)	< 0.05, 1.78*
	11-	86.11(6.01)	76.56(3.87)	0.09	0.38 (0.02)	0.36 (0.02)	0.10
	12-	90.83(5.9)	81.04(5.83)	0.43	0.38 (0.06)	0.36 (0.03)	0.63
	13-	96.26(5.67)	83.03(5.68)	0.11	0.38 (0.03)	0.36 (0.02)	0.09
	14-	96.80(2.26)	87.55(7.23)	0.08	0.38 (0.02)	0.36 (0.02)	0.10
HW	7-	47.88(4.09)	48.77(3.55)	0.09	0.25 (0.02)	0.27 (0.02)	< 0.05, 1.00*
	8-	49.14(3.9)	50.54(3.19)	0.08	0.25 (0.02)	0.27 (0.02)	< 0.05, 1.00*
	9-	51.05(4.11)	53.07(3.52)	< 0.05, 0.53*	0.25 (0.01)	0.27 (0.02)	< 0.05, 1.26*
	10-	53.00(5.03)	55.70(3.82)	< 0.05, 0.61*	0.25 (0.01)	0.27 (0.02)	< 0.05, 1.26*
	11-	55.88(3.62)	57.68(3.50)	0.27	0.25 (0.02)	0.26 (0.01)	0.42
	12-	59.86(5.10)	61.42(4.43)	0.18	0.25 (0.01)	0.26 (0.02)	0.42
	13-	60.74(7.16)	62.00(4.60)	0.12	0.25 (0.01)	0.26 (0.01)	0.28
	14-	63.50(6.05)	65.06(4.33)	0.09	0.25 (0.01)	0.26 (0.02)	0.24

Group 1: Chinese children, Group 2: Mongolian children.

**p* represents significant difference between Group 1 and Group 2

Table 5: Mean (SD) values of absolute and normalized foot height dimensions with *p* values and effect sizes for significant results for the two groups

Variables	Age (yrs)	Absolute (mm)		<i>p</i> value, ES*	Normalized (to foot length)		<i>p</i> value, ES*
		Group 1	Group 2		Group 1	Group 2	
GT	7-	14.64(1.46)	25.71(3.34)	< 0.01, 4.29*	0.07 (0.01)	0.14 (0.02)	< 0.01, 4.42*
	8-	15.89(1.70)	26.57(3.28)	< 0.01, 4.08*	0.08 (0.02)	0.14 (0.01)	< 0.01, 3.78*
	9-	15.9(1.52)	28.13(2.16)	< 0.01, 6.54*	0.08 (0.02)	0.14 (0.01)	< 0.01, 3.00*
	10-	16.78(1.35)	29.35(2.76)	< 0.01, 5.78*	0.08 (0.01)	0.14 (0.02)	< 0.01, 3.79*
	11-	17.28(1.24)	29.38(2.23)	< 0.01, 6.70*	0.08 (0.02)	0.14 (0.01)	< 0.01, 3.79*
	12-	17.69(1.44)	30.64(2.70)	< 0.01, 5.98*	0.07 (0.01)	0.14 (0.02)	< 0.01, 4.42*
	13-	19.14(2.34)	31.87(1.69)	< 0.01, 6.23*	0.08 (0.02)	0.14 (0.03)	< 0.01, 2.35*
	14-	19.44(2.85)	32.77(2.16)	< 0.01, 5.27*	0.08 (0.01)	0.14 (0.02)	< 0.01, 3.79*
IH	7-	43.09(5.60)	51.42(3.35)	< 0.05, 1.80*	0.22 (0.02)	0.27 (0.02)	< 0.05, 2.50*
	8-	45.13(4.85)	53.21(4.02)	< 0.05, 1.81*	0.22 (0.02)	0.27 (0.02)	< 0.05, 2.50*
	9-	47.90(4.95)	53.81(2.79)	< 0.05, 1.47*	0.23 (0.02)	0.27 (0.02)	< 0.05, 2.00*
	10-	53.18(5.16)	56.41(3.64)	0.11	0.24 (0.02)	0.27 (0.02)	0.09
	11-	53.49(6.94)	58.53(3.99)	< 0.05, 0.89*	0.24 (0.02)	0.28 (0.02)	< 0.05, 2.00*
	12-	55.10(6.38)	59.79(3.69)	< 0.05, 0.90*	0.25 (0.02)	0.28 (0.02)	< 0.05, 1.50*
	13-	64.22(4.77)	60.32(3.89)	0.15	0.26 (0.02)	0.28 (0.01)	0.10
	14-	67.45(4.74)	62.00(5.23)	0.06	0.26 (0.02)	0.28 (0.02)	0.09
NH	7-	60.37(3.90)	65.96(4.92)	0.09	0.31 (0.02)	0.33 (0.02)	0.06
	8-	61.53(3.91)	67.21(4.95)	0.07	0.31 (0.02)	0.33 (0.03)	0.11
	9-	64.41(3.72)	69.81(5.59)	0.09	0.31 (0.02)	0.33 (0.02)	0.09
	10-	68.86(5.73)	71.88(3.43)	0.13	0.32 (0.02)	0.34 (0.02)	0.31
	11-	71.79(4.09)	74.97(5.15)	0.09	0.32 (0.02)	0.34 (0.03)	0.15
	12-	76.49(5.06)	77.68(4.36)	0.17	0.32 (0.01)	0.34 (0.02)	0.09
	13-	79.06(4.58)	78.61(4.58)	0.21	0.32 (0.01)	0.34 (0.01)	0.10
	14-	81.18(5.27)	80.41(8.29)	0.37	0.32 (0.02)	0.34 (0.02)	0.30
LMH	7-	35.76(5.09)	50.46(5.12)	< 0.01, 2.88*	0.18 (0.01)	0.28 (0.02)	< 0.01, 6.32*
	8-	38.49(3.44)	51.79(6.33)	< 0.01, 2.61*	0.19 (0.02)	0.27 (0.01)	< 0.01, 5.06*
	9-	40.88 (5.21)	52.94(4.20)	< 0.01, 2.54*	0.19 (0.02)	0.27 (0.02)	< 0.01, 4.00*
	10-	45.52(5.95)	58.88(3.30)	< 0.01, 2.62*	0.22 (0.02)	0.28 (0.02)	< 0.01, 3.00*
	11-	45.71(4.82)	59.53(5.67)	< 0.01, 2.75*	0.21 (0.02)	0.28 (0.03)	< 0.01, 2.75*
	12-	50.36(5.50)	60.75(4.32)	< 0.01, 2.06*	0.21 (0.02)	0.27 (0.01)	< 0.01, 3.79*
	13-	54.40(3.75)	62.45(5.48)	< 0.01, 1.71*	0.22 (0.01)	0.27 (0.02)	< 0.01, 3.16*
	14-	56.53(4.46)	66.05(6.97)	< 0.01, 1.63*	0.22 (0.01)	0.27 (0.03)	< 0.01, 2.23*

Group 1: Chinese children, Group 2: Mongolian children.

**p* represents significant difference between Group 1 and Group 2

Table 6: Mean (SD) values of absolute and normalized foot breadth dimensions with *p* values and effect sizes for significant results for the two groups

Variables	Age (yrs)	Absolute (mm)		<i>p</i> value, ES*	Normalized (to foot length)		<i>p</i> value, ES*
		Group 1	Group 2		Group 1	Group 2	
BG	7-	190.19(11.63)	184.58(13.28)	0.06	0.97 (0.01)	0.99 (0.02)	< 0.05, 1.26*
	8-	197.25(10.32)	190.43(14.85)	0.09	0.97 (0.02)	0.99 (0.02)	0.15
	9-	205.65(10.83)	195.69(9.53)	0.43	0.97 (0.03)	0.99 (0.02)	0.33
	10-	208.54(5.84)	208.18(12.57)	0.83	0.96 (0.06)	0.99 (0.04)	0.59
	11-	216.85(14.82)	205.32(11.01)	0.47	0.94 (0.02)	0.96 (0.03)	0.31
	12-	227.03(13.09)	217.5(14.29)	0.09	0.95 (0.02)	0.96 (0.02)	0.29
	13-	238.65(12.15)	222.74(13.07)	0.07	0.96 (0.01)	0.97 (0.02)	0.42
	14-	242.15(4.94)	235.41(16.06)	0.10	0.94 (0.02)	0.96 (0.03)	< 0.05, 0.78*
IG	7-	199.53(12.00)	185.42(11.56)	0.37	1.02 (0.03)	1.01 (0.03)	0.59
	8-	202.54(19.7)	192.00(13.39)	0.51	1.00 (0.02)	0.99 (0.04)	0.83
	9-	206.86(11.85)	197.00(9.08)	0.43	0.99 (0.03)	0.98 (0.02)	0.09
	10-	203.01(12.31)	207.18(11.07)	0.81	0.96 (0.05)	0.96 (0.04)	0.91
	11-	224.31(18.67)	206.71(9.54)	0.23	0.97 (0.05)	0.96 (0.03)	0.76
	12-	219.8(22.39)	216.68(15.48)	0.75	0.93 (0.04)	0.95 (0.02)	0.42
	13-	241.55(15.15)	222.97(14.48)	0.11	0.98 (0.02)	0.96 (0.01)	0.33
	14-	252.41(5.05)	235.55(14.76)	0.21	0.96 (0.04)	0.96 (0.02)	0.83
HG	7-	263.46(17.25)	243.92(12.8)	0.23	1.32 (0.05)	1.34 (0.03)	0.42
	8-	269.45(34.51)	254.5(15.82)	0.51	1.34 (0.03)	1.33 (0.02)	0.55
	9-	272.72(14.18)	264.00(12.21)	0.43	1.30 (0.03)	1.33 (0.03)	0.10
	10-	277.71(30.56)	280.82(15.08)	0.79	1.32 (0.07)	1.31 (0.05)	0.81
	11-	300.33(38.96)	280.53(11.53)	0.11	1.28 (0.07)	1.31 (0.03)	0.61
	12-	304.95(28.28)	296.57(18.50)	0.83	1.28 (0.03)	1.30 (0.03)	0.18
	13-	311.22(16.28)	301.65(16.07)	0.41	1.27 (0.01)	1.31 (0.03)	0.30
	14-	328.13(17.18)	317.95(19.19)	0.37	1.25 (0.04)	1.29 (0.02)	0.18

Group 1: Chinese children, Group 2: Mongolian children.

**p* represents significant difference between Group 1 and Group 2

Correlation of Foot Parameters

The foot length and ball girth are considered to be the main functional foot parameters for shoe fitting [20]. Linear regression analysis was used to identify the relationship between foot length and ball girth for both genders. The regression results are shown in Figure 3 as follows:

(1) For Chinese boys: Ball girth = $(0.847 \times \text{foot length}) + 39.85$, $r^2 = 0.717$;

(2) For Chinese girls: Ball girth = $(0.859 \times \text{foot length}) + 26.91$, $r^2 = 0.738$;

(3) For Mongolian boys: Ball girth = $(0.791 \times \text{foot length}) + 39.11$, $r^2 = 0.802$;

(4) For Mongolian girls: Ball girth = $(0.768 \times \text{foot length}) + 31.26$, $r^2 = 0.794$.

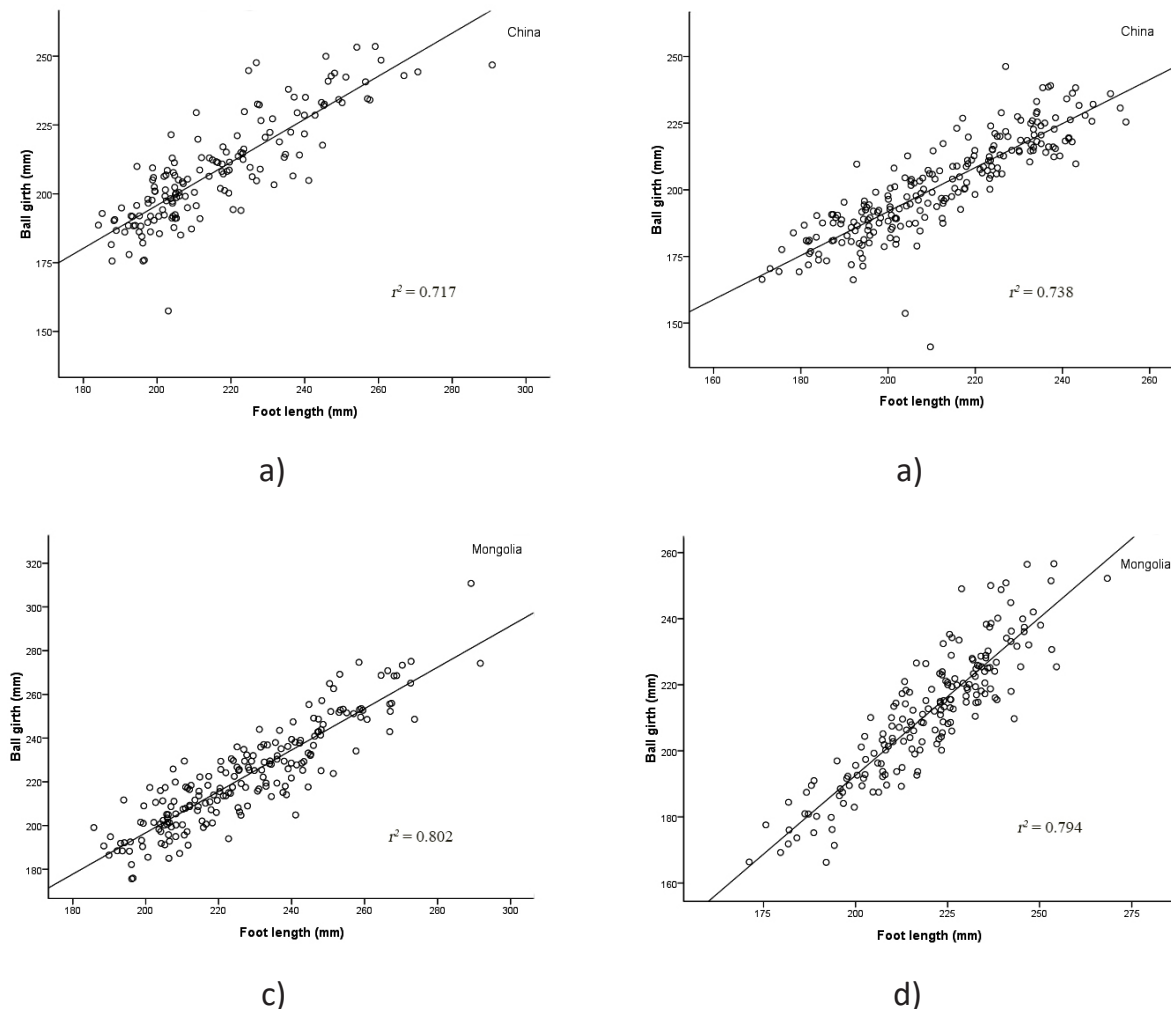


Figure 3. Correlation between foot length and ball girth for both genders, by countries.

(a): Chinese boys; (b): Chinese girls; (c): Mongolian boys; (d): Mongolian girls

Hallux Valgus

Measures of absolute *hallux valgus* angles are shown in Table 7. It was observed that *hallux valgus* angles of Chinese children were significantly greater than those of Mongolian children ($p < 0.05$). The degrees of *hallux valgus* were divided into three grades in Table 8: "Straight or mild", "Moderate" and "Severe" [12]. Chi-square test was used to determine the difference of the *hallux valgus* rate between

genders and countries. The results showed that Chinese children appeared to demonstrate higher incidences of *hallux valgus* compared to Mongolian children of both sexes (for boys: $\chi^2 = 10.97$, $p = 0.004$; for girls: $\chi^2 = 14.48$, $p = 0.001$, respectively). Results revealed that girls appeared to demonstrate higher incidences of *hallux valgus* compared with boys in both countries for all ages (for China: $\chi^2 = 12.90$, $p = 0.002$; for Mongolia: $\chi^2 = 10.68$, $p = 0.005$, respectively).

Table 7: Comparison of means (standard deviations) of *hallux valgus* of the Chinese and Mongolian populations

Foot dimension	Boys		Girls	
	China	Mongolia	China	Mongolia
<i>Hallux valgus</i> angles (°)	8.16 (4.49)	6.05 (3.21)	10.04 (4.53)	7.31 (3.05)

Table 8: The number and proportion of participants with *hallux valgus*

Classification of hallux valgus	Girls, n (%)		Boys, n (%)	
	China	Mongolia	China	Mongolia
Straight or mild (> - 10° and < + 10°)	128(57.15%)	112(73.20%)	114(73.55%)	162(87.10%)
Moderate (> + 11° and < + 15°)	67(29.91%)	36(23.53%)	34(21.93%)	22(11.82%)
Severe (> + 16°)	29(12.95%)	5(3.27%)	7(4.52%)	2(1.08%)
Total	224	153	155	186

DISCUSSION

The results of this study showed that the foot length of Chinese children was significantly greater than that of Mongolian children of the same age. Studies have already shown the significant association between body height, body mass and foot length [21-23]. To match the Mongolian database, the Chinese database was controlled for age, body height and body mass as variable factors. But the tendency of higher height and body mass of Chinese children could be a reason for the difference in foot length. Previous study assumed that the differences in daily diet (especially protein intake) may be related to the differences in children' growth [6].

In comparison to the Chinese children, Mongolian children showed significantly greater toe thickness, instep height and lateral malleolus height. It implies that the vamp designed for Mongolian children should be of sufficient depth. Results showed that the foot width of Chinese children is significantly greater than that of Mongolian children. It indicates that the vamp designed for Chinese children should allow sufficient space around the metatarsal joint area, in order not to damage the soft cartilaginous toes or toe nails [18]. In this study, the absolute foot width of the Chinese children was similar to that of the Filipino children in Kusumoto's study [7], while Chinese children had a larger foot length compared to Filipino children. It is postulated that not only differences in dietary habit, but also differences in ethnicities and region may be responsible for modifying the shape of foot. The normalized foot dimensions provide the necessary information for describing the foot characteristics [24]. Interestingly, when the foot measures were normalized to the length of the foot, significantly greater ball girth and heel width were found in Mongolian children.

The most common foot deformity known and irregularity treated is *hallux valgus*, which

affects more than 35% of individuals [25]. The results obtained in our study showed that girls appeared to demonstrate higher rates of moderate *hallux valgus* compared to boys of the same age in both countries, which have been proved in early literature [26]. However, Chinese children could be at a higher risk for *hallux valgus* compared to Mongolian children. Results showed that 30.11% of Chinese girls and 22.3% of Chinese boys aged from 7 to 14 years had *hallux valgus* deformity (greater than 8°). But the exact prevalence rate of *hallux valgus* is difficult to determine because of the paucity of large-scale epidemiological studies and varying definitions used in the literature. There is no unified explanation of what angle represents a healthy or deformed foot in the big toe area. Some authors indicated 8°, others used 10°, or 15° [25-29]. Specifically, *hallux valgus* found in different populations proved to be related to poorly-fitting footwear [25, 28, 29]. The prevalence of *hallux valgus* is higher in Chinese children, mainly due to the habit of wearing shoes with a narrow toe box. Because shoe styles for children tend to follow the fashion trends for adults, more so in regards to shape rather than the comfort [4]. Therefore, the footwear industry should vary the last dimensions on the basis of foot morphology when exporting products to specific countries.

CONCLUSION

In comparison to the Mongolian children, Chinese children had significantly greater foot length and foot width. However, Mongolian children showed significantly greater toe thickness, instep height, lateral malleolus height, heel width and ball girth than those of Chinese children. The hypothesis is proved that there is obvious difference in foot morphology between Chinese children and Mongolian children. This study thus suggests that small variations in foot

morphology should be considered in the shoe design for specific children. It is hoped that prospective studies could measure more foot parameters, like Chippaux-Smirak and Staheli indices of the longitudinal arch, which are also important variables for the footwear industry.

Conflict of Interest

There were no conflicts of interest with other authors or institution for this study.

Acknowledgments

This research was supported by the National Natural Science Foundation of China [grant number: 11502154]. The authors would express sincere gratitude to all the experimenters and participants who made this study possible.

REFERENCES

1. Noviani, A.D., Widyanti, A., Integrating Anthropometry Approach and Kansei Engineering in the Design of Children Shoe, *Leather and Footwear Journal*, **2018**, 18, 4, 295-306, <https://doi.org/10.24264/lfj.18.4.5>.
2. Martinez-Nova, A., Gijon-Nogueron, G., Alfageme-Garcia, P., Montes-Alguacil, J., Evans, A.M., Foot posture development in children aged 5 to 11 years: A three-year prospective study, *Gait Posture*, **2018**, 62, 280-4, <https://doi.org/10.1016/j.gaitpost.2018.03.032>.
3. Feng, Y., Xu, B., Zhou, J., Effects of the stride length on the gait and intra-limbs coordination of healthy children aged 3 to 6, *Leather and Footwear Journal*, **2019**, 19, 1, 3-10, <https://doi.org/10.24264/lfj.19.1.1>.
4. Xu, M., Wang, L., Foot growth and foot types in children and adolescents: a narrative review, *Sheng Wu Yi Xue Gong Cheng Xue Za Zhi*, **2017**, 34, 648-52.
5. Shariff, S.M., Merican, A.F., Shariff, A.A., Foot morphological between ethnic groups, Anthropometry, Apparel Sizing and Design, **2020**, 317-30, <https://doi.org/10.1016/B978-0-08-102604-5.00012-3>.
6. Sacco, I.C., Onodera, A.N., Bosch, K., Rosenbaum, D., Comparisons of foot anthropometry and plantar arch indices between German and Brazilian children, *BMC Pediatr*, 2015, 15, 4, <https://doi.org/10.1186/s12887-015-0321-z>.
7. Kusumoto, A., Comparative foot dimensions in Filipino rural children and Tokyo children, *Ann Hum Biol*, **1990**, 17, 249- 55, <https://doi.org/10.1080/03014469000001022>.
8. Mauch, M., Mickle, K.J., Munro, B.J., Dowling, A.M., Grau, S., Steele, J.R., Do the feet of German and Australian children differ in structure? Implications for children's shoe design, *Ergonomics*, **2008**, 51, 4, 527-39, <https://doi.org/10.1080/00140130701660520>.
9. Gurney, J.K., Kersting, U.G., Rosenbaum, D., Dynamic foot function and morphology in elite rugby league athletes of different ethnicity, *Ergonomics*, **2009**, 40, 554-9, <https://doi.org/10.1016/j.apergo.2008.11.001>.
10. Ashizawa, K., Kumakura, C., Kusumoto, A., Relative foot size and shape to general body size in Javanese, Filipinas and Japanese with special reference to habitual footwear types, *Ann Hum Biol*, **1997**, 24, 117-29, <https://doi.org/10.1080/03014469700004862>.
11. Hawes, M.R., Sovak, D., Miyashita, M., Kang, S.J., Yoshihuku, Y., Tanaka, S., Ethnic differences in forefoot shape and the determination of shoe comfort, *Ergonomics*, **1994**, 37, 187-96, <https://doi.org/10.1080/00140139408963637>.
12. Batbaatar, T., The influence of the origin of country on consumer intentions – An empirical investigation into reviews on Mongolian consumers: East China Normal University, **2015**.
13. Yanjia, Y., The impact of China's direct investment in Mongolia on Sino-Mongolian Trade and Its Countermeasures, Beijing Jiaotong University, **2017**.
14. Aiyer, A., Hennrikus, W., Foot pain in the child and adolescent, *Pediatr Clin North Am*, **2014**, 61, 1185-205, <https://doi.org/10.1016/j.pcl.2014.08.005>.
15. Menz, H.B., Two feet, or one person? Problems associated with statistical analysis of paired data in foot and ankle medicine, *The Foot*, **2004**, 14, 2-5, [https://doi.org/10.1016/S0958-2592\(03\)00047-6](https://doi.org/10.1016/S0958-2592(03)00047-6).
16. Manna, I., Pradhan, D., Ghosh, S., Kar, S.K., Dhara, P., A Comparative Study of Foot Dimension between Adult Male and Female and Evaluation of Foot Hazards due to Using

- of Footwear, *J Physiol Anthropol Appl Human Sci*, **2001**, 20, 241–6, <https://doi.org/10.2114/jpa.20.241>.
17. Leung, L.A.K., Cheng, J.C.Y., Mak, A.F.T., A cross-sectional study on the development of foot arch function of 2715 Chinese children, *Prosthet Orthot Int*, **2005**, 29, 241–53, <https://doi.org/10.1080/03093640500199695>.
 18. Mauch, M., Grau, S., Krauss, I., Maiwald, C., Horstmann, T., A new approach to children's footwear based on foot type classification, *Ergonomics*, **2009**, 52, 999–1008, <https://doi.org/10.1080/00140130902803549>.
 19. A New View of Statistics, <http://www.sportsci.org/resource/stats/>, **2016**.
 20. Furong, H., Meiling, R., Shiyang, Y., Luming, Y., Research on Foot Shape and Plantar Pressure Distribution of Contemporary Chinese Young Women, *Leather Science and Engineering*, **2013**, 23, 47-51.
 21. Yousefi Azarfam, A.A., Ozdemir, O., Altuntas, O., Cetin, A., Gokce Kutsal, Y., The relationship between body mass index and footprint parameters in older people, *Foot (Edinb)*, **2014**, 24, 186-9, <https://doi.org/10.1016/j.foot.2014.08.009>.
 22. Price, C., Nester, C., Foot dimensions and morphology in healthy weight, overweight and obese males, *Clin Biomech (Bristol, Avon)*, **2016**, 37, 125-30, <https://doi.org/10.1016/j.clinbiomech.2016.07.003>.
 23. Kouchi, M., Foot dimension and foot shape: Different due to growth, generation and ethic origin, *Anthropol Sci*, **1998**, 106, 161-88, https://doi.org/10.1537/ase.106.Supplement_161.
 24. Delgado-Abellán, L., Aguado, X., Jiménez-Ormeño, E., Mecerreyres, L., Alegre, L.M., Foot morphology in Spanish school children according to sex and age, *Ergonomics*, **2014**, 57, 787-97, <https://doi.org/10.1080/00140139.2014.895055>.
 25. Robinson, C., Bhosale, A., Pillai, A., Footwear modification following hallux valgus surgery: The all-or-none phenomenon, *World J Methodol*, **2016**, 6, <https://doi.org/10.5662/wjm.v6.i2.171>.
 26. Nishimura, A., Kato, K., Fukuda, A., Prevalence of hallux valgus and risk factors among Japanese community dwellers, *J Orthop Sci*, **2013**, 19, 257-62, <https://doi.org/10.1007/s00776-013-0513-z>.
 27. Hao, G., Zhicheng, S., Recent advances in X ray observation index of hallux valgus and their applications, *China J Orthop Trauma*, **2013**, 26, 171-4.
 28. Barnett, C.H., The normal orientation of the human hallux and the effect of footwear, *J Anat*, **1962**, 96, 94-489.
 29. Shine, B.L., Incidence of Hallux Valgus in a Partially Shoe-wearing Community, *Br Med J*, **1965**, 1648-50, <https://doi.org/10.1136/bmj.1.5451.1648>.

© 2020 by the author(s). Published by INCDTP-ICPI, Bucharest, RO. This is an open access article distributed under the terms and conditions of the Creative Commons Attribution license (<http://creativecommons.org/licenses/by/4.0/>).

CHARACTERIZATION OF SILICA/SILVER-BASED ANTIBACTERIAL LEATHER

Nur Mutia ROSIATI^{1*}, Fitrilia SILVIANTI², Mustafidah UDKHIYATI¹

¹Department of Leather Processing Technology, Politeknik ATK Yogyakarta, Sewon, Bantul 55281, Yogyakarta, Indonesia,
mutia.rosiati92@gmail.com

²Department of Rubber and Plastic Processing Technology, Politeknik ATK Yogyakarta, Sewon, Bantul 55281, Yogyakarta,
Indonesia

Received: 06.02.2020

Accepted: 06.05.2020

<https://doi.org/10.24264/lfj.20.2.2>

CHARACTERIZATION OF SILICA/SILVER-BASED ANTIBACTERIAL LEATHER

ABSTRACT. The hydrophilic character of vegetable tanned leather is potentially a medium for bacterial growth. A treatment using an antibacterial agent applies to prevent bacterial growth on it. The vegetable tanned leather in this study was obtained from the tanning of goat skin using mimosa as a tanning agent. The utilization of silica from volcanic ash modified with silver was employed in this study as an antibacterial agent. The functional groups of materials were analysed using FTIR spectrophotometer and evaluated. The results of thermal studies using TG/DTA show that vegetable tanned leather coated with silica (leather@SiO₂) and vegetable tanned leather coated with silica/silver (leather@SiO₂/Ag) are thermally stable materials. The inhibition zones of *Staphylococcus aureus* for leather@SiO₂ and leather@SiO₂/Ag were larger compared to vegetable tanned leather with inhibition area of 21.25 ± 0.50 mm, 24.80 ± 1.64 mm and 11.40 ± 0.55 mm, respectively. This confirmed the effectiveness of utilization of silica-based volcanic ash and silver as an antibacterial agent.

KEY WORDS: leather, silica, silver, antibacterial agent

CARACTERIZAREA PIELII CU PROPRIETĂȚI ANTIBACTERIERE TRATATE CU SILICE/ARGINT

REZUMAT. Având în vedere caracterul său hidrofil, pielea tăbăcătă vegetal poate fi un mediu propice pentru creșterea bacteriilor. Se poate aplica un tratament care utilizează un agent antibacterian pentru a preveni creșterea bacteriilor pe piele. Pielea tăbăcătă vegetal din acest studiu a fost obținută prin tăbăcirea pielii de capră folosind mimosă ca agent de tăbăcire. Silicea din cenușă vulcanică modificată cu argint a fost utilizată în acest studiu ca agent antibacterian. Grupările funcționale ale materialelor au fost analizate folosind spectrofotometru FTIR și apoi evaluate. Rezultatele studiilor termice efectuate folosind TG/DTA arată că pielea tăbăcătă vegetal acoperită cu silice (leather@SiO₂) și pielea tăbăcătă vegetal acoperită cu silice/argint (leather@SiO₂/Ag) sunt materiale stabilă din punct de vedere termic. Zonele de inhibare ale *Staphylococcus aureus* pentru leather@SiO₂ și leather@SiO₂/Ag au fost mai mari comparativ cu pielea tăbăcătă vegetal cu suprafață de inhibare de 21,25 ± 0,50 mm, 24,80 ± 1,64 mm și, respectiv, 11,40 ± 0,55 mm. Acest lucru a confirmat eficacitatea utilizării cenușii vulcanice pe bază de silice și a argintului ca agent antibacterian.

CUVINTE CHEIE: piele, silice, argint, agent antibacterian

CARACTÉRISATION DU CUIR ANTIBACTÉRIEN TRAITÉ AVEC DE SILICE/D'ARGENT

RÉSUMÉ. En raison de sa nature hydrophile, le cuir au tannage végétal peut être un environnement approprié pour la croissance des bactéries. Un traitement peut être appliqué qui utilise un agent antibactérien pour empêcher la croissance bactérienne sur la peau. Le cuir au tannage végétal dans cette étude a été obtenu en tannant la peau de chèvre en utilisant du mimosa comme agent de tannage. La silice provenant des cendres volcaniques modifiée par l'argent a été utilisée dans cette étude comme agent antibactérien. Les groupes fonctionnels des matériaux ont été analysés à l'aide du spectrophotomètre FTIR puis évalués. Les résultats des études thermiques utilisant TG/DTA montrent que le cuir tanné végétal traité avec de silice (leather@SiO₂) et le cuir tanné végétal traité avec de silice/argent (leather@SiO₂/Ag) sont des matériaux thermiquement stables. Les zones d'inhibition de *Staphylococcus aureus* pour leather@SiO₂ et leather@SiO₂/Ag étaient plus grandes par rapport au cuir au tannage végétal avec une surface inhibitrice de 21,25 ± 0,50 mm, 24,80 ± 1,64 mm et 11,40 ± 0,55 mm. Cela a confirmé l'efficacité de l'utilisation de cendres volcaniques à base de silice et d'argent comme agent antibactérien.

MOTS CLÉS : cuir, silice, argent, agent antibactérien

* Correspondence to: Nur Mutia ROSIATI, Department of Leather Processing Technology, Politeknik ATK Yogyakarta, Sewon, Bantul 55281, Yogyakarta, Indonesia, mutia.rosiati92@gmail.com

INTRODUCTION

The processes of leather tanning play an important role in obtaining the character of the product, especially the tanning process. In general, the skin is tanned using mineral or vegetable tanning agents. Mineral tanning agents that are usually used are chrome compounds derived from Cr(III) salts. This species of Cr(III) may be oxidized forming Cr(VI) which is known to be a hazardous material to the environment. Therefore, the tanning of skin using chrome compounds needs to be minimized.

The alternative tanning process may be conducted using vegetable tanning agents. These vegetable tanning agents are extracted from plants that are known as renewable natural resources. Vegetable tanning agents generally contain a high number of hydroxyl ($-OH$) groups, increasing the hydrophilicity and the humidity of the tanned leather. As a result, vegetable tanned skin is potentially a good bacterial growth medium. Bacteria that grow on vegetable tanned skin can lead to a disease for consumers. Hence, it is necessary to make an effort to obtain antibacterial tanned skin.

Antibacterial agents such as pentachlorophenol, polyhalogenated phenolic compounds, dimethylfumarate, quaternary ammonium salts, silylquaternary compounds, etc., have been used in leather industry. However, some of them are harmful to human health and the environment [1-3]. Therefore, studies to find alternative antibacterial agents have been widely developed.

Silica is one of the antimicrobial agents which has been studied in several fields [4-8]. It can be utilized as antibacterial particles or as delivery systems for antibacterial agents [6, 8]. Various sources of silica have been used as silica precursors, such as tetraethoxysilane (TEOS) [9-11] and water glass [12]. Volcanic ash is solid waste from an eruption that has the potential to be used as a raw material for the preparation of a silica precursor due to its high silica content. Furthermore, volcanic ash of Mount Merapi has been known to contain 51.31% silica [13]. However, the utilization of silica as an antibacterial agent has a limited effect against bacteria [6]. One attempt to enhance the antibacterial activity of silica is by modification via metal particles [5, 11, 14]. The

previous studies found that silver (Ag) can be used as an antibacterial agent in leather [15-17]. Silver has attracted attention due to its excellent antibacterial activity and non-toxic character [6, 15, 16]. Moreover, it has been reported that the attachment of silica-silver for various fields giving good antibacterial effect [5, 9, 10, 12, 16]. Thus, this study focuses on applying the silica-based coating modified with silver on leather.

EXPERIMENTAL

Materials and Methods

Materials

The materials used for the vegetable tanning process were three pieces of pickled goat skins and mimosa as a tanning agent. Silica was extracted from ash of Merapi Volcano, Yogyakarta, Indonesia using sodium hydroxide. Other chemicals used included sodium formate, naphthalene sulphonate (Coralon OT produced by STAHL), replacement syntan (Tanicor PWB produced by STAHL), sulphited oil (Derminol OCS produced by STAHL) and silver nitrate (Merck).

Methods

Synthesis of Silica from Volcanic Ash

The synthesis of silica was employed as conducted by Sudjarwo and Bee (2017) [20]. Merapi Volcano ash was mixed with sodium hydroxide by the ratio (w/w) of 1:1. The mixture was heated to 900°C in the furnace for 3 (three) hours. Afterward, the solid product was dissolved in water, after which 2 M hydrochloric acid was added. This mixture was stirred for a day then filtered. The filtrate containing silica was used as a material for coating leather.

Coating Leather with Silver Modified Silica

The pickled goat skins were processed by the vegetable tanning method for insole shoes (Table 1). Two obtained pieces of leather were coated using the impregnation method [21]. One leather was coated by silica while the other one was coated by silica and $AgNO_3$ solution. These coated leathers were dried and stored in closed plastic bags before the treatment for antibacterial activity assays.

Table 1: The stages of leather preparation process

Stage Process	Chemical Material (%)
pH Adjustment	200% water 0.1% Sodium Formate (60 minutes)
Tanning	200% water 5% Dispersing Agent (Coralon OT) (30 minutes) 10% Mimosa Sul (60 minutes) 10% Mimosa (60 minutes) 10% Mimosa (60 minutes) 5% Tanicor PWB (60 minutes)
Post Tanning	
Fatliquoring	4% Derminol OCS (45 minutes)
Coating processes	1% Silica Solution (2 hours)
Fixation	1% Formic Acid (45 minutes) 1% AgNO_3 solution

Identification of Functional Groups with Fourier Transform Infrared (FTIR) Spectrophotometry

FTIR spectrophotometry analysis was performed using Shimadzu FTIR Prestige 21. An amount of 2 mg of sample was homogenized with 200 mg of KBr powder. It was made into a pellet using 2000 psi in pressure. The absorbance of the sample was recorded at a wavenumber range of 400-4000 cm^{-1} .

Thermal Analysis with Thermo-Gravimetry and Differential Thermal Analysis (TG/DTA)

TG/DTA analysis was conducted using Perkin-Elmer under a nitrogen gas flow with a heating rate of 10.00°C/min within the temperature range of 30.00-750.00°C. About 5 mg of sample was prepared in aluminium sample holder then heated according to the standard operating above.

Antibacterial Activity Assays

The bacteria inoculum was prepared by aseptically transferring isolated colonies (*Staphylococcus aureus*) to the nutrient broth, then incubated during 24 h at 37 ± 1°C. The inoculum was diluted to 0.5 McFarland turbidity standards (corresponding to a concentration of 1.5 – 3.0 × 10⁸ CFU/mL). For antibacterial activity evaluation purposes, a coated leather sample (2 cm × 2 cm) was placed on a Petri dish containing 0.5 mL of the working bacterial dilution in 20 ml nutrient agar solution. Afterward, the Petri dishes were incubated for 24 h at 37 ± 1°C.

The evaluation of the antibacterial activity was conducted on the presence of an inhibition growth zone around the edges of the tested leather sample.

RESULTS AND DISCUSSIONS

The tanning process in this study was employed using goat skin as raw material and mimosa as a vegetable tanning agent. Mimosa contains polyphenols that can interact with collagen of goat skin via hydrogen and covalent bonding. The abundance of hydroxyl groups on the vegetable tanned surface makes it a good bacterial growth medium. Therefore, the vegetable tanned leather was coated using silica and silver to give the antibacterial effect on the leather.

The tanning process leads to an increase in weight of leather (Table 2). This indicates the formation of the bond between the tanning agent and goat skin [22]. As can be seen in Table 2, leather@ SiO_2 and leather@ SiO_2/Ag show a higher percentage of weight increase compared to vegetable tanned leather. This can be explained by the modification of leather with silica and Ag that generated the interaction between modifier and leather.

Table 2: Percentage of weight increase after process

Sample	Weight of pickled skin (g)	Weight of leather (g)	Percentage of increase (%)
Vegetable tanned leather	398.8	458.5	14.52
Leather@SiO ₂	279.6	321.3	14.90
Leather@SiO ₂ /Ag	379.8	437.5	15.19

The silica was obtained from the Merapi volcanic ash which is abundant and unused material. The treatment of volcanic ash was conducted using sodium hydroxide and hydrochloric acid resulting in sodium silicate. Sodium silicate can react with the hydroxyl groups of vegetable tanned leather forming

other hydroxyl groups on the coated vegetable tanned leather. The modification of the coating layer was done using silver. The positive charges of silver interacted with negative charges of protonated oxygen resulting in electrostatic interaction. The illustrations of coated vegetable tanned leather surface are shown in Figure 1.

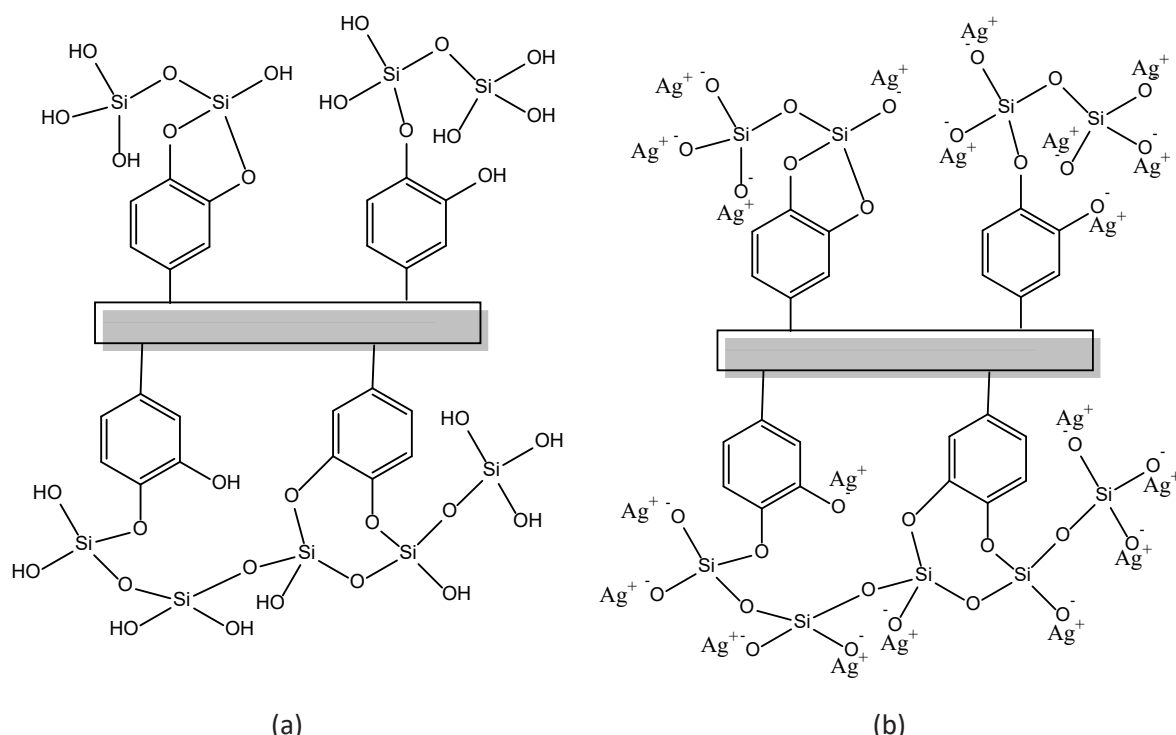


Figure 1. Interaction model of vegetable tanned leather coated with: (a) silica-based volcanic ash and (b) silica-based volcanic ash/Ag

Identification of Functional Groups of Leather

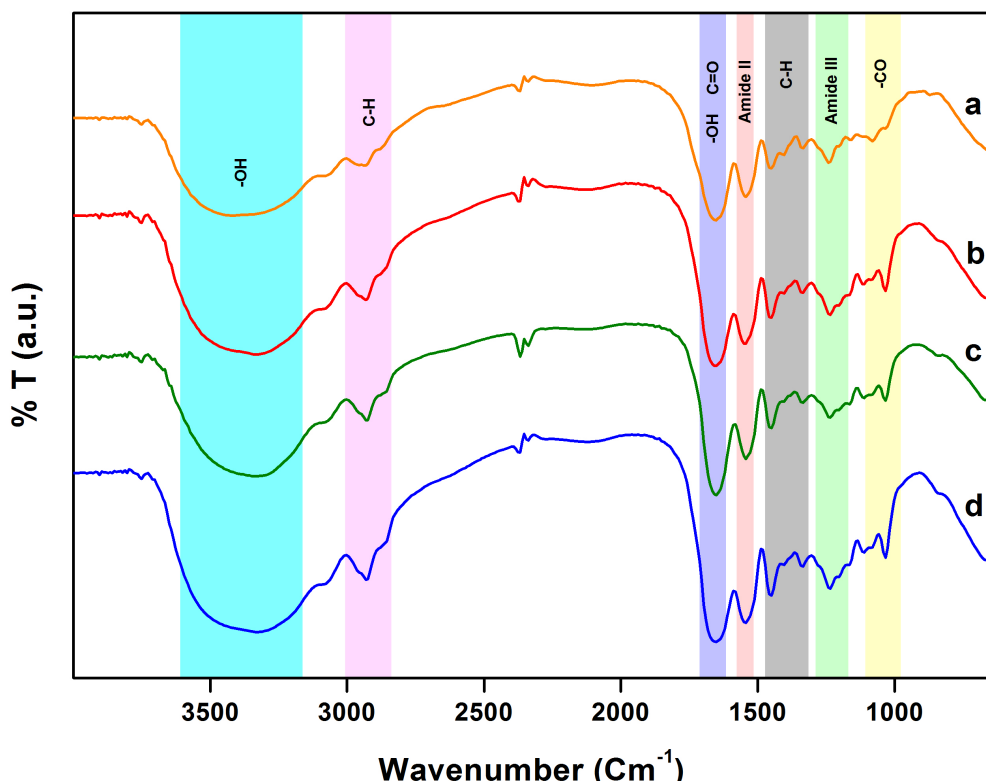


Figure 2. FTIR spectra of (a) pickled goat skin, (b) vegetable tanned leather, (c) leather@ SiO_2 , and (d) leather@ SiO_2/Ag

The amide groups of leather were identified in several wavelength regions. Amide I band resulted in absorbance at 1651 cm^{-1} corresponding to C=O stretching vibration of pure collagen [23]. This band overlapped with –OH bending vibration. The absorption band at 1543 cm^{-1} appeared from the amide II band [23, 24]. Amide III band is shown between $1234\text{--}1242\text{ cm}^{-1}$ attributing to symmetrical stretching of carboxylate groups [17, 24]. The absorption bands at $1335\text{; }1450$ and around $2924\text{--}2932\text{ cm}^{-1}$ appeared as C–H bending, C–H wagging, and C–H asymmetric stretching vibration respectively, verifying the presence of C–H bonding in collagen [25–27].

It is shown in the FTIR spectra that the coating with silica does not change the absorption bands of tanned leather. This can be explained by the silica characteristic bands that commonly appeared around $1034\text{--}1080\text{ cm}^{-1}$ and 3400 cm^{-1} overlapped with –CO and –OH stretching bands of tannin [7, 12, 28–31]. However, the attachment of Ag on leather is not

revealed in the FTIR spectra. This phenomenon suggests that no bond occurs between Ag and the modified leather, indicating that Ag and modified leather interact electrostatically. It also confirmed that the modification of leather using Ag does not affect the structure of modified leather [24]. The FTIR spectra revealed no difference in characteristic absorption band between one another. It implies that the modifiers' penetration occurs almost uniformly from the flesh to the grain of the leather.

Stability at Thermal Decomposition

The TG analysis curves of samples are shown in Figure 3. The thermal degradation of samples showed three stages of weight loss over a temperature range of $30\text{--}750^\circ\text{C}$. The first stages occurred at $40\text{--}90^\circ\text{C}$ due to the water content of samples [32, 33]. The second stage ranges between $150\text{--}500^\circ\text{C}$ and was identified as the decomposition of the organic moiety [34]. The last stage was observed above 500°C , caused by the weight loss of carbonized residues [33].

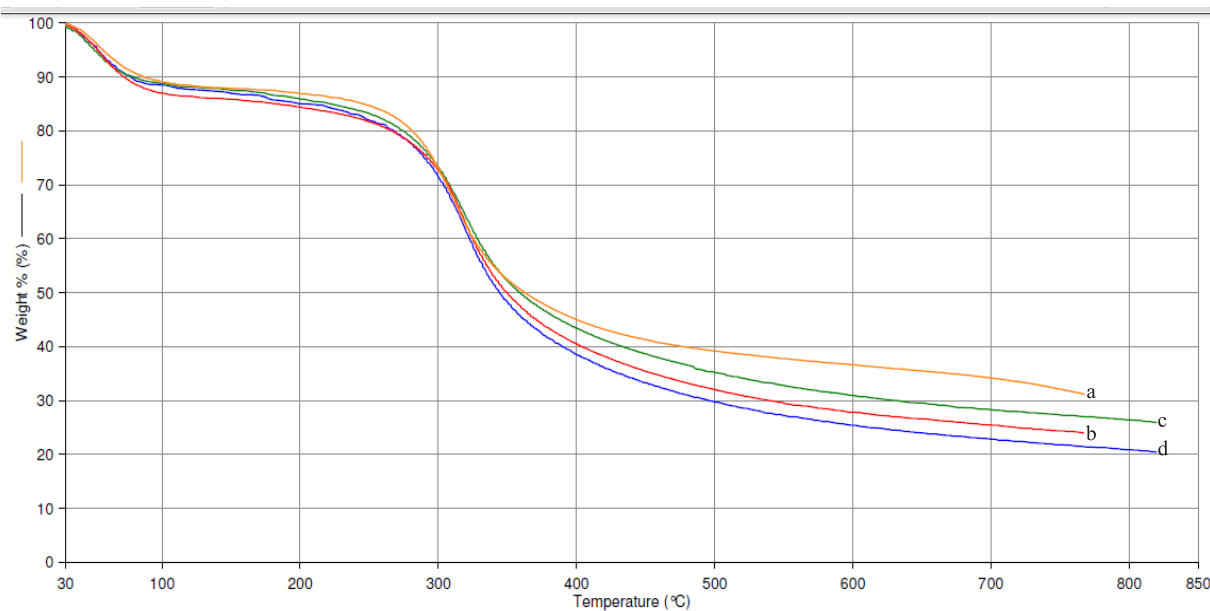


Figure 3. TG curves of (a) pickled goat skin, (b) vegetable tanned leather, (c) leather@ SiO_2 and (d) leather@ SiO_2/Ag

Based on the TG analysis, it was confirmed that the weight loss ratio was almost similar for all the samples. The first stage required a higher temperature than the other stages, corresponding

to the decomposition temperature of water. The slight differences in temperature of the second stage were identified for all samples.

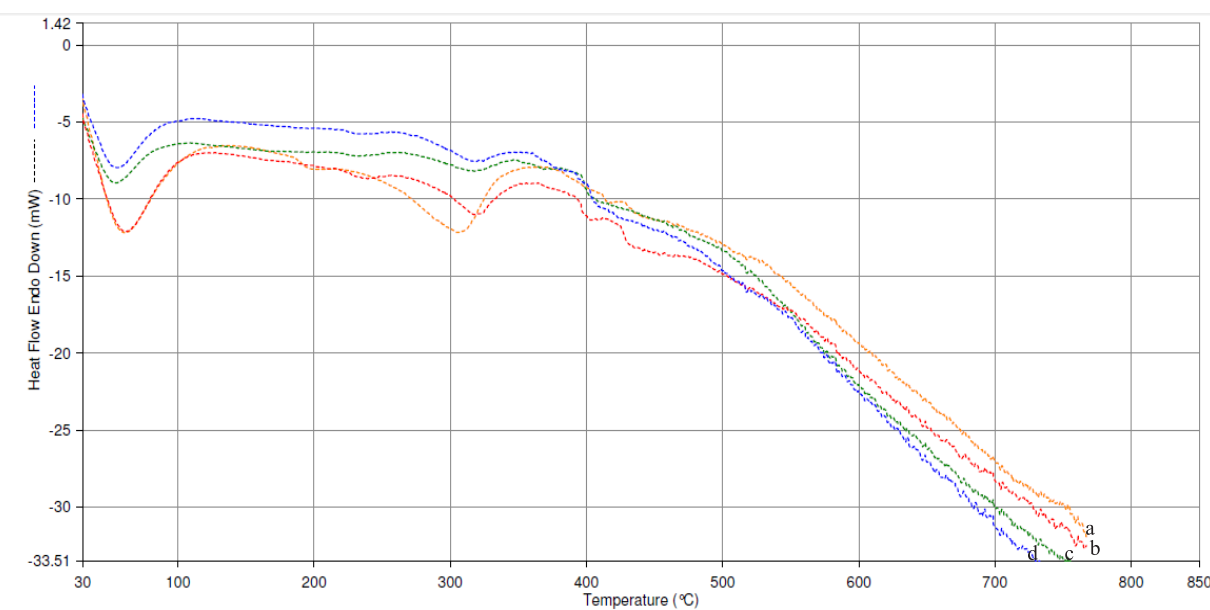


Figure 4. DTA curves of (a) pickled goat skin, (b) vegetable tanned leather, (c) leather@ SiO_2 and (d) leather@ SiO_2/Ag

The DTA curves informed two endothermic peaks of samples (Figure 4). The phase change observed at around 56 and 62°C corresponds to evaporation of water in pickled skin and coated leathers. The water evaporation temperatures of leather@ SiO_2 and that of leather@ SiO_2/Ag

were identified slightly lower than that of pickled goat skin and vegetable tanned leather. The increase of hydroxyl groups in leather@ SiO_2 and leather@ SiO_2/Ag can explain this difference in temperature. The endotherm at 300-325°C reflects to the release of organic moiety of

samples. The heat flow of pickled skin and the tanned leather were higher than the silica

treated leather, expressing that the coating of silica on leather increases the thermal stability of leather.

Antibacterial Activity

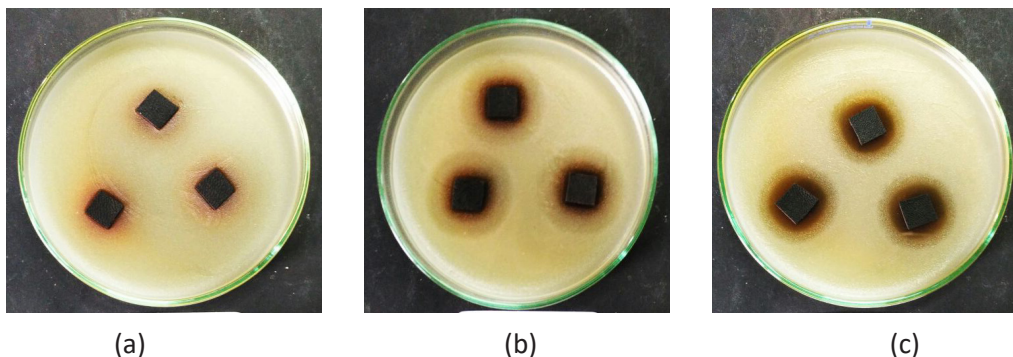


Figure 5. *Staphylococcus aureus* inhibition zone of (a) vegetable tanned leather, (b) leather@ SiO_2 , and (c) leather@ SiO_2/Ag

The antibacterial activity assay was investigated by the agar diffusion method using *Staphylococcus aureus* to identify the bacteria inhibition zone diameter (Figure 5). The measurement data are written in Table 3. The results imply that the inhibition zones of leather@ SiO_2 and leather@ SiO_2/Ag were 21.25 ± 0.50 mm and 24.80 ± 1.64 mm, respectively. This area was larger than the inhibition zone of vegetable tanned leather that is equal to 11.40 ± 0.55 mm. Anova test shows a significant difference for every data. This confirmed the successful working of silica-based volcanic ash and silver as an antibacterial agent on vegetable tanned leather.

Table 3: Inhibition zone of samples

Sample	Inhibition Zone (mm)
Vegetable tanned leather	11.40 ± 0.55
Leather@ SiO_2	21.25 ± 0.50
Leather@ SiO_2/Ag	24.80 ± 1.64

The antibacterial mechanism of silica is different from that of silver. Silica increased the hydrophobicity of vegetable tanned leather, thus reducing bacteria growth on vegetable tanned leather. While silver ions interact with disulfide or sulphydryl groups of enzymes, causing structural changes leading to disruption of metabolic processes followed by cell death [35, 36]. Recently, it has been suggested that the

antibacterial mechanism of silver nanoparticles may also be related to membrane damage due to free radicals that are derived from the surface of the nanoparticles [37]. This bacterial activity also appeared to be dependent on the size and shape of the silver nanoparticles [38].

CONCLUSIONS

The utilization of silica-based volcanic ash modified with silver as an antibacterial agent in leather production was investigated in this study. The leather was obtained from the tanning process of goat skin using mimosa as a tanning agent. The antibacterial assay showed that the inhibition zones of *Staphylococcus aureus* for vegetable tanned leather, leather@ SiO_2 and leather@ SiO_2/Ag are 11.40 ± 0.55 mm, 21.25 ± 0.50 mm and 24.80 ± 1.64 mm, respectively. It verified the effectiveness of leather coating with silica-based volcanic ash/silver as an antibacterial agent.

Acknowledgements

This work was funded by Politeknik ATK Yogyakarta through Research Grant of Riset Pembinaan, No. 74.1/SK/SJ-IND.7.7/11/2018. The authors would like to acknowledge Laura Boetje for the valuable proofreading and suggestions, and Wisnu A.A. Sudjarwo for the valuable discussions and providing chemicals.

REFERENCES

1. Sirvaityte, J., Siugzdaite, J., Valeika, V., Application of commercial essential oils of Eucalyptus and Lavender as natural preservative for leather tanning industry, *Rev Chim*, **2011**, 62, 9, 885-893.
2. Türkan, M.F., Yapici, A.N., Yapici, B.M., Bilgi, S.D., Assessment of antimicrobial activity of natural leathers treated with *Pseudoevernia furfuracea* (L.) Zopf extracts, *Tekstil ve Konfeksiyon*, **2013**, 23, 2, 176-180.
3. Koizhaiganova, M., Yaşa, I., Gürümser, G., Assessment of antibacterial activity of lining leather treated with silver doped hydroxyapatite, *Int Biodeterior Biodegradation*, **2015**, 105, 262-267, <https://doi.org/10.1016/j.ibiod.2015.09.017>.
4. Mahltig, B., Fiedler, D., Bottcher, H., Antimicrobial sol-gel coatings, *J Sol-Gel Sci Techn*, **2004**, 32, 219-222, <https://doi.org/10.1007/s10971-004-5791-7>.
5. Nischala, K., Rao, T.N., Hebalkar, N., Silica-silver core-shell particles for antibacterial textile application, *Colloids Surf B Biointerfaces*, **2011**, 82, 1, 203-208, <https://doi.org/10.1016/j.colsurfb.2010.08.039>.
6. Besines, A., Peralta, T.D., Handy, R.D., The antibacterial effects of silver, titanium dioxide and silica dioxide nanoparticles compared to the dental disinfectant chlorhexidine on *Streptococcus mutans* using a suite of bioassays, *Nanotoxicology*, **2014**, 8, 1, 1-16, <https://doi.org/10.3109/17435390.2012.742935>.
7. Maestre-López, M.I., Payá-Nohales, F.J., Arán-Ais, F., Martínez-Sánchez, M.A., Orgilés-Barceló, C., Bertazzo, M., Antimicrobial effect of coated leather based on silver@silicananocomposites: synthesis, characterisation and microbiological evaluation, *Journal of Biotechnology and Biomaterials*, **2015**, 5, 171-181, <https://doi.org/10.4172/2155-952X.1000171>.
8. Karaman, D.S., Manner, S., Rosenholm, J.M., Mesoporous silica nanoparticles as diagnostic and therapeutic tools: how can they combat bacterial infection?, *Ther Deliv*, **2018**, 9, 4, 1-4, <https://doi.org/10.4155/tde-2017-0111>.
9. Kawashita, M., Tsuneyama, S., Miyaji, F., Kokubo, T., Kozuka, H., Yamamoto, K., Antibacterial Silver-Containing Silica Glass Prepared by Sol-Gel Method, *Biomaterials*, **2000**, 21, 4, 393-398, [https://doi.org/10.1016/S0142-9612\(99\)00201-X](https://doi.org/10.1016/S0142-9612(99)00201-X).
10. Xu, K., Wang, J.X., Kang, X.L., Chen, J.F., Fabrication of antibacterial monodispersed Ag-SiO₂ core-shell nanoparticles with high concentration, *Mater Lett*, **2009**, 63, 31-33, <https://doi.org/10.1016/j.matlet.2008.08.039>.
11. Berendjchi, A., Khajavi, R., Yazdanshenas, E., Fabrication of superhydrophobic and antibacterial surface on cotton fabric by doped silica-based sols with nanoparticles of copper, *Nanoscale Res Lett*, **2011**, 6, 594, 1-8, <https://doi.org/10.1186/1556-276X-6-594>.
12. Xing, Y., Yang, X., Dai, J., Antimicrobial finishing of cotton textile based on water glass by sol-gel method, *J Sol-Gel Sci Techn*, **2007**, 43, 187-192, <https://doi.org/10.1007/s10971-007-1575-1>.
13. Latif, D.O., Rifa'i, A., Suryolelono, K.B., Chemical characteristics of volcanic ash in Indonesia for soil stabilization: Morphology and mineral content, *Int J GEOMATE*, **2016**, 11, 26, 2606-2610.
14. Wang, Y., Ding, X., Chen, Y., Guo, M., Zhang, Y., Guo, X., Gu, H., Antibiotic-loaded, silver core-embedded mesoporous silica nanovehicles as a synergistic antibacterial agent for the treatment of drug-resistant infections, *Biomaterials*, **2016**, 101, 207-216, <https://doi.org/10.1016/j.biomaterials.2016.06.004>.
15. Ionita, I., Dragne, A.M., Gaidau, C., Dragomir, T., Collagen fluorescence measurements on nanosilver treated leather, *Rom Rep Phys*, **2010**, 62, 3, 634-643.
16. Pollini, M., Paladani, F., Licciulli, A., Maffezzoli, A., Sannino, A., Nicolais, L., Antibacterial natural leather for application in the public transport system, *J Coat Technol Res*, **2013**, 10, 2, 239-245, <https://doi.org/10.1007/s11998-012-9439-1>.
17. Velmurugan, P., Lee, S.M., Cho, M., Park, J.H., Seo, S.K., Myung, H., Bang, K.S., Oh, B.T., Antibacterial activity of silver nanoparticle-coated fabric and leather against odor and skin infection causing bacteria, *Appl Microbiol Biotechnol*, **2014**, 98, 8179-8189, <https://doi.org/10.1007/s00253-014-5945-7>.
18. Velmurugan, P., Cho, M., Lee, S., Park, J., Bae, S., Oh, B., Antimicrobial fabrication of cotton

- fabric and leather using green-synthesized nanosilver, *Carbohydr Polym*, **2014**, 106, 319-325, <https://doi.org/10.1016/j.carbpol.2014.02.021>.
19. Liu, G., Gao, H., Li, K., Xiang, J., Lan, T., Zhang, Z., Fabrication of silver nanoparticle sponge leather with durable antibacterial property, *J Colloid Interface Sci*, **2018**, 514, 338-348, <https://doi.org/10.1016/j.jcis.2017.09.049>.
20. Sudjarwo, W.A.A., Bee, M.M.F., Synthesis of silica gel from waste glass bottles and its application for the reduction of Free Fatty Acid (FFA) on waste cooking oil, AIP Conference, **2017**, 1855, 020019, <https://doi.org/10.1063/1.4985464>.
21. Fernandes, I.P., Amaral, J.S., Pinto, V., Ferreira, M.J., Barreiroa, M.F., Development of chitosan-based antimicrobial leather coatings, *Carbohydr Polym*, **2013**, 98, 1229–1235, <https://doi.org/10.1016/j.carbpol.2013.07.030>
22. Kasim, A., Novia, D., Mutiar, S., Pinem, J., Characterization of goat skin on preparation of leather tanned with gambir and properties of leather, *Majalah Kulit, Karet dan Plastik*, **2013**, 29, 1, 01-12, <http://dx.doi.org/10.20543/mkkp.v29i1.213>.
23. Ramalingam, S., Sreeram, K.J., Rao, J.R., Nair, B.U., Organic Nano-colourants: A self-fixed, optothermal resistive silica supported dyes for sustainable dyeing of leather, *ACS Sustain Chem Eng*, **2016**, 4, 5, 2706-2714, <https://doi.org/10.1021/acssuschemeng.6b00218>.
24. Lu, Z., Xiao, J., Wang, Y., Meng, M., In situ synthesis of silver nanoparticles uniformly distributed on polydopamine-coated silk fibers for antibacterial application, *J Colloid Interface Sci*, **2015**, 452, 8-14, <https://doi.org/10.1016/j.jcis.2015.04.015>.
25. Zahran, M.K., Ahmed, H.B., El-Rafie, M.H., Surface modification of cotton fabrics for antibacterial application by coating with AgNPs-alginate composite, *Carbohydr Polym*, **2014**, 108, 145-152, <https://doi.org/10.1016/j.carbpol.2014.03.005>.
26. Pan, H., Li, G.L., Liu, R.Q., Wang, S.X., Wang, X.D., Preparation, characterization and application of dispersible and spherical nano-SiO₂@copolymer nanocomposite in leather tanning, *Appl Surf Sci*, **2017**, 426, 376-385, <https://doi.org/10.1016/j.apsusc.2017.07.106>.
27. Nuryono, N., Rosiati, N.M., Rusdiarso, B., Sakti, S.C.W., Tanaka, S., Coating of magnetite with mercapto modified rice hull ash silica in a one-pot process, *SpringerPlus*, **2014**, 3, 515, 1-12, <https://doi.org/10.1186/2193-1801-3-515>.
28. Latif, D.O., Rifa'i, A., Suryolelono, K.B., Chemical characteristics of volcanic ash in Indonesia for soil stabilization: Morphology and mineral content, *Int J GEOMATE*, **2016**, 11, 26, 2606-2610.
29. Djobo, Y.J.N., Elimbi, A., Dika Manga, J., Djon Li Ndjock, I.B., Partial replacement of volcanic ash by bauxite and calcined oyster shell in the synthesis of volcanic ash-based geopolymers, *Constr Build Mater*, **2016**, 113, 673-681, <https://doi.org/10.1016/j.conbuildmat.2016.03.104>.
30. Nuryono, Rosiati, N.M., Rettob, A.L., Suyanta, Arryanto, Y., Coating of 2-aminobenzimidazole and 1-(o-tolyl)biguanide functionalized silicas on iron sand magnetic material for sorption of [AuCl₄]⁻, *Indones J Chem*, **2019**, 19, 2, 395-404, <https://doi.org/10.22146/ijc.34653>.
31. Chupin, L., Motillon, C., Charrier-El-Bouhtoury, F., Pizzi, A., Charrier, B., Characterisation of maritime, pine (*Pinus pinaster*) bark tannins extracted under different conditions by spectroscopic methods FTIR and HPLC, *Ind Crops Prod*, **2013**, 49, 897-903, <https://doi.org/10.1016/j.indcrop.2013.06.045>.
32. Sahu, S., Sahu, U.K., Patel, R.K., Modified thorium oxide polyanilie core-shell nanocomposite and its application for the efficient removal of Cr(VI), *J Chem Eng Data*, **2019**, 64, 3, 1294-1304, <https://doi.org/10.1021/acs.jced.8b01225>.
33. Wu, J., Liao, W., Zhang, J., Chen, W., Thermal behavior of collagen crosslinked with tannic acid under microwave heating, *J Therm Anal Calorim*, **2019**, 135, 2329-2335, <https://doi.org/10.1007/s10973-018-7341-5>.
34. Yousef, S., Eimontas, J., Strūgas, N., Tatariants, M., Abdelnaby, M.A., Tuckute, S., Kliucininkas, L., A sustainable bioenergy conversion strategy for textile waste with self-catalysts using mini-pyrolysis plant, *Energy Convers Manag*, **2019**, 196, 688-704, <https://doi.org/10.1016/j.enconman.2019.06.050>.
35. Butkus, M.A., Edling, L., Labare, M.P., The efficacy of silver as a bactericidal agent:

- advantages, limitations and considerations for future use, *J Water Supply Res T*, **2003**, 52, 407–416, <https://doi.org/10.2166/aqua.2003.0037>.
36. Feng, Q.L., Wu, J., Chen, G.Q., Cui, F.Z., Kim, T.N., Kim, J.O., A mechanistic study of the antibacterial effect of silver ions on *Escherichia coli* and *Staphylococcus aureus*, *J Biomed Mater Res*, **2000**, 52, 4, 662–668, [https://doi.org/10.1002/1097-4636\(20001215\)52:4<662::AID-JBM10>3.0.CO;2-3](https://doi.org/10.1002/1097-4636(20001215)52:4<662::AID-JBM10>3.0.CO;2-3).
37. Kim, J.S., Kuk, E., Yu, K.N., Kim, J.H., Park, S.J., Lee, H.J., Kim, S.H., Park, Y.K., Park, Y.H., Hwang, C.Y., Kim, Y.K., Lee, Y.S., Jeong, D.H., Cho, M.H., Antimicrobial effects of silver nanoparticles, *Nanomed Nanotechnol*, **2007**, 3, 1, 95–101, <https://doi.org/10.1016/j.nano.2006.12.001>.
38. Pal, S., Tak, Y.K., Song, J.M., Does the antibacterial activity of silver nanoparticles depend on the shape of the nanoparticle? A study of the Gram-negative bacterium *Escherichia coli*, *Appl Environ Microbiol*, **2007**, 73, 1712–1720, <https://doi.org/10.1128/AEM.02218-06>.

© 2020 by the author(s). Published by INCDTP-ICPI, Bucharest, RO. This is an open access article distributed under the terms and conditions of the Creative Commons Attribution license (<http://creativecommons.org/licenses/by/4.0/>).

DEVELOPMENT OF A DEGREASING PROCESS FOR PAICHE SKINS (*Arapaima gigas*) FOR TANNING PRESERVING THE NATURAL PATTERN AND COLOR

Abdón SEGUNDO ESPADA, Liliana MARRUFO SALDAÑA*, Julio BARRA HINOJOSA, Rosa CONTRERAS PANIZO

Productive Innovation and Technological Transfer Center of Leather, Footwear and related industries (CITEccal Lima), Technological Institute of Production (ITP), Caquetá Ave. 1300, Rímac, 15094, Lima, Perú, aseguardo@itp.gob.pe, lmarrufo@itp.gob.pe, julio.barra.h@uni.pe, rcontreras@itp.gob.pe

Received: 28.11.2019

Accepted: 29.04.2020

<https://doi.org/10.24264/lfj.20.2.3>

DEVELOPMENT OF A DEGREASING PROCESS FOR PAICHE SKINS (*Arapaima gigas*) FOR TANNING PRESERVING THE NATURAL PATTERN AND COLOR

ABSTRACT. The utilization of Amazonian fish skins, like paiche, to obtain leather, has been gaining importance in Peru. The beauty of the pattern of this fish skin comes from its light beige color and the black strip that runs through its back. This research aimed to develop a degreasing process for the tanning of paiche skin, that allows to preserve its natural pattern and color in the finished leather. For this purpose, a mixture of degreasers, diesel oil, lipases, and surfactants was used. In tanned skins, physical-mechanical properties, such as tear strength, tensile strength, elongation percentage, and shrinkage temperature, were evaluated. The presence of fishy smell in tanned paiche skins was evaluated through an analysis of fat content, fatty acid profiles, and sensorial tests. Besides, wastewater of the process was characterized to determine BOD₅, COD, TSS, oils, and greases, TPH, phenols, and pH. This wastewater was treated by a laboratory-scale system, based on sedimentation, sifting, and flocculation-coagulation. As a result, a degreasing process using 8% of diesel oil, 18% of surfactants and 1.2% of lipidic enzymes, applied in cycles before and after the pickling process, was established. This process allowed the conservation of pattern and color of skin and the reduction of polyunsaturated fatty acids that cause the fishy smell in the leather, which complied with physical-mechanical standards for making footwear, bags, and clothing. Thus, a reduction in the pollutant charge in wastewater was achieved to acceptable environmental levels.

KEY WORDS: paiche, *Arapaima gigas*, fishskin, tanning process, degreasing

DEZVOLTAREA UNUI PROCES DE DEGRESARE PENTRU TĂBĂCIREA PIELII DE PEŞTE PAICHE (*Arapaima gigas*) PĂSTRÂND MODELUL ŞI CULOAREA NATURALE ALE ACESTEIA

REZUMAT. Utilizarea pieilor de pești amazonieni, cum ar fi cea a peștelui paiche, pentru a obține piele finită, este o activitate care a căpătat importanță în ultimii ani în Perú. Frumusețea modelului pielii acestui pește este dată de culoarea sa bej deschis și de dunga neagră care îi străbate spatele. Această cercetare și-a propus să dezvolte un proces de degresare pentru tăbăcirea pielii de pește paiche, care să permită păstrarea modelului și a colorii naturale în pielea finisată. În acest scop, s-a utilizat un amestec de agenți de degresare, motorină, lipaze și agenți tensioactivi. S-au evaluat proprietățile fizico-mecanice ale pieilor tăbăcite, cum ar fi rezistența la sfâșiere, rezistența la rupere, procentul de alungire și temperatura de contracție. Prezența miroslui caracteristic al pieilor de pește paiche tăbăcite a fost evaluată prin analiza conținutului de grăsimi, a profilurilor acizilor grași și prin teste senzoriale. Pe de altă parte, apa uzată a fost caracterizată pentru a determina CBO₅, CCO, totalul materiilor solide în suspensie, uleiuri și grăsimi, totalul hidrocarburilor din petrol, fenoli și pH. Aceste ape uzate au fost tratate printr-un sistem de laborator, bazat pe sedimentare, cernere și floculare-coagulare. Drept urmare, s-a stabilit un proces de degresare folosind 8% hidrocarburi, 18% surfațanți și 1,2% enzime lipidice, aplicate în cicluri înainte și după procesul de piclare. Acest proces a permis conservarea modelului și a colorii pielii și reducerea acizilor grași polinesaturați care provoacă miroslul caracteristic al pielii de pește, respectând standardele fizico-mecanice pentru confecționarea încălțăminte, gențiilor și îmbrăcămintei. Astfel, s-a obținut reducerea poluanților din apele uzate la niveluri acceptabile.

CUVINTE CHEIE: paiche, *Arapaima gigas*, piele de pește, proces de tăbăcire, degresare

DÉVELOPPEMENT D'UN PROCÉDÉ DE DÉGRAISSEMENT DES PEAUX DE PAICHE (*Arapaima gigas*) POUR LE TANNAGE, EN PRÉSERVANT LE MOTIF ET LA COULEUR NATURELS

RÉSUMÉ. L'utilisation de peaux de poisson amazoniennes, telles que la paiche, pour obtenir du cuir, est une activité qui a pris de l'importance ces dernières années au Pérou. La beauté du motif de peau de ce poisson est donnée par sa couleur beige clair et par la bande noire qui traverse son dos. Cette recherche vise à développer un procédé de dégraissage pour le tannage de la peau des poissons paiche, qui permet de conserver le motif et la couleur naturels du cuir fini. À cette fin, un mélange de dégraissants, d'hydrocarbures, de lipases et de tensioactifs a été utilisé. On a évalué les propriétés physico-mécaniques du cuir fini, telles que la résistance à la déchirure, la résistance à la traction, le pourcentage d'allongement et la température de retrait. La présence d'une odeur de poisson caractéristique dans les peaux de paiche tannées a été évaluée par une analyse de la teneur en matière grasse, des profils d'acides gras et des tests sensoriels. D'autre part, les eaux usées du procédé ont été caractérisées pour déterminer la DBO₅, la DCO, le TSS, les huiles et les graisses, la TPH, les phénols et le pH. Ces eaux usées ont été traitées par un système de laboratoire basé sur la sédimentation, le tamisage et la flocculation-coagulation. En conséquence, un processus de dégraissage utilisant 8% d'hydrocarbures, 18% de tensioactifs et 1,2% d'enzymes lipidiques, appliqué par cycles avant et après le processus de picklage, a été mis en place. Ce processus a permis de conserver le motif et la couleur de la peau et de réduire les acides gras polyinsaturés responsables de l'odeur caractéristique du cuir de poisson, conformément aux normes physico-mécaniques applicables à la fabrication de chaussures, de sacs et de vêtements. Ainsi, une réduction de la charge polluante dans les eaux usées a été atteinte à des niveaux environnementaux acceptables.

MOTS CLÉS : paiche, *Arapaima gigas*, peau de poisson, procédé de tannage, dégraissage

* Correspondence to: Liliana MARRUFO SALDAÑA and Julio BARRA HINOJOSA, Productive Innovation and Technological Transfer Center of Leather, Footwear and related industries (CITEccal Lima), Technological Institute of Production (ITP), Caquetá Ave. 1300, Rímac, 15094, Lima, Perú, lmarrufo@itp.gob.pe, julio.barra.h@uni.pe.

INTRODUCTION

Paiche is an Amazonian fish species whose nutritional properties make it an important source of food [1, 2] with projections for the international market that has gained popularity in Peru. Its richness, however, lies not only in its meat but also in the waste generated from its use, from which, for example, scales with a high protein and mineral content can be obtained. The skin containing a peculiar pattern and color gives natural beauty and when tanned, items of clothing can be made with a high value.

The specialized report of PROMPERU stated that approximately 1227 tons of paiche were obtained from aquaculture and capture activities in 2015 [3], resulting in the production of around 400 tons of skin that could have a by-product such as leather. It is true that significant efforts have been made in Peru to highlight the skin properties of this species as leather. There is a great deal of potential to exploit this commodity, which will make to add value to the aquaculture sector, resulting in major projects focused on the manufacturing of tanned fish skin that should be targeted to markets with high fashion standards, sophistication, and valuation of biodiversity.

Using paiche skins for tanning implies the development of a process adapted to the characteristics of this skin. The presence of high-fat content in the tanned skins can cause yellowing and the appearance of an unpleasant fishy smell. In contrast, preserving the natural color and pattern, comprising a light beige color and a black strip that crosses the back, means avoiding the use of materials that can either alter or deteriorate it, as happens in the case of conventional degreasing. The objective of this research was to develop a degreasing process based on diesel oil, enzymes, and surfactants that would allow a tanned skin with adequate physical, mechanical and sensory characteristics and particularly an imperceptible fishy smell to be obtained without deteriorating the natural color and pattern of the species. The development of this process also included the characterization of the effluents produced and treating them on a laboratory scale.

EXPERIMENTAL

Materials and Methods

The present research was developed in the tanning pilot plant of CITEccal Lima. The tanned paiche skins came from the aquaculture activity taking place in the region of Ucayali. To avoid microbiological degradation of the collagenic structure, it was recommended that once removed from the meat, they should be preserved immediately in a container containing brine at 20° Baumé until the end of the fillet day. Afterward, they were scaled and treated with salt at 30% w/w on both sides, putting one skin above the other, allowing them to drain for 12 hours and freezing them until they are processed.

Leather Processing

Before starting the tanning process, the skins were conditioned by fleshing that allowed the removal of meat and fat adhered to the skin. Commercial chemicals were used in leather process: Wetting agent (UD-800), bactericide (Tensocide 85), probiotics (Prosoak™), degreasing surfactant (Cletapon FU-100), formaldehyde, lipid enzyme (Degreasing enzyme 7707), diesel oil (Diesel B5), emulsifier (Garapon HE), salt, organic acid (Unictan TC-400), sodium bicarbonate, glutaraldehyde (GT-50), phenolic retanning agent (Floretan SF-Extra), fungicide (Tensocide EB), neutralizing agent (Trupotan NL), fatliquoring agent (Fospholicker 6146L), resin (Krotan DC), synthetic tanning agent (Blancotan W), filler (Filler FJ), mix of protein binder and wax (LA 5269), penetrating agent (PT Penetrante), urethane resin (PUR 3365) and mix of protein binder and polishing wax (LVH67).

The tanning process started with a two-phase soaking, process that allowed the skins to return to their natural swelling state while removing dirt, soluble protein substances and preservatives [4-6]. In the pre-soaking phase, room temperature water, wetting agent, bactericide, formaldehyde, and degreasing surfactant were used. Following, in the main soaking, besides the products used in the pre-soaking, lipid enzymes were added, then, skins were washed and drained.

To establish the optimal degreasing process, tests were carried out with mixtures of diesel oil, probiotics, degreasing surfactants,

and lipid enzymes, according to the formulations listed in Table 1 (all weights were measured in w/w) [5-8].

Table 1: Degreasing processes evaluated in the tanning of paiche skins

Test code	Process	Product	Amount (%)	Temp. (°C)	Duration (min)
A	Degreasing	Diesel oil	5	28	130
		Probiotics	3		
	Tanning	Glutaraldehyde	2.25	28	440
		Phenol-sulphonic syntan	7.5		
B	Degreasing	Diesel oil	5	28	100
		Degreasing surfactant	3		
		Lipid enzyme	0.1		
	Tanning	Glutaraldehyde	3	28	360
		Phenol-sulphonic syntan	10		
C	Degreasing	Diesel oil	4		290
		Degreasing surfactant	15	28	
		Lipid enzyme	1		
		Emulsifier	0.7		
	Resting	2 weeks			
		Degreasing surfactant	4.5	28	275
	Degreasing after pickling	Lipid enzyme	0.2		
		Wetting surfactant	0.2		
		Glutaraldehyde	2.25	28	390
	Tanning	Phenol-sulphonic syntan	7.5		
D	Degreasing	Diesel oil	4		290
		Degreasing surfactant	15	28	
		Lipid enzyme	1		
		Emulsifier	0.7		
	Resting	1 week			
		Degreasing surfactant	4.5	28	280
	Degreasing after pickling	Lipid enzyme	0.2		
		Wetting surfactant	0.2		
		Glutaraldehyde	2.25	28	390
	Tanning	Phenol-sulphonic syntan	7.5		

	Degreasing	Diesel oil	6	28	380
		Degreasing surfactant	18		
		Lipid enzyme	1.2		
		Emulsifier	2.3		
		Humectant	3		
CP-6	Resting	1 week			
		Degreasing surfactant	6	28	295
	Degreasing after pickling	Lipid enzyme	0.4		
		Emulsifier	0.4		
		Humectant	2		
	Tanning	Glutaraldehyde	2.5	28	390
		Phenol-sulphonic syntan	7.5		
CP-8	Degreasing	Diesel oil	8	28	380
		Degreasing surfactant	18		
		Lipid enzyme	1.2		
		Emulsifier	2.3		
		Humectant	3		
	Resting	1 week			
CP-F		Degreasing surfactant	6	28	295
	Degreasing after pickling	Lipid enzyme	0.4		
		Emulsifier	0.4		
		Humectant	2		
	Tanning	Glutaraldehyde	2.5	28	390
		Phenol-sulphonic syntan	7.5		
CP-F	Degreasing	Diesel oil	8	28	380
		Degreasing surfactant	18		
		Lipid enzyme	1.2		
		Emulsifier	2.3		
		Humectant	3		
	Resting	1 week			
CP-F		Degreasing surfactant	3	28	115
	Degreasing after pickling	Lipid enzyme	0.3		
		Emulsifier	0.2		
	Tanning	Glutaraldehyde	2.5	28	390
		Phenol-sulphonic syntan	7.5		

The degreasing and tanning processes were the only ones to suffer modifications, that is why they need a more detailed explanation as presented in Table 1. The processes A, B, C and D were developed first, to explore and adjust the characteristics of the degreasing of paiche skins, and processes CP-6, CP-8 and CP-F were carried out to improve the degreasing process.

In the case of the pickling process, it took place after degreasing in two phases, the first one consisted in adding a salt solution, and in the second, acidification by adding two parts of organic acid (1% per part), until the pH of the skins reached the value 3.

A degreasing after pickling process was done, starting with the skin depickling with brine and basification with two parts of 0.5% sodium bicarbonate. Then degreasing was performed as presented in Table 1. Subsequently, the pickling process described above was repeated, leaving the skins prepared for tanning, a process where glutaraldehyde and phenol-sulphonic syntan compounds were applied as tanning agents. The shrinkage temperature of the tanned hides, determined by the NTP 291.036:2007 method, indicated a shrinkage of not over 5% at a temperature between 70 and 75°C, maintaining a pH between 4 and 4.2.

The skins thus obtained were washed and neutralized, then were fatliquored with a fatliquoring agent and a mixture of retanning agents. The leathers were smoothed, dried and softened before finishing, which consisted in adding a mixture of penetrating protein binders, waxes for polishing and urethane resin by spraying [5, 9].

Evaluation of Fat Removal

Fat removal in tanned leather was quantified by determining the fat content in raw and tanned leather using the method NTP 201.016 2002 (Rev 2017) MEAT AND MEAT PRODUCTS. The fatty acids profile was characterized using the method ISO 12966. To determine the fishy smell, sensory tests were performed on tanned skins using a specified attribute grade test carried out by a panel of experts, specialized in the chemical analysis of leather samples from the CITEccal Lima Laboratory. Each expert was assigned nine test pieces per sample. Negative control was included in the specimens submitted

for a test of tanned paiche skin with tannins without a fishy smell. The specimen showing the attribute to be tested was a tanned paiche skin with a highly perceptible fishy smell. The samples were randomly assigned to the analysts and their analysis was performed at least one month after their tanning process. It should be noted here that the analysts were blindfolded to avoid associating the color of the sample pieces with the degree of smell. The qualification criteria used in the sensory test were Imperceptible (1), Slightly perceptible (2), Moderately perceptible (3) and Highly perceptible (4).

For each expert, statistical analysis of the results was conducted using ANOVA analysis and multiple comparison tests (Tukey HSD/Kramer Test and Dunnett Test) at a confidence level of 95%, to establish significant differences of process samples (A, B, C, and D) with negative control and between samples. Statistical analysis was performed with the use of Real Statistics in MS Excel.

Evaluation of the Physical-Mechanical Quality of Tanned Leather

The tanned samples were tested in the laboratory of CITEccal Lima to determine their physical-mechanical properties. The tests performed are tear resistance (NTP ISO 3377-2:2008. LEATHER: Physical and mechanical tests. Determination of resistance to tearing. Part 2: Double tear), tensile strength and percentage elongation (NTP ISO 3376:2012. LEATHER: Physical and mechanical tests. Determination of tensile strength and elongation percentage) and shrinkage temperature with the method (NTP 291.036:2007. PELETERIA. Physical tests. Determination of shrinkage temperature).

Effluent Characterization and Treatment

The tanning system effluents are defined by the parameters established by Supreme Decree No. 003-2002-PRODUCE, analyzing the content of Total Suspended Solids (TSS) (SMEWW-APHA-AWWA-WEF Part 2540-D; 23rd Ed: 2017. Total Suspended Solids dried at 103-105°C), oils and fat content (ASTM D3921 - 96 (Reapproved 2011). Standard Test Method for oil and Grease and Petroleum Hydrocarbons in Water (Validated) 2014), Biochemical Oxygen Demand (BOD5) (SMEWW-APHA-AWWA-WEF Part 5210 B; 23rd

Ed:2017). Biochemical Oxygen Demand (BOD): 5-day BOD test), Chemical Oxygen Demand (COD) (SMEWW-APHA-AWWA-WEF Part 5220 D; 23rd Ed:2017. Chemical Oxygen Demand, Closed Reflux. Colorimetric Method) and potential of hydrogen (pH) (SMEWW-APHA-AWWA-WEF Part 4500-H+-B; 23rd Ed: 2017. pH Value: Electrometric Method.), likewise, the content of phenols was evaluated (EPA Method 420.2:1974 Phenolics-Colorimetric, Automated 4-AAP With Distillation//EPA Method 420.4 Rev. 01.1993 Determination of Total Recoverable Phenolics By Semi-Automated Colorimetry. Validity 2013) and Total Petroleum Hydrocarbons (TPH) (EPA Method 8015C Rev.3: 2007. Naphthalogenated Organics by Gas Chromatography).

The global effluent of the process, constituted by the contribution of the subprocesses, was submitted to a treatment based on the principles of sedimentation, liquid-solid separation (sieving) and coagulation-flocculation, at laboratory scale for the reduction of the contaminant load. The procedure was carried out as follows: first, the grease was separated from the effluent by means of a decantation pear, leaving it to rest for 30

minutes, and then the solids were filtered with a Tyler mesh N° 200 (74 µm). Once the sample was filtered, it was diluted to a ratio of 1:9 with tap water. Next, a 10% ferric sulfate solution was prepared as a coagulant and Arisfloc 606 at 0.1% as a flocculant. The operating conditions are as follows: stirring speed = 200 rpm, stirring time = 5 minutes/flocculation: stirring speed = 40 rpm, and stirring time = 10 minutes. Post-treatment sedimentation time was 10 minutes, after which samples were taken and preserved for analysis of TSS, oils and fats, BOD5, COD, pH, phenols, and TPH. The effluent samples were analyzed in an accredited Laboratory under the requirements of ISO 17025.

RESULTS AND DISCUSSIONS

Table 2 presents the results obtained in the determination of fat and the percentage concentration of fatty acids. The data shows that paiche skins have high-fat content, approximately 45% which is higher than those of sheep with values 30%-40% [10]. Other species, for example, cattle (2-4%) and goats (12-15%) have relatively lower fat concentration [11].

Table 2: Results of characterization of fatty acid types in raw and tanned skin

Types of fatty acids	Paiche skin crude	Types of fatty acids expressed as %	
		Tanned paiche leather - Sample D	Tanned paiche leather - Sample CP-6
Saturated fatty acids	20.53	6.38	--
Monounsaturated fatty acids	11.63	3.30	--
Polyunsaturated fatty acids	7.65	0.54	--
Fat percentage	45.00	11.30	11.00

The removal of fats for the tanning of conventional hides is done during pre-tanning operations, including unhairing using alkaline substances [4, 12]. In the case of fish skins, the use of sulphides and alkalis leads to the removal of scales and pigments from the skins [13, 14], for this reason, in the present research this procedure was removed, as the aim of this project is to preserve the natural color and pattern of paiche skin, so degreasing process was done after soaking.

The difficulty in the degreasing process is that most of the natural fat is available in

the dermis and is contained within fat cells, whose walls consist of a protoplasmic envelope inverted in reticular tissue. Hence, degreasing involves the release of fat from cell confinement and for this, it is necessary to achieve the diffusion of degreasers in the skin that has a three-dimensional tissue of collagen fibers. The diffusion includes transport of degreasing chemicals into the skin, emulsification of fat and the removal of emulsified fat [15]. One of the most effective ways used for fat removal in the tanning industry is the degreasing process using organic solvents, emulsifiers and/or a

mixture of them [11, 15]. The organic solvents used are kerosene [15], petroleum, diesel oil, trichloroethylene, and perchloroethylene [16]. An alternative to these materials, developed in recent years, is the use of enzymes, that are used for soaking, liming, deliming, degreasing and bating [16]. Protease and lipase are the main enzymes commercialized, making possible to decrease the amount of organic solvents and emulsifiers in the effluents, contributing to the efficiency of the degreasing process.

It is important to point out that a process of yellowing occurs when fats are not removed sufficiently, it is produced because of the oxidation of polyunsaturated fatty acids, which have two or more double bonds that are easily oxidized and converted to hydroperoxides, this process is produced by heat, light and humidity, and is favoured by the action of bacterial degradation [17, 18], responsible of giving off the fishy smell [19, 20]. The results of the tests A and B presented good characteristics in tanned leather, nevertheless, after some days of finished the process, yellowing and giving off of fishy smell was observed in the tanned leather obtained in these processes, which meant that fats had not been removed enough. Thus, it was discarded to continue researching on the application of probiotics, as the defects presented by the skins implied the use of a larger quantity of this product, which increased the cost of the scaling process.

So, processes C and D were developed considering the emanation and oxidation of fats observed after tanning, that is why in these processes was considered a resting time after pickling, thought to evaluate the emanation of fats, in order to remove them in a second degreasing. Test C consider two weeks of resting time, and D, one week, because of the great emanation and oxidation of fat observed during resting time in process C, so results in process D seemed to be better, as finished leather does not show a significantly yellowing or fishy smell, these results were proved with fat analysis and odour tests. As result, the percentage of fats in tanned leather from process D decreased significantly compared to raw leather, establishing a fat content of 11.3%. The recommended fat level for leather according to G. John (1997) is in the range of 4-10%. Table 2 lists the percentage

of polyunsaturated fatty acids as 7.65%. The removal of fat using degreasing formula D resulted in a tanned skin with a concentration of polyunsaturated fatty acids of 0.54%.

The detail analyses of the sensory odour test are listed in Tables 3, 4 and 5 while Figures 1, 2 and 3 present the graphical representation of the data. It is observed that Judge 1 established significant differences between the negative control and the samples A and B. Comparing samples from tests A and B, both with mode 4 (highly perceptible) as calification, correspond to the tanned samples that presented high yellowing, the negative control, with calification 2 (slightly perceptible), is a sample without fishy smell coming from a vegetable tanning. Sample C does not present significant differences with the negative control after almost three months have elapsed since its tanning. Sample D (assayed after one month of tanning) presents significant differences with respect to others, its valuation being 1, imperceptible, establishing significant differences regarding the negative control and the C sample. Regarding Judge 2, statistical analysis indicates that there are significant differences between the A, B, and negative control samples. The statistical mode for each of them was 3, 4 and 1, respectively. Sample C with mode 2 and sample D with mode 1, do not present significant differences with respect to the negative control, however, sample D and sample C present significant differences between them. Statistical analysis for Judge 3 indicates that samples A, B, C, D present modes 4, 4, 3 and 1 respectively, which differ significantly from the negative control presented by mode 2. Samples A and B are significantly different from sample C and this is statistically different from sample D.

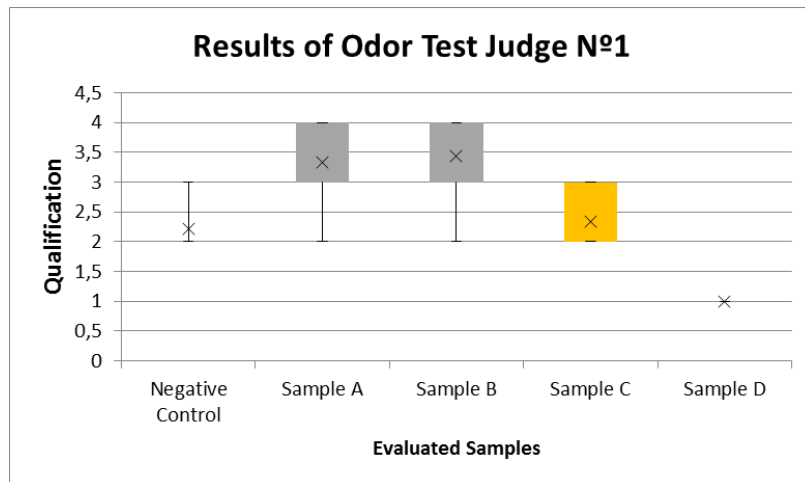


Figure 1. Results obtained by Judge 1 in the odour sensory test

Table 3: Analysis of the results obtained by Judge 1 Test Tukey HSD/Kramer

TUKEY HSD/KRAMER		alpha		0.05		q-crit			
group	me	n	ss	df					
Negative control	2.2222	9	1.5556						
Sample A	3.3333	9	6.0000						
Sample B	3.4444	9	4.2222						
Sample C	2.3333	9	2.0000						
Sample D	1.0000	9	0.0000						
		45	13.7778	40		4.039			
Q TEST									
group 1	group 2	me	std err	q-stat	lower	upper	p-value	mean-crit	Cohen d
Negative control	Sample A	1.1111	0.1956	5.6796	0.3210	1.9013	0.0022	0.7902	1.8932
Negative control	Sample B	1.2222	0.1956	6.2476	0.4321	2.0124	0.0007	0.7902	2.0825
Negative control	Sample C	0.1111	0.1956	0.5680	-0.6790	0.9013	0.9943	0.7902	0.1893
Negative control	Sample D	1.2222	0.1956	6.2476	0.4321	2.0124	0.0007	0.7902	2.0825
Sample A	Sample B	0.1111	0.1956	0.5680	-0.6790	0.9013	0.9943	0.7902	0.1893
Sample A	Sample C	1.0000	0.1956	5.1117	0.2098	1.7902	0.0070	0.7902	1.7039
Sample A	Sample D	2.3333	0.1956	11.9272	1.5432	3.1235	0.0000	0.7902	3.9757
Sample B	Sample C	1.1111	0.1956	5.6796	0.3210	1.9013	0.0022	0.7902	1.8932
Sample B	Sample D	2.4444	0.1956	12.4952	1.6543	3.2346	0.0000	0.7902	4.1651
Sample C	Sample D	1.3333	0.1956	6.8155	0.5432	2.1235	0.0002	0.7902	2.2718

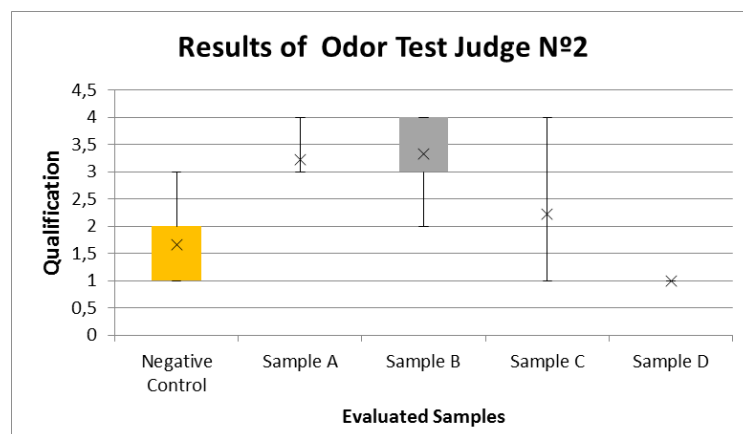


Figure 2. Results obtained by Judge 2 in the odour sensory test

Table 4: Analysis of the results obtained by Judge N°2 Test Tukey HSD/Kramer

TUKEY HSD/KRAMER		alpha		0.05		q-crit
group	me	n	ss	df		
Negative control	1.6667	9	6.0000			
Sample A	3.2222	9	1.5556			
Sample B	3.3333	9	6.0000			
Sample C	2.2222	9	5.5556			
Sample D	1.0000	9	0.0000			
		45	19.1111	40		4.039

Q TEST

group 1	group 2	me	std err	q-stat	lower	upper	p-value	mean-crit	Cohen d
Negative control	Sample A	1.5556	0.2304	6.7514	0.6250	2.4862	0.0002	0.9306	2.2505
Negative control	Sample B	1.6667	0.2304	7.2336	0.7361	2.5973	0.0001	0.9306	2.4112
Negative control	Sample C	0.5556	0.2304	2.4112	-0.3750	1.4862	0.4425	0.9306	0.8037
Negative control	Sample D	0.6667	0.2304	2.8935	-0.2639	1.5973	0.2635	0.9306	0.9645
Sample A	Sample B	0.1111	0.2304	0.4822	-0.8195	1.0417	0.9970	0.9306	0.1607
Sample A	Sample C	1.0000	0.2304	4.3402	0.0694	1.9306	0.0298	0.9306	1.4467
Sample A	Sample D	2.2222	0.2304	9.6449	1.2916	3.1528	0.0000	0.9306	3.2150
Sample B	Sample C	1.1111	0.2304	4.8224	0.1805	2.0417	0.0123	0.9306	1.6075
Sample B	Sample D	2.3333	0.2304	10.1271	1.4027	3.2639	0.0000	0.9306	3.3757
Sample C	Sample D	1.2222	0.2304	5.3047	0.2916	2.1528	0.0048	0.9306	1.7682

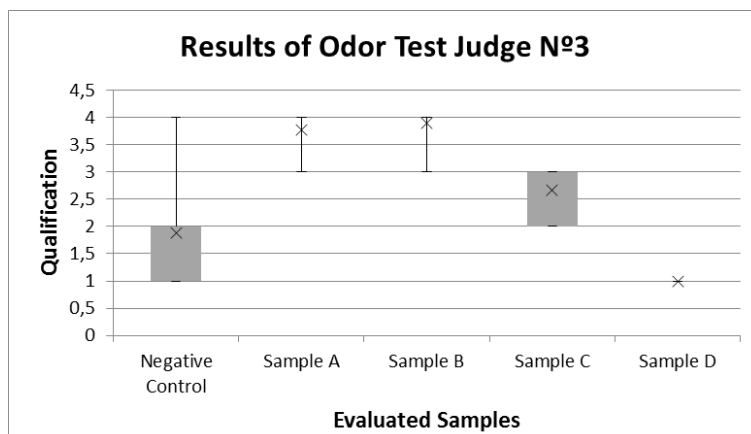


Figure 3. Results obtained by Judge 3 in the odour sensory test

Table 5: Analysis of the results obtained by Judge 3 Test Tukey HSD/Kramer

TUKEY HSD/KRAMER		alpha		0.05		q-crit
group	me	n	ss	df		
Negative control	1.8889	9	6.8889			
Sample A	3.7778	9	1.5556			
Sample B	3.8889	9	0.8889			
Sample C	2.6667	9	2.0000			
Sample D	1.0000	9	0.0000			
		45	11.3333	40		4.039

Q TEST

group 1	group 2	me	std err	q-stat	lower	upper	p-value	mean-crit	Cohen d
Negative control	Sample A	1.8889	0.1774	10.6458	1.1722	2.6055	0.0000	0.7166	3.5486
Negative control	Sample B	2.0000	0.1774	11.2720	1.2834	2.7166	0.0000	0.7166	3.7573
Negative control	Sample C	0.7778	0.1774	4.3836	0.0611	1.4944	0.0276	0.7166	1.4612
Negative control	Sample D	0.8889	0.1774	5.0098	0.1722	1.6055	0.0086	0.7166	1.6699
Sample A	Sample B	0.1111	0.1774	0.6262	-0.6055	0.8278	0.9917	0.7166	0.2087

Sample A	Sample C	1.1111	0.1774	6.2622	0.3945	1.8278	0.0007	0.7166	2.0874
Sample A	Sample D	2.7778	0.1774	15.6556	2.0611	3.4944	0.0000	0.7166	5.2185
Sample B	Sample C	1.2222	0.1774	6.8885	0.5056	1.9389	0.0002	0.7166	2.2962
Sample B	Sample D	2.8889	0.1774	16.2818	2.1722	3.6055	0.0000	0.7166	5.4273
Sample C	Sample D	1.6667	0.1774	9.3934	0.9500	2.3833	0.0000	0.7166	3.1311

The “imperceptible” rating given by the three judges for the sample from process D in the odour test would be supported by the decrease in the percentage of polyunsaturated fats and fatty acids achieved by the applied degreasing process. As observed in the sensory test, the three judges establish significant differences between samples C and D, which would mean that oxidation of polyunsaturated fatty acids could have originated over time in process C, making the difference in smell perceptible.

Thus, resting time was established in one week, and further processes were tested to evaluate the amount of degreasing products. Process CP-6 and CP-8 increase the amount of degreasing surfactant to 18 % (w/w), and diesel oil to 6 % and 8 % respectively (Table 2). The results obtained for fat content in CP-6 indicate that the removal is slightly higher than process D. In addition, the paiche leathers from CP-8 were lighter (absence of yellowing) compared with those obtained in previous processes, indicating a further removal of fat, so degreasing was established at 8 % (w/w).



Figure 4. Samples of skins corresponding to tanning processes A and D respectively

The results of physical-mechanical properties presented in Table 6 show the evaluation of tear resistance, tensile strength and elongation percentage for tanned leather, values are within the standards as established by the technical norms and recommendations for manufacturing of footwear and articles of clothing and leather goods. The shrinkage temperature determined for skins tanned in this research with phenolic compounds syntan sulfonic and glutaraldehyde remains within the recommended minimum values for leather (>75%) [21]. Tanning with alternative agents replacing chromium, in many cases, is not comparable to this metal because

of the weak cross-linking capacity of these substitutes [5, 22]. Researchers have reported earlier that the contraction temperatures for tanning with synthetic tanning agents such as polymerized phenols in the range of 75-85°C and glutaraldehyde in the range of 80-85°C [23]. The properties attained in tanned leather make it viable for use in the manufacture of footwear, clothing and leather goods. Figure 5 presents the prototypes elaborated with the tanned paiche skins obtained in the framework.

Table 6: Physical-mechanical characteristics of tanned paiche skins

PARAMETER	Application					Range of values obtained for paiche leather	Test Methods
	Casual Shoes ¹	Men Shoes ²	Ladies Shoes ³	Clothing ⁴	Leather goods ⁵		
Tear Resistance	Unlined: ≥ 100 N With lining: ≥ 70 N	≥ 40 N	≥ 40 N	Greater than 20 N*	Minimum 400 N/cm	147 N -187 N	NTP ISO 3377-02:2008
Tensile strength	≥ 10.0 N/mm ²	≥ 15.0 N/mm ² in splits	≥ 15.0 N/mm ² in splits	--	Minimum 2250 N/cm ²	9.79 N/mm ² /12.24 N/mm ²	NTP ISO 3376:2012
Elongation at break	≥15% (→) ≥ 7% (↑)	--	--	--	Maximum 50%.	76.40 -94.47%	NTP ISO 3376:2012
Shrinkage temperature	At least 70°C to 75°C with a shrinkage of no more than 5%.					Above 75°C: shrinkage 4%.	NTP 291.036:2007
Odour	--	--	--	--	--	Imperceptible to the fishy smell	Sensory Testing

¹ NTP 241.023:2014. SHOES. Casual footwear. Railway applications - Requirements and test methods² NTP 241.021:2015 FOOTWEAR. Men's footwear. Railway applications - Requirements and test methods³ NTP 241.022:2015 FOOTWEAR. Lady's footwear. Railway applications - Requirements and test methods⁴ NTP ISO 14931:2016. LEATHER: Guide for the selection of leather for clothing (excluding fur skins).⁵ Gerhard, J. (1996). Possible defects in leather production

*leathers with tear resistance greater than 10 N can be used as long as attention is paid to the design and construction of the garment.



Figure 5. Items made with paiche skin preserving the pattern and color

Finally, the effluents from tanning process were collected and characterized to determine its content of total suspended solids (TSS), pH, oils and fats, biological oxygen demand (BOD5), chemical oxygen demand (COD), phenols, total petroleum hydrocarbons, which are presented in Table 7. Different samples were evaluated. First, in order to compare the effectiveness of degreasing after pickling process, effluents of degreasing from process CP-8 (sample DP-8) and effluents of degreasing from a process without second degreasing (DP-F) were characterized. From the results, it was determined that sample DP-8 is more efficient removing fats than DP-F, as its results of oils and fats are higher. Besides, effluents from whole process CP-8, and treated effluents from this process were characterized. The treatment was then carried out at laboratory scale, including sedimentation,

filtration and coagulation-flocculation, achieving the removal of polluting charge at acceptable levels by national legislation for effluents from tanneries to be discharged to the sewage system, according to DS N° 002-2003-PRODUCE for TSS, pH, BOD5. The values of COD and oils and fats were exceeded by 18 mg/L and 116.3 mg/L, respectively. Although the legislation for tanning liquid effluents does not include permissible values for phenols and hydrocarbons, the results obtained were compared with maximum admissible values established by the company that manages the potable water supply for Metropolitan Lima (SEDAPAL) and with permissible limits for refinery effluents regulated in DS N° 0.37-2008 -PCMO, respectively. With phenols, the values were not exceeded although the hydrocarbons exceeded the standard by 36.5 mg/L.

Table 7: Results obtained in degreasing effluents from the tanning process and in the treated effluent

Parameter	Maximum permissible limit - sewer ¹	DP-8 ²	CP-8 ³	DP-F ⁴	Treated effluent ⁵
pH	6.0-9.0	5.30	4.19	5.70	6.11
Total suspended solids (mg/l)	500	2135.0	2500	2124	93
Oils and fats (mg/L)	50	11167.7	8318.2	9796.6	166.3
BOD5 (mg/L)	500	11270	9120	11500	358
COD (mg/L)	1500	33617	27366	25004	1519
Phenols *(mg/L)	0.5	--	5.02	--	0.21
Total petroleum hydrocarbons ** (C10-C40) (mg/L)	20	2622.1	2698.8	1571.2	56.5

¹ Supreme Decree N° 003-2002-PRODUCE - Peru

² Sample of effluent of degreasing from process CP-8.

³ Sample of effluent from whole process CP-8.

⁴ Sample of effluent of degreasing from process CP-F.

⁵ Sample of treated effluent from whole process CP-F.

* Maximum admissible values SEDAPAL

** Maximum permissible limit for refinery effluents D.S. N° 037-2008-PCMO

CONCLUSIONS

The degreasing of paiche skins for tanning, preserving color and pattern, is a process that must be controlled in such a way to avoid the yellowing of the tanned skins and the giving off of fishy smell. In this research, optimal fat removal was achieved through the use of a mixture of 8% diesel oil, 18% degreasing surfactants, and 1.2% lipid enzymes in repetitive cycles before and after pickling. The level of fat

in the tanned skins reached a concentration of 11%, a value that ensures an imperceptible level of fishy odour. The shrinkage temperature of the tanned leather and its physical-mechanical properties were within the standards established and recommended for use in the manufacture of footwear, clothing and leather goods. Based on the results obtained, it is recommended to study more about another degreasing processes using enzymes and biodegradable products, in order

to improve the removal of fat and avoid the utilization of diesel oil in the degreasing process.

The effluents from the tanning process present high levels of organic pollutants, which, although were reduced on a laboratory scale through sedimentation, sieving, and coagulation-flocculation processes could not reach the permissible limits in all the parameters of the standard for discharge of effluents to the sewage system, so the removal process must be complemented with other methods to improve it, above all, the high content of oils and fats that characterizes this process, even more so, if it is projected to be implemented in regions where the discharge of liquid effluents is made directly in water surfaces that involve much lower permissible limits. The tanning of Amazonian fish skins is an activity that should be considered as an important opportunity to value these resources; however, the skins should come from formal aquaculture activity to avoid depredating them. Also, the tanning must be scaled up including the treatment of effluents to avoid negative impacts on the environment.

Acknowledgements

We acknowledge the National Innovation Program for Competitiveness and Productivity (Innovate Perú) of the Ministry of Production of Peru for funding this research.

REFERENCES

1. Alcántara Bocanegra, F., Wust, W.H., Tello Martín, S., Rebaza Alfaro, M., Del Castillo Torres, D., Paiche el gigante del Amazonas, WUST Ediciones, **2006**, 70 p.
2. Chu Koo, F., Fernández Méndez, C., Rebaza Alfaro, C., Darias, M.J., García Dávila, C.R., García Vásquez, A. et al., El cultivo del paiche: biología, procesos productivos, tecnologías y estadísticas, Repositorio Institucional – IIAP, **2017**, 110 p, available from: <http://repositorio.iiap.gob.pe/handle/IIAP/267>.
3. PROMPERÚ. Informe Especializado Oportunidades Comerciales para el Paiche en Europa, Lima, **2017**.
4. China Leather and Footwear Industry Research Institute, Developing countries training course on eco-leather manufacture technology.
5. Krishnamoorthy, G., Sadulla, S., Sehgal, P.K., Mandal, A.B., Green chemistry approaches to leather tanning process for making chrome-free leather by unnatural amino acids, *J Hazard Mater*, **2012**, 215–216, 173–82, <https://doi.org/10.1016/j.jhazmat.2012.02.046>.
6. Fotouh, D.M.A., Bayoumi, R.A., Hassan, M.A., Production of Thermoalkaliphilic Lipase from *Geobacillus thermolevorans* DA2 and Application in Leather Industry, *Enzyme Res*, **2016**, <https://doi.org/10.1155/2016/9034364>.
7. Singhania, R.R., Patel, A.K., Thomas, L., Goswami, M., Giri, B.S., Pandey, A., Industrial enzymes, *Ind Biorefineries White Technol*, **2015**, 473–97, <https://doi.org/10.1016/B978-0-444-63453-5.00015-X>.
8. Kılıç, E., Evaluation of degreasing process with plant derived biosurfactant for leather making: An ecological approach, *Tekstil ve Konfeksiyon*, **2013**, 23, 2, 181–7.
9. Fischer, C., Izquierdo, F., Mähner, P., Drexler, J., Reetz, I., Segura, R., Fatliquoring from a viewpoint of sustainability, 31st IULTCS Congress, Valencia, **2011**.
10. Afsar, A., Cetinkaya, F., Studies on the degreasing of skin by using enzyme in liming process, *Indian J Chem Technol*, **2008**, 15, 5, 507–10.
11. Choudhary, R.B., Jana, A.K., Jha, M.K., Enzyme technology applications in leather processing, *Indian J Chem Technol*, **2004**, 11, 5, 659–71.
12. Escoto-Palacios, M.J., Pérez-Limiñana, M.Á., Arán-Ais, F., From leather waste to functional leather, **2016**, INESCOP, ISBN: 978-84-934261-9-4, 60 p.
13. Hermiyati, I.H., Syabani, M.W.S., Silvanti, F.S. Vegetable Tanning Process of Starry Trigger Fish (*Abalistes Stellaris*) and its Plotting to Leather Products, 7th International Seminar on Tropical Animal Production (ISTAP), September **2017**, 475–474.
14. Duraisamy, R., Shama, S., Berekete, A.K., A Review of Bio-tanning Materials for Processing of Fish Skin into Leather, *International Journal of Engineering Trends and Technology*, **2016**, 39, 1, 19.
15. Sivakumar, V., Chandrasekaran, F., Swaminathan, G., Rao, P.G., Towards cleaner degreasing method in industries: ultrasound-assisted aqueous degreasing

- process in leather making, *J Clean Prod*, **2009**, 17, 1, 101–4, <https://doi.org/10.1016/j.jclepro.2008.02.012>.
16. Nawaz, H.R., Solangi, B.A., Nadeem, U., Zehra, B., Zeeshan, M., Preparation and Application of Degreasing Enzyme for Leather from Indigenous Resource: A Step for Reduction of Tannery Pollutants, **2011**, Fourth International Conference Environmentally Sustainable Development, Pakistan.
17. Fujita, A., Isogai, A., Endo, M., Utsunomiya, H., Nakano, S., Iwata, H., Effects of sulfur dioxide on formation of fishy off-odor and undesirable taste in wine consumed with seafood, *J Agric Food Chem*, **2010**, 58, 7, 4414–20, <https://doi.org/10.1021/jf9041547>.
18. Sohn, J.-H., Taki, Y., Ushio, H., Kohata, T., Shioya, I., Ohshima, T., Lipid Oxidations in Ordinary and Dark Muscles of Fish: Influences on Rancid Off-odor Development and Color Darkening of Yellowtail Flesh During Ice Storage, *J Food Sci*, **2005**, 70, 7, s490–6, <https://doi.org/10.1111/j.1365-2621.2005.tb11497.x>.
19. Afşar, A., Çetinkaya, F., A research on increasing the effectiveness of degreasing process by using enzymes, *Tekstil ve Konfeksiyon*, **2008**, 18, 4, 278–83.
20. Sae-leaw, T., Benjakul, S., Fatty acid composition, lipid oxidation, and fishy odour development in seabass (*Lates calcarifer*) skin during iced storage, *Eur J Lipid Sci Technol*, **2014**, 116, 7, 885–94, <https://doi.org/10.1002/ejlt.201300381>.
21. Kuria, A., Ombui, J., Onyuka, A., Sasia, A., Kipyegon, C., Kaimenyi, Ngugi, A., Quality Evaluation of Leathers Produced by Selected Vegetable Tanning Materials from Laikipia County, Kenya, *IOSR J Agric Vet Sci Ver I*, **2016**, 9, 4, 13–17, <https://doi.org/10.9790/2380-0904011317>.
22. Valeika, V., Širvaitytė, J., Beleška, K., Estimation of chrome-free tanning method suitability in conformity with physical and chemical properties of leather, *Medziagotyra*, **2010**, 16, 4, 330–6.
23. Covington, A.D., Song, L., Suparno, O., Koon, H.E.C., Collins, M.J., Link-lock: An explanation of the chemical stabilisation of collagen, *J Soc Leather Technol Chem*, **2008**, 92, 1, 1–7.

© 2020 by the author(s). Published by INCOTP-ICPI, Bucharest, RO. This is an open access article distributed under the terms and conditions of the Creative Commons Attribution license (<http://creativecommons.org/licenses/by/4.0/>).

ANTIFUNGAL ACTIVITY OF LEATHER TREATED WITH *Anethum graveolens* AND *Melaleuca alternifolia* ESSENTIAL OILS AGAINST *Trichophyton interdigitale*

**Mariana Daniela BERECHET^{1*}, Corina CHIRILĂ¹, Demetra SIMION¹, Olga NICULESCU¹,
Maria STANCA¹, Cosmin-Andrei ALEXE¹, Ciprian CHELARU¹, Maria RÂPĂ², Dana Florentina GURĂU¹**

¹INCDTP - Division: Leather and Footwear Research Institute (ICPI), Bucharest, 031215, Romania, marianadanielaberechet@yahoo.co.uk

²Polytechnic University of Bucharest

Received: 18.10.2019

Accepted: 25.05.2020

<https://doi.org/10.24264/lfj.20.2.4>

ANTIFUNGAL ACTIVITY OF LEATHER TREATED WITH *Anethum graveolens* AND *Melaleuca alternifolia* ESSENTIAL OILS AGAINST *Trichophyton interdigitale*

ABSTRACT. *Trichophyton interdigitale* is a common fungus causing onychomycosis of the nail in humans. Plants are a rich source of bioactive compounds with antifungal properties used in various compositions in pharmaceuticals, cosmetics or various industrial products. In the present paper, the antifungal activity of two kinds of leathers was tested: ecologically processed sheepskin leather lining (Eco) and sheepskin leather lining processed with basic chromium salts (Cr), treated with *Anethum graveolens* and *Melaleuca alternifolia* essential oils. Dill (*Anethum graveolens*) essential oil rich in o-cymene (30.71%) and α-phellandrene (23.21%) and tea tree (*Melaleuca alternifolia*) essential oil rich in terpinene-4-ol (23.06%) were used. The results obtained in this study show that the essential oil of *Anethum graveolens* and *Melaleuca alternifolia* had a high antifungal effect against *Trichophyton interdigitale*. Tea tree and dill essential oils offer a much safer alternative protection against fungi as compared to synthetic compounds with adverse reactions to body and environment. The results of this study may have potential for use in developing applications for cosmetics, pharmaceuticals, obtaining leathers and textiles with selective bioproperties.

KEY WORDS: *Anethum graveolens* and *Melaleuca alternifolia* essential oil, antifungal activity, *Trichophyton interdigitale*, sheepskin leather lining

ACTIVITATEA ANTIFUNGICĂ A PIEILOR TRATATE CU ULEIURI ESENȚIALE DE *Anethum graveolens* ȘI *Melaleuca alternifolia* ÎMPOTRIVA *Trichophyton interdigitale*

REZUMAT. *Trichophyton interdigitale* este un fung comun care provoacă onicomicoza unghiei la om. Plantele sunt o sursă bogată de compuși bioactivi cu proprietăți antifunzice utilizate în diferite compozitii în produse farmaceutice, produse cosmetice sau diverse produse industriale. În lucrarea de față s-a testat activitatea antifungică pe două tipuri de piele: cătușeala din piele de oaie procesată ecologic (piele Eco) și cătușeala din piele de oaie procesată cu săruri bazice de crom (piele Cr) tratată cu uleiuri esențiale de *Anethum graveolens* și *Melaleuca alternifolia*. S-a folosit ulei esențial de mărăr (*Anethum graveolens*) bogat în o-cimol (30,71%) și α-felandren (23,21%) și ulei esențial de arbore de ceai (*Melaleuca alternifolia*) bogat în terpinen-4-ol (23,06%). Rezultatele obținute în acest studiu arată că uleiurile esențiale de *Anethum graveolens* și *Melaleuca alternifolia* au avut un efect antifungic ridicat împotriva *Trichophyton interdigitale*. Uleiurile esențiale de arbore de ceai și mărăr oferă o alternativă de protecție mult mai sigură împotriva ciupercilor, comparativ cu compuși sintetici, care prezintă reacții adverse pentru corp și mediu. Rezultatele acestui studiu pot avea potențial de utilizare în dezvoltarea aplicațiilor în produse cosmetice, farmaceutice, obținerea de piei și textile cu bioproprietăți selective.

CUVINTE CHEIE: ulei esențial de *Anethum graveolens* și *Melaleuca alternifolia*, activitate antifungică, *Trichophyton interdigitale*, piei ovine pentru cătușeli

L'ACTIVITÉ ANTIFONGIQUE DES CUIRS TRAITÉS AVEC DES HUILES ESSENTIELLES D'*Anethum graveolens* ET *Melaleuca alternifolia* CONTRE *Trichophyton interdigitale*

RÉSUMÉ. *Trichophyton interdigitale* est un champignon commun provoquant l'onychomycose des ongles chez l'homme. Les plantes sont une riche source de composés bioactifs aux propriétés antifongiques utilisés dans diverses compositions pharmaceutiques, cosmétiques ou divers produits industriels. Dans cet article, on a testé l'activité antifongique de deux types de cuirs : la doublure en cuir de mouton traitée écologiquement (Eco) et la doublure en cuir de mouton traitée avec des sels basiques de chrome (Cr), traités avec des huiles essentielles d'*Anethum graveolens* et *Melaleuca alternifolia*. L'huile essentielle d'aneth (*Anethum graveolens*) riche en o-cymène (30,71%) et α-phellandrène (23,21%) et l'huile essentielle d'arbre à thé (*Melaleuca alternifolia*) riche en terpinène-4-ol (23,06%) ont été utilisées. Les résultats obtenus dans cette étude montrent que l'huile essentielle d'*Anethum graveolens* et *Melaleuca alternifolia* ont eu un effet antifongique élevé contre *Trichophyton interdigitale*. Les huiles essentielles d'arbre à thé et d'aneth offrent une protection alternative beaucoup plus sûre contre les champignons par rapport aux composés synthétiques ayant des réactions indésirables au corps et à l'environnement. Les résultats de cette étude peuvent avoir un potentiel d'utilisation dans le développement d'applications dans les cosmétiques, les produits pharmaceutiques, l'obtention de cuirs et de textiles à propriétés biologiques sélectives.

MOTS CLÉS : huile essentielle d'*Anethum graveolens* et *Melaleuca alternifolia*, activité antifongique, *Trichophyton interdigitale*, peau de mouton pour doublures

* Correspondence to: Mariana Daniela BERECHET, INCDTP - Division: Leather and Footwear Research Institute (ICPI), Bucharest, 031215, Romania, marianadanielaberechet@yahoo.co.uk

INTRODUCTION

Plants are a rich source of bioactive compounds with antifungal properties used in various compositions in pharmaceuticals, cosmetics or various industrial products [1]. Medicinal plants have been used to treat various afflictions for thousands of years, because they are vast and diverse compositions of natural compounds that can have important selective bioproperties. The most important of these compounds are alkaloids, tannins, flavonoids, terpenoids, saponins and phenolic compounds. Researchers, pharmacists, doctors are interested in these compounds due to their bioactivity and low toxicity [2]. Many compounds were isolated from plants that could be used for the development of new compositions to inhibit growth of fungal pathogens with possibly new mechanisms of action [3]. Extensive studies have already been reported for the use of essential oils from plants as biocides in leather processing [4-9] and in the protection of footwear against the growth of microorganisms which are mainly responsible for the appearance of fungal infections on the nails [4, 10-13]. Considering the side effects of antifungal drugs obtained by chemical synthesis, remedies based on natural compounds are a safe choice for treating fungal infections. They have no side effects as have other medicines. Essential oils are a natural remedy to prevent and treat fungal infections. If used in optimal proportions, essential oils with antifungal properties are a natural way to cure fungal diseases of the foot such as athlete's foot, or treat other demanding areas of the foot [4]. The use of essential oils in biological control against fungi is mainly due to their richness in antifungal substances [14-18]. Numerous studies have established the efficacy of *Anethum graveolens* essential oil from the *Apiaceae* family [1] and *Melaleuca alternifolia* essential oil from the *Myrtaceae* family [19] against fungi [20-22]. Many members from these families are economically useful for medicines, cosmetics and various commercial uses [23]. Previous studies on the essential oils of *Apiaceae* and *Myrtaceae* have shown that these plants have a wide range of biological activities, in particular antifungal and antimicrobial potential. The chemical nature of the main ingredients was directly related to this activity [24]. Several

previous studies have focused on chemical composition and antifungal effect of *Anethum graveolens* and *Melaleuca alternifolia* essential oils. Thus, their rich content in monoterpenes, gives an antifungal, antioxidant and antimicrobial activity. These properties promise their use as a natural antifungal in various pharmaceutical, cosmetic, industrial applications [25, 26]. There is much interest to find antimicrobial and antifungal agents to treat the shoe lining leather. For example, Koizhaiganova *et al.* studied the leather treated with silver doped hydroxyapatite. Good antibacterial properties against *S. aureus*, *B. subtilis*, *E. faecalis* as Gram positive bacteria, *E. coli*, *S. typhimurium*, *K. pneumoniae* and *P. aeruginosa* as Gram negative bacteria and the yeast *C. albicans* were reported with the increasing concentration of Ag [27]. In our previous paper, we presented the antifungal and antibacterial effects of geranium, pine, and rosemary essential oils on the cotton and leather linings with good results [28]. This fungus causes onychomycosis (also known as *tinea unguium*, a fungal infection on the nail) and *tinea pedis* (skin infection on the feet causes by fungus) in humans [30-32].

The aim of this paper is to test the antifungal effect of the essential oil extracted from dill (*Anethum graveolens*) and tea tree (*Melaleuca alternifolia*) against *Trichophyton interdigitale* on sheepskin lining leather used in the production of footwear, to avoid the appearance of nail fungus or bad smell of shoes by using natural antifungal agents.

EXPERIMENTAL

Materials and Methods

Materials

Anethum graveolens essential oil (EO) was acquired from S.C. Herbavit S.R.L. Oradea, Romania. *Melaleuca alternifolia* essential oil (EO) was acquired from S.C. Solaris Plant Radix S.R.L. Bucharest, Romania and Borron SE from Triderma SRL Bucharest. Sheepskin leather lining was processed at the National Research and Development Institute for Textiles and Leather – Division: Leather and Footwear Research Institute (INCDTP-ICPI), Bucharest.

Methods

Sheepskin Lining Leather

Sheepskin lining leather obtained by ecological processing without basic chromium salts (lining leather Eco) and sheepskin lining leather obtained by processing with basic chromium salts (lining leather Cr) were used. The samples of sheepskin lining leather were treated by immersion in 200% aqueous float with 5% essential oil and 5% Borron SE, relative to the weight of the lining materials, at 25°C for 30 minutes with stirring and then free dried at 25°C.

GC-MS Analysis

Chemical composition of essential oils was determined by Gas chromatography-Mass Spectrometry (GC-MS) with Agilent 6890 N and the majority constituent compounds were identified [29].

ATR-FTIR Analysis

The chemical structures of investigated leather samples were analyzed by use of Fourier Transform Infrared Spectroscopy-Attenuated Total

Reflectance FT-IR/ATR spectrometer JASCO FT-IR 4200. The spectra were accumulated from 16 scans in a range of 4000-400 cm⁻¹ scale, with a scan speed of 2.2 KHz and a resolution of 4 cm⁻¹, single-beam, with ATR accessory with diamond sensor.

Antifungal Activity Assessment

The antifungal activity was evaluated using *Trichophyton interdigitale* fungus. Figure 1 shows the culture of 7-day-old *Trichophyton interdigitale* grown on Sabouraud dextrose agar culture medium and analyzed using an optical microscope. The tests were performed in accordance with ASTM D4576-86:2016 – Standard Test Method for Mold Growth Resistance of Wet Blue and Wet White. In each Petri dish a Dextrose Agar Sabouraud culture medium was poured. Treated samples and control samples were placed in Petri dishes in the center of the surface of the culture medium, and then the culture medium was seeded in 3 points around the sample with *Trichophyton interdigitale* fungus, as an equilateral triangle. Petri dishes were placed in thermo-hygrostat (Memmert) at the temperature of 30°C and were analyzed after 3, 7, 14 and 21 days.



Figure 1. *Trichophyton interdigitale* fungus, optical microscopy images, 40x

Optical Microscopy Investigation

Optical microscopy images were captured using a Leica stereomicroscope S8APO model with optical fiber cold light source, L2, with three levels of intensity, and 40X magnification.

RESULTS AND DISCUSSIONS

GC-MS Analysis of Essential Oils

The major compounds identified in *Anethum graveolens* essential oil were o-cymene with an area percentage of 30.71%,

and α-phellandrene with an area percentage of 23.21%; other compounds had lower area percentages [1, 29]. The GC-MS analysis in the case of *Melaleuca alternifolia* essential oil showed that the major compound was terpinene-4-ol with an area percentage of 23.06% [14] (Figure 2). The chemical composition of tea tree essential oil consists largely of cyclic monoterpenes of which about 50% are oxygenated and about 50% are hydrocarbons [20].

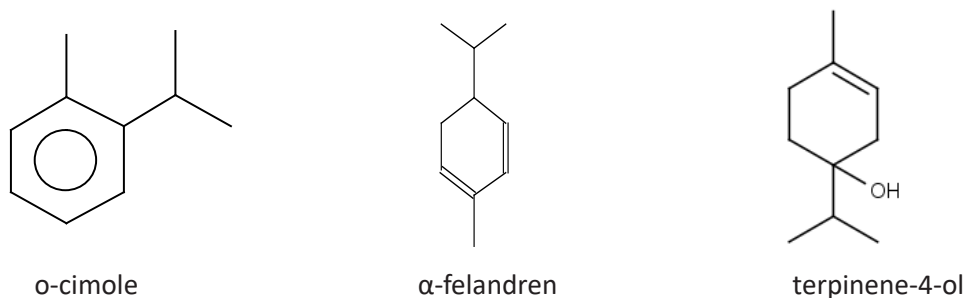
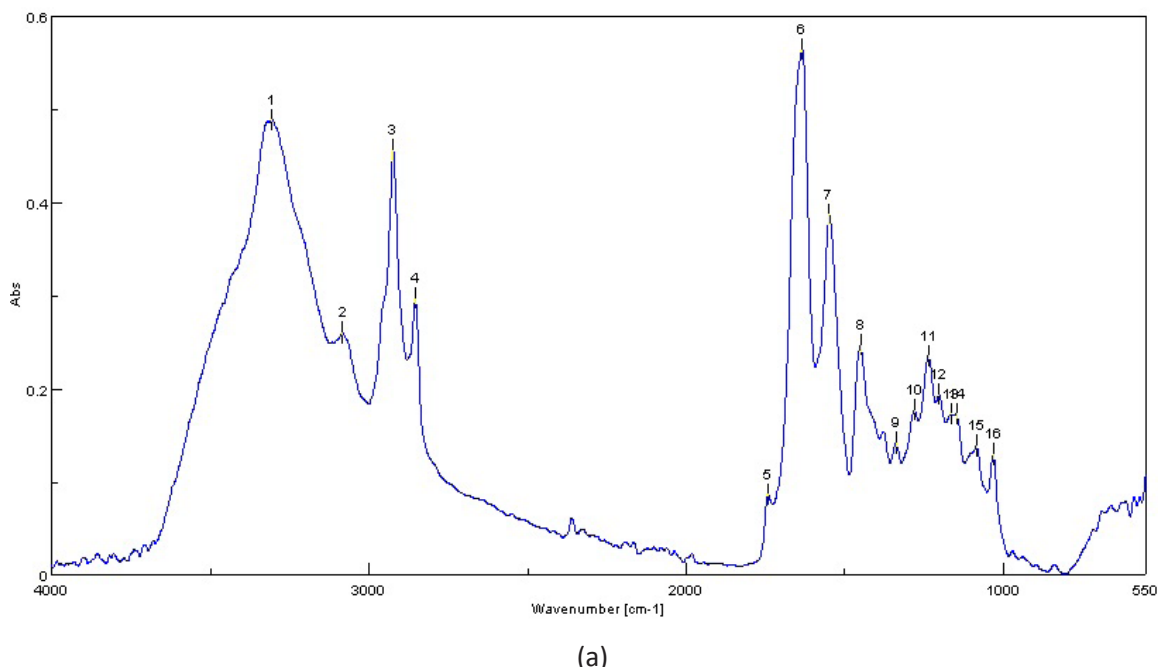


Figure 2. The main components of dill and tea tree essential oils

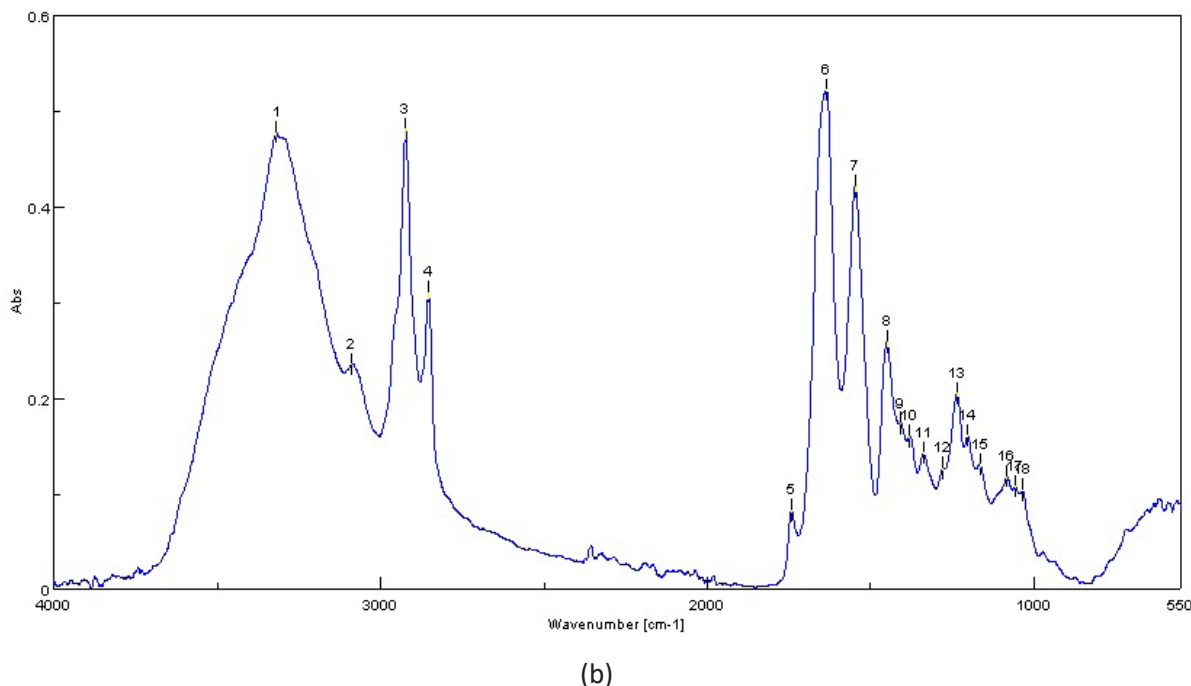
ATR-FTIR Analysis of Leathers

Mid-infrared spectra for un-treated leather lining - Eco control and leather lining - Cr control and leather samples treated with dill or tea tree essential oil are shown in Figures 3, 4 and 5. According to FTIR spectra from Figure 3, the characteristic bands of sheepskin leather lining - Eco control (a) and sheepskin leather lining - Cr control (b) are observed. Vibration bands at 1449 cm^{-1} , 2853 cm^{-1} and 3086 cm^{-1} are attributed to hydrogen bonds of associated

functional groups C-H and those at 1082 cm^{-1} and 3318 cm^{-1} are attributed to hydrogen bonds of associated functional groups C-O [27]. Bands in the range of $3318\text{-}3307\text{ cm}^{-1}$ are related to O-H stretching. Peaks in the ranges of $1636\text{-}1633\text{ cm}^{-1}$ ($-\text{C}=\text{C}$ stretch), $1548\text{-}1547\text{ cm}^{-1}$ and at 1236 cm^{-1} are attributed to I, II and III amide bands, respectively. Peaks of the C-O band were observed at 1032 cm^{-1} in the case of sheepskin leather lining - Eco control, $1085\text{-}1082\text{ cm}^{-1}$ and $1166\text{-}1155\text{ cm}^{-1}$ in all samples.



(a)



(b)

Figure 3. ATR-FTIR spectra for (a) sheepskin leather lining - Eco control, and (b) sheepskin leather lining - Cr control

The chemical changes occurring in the functional groups in the leather lining treated

with tea tree essential oils are shown in Figure 4 compared to spectra for tea tree essential oil.

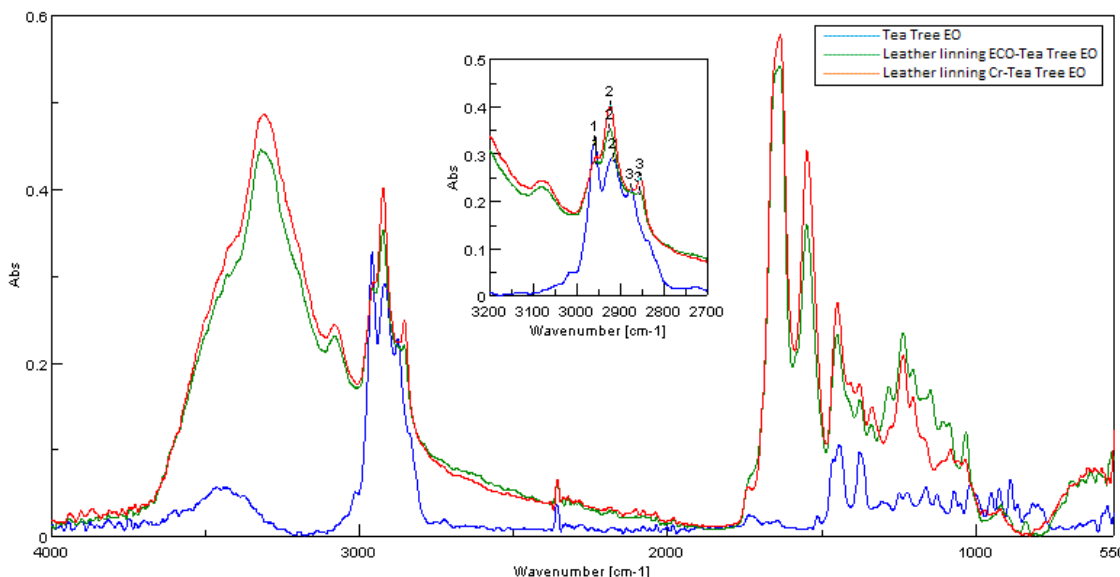


Figure 4. ATR-FTIR spectra of tea tree EO, leather lining - Eco and leather lining - Cr treated with tea tree EO

The treatment of sheepskin lining - Eco and sheepskin lining - Cr, respectively with tea tree essential oil leads to the evidence of absorption bands at 2958-2956 cm⁻¹ (C-H stretch), 1449-1448 cm⁻¹ (C-H bending) specific for this EO

[33]. The absorption band at 2919 cm⁻¹ (-CH₂) as well as from the asymmetric -CH(CH₃) stretching vibration [34]) is shifted to 2925-2924 cm⁻¹ in the case of treated leather lining samples. The band at 2877 cm⁻¹ (-CH(CH₂)-, symmetric and

asymmetric stretching vibrations) identified at tea tree spectrum [34] is found in the range of 2856-2855 cm⁻¹ in the spectra of leather samples treated with tea tree EO. The bands at 3318-3307 cm⁻¹, 1548-1547 cm⁻¹ found in control samples are also observed at the treated samples with tea tree essential oil. The band at 1441 cm⁻¹

observed in the case of tea tree EO due the -CH₂- and -CH₃ scissoring vibration [34] is shifted in the range of 1449-1449 cm⁻¹ for treated leather samples.

Figure 5 shows comparative spectra for dill EO, leather lining - Eco and leather lining - Cr treated with dill essential oil.

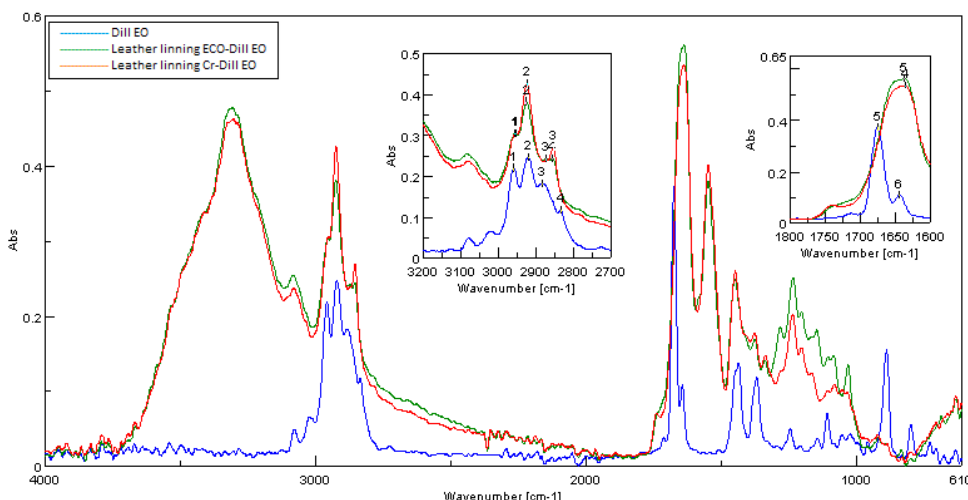


Figure 5. ATR-FTIR spectra of dill EO, leather lining - Eco treated with dill EO and leather lining - Cr treated with dill EO

The FTIR analysis of treated lining leather samples with dill essential oil is accompanied by the shifting of wave number from 2953 cm⁻¹ and 2922 cm⁻¹ (C-H stretch) assigned to EO to 2957-2955 cm⁻¹ and 2925-2924 cm⁻¹. The characteristic band of EO from 2884 cm⁻¹ assigned to CH₃ stretching is moved to lower wave number (2874 cm⁻¹) in the case of treated sheepskin lining Eco leather.

The bands at 3318 cm⁻¹ and 3307 cm⁻¹ (O-H stretching) from sheepskin lining - Cr spectrum and sheepskin lining - Eco spectrum are found in the treated samples with dill EO. The bands at 1644 cm⁻¹ (-C=C stretch) and 1675 cm⁻¹ (α - β unsaturated C = O stretch) [33] from dill EO are shifted to 1637-1637 cm⁻¹ for treated samples.

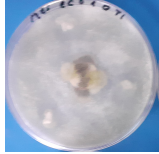
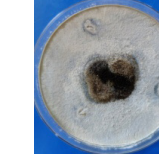
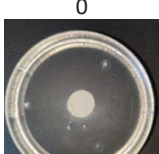
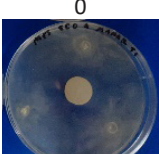
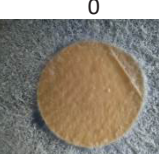
The spectra presented in Figures 4-5 confirm the presence of tea tree or dill essential oils in the sheepskin lining samples.

Antifungal Activity against *Trichophyton interdigitale*

Samples of sheepskin leather lining - Eco control and treated with tea tree and dill essential oil was incubating at 30°C and the antifungal activity towards the grown of

Trichophyton interdigitale was evaluated after 3, 7, 14, and 21 days (Table 1). Antifungal activity against *Trichophyton interdigitale* was ranked with indicators between 0-5, where 0 means that no microorganisms grew on the sample surface, 1 shows growth between 10-20%, 2 between 30-45%, 3 between 50-75%, 4 between 80-90% and 5 shows 100% growth of microorganisms on the evaluated sample surface. Control sheepskin leather lining - Eco samples show growth of microorganisms after 3 days on 90% of leather surface and it increases at 100% after 7 days. Sheepskin leather lining - Eco samples treated with tea tree essential oil show no growth of microorganisms after 3 days, 7 days and 14 days respectively, remaining without growth of *Trichophyton interdigitale* fungus on leather surface and on culture environment. After 21 days their growth covers 80% of the leather sample surface. Sheepskin leather lining - Eco samples treated with dill essential oil show no growth of microorganisms after 3 days and 7 days, respectively. After 14 days the microorganism growth was 10% on the surface of leather and it did not evolve after 21 days.

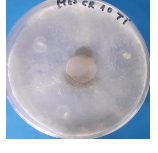
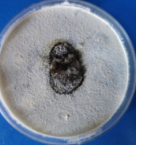
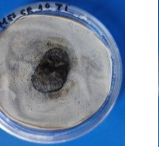
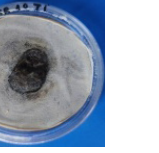
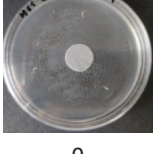
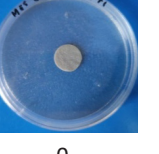
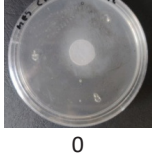
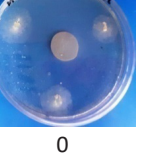
Table 1: Sheepskin lining leathers - Eco treated with tea tree and dill essential oil tested against *Trichophyton interdigitale* fungus as compared with control samples

Sample	3 days	7 days	14 days	21 days
Control sheepskin leather lining - Eco				
Grading	4	5	5	5
Sheepskin leather lining - Eco with tea tree EO				
Grading	0	0	0	4
Sheepskin leather lining - Eco with dill EO				
Grading	0	0	1	1

Also, samples of sheepskin leather lining - Cr control and treated with tea tree and dill essential oil, respectively, were incubated at 30°C for 3, 7, 14, and 21 days, respectively. After each test period, the antifungal activity was evaluated against *Trichophyton interdigitale* (Table 2). Control sheepskin leather lining - Eco samples show growth of microorganisms after 3 days on 20% from leather surface and increases

at 100% after 7 days. Sheepskin leather lining - Cr samples treated with tea tree essential oil show no growth of microorganisms on the leather surface after 21 days of exposure. Sheepskin leather lining - Cr samples treated with dill essential oil show no growth of microorganisms after 3 days and 7 days, respectively. After 14 days, the microorganism growth was 100% on the surface of leather.

Table 2: Sheepskin lining leathers - Cr treated with tea tree and dill essential oil tested against *Trichophyton interdigitale* fungus as compared with control samples

Sample	3 days	7 days	14 days	21 days
Control sheepskin leather lining - Cr				
Grading	2	5	5	5
Sheepskin leather lining - Cr with tea tree EO				
Grading	0	0	0	0
Sheepskin leather lining - Cr with dill EO				
Grading	0	0	5	5

In the case of treatment of leather - Eco samples with tea tree EO, a good resistance against *Trichophyton interdigitale* microorganism with zero growth after 14 days, and no microorganism growth on leather with Cr sample were recorded throughout the experiment. Tea tree essential oil compounds affected cell membranes in microorganisms and induced cell membrane rupture [23]. Tea tree oil has a broad spectrum of antifungal and antimicrobial activity [35] which can be mainly attributed to the major compound, terpinen-4-ol [36, 37], through an action of penetrating the cell wall and cell membrane structures that stops the development of microorganisms [25].

Leather samples treated with dill essential oil has improved/better antifungal activity in the case of sheepskin leather lining Eco with zero growth of microorganism up to 7 days and an increase up to 10% surface coverage after 14 days. Sheepskin leather lining - Cr has also no growth of *Trichophyton interdigitale* up to 7 days and shows 100% increase after 14 days. In another study, it was reported that the dill seed essential oil (1.00 µL/mL) completely inhibited the growth of *S. sclerotiorum* fungus after 4 days of incubation due to the carvone and limonene content [22]. A completely inhibition of the growth of *Trichophyton interdigitale* species during 28 days on the sheepskin leather for lining finished with synthetic film was observed in the case of treatment with thyme essential oil [4]. The mechanism of the dill essential oil on the fungal inhibition could be explained by the low molecular weight and highly lipophilic compounds (terpene) that disrupt the fungus membrane [38]. In the case of tea tree essential oil, the fungal activity was assigned to the terpene-4-ol that exhibits antimycotic activities by disrupting cell walls, membranes and cytoplasm, which led to compromising fungal life processes [39].

A wide variety of essential oils have antifungal and antimicrobial properties and in many cases this activity is due to the presence of active monoterpenic constituents [40-42]. Several studies have also shown that

monoterpenes exert a membrane dam with effects of cell aging and stopping the development of microorganisms [25, 43]. Essential oils used in optimal proportions have selective bioactive properties and no side effects [44]. The antifungal activity of tea tree and dill essential oils against *Trichophyton interdigitale* makes it possible to develop antifungal compositions based on natural compounds for footwear, gloves and other specific products [44].

CONCLUSIONS

The results obtained in this study show that the essential oils of *Anethum graveolens* and *Melaleuca alternifolia* had different antifungal effects against *Trichophyton interdigitale* depending on the tested period and type of leather tanning. The experiments showed that the tea tree essential oil totally inhibited the growth of *Trichophyton interdigitale* fungus on the sheepskin leather lining - Cr up to 21 days of exposure and on the sheepskin leather lining - Eco up to 14 days of exposure. The dill essential oil shown to enhance the growth inhibition of the *Trichophyton interdigitale* fungus up to 7 days. The results are promising for treatment of lining leather with essential oils having a great importance for foot health and hygiene. Also, tea tree and dill essential oils could offer a much safer alternative protection against fungus as compared to synthetic compounds with adverse reactions to body and environment. The results of this study may have potential for use in application development in cosmetics, pharmaceuticals, obtaining leathers and textiles with selective bioproperties.

Acknowledgements

The research was carried out under project number 19 Nucleu / 2019, PN 19_17_01_02, CREATIV_PIEL, 6PFE_4PERFORM-TEX-PEL/2018 project, and funded by Romanian Ministry of Education and Research.

REFERENCES

1. Akhtar, N., Ihsan-ul-Haq, Mirza, B., Phytochemical analysis and comprehensive evaluation of antimicrobial and antioxidant properties of 61 medicinal plant species, *Arab J Chem*, **2018**, 11, 1223–1235, <https://doi.org/10.1016/j.arabjc.2015.01.013>.
2. Inayatullah, S., Prenzler, P.D., Obied, H.K., Rehman, A.U., Mirza, B., Bioprospecting traditional Pakistani medicinal plants for potent antioxidants, *Food Chem*, **2012**, 132, 222–229, <https://doi.org/10.1016/j.foodchem.2011.10.060>.
3. Ahmad, I., Aqil, F., *In vitro* efficacy of bioactive extracts of 15 medicinal plants against ESBL-producing multidrug-resistant enteric bacteria, *Microbiol Res*, **2007**, 162, 264–275, <https://doi.org/10.1016/j.micres.2006.06.010>.
4. Chirila, C., Deselnicu, V., Berechet, M.D., Footwear protection against fungi using thyme essential oil, *Leather and Footwear Journal*, **2017**, 17, 3, <https://doi.org/10.24264/lfj.17.3.7>.
5. Berechet, M.D., Chirila, C., Deselnicu, V., Antifungal Activity of Thyme Essential Oil on Woolen Sheepskins, Proceedings of the 6th International Conference on Advanced Materials and Systems – ICAMS 2016, 20-23 October **2016**, Bucharest, Romania, 203-208, <https://doi.org/10.24264/icams-2016.II.2>.
6. Chirila, C., Berechet, M.D., Deselnicu, V., Thyme Essential Oil as Natural Leather Preservative against Fungi, Proceedings of the 6th International Conference on Advanced Materials and Systems – ICAMS 2016, 20-23 October **2016**, Bucharest, Romania, 227-232, <https://doi.org/10.24264/icams-2016.II.6>.
7. Chirila, C., Crudu, M., Deselnicu, V., Comparative Study regarding Resistance of Wet-White and Wet-Blue Leather to the Growth of Fungi, *Leather and Footwear Journal*, **2014**, 14, 2, 107-120, <https://doi.org/10.24264/lfj.14.2.4>.
8. Chirila, C., Crudu, M., Deselnicu, V., Study regarding the Resistance to the Growth of Fungi of Wet-White Leather Tanned with Titanium – Aluminum, Proceedings of the 5th International Conference on Advanced Materials and Systems – ICAMS 2014, 23-25 October **2014**, Bucharest, Romania, 31-36, ISSN: 2068-0783, CERTEX press.
9. Chirila, C., Deselnicu, V., Crudu, M., Study regarding the Resistance of Wet-White Leather Organic Tanned to the Growth of Fungi, Proceedings of the 5th International Conference on Advanced Materials and Systems – ICAMS 2014, 23-25 October **2014**, Bucharest, Romania, 37-42, ISSN: 2068-0783, CERTEX press.
10. Deselnicu, D.C., Vasilescu, A.M., Purcarea, A.A., Militaru, G., Sustainable Consumption and Production in the Footwear Sector, *Leather and Footwear Journal*, **2014**, 14, 3, 159-180, <https://doi.org/10.24264/lfj.14.3.3>.
11. Deselnicu, V., Deselnicu, D.C., Vasilescu, A.M., Militaru, G., EU Policy for Sustainable Consumption and Production – EU Ecolabel for Footwear, Proceedings of the 5th International Conference on Advanced Materials and Systems – ICAMS 2014, 23-25 October **2014**, Bucharest, Romania, 641-646, ISSN: 2068-0783, CERTEX press.
12. Deselnicu, V., Maier, S.S., Albu, L., Buruntea, N., Antimicrobial and Antifungal Leathers for Increasing the Health and the Comfort of the Individuals, CORTEP 2007, 18-21 October **2007**, Iasi, Romania.
13. Deselnicu, V., Maier, S.S., Deselnicu, O.C., Florescu, M., Impact of Technological Changes on Increased Health and Comfort Efficiency, Proceedings of the 4th International Conference in Management of Technological

- Change, Book 1, Chania, Greece, 19-20 August **2005**, 87-92.
14. Chidi, F., Bouhoudan, A., Khaddor, M., Antifungal effect of the tea tree essential oil (*Melaleuca alternifolia*) against *Penicillium griseofulvum* and *Penicillium verrucosum*, *J King Saud Univ Sci*, **2020**, 2041–2045, <https://doi.org/10.1016/j.jksus.2020.02.012>.
 15. Foganholi, A.P. do A.M., Daniel, J.F.S., Santiago, D.C., Orives, J.R., Pereira, J.P., Faria, T. de J., Chemical composition and antifungal activity of pennyroyal essential oil in different stages of development, *Semina Ciênc Agrár, Londrina*, **2015**, 36, 3091–3100, <https://doi.org/10.5433/1679-0359.2015v36n5p3091>.
 16. Hmiri, S., Rahouti, M., Habib, Z., Satrani, B., Ghanmi, M., El Ajouri, M., Évaluation du potential antifongique des huiles essentielles de *Mentha pulegium* et d'*Eucalyptus camaldulensis* dans la lute biologique contre les champignons responsables de la détérioration des pommes en conservation, *Bull Soc R Sci Liège*, **2011**, 80, 824–836, available at <https://popups.uliege.be:443/0037-9565/index.php?id=3375>.
 17. Khaddor, M., Saidi, R., Aidoun, A., Lamarti, A., Tantaoui-Elaraki, A., Ezziyyani, M., Castillo, M.C., Badoc, A., Antibacterial effects and toxigenesis of *Penicillium aurantiogriseum* and *P. viridicatum*, *Afr J Biotechnol*, **2007**, 6, 2314–2318, <https://doi.org/10.5897/AJB2007.000-2362>.
 18. Louhibi, S., Amiri, S., Elghadraoui, L., Chemical composition and antimicrobial activity of essential oils, *Thymus vulgaris* L. and *Mentha L. pulegium* against the major post harvest diseases of citrus in Morocco, *Int J Sci Res*, **2015**, 4, 1181–1184.
 19. Cheng, S., Xingfeng, S., *In vivo* antifungal activities of the tea tree oil vapor against *Botrytis cinerea*, in: 2011 International Conference on New Technology of Agricultural, Presented at the 2011 International Conference on New Technology of Agricultural Engineering (ICAE), IEEE, Zibo, China, **2011**, pp. 949–951.
 20. Brophy, J.J., Davies, N.W., Southwell, I.A., Stiff, I.A., Williams, L.R., Gas chromatographic quality control for oil of melaleuca terpinen-4-ol type (Australian Tea Tree), *J Agric Food Chem*, **1989**, 37, 1330–1335, <https://doi.org/10.1021/jf00089a027>.
 21. Ebani, V.V., Najar, B., Bertelloni, F., Pistelli, L., Mancianti, F., Nardoni, S., Chemical composition and *in vitro* antimicrobial efficacy of sixteen essential oils against *Escherichia coli* and *Aspergillus fumigatus* isolated from poultry, *Vet Sci*, **2018**, 5, 62–74, <https://doi.org/10.3390/vetsci5030062>.
 22. Ma, B., Ban, X., Huang, B., He, J., Tian, J., Zeng, H., et al., Interference and Mechanism of Dill Seed Essential Oil and Contribution of Carvone and Limonene in Preventing Sclerotinia Rot of Rapeseed, *PLoS ONE*, **2015**, 10(7), e0131733, <https://doi.org/10.1371/journal.pone.0131733>.
 23. Lang, G., Buchbauer, G., A review on recent research results (2008–2010) on essential oils as antimicrobials and antifungals. A review, *Flavour Fragr J*, **2012**, 27, 13–39, <https://doi.org/10.1002/ffj.2082>.
 24. Nuzhat, T., Vidyasagar, G.M., Antifungal investigations on plant essential oils. A review, *Int J Pharm Pharm Sci*, **2013**, 5, 19–28.
 25. Cox, S.D., Mann, C.M., Markham, J.L., Bell, H.C., Gustafson, J.E., Warmington, J.R., Wyllie, S.G., The mode of antimicrobial action of the essential oil of *Melaleuca alternifolia* (tea tree oil), *J Appl Microbiol*, **2001**, 88, 170–175, <https://doi.org/10.1046/j.1365-2672.2000.00943.x>.
 26. Zhang, X., Guo, Y., Guo, L., Jiang, H., Ji, Q., *In vitro* evaluation of antioxidant and antimicrobial activities of *Melaleuca alternifolia* essential oil, *BioMed Res Int*, **2018**, 8, <https://doi.org/10.1155/2018/2396109>.
 27. Koizhaiganova, M., Yaşa, I., Gülmser, G., Assessment of antibacterial activity

- of lining leather treated with silver doped hydroxyapatite, *Int Biodeterior Biodegradation*, **2015**, 105, 262–267, <https://doi.org/10.1016/j.ibiod.2015.09.017>.
28. Berechet, M.D., Constantinescu, R.R., Răpă, M., Chirilă, C., Stanca, M., Simion, D., Surdu, L., Gurău, D.F., Antifungal and antibacterial treatments based on natural compounds for lining leather and footwear articles, *Leather and Footwear Journal*, **2019**, 19, 4, 201-216, <https://doi.org/10.24264/lfj.19.4.5>.
29. Berechet, M.D., Essential Oils – Their Use in Practice and Research, Doctoral Thesis, Faculty of Applied Chemistry and Materials Science, “Politehnica” University of Bucharest, **2015**.
30. de Hoog, G.S., Dukik, K., Monod, M., Packeu, A., Stubbe, D., Hendrickx, M., Kupsch, C., Stielow, B., Freeke, J., Göker, M., Rezaei-Matehkolaie, A., Mirhendi, H., Gräser, Y., Toward a Novel Multilocus Phylogenetic Taxonomy for the Dermatophytes, *Mycopathologia*, **2017**, 182, 5–31, <https://doi.org/10.1007/s11046-016-0073-9>.
31. Rodgers, P., Bassler, M., Treating onychomycosis, *Am Fam Physician*, **2001**, 63, 4, 663–72, 677–8, PMID 11237081.
32. Westerberg, D.P., Voyack, M.J., Onychomycosis: current trends in diagnosis and treatment, *Am Fam Physician*, **2013**, 88, 11, 762–70, PMID 24364524.
33. Kaur, N., Chahal, K.K., Kumar, A., Singh, R., Bhardwaj, U., Antioxidant activity of *Anethum graveolens* L. essential oil constituents and their chemical analogues, *J Food Biochem*, **2019**, e12782, <https://doi.org/10.1111/jfbc.12782>.
34. Gallart-Mateu, D., Largo-Arango, C.D., Larkman, T., Garrigues, S., de la Guardia, M., Fast authentication of tea tree oil through spectroscopy, *Talanta*, **2018**, 189, 404–410, <https://doi.org/10.1016/j.talanta.2018.07.023>.
35. Markham, J.L., Biological activity of tea tree oil, in: Tea Tree, the Genus *Melaleuca*, ed. Southwell, I. and Lowe, R., Amsterdam: Harwood Academic Publishers, **1999**, 169–190.
36. Southwell, I.A., Hayes, A.J., Markham, J.L., Leach, D.N., The search for optimally bioactive Australian tea tree oil, *Acta Hortic*, **1993**, 334, 265–275, <https://doi.org/10.17660/ActaHortic.1993.344.30>.
37. Carson, C.F., Riley, T.V., Antimicrobial activity of the major components of the essential oil of *Melaleuca alternifolia*, *J Appl Bacteriol*, **1995**, 78, 264–269, <https://doi.org/10.1111/j.1365-2672.1995.tb05025.x>.
38. Tian, J., Ban, X., Zeng, H., Huang, B., He, J., & Wang, Y., *In vitro* and *in vivo* activity of essential oil from dill (*Anethum graveolens* L.) against fungal spoilage of cherry tomatoes, *Food Control*, **2011**, 22, 12, 1992–1999, <https://doi.org/10.1016/j.foodcont.2011.05.018>.
39. An, P., Yang, X., Yu, J., Qi, J., Ren, X., Kong, Q., α-terpineol and terpene-4-ol, the critical components of tea tree oil, exert antifungal activities *in vitro* and *in vivo* against *Aspergillus niger* in grapes by inducing morphous damage and metabolic changes of fungus, *Food Control*, **2018**, <https://doi.org/10.1016/j.foodcont.2018.11.013>.
40. Knobloch, K., Pauli, A., Iberl, B., Weis, N., Weigand, H., Antibacterial activity and antifungal properties of essential oil components, *J Essent Oil Res*, **1988**, 1, 119–128, <https://doi.org/10.1080/10412905.1989.9697767>.
41. Beylier, M., Bacteriostatic activity of some Australian essential oils, *Perfum Flavour*, **1979**, 4, 23–25.
42. Morris, J.A., Khettry, A., Seitz, E.W., Antimicrobial activity of aroma chemicals and essential oils, *J Am Chem Soc*, **1979**, 56, 595–603, <https://doi.org/10.1007/BF02660245>.
43. Sikkema, J., de Bont, J.A.M., Poolman, B., Mechanisms of membrane toxicity of hydrocarbons, *Microbiol Rev*, **1995**, 59, 201–222, <https://doi.org/10.1128/MMBR.59.2.201-222.1995>.

44. Hammer, K.A., Carson, C.F., Riley, T.V., Nielsen, J.B., A review of the toxicity of *Melaleuca alternifolia* (tea tree) oil, *Food Chem Toxicol.*, **2006**, 44, 616–625, <https://doi.org/10.1016/j.fct.2005.09.001>.

© 2020 by the author(s). Published by INCDTP-ICPI, Bucharest, RO. This is an open access article distributed under the terms and conditions of the Creative Commons Attribution license (<http://creativecommons.org/licenses/by/4.0/>).

NOVEL USE OF THE INTEL REALSENSE SR300 CAMERA FOR FOOT 3D RECONSTRUCTION

Fangchuan LI¹, Shuangjia LIU¹, Luyu JIANG¹, Weihua ZHANG², Jin ZHOU^{3*}

¹College of Software Engineering, Sichuan University; Chengdu 610065, P. R. China

²College of Computer Science, Sichuan University; Chengdu 610065, P. R. China

³The Key Laboratory of Leather Chemistry and Engineering Ministry of Education, Sichuan University; Chengdu 610065, P. R. China

Received: 05.02.2020

Accepted: 07.05.2020

<https://doi.org/10.24264/lfj.20.2.5>

NOVEL USE OF THE INTEL REALSENSE SR300 CAMERA FOR FOOT 3D RECONSTRUCTION

ABSTRACT. Foot three-dimensional (3D) reconstruction is increasingly used in real life at present; however, current 3D measuring devices are usually expensive and have a large volume. So they are limited used in a specific domain and feasible method for accurate, fast and low-cost foot 3D reconstruction are required. Since the Intel RealSense SR300 camera has advantages on 3D scanning, such as high efficiency, portable, low-cost and simple operation, this camera has been widely applied in multi-scenario, such as gaming. But its performance on foot scanning is still unknown. Thereby this study first aimed to design and develop a foot 3D scanning protocol based on the Intel RealSense SR300 camera and then to contrast this new method with a traditional one in terms of accuracy. Fifteen healthy adults without any foot deformity or foot disease participated and their feet were measured by our simulated measurements (SM) and manual measurements (MM). 13 variables were calculated and contrasted and their significant differences were assessed by Single-Sample T Test with significant level of 0.05 and confident interval of 95%. The results show that the SR300 presented a precise foot 3D reconstruction on the mean differences ranged from -1.3 mm to 5.2 mm; meanwhile eight of the thirteen foot parameters exhibited no significant differences between the two methods. Overall, these findings above demonstrate that the SR300 is a valid tool for foot 3D scanning and it can be widely applied in the both medical and commercial fields.

KEY WORDS: Intel RealSense SR300, foot 3D scanning, foot measurement, footwear customization

UTILIZARE NOUĂ A CAMEIEI INTEL REALSENSE SR300 PENTRU RECONSTRUCȚIA 3D A PICIORULUI

REZUMAT. Reconstituirea tridimensională (3D) a piciorului este folosită din ce în ce mai mult în viața reală în prezent; cu toate acestea, dispozitivele de măsurare 3D actuale sunt de obicei costisitoare și au un volum mare. Așadar utilizarea este limitată la un anumit domeniu și este necesară o metodă fezabilă pentru o reconstrucție 3D a piciorului exactă, rapidă și cu costuri reduse. Întrucât camera Intel RealSense SR300 are avantaje în ceea ce privește scanarea 3D, cum ar fi eficiență ridicată, portabilitate, costuri reduse și operare simplă, această cameră a fost aplicată pe scară largă în mai multe domenii, cum ar fi jocurile. Însă performanțele acesteia la scanarea piciorului nu sunt cunoscute încă. Prin urmare, acest studiu a avut ca scop mai întâi de a proiecta și dezvolta un protocol de scanare 3D pentru picioare bazat pe camera Intel RealSense SR300 și apoi de a compara această nouă metodă cu una tradițională din punctul de vedere al preciziei. La studiu au participat cincisprezece adulți sănătoși fără deformări sau boli ale piciorului, efectuându-se măsurători simulate (SM) și măsurători manuale (MM) ale piciorului. S-au calculat și comparat 13 variabile, iar diferențele semnificative ale acestora au fost evaluate prin testul T cu un singur eșantion, cu un nivel de semnificație de 0,05 și un interval de încredere de 95%. Rezultatele arată că SR300 a prezentat o reconstrucție 3D precisă a piciorului, diferențele medii fiind cuprinse între -1,3 mm și 5,2 mm; pe de altă parte, opt dintre cei treisprezece parametri ai piciorului nu au prezentat diferențe semnificative între cele două metode. În general, aceste concluzii de mai sus demonstrează că SR300 este un instrument valid pentru scanarea 3D a picioarelor și poate fi aplicat pe scară largă atât în domeniul medical cât și în cel comercial.

CUVINTE CHEIE: Intel RealSense SR300, scanare 3D a piciorului, măsurarea piciorului, personalizarea încălțămintei

UNE NOUVELLE UTILISATION DE LA CAMÉRA INTEL REALSENSE SR300 POUR LA RECONSTRUCTION 3D DU PIED

RÉSUMÉ. La reconstruction tridimensionnelle (3D) du pied est de plus en plus utilisée dans la vie réelle à l'heure actuelle ; cependant, les appareils de mesure 3D actuels sont généralement chers et ont un grand volume. Ils sont donc limités dans un domaine spécifique et une méthode réalisable pour une reconstruction 3D précise, rapide et peu coûteuse du pied est requise. Étant donné que la caméra Intel RealSense SR300 présente des avantages sur la numérisation 3D, tels qu'une efficacité élevée, un fonctionnement portable, peu coûteux et simple, cette caméra a été largement appliquée dans plusieurs scénarios, tels que les jeux. Mais les performances sur le balayage des pieds sont encore inconnues. Ainsi, cette étude visait d'abord à concevoir et à développer un protocole de numérisation 3D du pied basé sur la caméra Intel RealSense SR300, puis à comparer cette nouvelle méthode avec une méthode traditionnelle en termes de précision. Quinze adultes en bonne santé sans aucune déformation du pied ou maladie du pied ont participé et on a fait de mesures simulées (SM) et mesures manuelles (MM) sur leurs pieds. On a calculé et comparé 13 variables et leurs différences significatives ont été évaluées par le test T à échantillon unique avec un niveau de signification de 0,05 et un intervalle de confiance de 95%. Les résultats montrent que le SR300 présentait une reconstruction 3D précise du pied avec des différences moyennes variant de -1,3 mm à 5,2 mm ; d'autre part, huit des treize paramètres du pied ne présentaient aucune différence significative entre les deux méthodes. Dans l'ensemble, ces résultats ci-dessus démontrent que le SR300 est un outil valide pour la numérisation 3D du pied et qu'il peut être largement appliqué dans les domaines médical et commercial.

MOTS CLÉS : Intel RealSense SR300, numérisation 3D du pied, mesure des pieds, personnalisation des chaussures

* Correspondence to: Assoc. Prof. Dr. Jin ZHOU, College of Biomass Science and Engineering, Sichuan University, Chengdu 610065, P. R. China, zj_scu@scu.edu.cn

INTRODUCTION

With the development of computer vision, virtual reality technology has been applied to various fields of life, including aerospace, manufacturing, reverse engineering and medical treatment, etc. While, 3D model reconstruction is one of key technologies in field of virtual reality and it has been intensively concerned by researchers [1, 2].

In shoe-making industry, accurate, fast and low-cost 3D scanning protocol is required for foot measurements. Different from the manual measurement, it provides a standard process and obtains consistent outcomes. At present, the mainstream technology of 3D reconstruction includes scanning technology [3, 4], structure from motion technology [5], and reverse mould technology, etc. However, in the past studies, the equipment commonly features the large volume, high price, long scanning time, and higher technical requirements upon the operators. For example, Menato *et al.* [6] obtained the foot 3D model through a self-developed 3D scanning App on the smartphone platform, although its precision reaches 0.15mm, the time-consuming of creating foot 3D model is nearly 15 minutes. Novak *et al.* [7] used four charge-coupled device cameras to wrap around participants' feet and scan with a laser line, requiring a huge and inconvenient walking stage with 4.7 m long and 0.8 m wide. Further, Gao *et al.* [8] used an active marking method, in which the participants wore socks with markers, and used 10 CCD cameras to capture video of foot movements; this method has complex experiment procedures with a series of operations, and it's hard to apply in real life. As shown above, most high-quality foot scanners are implausible regarding application. Hence, as an emerging depth camera, the Intel RealSense SR300 camera is a good tool which balancing convenience in use, clarity in visualization and accuracy in outcomes.

The SR300 may simultaneously capture the color, depth and other image information widely admitted in the real scenario, such as face direction recognition [9], robotic technology [10], gesture recognition [11], 3D model reconstruction, human body rehabilitation [12], and etc. As a result, we assumed whether this camera could be used in foot 3D scanning. Therefore, the objectives of this study were set

as follows: 1. to develop a foot 3D reconstruction method with the Intel RealSense SR300 camera; 2. to compare the result obtained in the new method with a traditional one to verify its accuracy.

EXPERIMENTAL

Methods

Participants

Fifteen students (gender = 11 males, 4 females; height = 1.73 ± 0.14 m; body mass = 65.20 ± 18.20 kg) from the Sichuan University were invited to this study. None of them had any types of foot deformities or foot diseases. All participants gave written informed consent before participation in this study.

Manual Foot Measurements (MM)

The methods used were in accordance with the guidelines developed by the research committee of Sichuan University. Before measuring, all participants' feet were disinfected and dried. Participants sat on stools and put their right legs horizontally on other ones. The operator measured thirteen foot parameters on each participant's right foot using a tape measure and a straightedge. There were three trials of MM for each foot parameter. All foot parameter definitions are as shown in Table 2 and the foot coordinate system we established is provided in Figure 2.

Simulated Foot Measurements (SM)

The foot scanner (Figure 1) adopted the Intel RealSense SR300 camera as the core hardware equipment, while the SR300 is a short-distance light coding 3D imaging camera [13-15]. We adopted the Visual Studio 2015 as the development platform and the Intel RealSense SDK 2016 R2 as our 3D scanning component library [9, 16]. All configuration parameters of SR300 are shown in Table 1. The main theory of the Intel RealSense SR300 camera is shown below: during the 3D scanning, the SR300 emits the specific "structured light" to the object surface via the infrared laser projector, which will be accepted by the high-speed VGA Infrared

Camera after the object reflection. Due to the variable distances from the infrared ray to the object surface, the distances and locations of "structured light" captured by the Infrared

Camera may vary [17]. It is feasible to calculate the space information on the object surface, and further restore the whole 3D space.

Table 1: Intel RealSense SR300 camera configuration parameters

Configuration	Parameters
Scanning Mode	HEAD
Scanning Range	40 cm~60 cm
Reconstruction Option	TEXTURE and SOLIDIFICATION
Max Triangles	0 (no limitation)
Max Vertices	0 (no limitation)
Max Texture Resolution Width	1920
Max Texture Resolution Height	1080
Flop Preview Image	False
Use Marker	False
File Format	OBJ

The foot scanner was mounted flush with the laboratory floor, and away from outside and windows, sunlight includes infrared light which may interfere with the depth imaging system; then we placed multiple diffuse lights around the foot scanner to improve the uniformity of the illumination and to avoid a too dark or corrupt scan color; besides, participants were asked to take off all foot ornaments before scanning, shiny or translucent portions of ornaments may corrupt the scan surface. Participants sat on stools about 70cm high and placed their right lower legs on the foot supporter in range of 40cm to 60cm from the Intel RealSense SR300 camera, the point cloud out of this range were automatically subtracted in head scanning mode (Table 1). They were instructed to remain as still as possible for the period of the SR300 scanning. Each foot was scanned for 50 seconds. A total of two successful trials were conducted for each participant and the foot scanner with 30 seconds of rest between trials and 2 minutes between each participant.

The following steps conducted for every frame of foot depth data during the working process: firstly, the foot depth data was transformed into the floating point cloud in meters; secondly, the bilateral filtering was used to carry out the denoising upon the depth floating point cloud, which could keep smooth at the edge; thirdly, the floating point cloud of

plane-coordinate system were mapped into the SR300 camera coordinate system; finally, the point cloud of the SR300 camera coordinate system were restored into the global coordinate system. The whole working process for foot 3D reconstruction is shown in Figure 3.

The foot 3D reconstruction data exported from the foot scanner in the .obj file format accompanied with an OBJ Material file (.mtl) and a texture map file (.png). We imported these files in meters into software 3D Builder (V18, Microsoft, USA) and used the split function in software to cut the excessive part (foot supporter, etc) of the point cloud; then meshed the point cloud; afterwards, the texture mapping technology was used to render the foot point cloud mesh. We manually measured thirteen foot parameters (Table 2) on the 3D foot model using the measuring tool in software. There were also three trials of SM for each foot parameter.

Data Processing and Statistical Analysis

The outcomes used in this study were MM and SM. The differences between them were chosen as the primary value to verify foot 3D model accuracy because of its widely recognized effectiveness in foot measurements assessment [18]. To avoid potential errors, we used the averaged value with standard deviation for each parameter. Meanwhile, the significant differences were assessed by Single-Sample T

Test (H_0 : there are no significant differences between the two groups). All statistical analyses

were operated under software SPSS (V21, IBM, USA) with significant level of 0.05 and confidence interval of 95%.

Table 2: Foot measurement parameter definitions

Location	Parameter definition
Foot length	Distance from pterion to acropodium
Foot width	Maximum width in parallel with the x-axis
Arch length	Distance from pterion to toe root on the y-axis
Waist girth	The distance around the circumference of the foot from foot length center
Ball girth	The distance around the circumference of the foot from toe root
Heel width	The width measured from the pterion at the 40mm along the y-axis and in parallel with the x-axis
Heel to the fifth toe	Distance measured from the heel to the fifth toe in parallel with the y-axis
Medial malleolus height	Distance of medial malleolus on the z-axis
Lateral malleolus height	Distance of lateral malleolus on the z-axis
Bimalleolar width	Distance of medial malleolus and lateral malleolus on the x-axis
Ankle girth	Horizontal girth at the foot and leg intersection
Heel to the medial malleolus	Distance from pterion to medial malleolus at the xOy mapping point on the y-axis
Heel to the lateral malleolus	Distance from pterion to lateral malleolus at the xOy mapping point on the y-axis

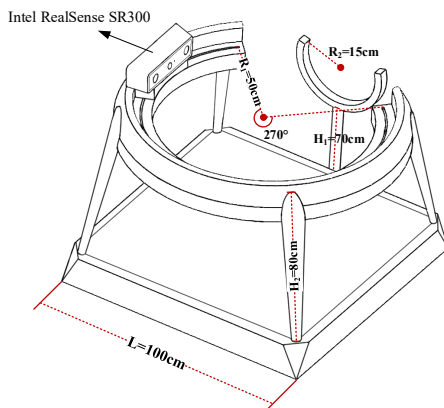


Figure 1. The self-developed foot scanner base on the Intel RealSense SR300 camera

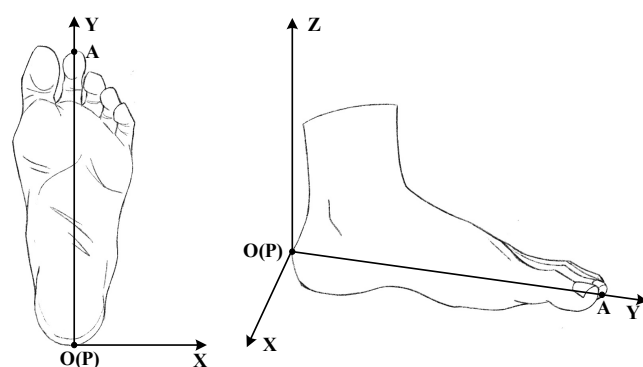


Figure 2. Foot coordinate system

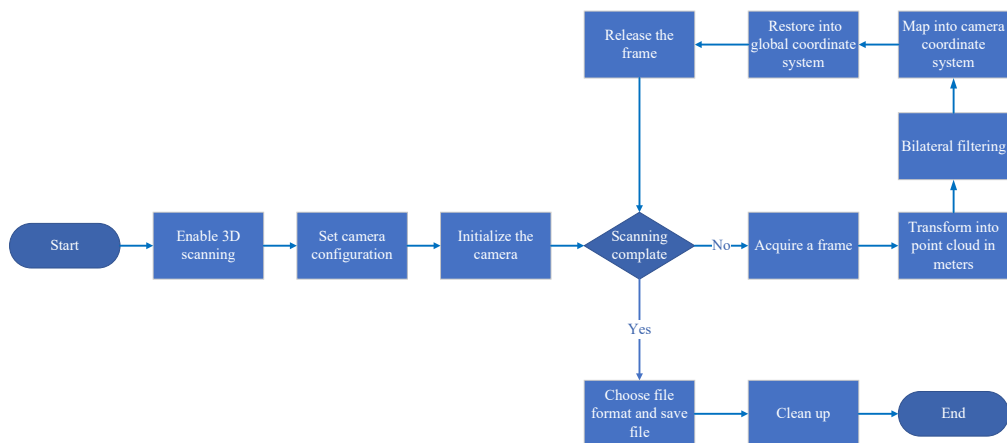


Figure 3. Foot 3D reconstruction working process flowchart

RESULTS

Table 3 shows a foot 3D reconstruction result of one of the male participants with four various angles and in two styles (meshed and rendered images).

Descriptive statistics and differences of the thirteen foot parameters measurements obtained from the two methods are given in Tables 4. It can be seen that the maximum mean difference was 5.2 mm between the

MM and the SM. Only the performance on the measurements of arch length and ankle girth had the mean differences greater than 3.0 mm, other measurements had the value of mean differences between -1.3 mm and 1.2 mm. Statistical analyses showed that the performance on the measurements of arch length, medial malleolus height, lateral malleolus height, ankle girth and heel to medial malleolus failing to reach an P value of 0.05.

Table 3: An overview of foot 3D reconstruction

Location	3D mesh images	3D rendered images
Plantar side		
Acrotarsium side		

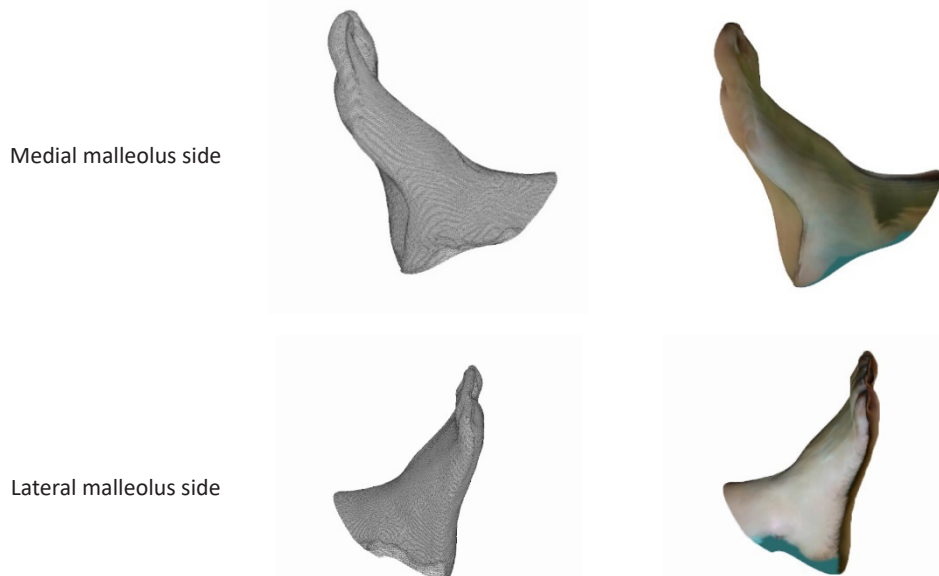


Table 4: Descriptive statistics and differences of thirteen foot parameters from the two methods

Foot measurement	MM		SM		Differences		P-value ($H_0:$ mean = 0)
	Mean	Std. dev.	Mean	Std. dev.	Mean	Std. dev.	
Foot length	259.0	11.4	259.0	12.2	-0.1	2.7	0.986
Foot width	93.1	3.4	93.2	3.7	-0.1	1.1	0.818
Arch length	190.1	6.8	186.2	7.6	3.8	3.1	< 0.001
Waist girth	237.7	13.1	236.5	14.2	1.2	4.0	0.280
Ball girth	231.0	6.8	230.6	6.7	0.5	2.1	0.443
Heel width	69.1	4.8	69.5	5.7	-0.4	2.3	0.506
Heel to the fifth toe	209.0	10.8	209.8	9.6	-0.8	3.1	0.377
Medial malleolus height	84.1	3.3	83.6	3.2	0.4	0.4	0.001
Lateral malleolus height	73.5	5.1	74.7	3.6	-1.2	1.9	0.048
Bimalleolar width	77.6	5.0	77.3	4.9	0.3	1.4	0.489
Ankle girth	256.7	11.3	251.5	13.8	5.2	3.6	< 0.001
Heel to medial malleolus	68.0	5.6	69.3	5.4	-1.3	2.7	0.006
Heel to lateral malleolus	60.7	4.2	60.8	3.1	-0.1	1.4	0.803

DISCUSSION

The purpose of our study was to evaluate the performance of the Intel RealSense SR300 camera in foot 3D reconstruction. Comparing MM with SM, we have shown that the SR300 exhibits excellent performance for foot 3D reconstruction and possesses concurrent accuracy with the manual method in traditional foot measurements. Meanwhile, it dramatically shortens the 3D reconstruction time, achieves consistent outcomes and performs a higher robustness.

Although the P-value in Table 4 showed that the two methods had no significant differences in the major 8 parameters, other five foot parameters were reported with significant differences. However, most of the mean differences were smaller than the foot differences in sensitivity (the shoe last size difference that people can feel, generally 6 mm for men and 2.08 mm for women [19]). We suggested that those significant differences might be attributed to two main reasons: smooth denoising and solidification. Smooth denoising upon the depth

image was used in filtering process which might lead to the most medially prominent point offset to an unreal location in the malleolus side measurements; meanwhile, for closed foot 3D model, we executed solidification orders, but it extends the surface curvature to fill the holes in foot 3D model surface.

The foot 3D reconstruction base on SR300 has fast, accurate and low-cost features. Therefore, this device may be put into use in the hospital, public community, and other places in large numbers, through foot 3D reconstruction made upon the feet of a large scale of population, a significant number of foot data may be obtained. Thereby, it may be prepared as per the foot big data, and the statistical analysis may be made in combination with the personal wear comfort data.

Although the current research results are promising, limitations existed and should be declared: firstly, the foot should be kept as still as possible while scanning and it might be difficult for children; secondly, rotational motion range of the SR300 on the foot scanner is 270° circumference, it is hard to obtain the front color and depth images of the acrotarsium side; thirdly, 3D model reconstruction is realized through the Color Camera and the Infrared Camera, it is required to obtain the color information and the depth information in the real space simultaneously [20, 21].

CONCLUSION

Overall, we approved that the Intel RealSense SR300 camera is a fast, accurate, and low-cost foot scanning protocol, with respect to the manual foot measurements protocol. We explored limitations and constraints may affect the foot 3D reconstruction result of the SR300. We also anticipated that it is likely to build a bridge between laboratory testing and practical application and can be widely applied in the both medical and commercial fields.

Acknowledgements

Thanks to the Support of the National Natural Science Foundation (31700813).

REFERENCES

1. Mu, G., Liao, M., Yang, R., Ouyang, D., Xu, Z., Guo, X., Complete 3D model reconstruction using a depth sensor, Proceedings of International Conference on Intelligent Computing and Integrated Systems, Guilin, **2010**, 175-179.
2. Zheng, M., Zhu, J., Xiong, X., Zhou, S., Zhang, Y., 3D model reconstruction with common hand-held cameras, Virtual Real, **2016**, 20, 4, 221-235, <https://doi.org/10.1007/s10055-016-0297-5>.
3. Shih, N.-J., Kuo, H.-C., Chang, C.-F., 3D scan for special urban evening occasion, 2016 International Conference on Applied System Innovation (ICASI), **2016**, 1-4, <https://doi.org/10.1109/ICASI.2016.7539742>.
4. Nowak, P. S., Sankowski, W., Krotewicz, P., 3D face and hand scans acquisition system dedicated for multimodal biometric identification, 2016 MIXDES-23rd International Conference Mixed Design of Integrated Circuits and Systems, **2016**, 389-393, <https://doi.org/10.1109/MIXDES.2016.7529772>.
5. Laksono, D., Open source stack for Structure from Motion 3D reconstruction: A geometric overview, The 6th International Annual Engineering Seminar (InAES), **2016**, 196-201.
6. Menato, S., Landolfi, G., Alge, M., Sorlini, M., Empowering widespread shoe personalization via a 3D foot scanning App, 2014 International Conference on Engineering, Technology and Innovation (ICE), **2014**, 1-7, <https://doi.org/10.1109/ICE.2014.6871556>.
7. Novak, B., Možina, J., Jezeršek, M., 3D laser measurements of bare and shod feet during walking, Gait Posture, **2014**, 40, 1, 87-93, <https://doi.org/10.1016/j.gaitpost.2014.02.015>.
8. Gao, F., Wang, Q., Geng, W., Pan, Y., Acquisition of time-varying 3D foot shapes from video, Science China Information Sciences, **2011**, 54, 11, 2256, <https://doi.org/10.1007/s11432-011-4361-1>.
9. Yamashita, T., Yamashita, Y., Masuda, S., Sato-Shimokawara, E., Yamaguchi, T., Face direction recognition system for robot control

- system using fingertip gesture, 2017 IEEE/SICE International Symposium on System Integration (SII), **2017**, 980-985, <https://doi.org/10.1109/SII.2017.8279350>.
10. Song, K.-T., Chang, Y.-H., Chen, J.-H., 3D Vision for Object Grasp and Obstacle Avoidance of a Collaborative Robot, 2019 IEEE/ASME International Conference on Advanced Intelligent Mechatronics (AIM), **2019**, 254-258, [https://doi.org/10.1109/ AIM.2019.8868694](https://doi.org/10.1109/AIM.2019.8868694).
 11. Liao, B., Li, J., Ju, Z., Ouyang, G., Hand gesture recognition with generalized hough transform and DC-CNN using realsense, 2018 Eighth International Conference on Information Science and Technology (ICIST), **2018**, 84-90, <https://doi.org/10.1109/ ICIST.2018.8426125>.
 12. Zhang, M., Liang, J., Liu, L., Liang, Y., Wang, X., Denoising method of body scanning point cloud obtained by SR300, J Cent South Univ, **2018**, 49, 9, 2225-2231.
 13. Siena, F.L., Byrom, B., Watts, P., Breedon, P., Utilising the Intel RealSense camera for measuring health outcomes in clinical research, J Med Syst, **2018**, 42, 3, 53, <https://doi.org/10.1007/s10916-018-0905-x>.
 14. Carfagni, M., Furferi, R., Governi, L., Servi, M., Uccheddu, F., Volpe, Y., On the performance of the Intel SR300 depth camera: metrological and critical characterization, IEEE Sens J, **2017**, 17, 14, 4508-4519, <https://doi.org/10.1109/JSEN.2017.2703829>.
 15. Zabatani, A., Surazhsky, V., Sperling, E., Ben Moshe, S., Menashe, O., Silver, D.H., Karni, T., Bronstein, A.M., Bronstein, M.M., Kimmel, R., Intel® RealSense™ SR300 Coded light depth Camera, IEEE Trans Pattern Anal Mach Intell, **2019**, <http://doi.org/10.1109/TPAMI.2019.2915841> (Early Access).
 16. Patil, J.V., Bailke, P., Real time facial expression recognition using RealSense camera and ANN, 2016 International Conference on Inventive Computation Technologies (ICICT), **2016**, vol. 2, 1-6, <https://doi.org/10.1109/INVENTIVE.2016.7824820>.
 17. Wang, L., Xu, W., Du, K., Lu, W., Zhu, J., Zhang, J., Portabella Mushrooms Measurement in Situ Based on SR300 Depth Camera, Transactions of The Chinese Society of Agricultural Machinery, **2018**, 49, 12, 13-19.
 18. Witana, C.P., Xiong, S., Zhao, J., Goonetilleke, R.S., Foot measurements from three-dimensional scans: A comparison and evaluation of different methods, Int J Ind Ergon, **2006**, 36, 9, 789-807, <https://doi.org/10.1016/j.ergon.2006.06.004>.
 19. Wang, M., Wang, X.A., Fan, Z., Zhang, S., Peng, C., Liu, Z., A 3D foot shape feature parameter measurement algorithm based on Kinect2, EURASIP J Image Vide, **2018**, vol. 2018, 1, 1-12, <https://doi.org/10.1186/s13640-018-0368-5>.
 20. Jung, J., Lee, J.-Y., Jeong, Y., Kweon, I.S., Time-of-flight sensor calibration for a color and depth camera pair, IEEE Trans Pattern Anal Mach Intell, **2014**, 37, 7, 1501-1513, <https://doi.org/10.1109/TPAMI.2014.2363827>.
 21. Zhang, C., Zhang Z., Calibration between depth and color sensors for commodity depth cameras, in Computer Vision and Machine Learning with RGB-D Sensors: Springer, **2014**, pp. 47-64, https://doi.org/10.1007/978-3-319-08651-4_3.

© 2020 by the author(s). Published by INCDTP-ICPI, Bucharest, RO. This is an open access article distributed under the terms and conditions of the Creative Commons Attribution license (<http://creativecommons.org/licenses/by/4.0/>).

DEVELOPMENT OF PROCESSES IN THE USE OF PEROXIDE AS AN INGREDIENT TO REDUCE FREE FORMALDEHYDE LEVELS IN THE SKIN

Emiliana ANGGRIYANI*, Laili RACHMAWATI, Nais Pinta ADETYA

Department of Leather Processing Technology, Politeknik ATK Yogyakarta, Sewon, Bantul, 55281 Yogyakarta, Indonesia,
emiliana.anggry@gmail.com

Received: 13.01.2020

Accepted: 22.05.2020

<https://doi.org/10.24264/lfj.20.2.6>

DEVELOPMENT OF PROCESSES IN THE USE OF PEROXIDE AS AN INGREDIENT TO REDUCE FREE FORMALDEHYDE LEVELS IN THE SKIN
ABSTRACT. This study aims to reduce the levels of free formaldehyde in the skin. The material used is goat skin. The process is carried out by formaldehyde (formalin) tanning on pickled goat skin. Furthermore, skin that has been tanned with formalin is washed with peroxide (H_2O_2) 0.5%, 1% and 2%. The formalin tanned skin produced was tested for formalin levels contained in the skin, then the data obtained was analysed by One Way ANOVA test. In addition, physical tests were carried out for the average value of tear strength and softness. The results showed that the higher the level of H_2O_2 used, the smaller the formalin content in the skin. The best results were obtained using 1% H_2O_2 which was $0.12 \pm 0.005\%$ ($p < 0.05$) taking into account the safety aspects of H_2O_2 . Furthermore, free formaldehyde levels of 0.045 mg/kg were obtained at 1% H_2O_2 . The value of tear strength with formaldehyde is higher than that of chrome tanning while the softness value is still below that of chrome tanning. Therefore, the use of H_2O_2 can be considered in an effort to reduce the levels of formaldehyde contained in formaldehyde as an alternative tanner substitute for chrome minerals.

KEY WORDS: reduce, formaldehyde, peroxide, skin

DEZVOLTAREA UNOR PROCESE DE UTILIZARE A PEROXIDULUI CA INGREDIENT PENTRU REDUCEREA NIVELULUI DE FORMALDEHIDĂ LIBERĂ ÎN PIELE

REZUMAT. Acest studiu își propune reducerea nivelului de formaldehidă liberă din piele. Materialul folosit este pielea de capră. Procesul se realizează prin efectuarea tăbăcirii cu formaldehidă (formalină) pe piele de capră piplată. Mai mult, pielea care a fost tăbăcită cu formalină este spălată cu 0,5%, 1% și 2% peroxid (H_2O_2). Pielea tăbăcită cu formalină obținută a fost testată pentru a determina nivelurile de formalină conținută în piele, apoi datele obținute au fost analizate prin testul One Way ANOVA. În plus, s-au efectuat teste fizico-mecanice pentru a determina valoarea medie a rezistenței la sfâșiere și moliciunea. Rezultatele au arătat că, cu cât este mai mare nivelul de H_2O_2 utilizat, cu atât conținutul de formalină este mai mic în piele. Cele mai bune rezultate s-au obținut utilizând H_2O_2 în proporție de 1%, și anume $0.12 \pm 0.005\%$ ($p < 0.05$), ținând cont de aspectele de siguranță ale H_2O_2 . Mai mult, s-au obținut concentrații de formaldehidă liberă de 0,045 mg/kg la utilizarea H_2O_2 în proporție de 1%. Valoarea rezistenței la sfâșiere a pielii cu conținut de formaldehidă este mai mare decât cea pentru pielea tăbăcită în crom, în timp ce valoarea moliciunii este încă sub cea obținută pentru pielea tăbăcită în crom. Prin urmare, se poate lua în considerare utilizarea H_2O_2 în efortul de a reduce nivelurile de formaldehidă ca o soluție alternativă de tăbăcire pentru utilizarea cromului.

CUVINTE CHEIE: reducere, formaldehidă, peroxid, piele

DÉVELOPPEMENT D'UN PROCÉDÉ D'UTILISATION DU PEROXYDE COMME INGRÉDIENT POUR RÉDUIRE LES NIVEAUX DE FORMALDÉHYDE LIBRE DANS LA PEAU

RÉSUMÉ. Cette étude vise à réduire les niveaux de formaldéhyde libre dans la peau. Le matériau utilisé est la peau de chèvre. Le processus est effectué par le tannage au formaldéhyde (formol) sur la peau de chèvre picklée. De plus, la peau tannée au formol est lavée au peroxyde (H_2O_2) en proportion de 0,5%, 1% et 2%. La peau tannée au formol a été testée pour déterminer les niveaux de formol contenus dans la peau, puis les données obtenues ont été analysées par le test One Way ANOVA. De plus, des tests physiques ont été effectués pour déterminer la valeur moyenne de la résistance à la déchirure et de la douceur. Les résultats ont montré que plus le niveau de H_2O_2 utilisé était élevé, plus la teneur en formol de la peau était faible. Les meilleurs résultats ont été obtenus en utilisant 1% de H_2O_2 qui était de $0,12 \pm 0,005\%$ ($p < 0,05$) en tenant compte des aspects de sécurité de H_2O_2 . De plus, on a obtenu des niveaux de formaldéhyde libre de 0,045 mg/kg en utilisant 1% de H_2O_2 . La valeur de la résistance à la déchirure avec le formaldéhyde est supérieure à celle du tannage au chrome tandis que la valeur de douceur est toujours inférieure à celle du tannage au chrome. Par conséquent, l'utilisation de H_2O_2 peut être envisagée dans le but de réduire les niveaux de formaldéhyde comme solution de tannage alternatif aux minéraux de chrome.

MOTS CLÉS : réduire, formaldéhyde, peroxyde, peau

* Correspondence to: Emiliana ANGGRIYANI, Department of Leather Processing Technology, Politeknik ATK Yogyakarta, Jl. Ringroad Selatan, Glugo, Panggungharjo, Sewon, Bantul, 55281, Yogyakarta, Indonesia, emiliana.anggry@gmail.com

INTRODUCTION

The tanning process is a process that converts raw skin into finished skin to be used as raw material for making leather products. The leather tanning process consists of beam house operation, tanning, post tanning and finishing processes. These processes use various kinds of chemicals. Chemicals used in the tanning process should be environmentally friendly materials that are safe to use and safe for the environment. During this time the tanning process with chrome tanning materials is widely used to produce quality products. On the one hand, the use of chrome tanning material must be reduced from time to time because of the side effects of its use.

Some previous studies mention that chromium can damage the environment, is carcinogenic. Carcinogenic risk of chrome is due to the formation of Cr (VI) from Cr (III), therefore the first step that can be done is to reduce the formation of Cr (VI). [1] Vegetable material used in the retanning process can reduce the formation of Cr (VI) because the vegetable contains phenol compounds which will be oxidized first if there are free radicals or oxidizing agents. In addition to preventing the formation of hazardous compounds, another thing that can be done to form a better environment is to reduce the use of chrome as a tanning agent. Therefore, its use must be really considered, to maintain a better environmental sustainability. Much research has been done to be able to replace the chrome tanning material as a tanner material with good quality, of course, with existing developments.

The use of non-chrome tanning agents is very necessary in the context of substitution for the tanning process. One of the ingredients that can be used is formalin tanning material for garment articles. The use of tanning agents in the future can be developed for chrome substitution. However, based on international regulations the final leather product should have maximum ≤ 75 mg/kg of free formaldehyde content.

The common source of free formaldehyde found in leathers comes from tanning or retanning agents. Unreacted free formaldehyde becomes the primary source of formaldehyde detected in the leather. One of the desirable processes for aldehyde-tanned leather to reduce the formaldehyde content that have been

studied is the modification of glutaraldehyde with polyurethane surfactant mixture solutions at different times. The formaldehyde content of mixture solution decreased by 5% when the solution mixed an hour later [2].

The use of formaldehyde as tanning agent, it is necessary to consider the presence of formaldehyde in the skin. Therefore it is important to reduce the presence of formaldehyde content in leather [3]. Taking advantage of the ability of polyphenols from vegetables to reduce the formaldehyde content of leathers treated with formaldehyde resins is an excellent example of clean technology in the tannery sector, especially given the known harmful nature of formaldehyde. Such measures help to achieve a more sustainable leather industry.

The decrease in the formaldehyde content in leather retanned with formaldehyde synthesized resins by the dyeing process could be explained by the reaction between formaldehyde and the amino groups present in the dyes structure. It should be noted that the extent of this decrease is a function not only of the number of the amino groups present in the dyes but also of their relative reactivity with formaldehyde. The vicinity of other functionalities, such as $-OH$, $-N=N-$ and $-NO_2$, to the amino groups can lead to the formation of relatively stable cyclic structures mediated by hydrogen bonds. When this occurs, the reactivity of this amino group with formaldehyde can decrease [4].

In addition to the availability of chrome substitutes, the thing to think about is the quality of the skin produced. Because after all the skin produced must have certain standards to be sold. Testing the physical quality of the skin must be considered in order to achieve the desired skin standard.

The existence of complaints of environmental security due to the use of chrome tanning materials encourage the search for chromic substitution materials, which can provide quality that resembles chrome tanned leather. This is of course by still paying attention to the safety standards for the use of these substitutes, in this case formaldehyde. Formaldehyde can be used as long as it can meet skin safety standards.

EXPERIMENTAL

Materials and Methods

Instruments

Drum process, knife, pH indicator, bucket, and scales.

Materials

6 pickle goats skin (5 SqFt/ 0,6 mm), formalin 70%, NaCl, water, wetting agent (Peramit MLN, Pulcra chemicals), Acid batting (Feliderm Bat AB, Stahl), Bleaching agent (NaOCl,

Brataco), Oxalic acid, NaHCO₃, Na-Formate, H₂O₂, Na-Bisulfit, dispersing agent (Coralon OT, Stahl), syntan (Tanicor PWB, Stahl), acrylic (Tergotan ESN, Stahl), sulphited oil (Derminol ASN, Stahl), Formic Acid, and fungicide (Preventol Cr, Lanxess).

Tanning Process

The tanning process is carried out by pretanning on pickle goat skin using formaldehyde, then washing with peroxide at the presentation of 0.5%, 1% and 2%. Then proceed with tanning using a replacement tanning agent (syntan).

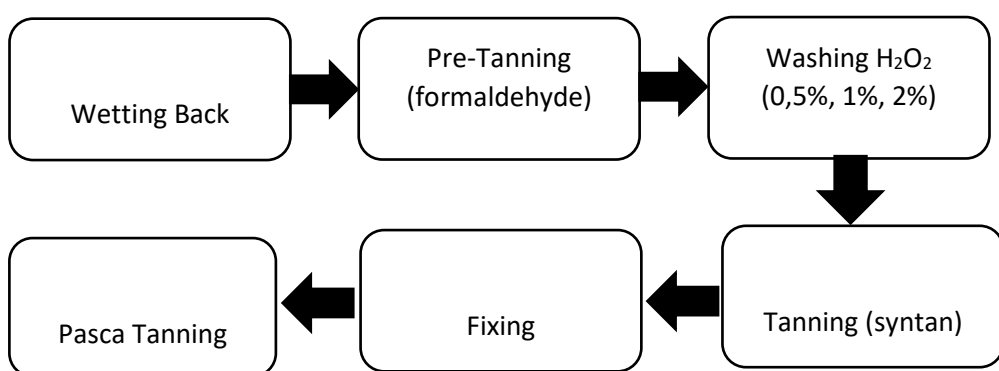


Figure 1. Tanning Process Diagram

Data Analysis

The results obtained (after fixing) were analyzed by the Different Test ANOVA, then continued with Independent Sample T-Test using the SPSS statistical 22 IBM. Further results from crust skin were analyzed using FTIR (Fourier Transmitted Infra Red). Furthermore, crust skin was also tested organoleptically to determine the value of tear strength and softness.

RESULTS AND DISCUSSIONS

Formaldehyde Content

The bound Formalin content contained in the skin decreases when washing by using H₂O₂ (peroxide) starting from 0.5%, 1% and 2% as shown in Table 1. This shows that the higher the percentage of peroxide used in the end of tanning can reduce bound formalin levels detected. Results in Table 1 show that there was a significant difference ($P < 0.05$) between 0.5%, 1% and 2% peroxide use. Whereas between 1%

and 2% peroxide use there was no significant difference (Independent Sample T-Test). Therefore, the best results used to produce the lowest formalin levels are enough to use 1% peroxide.

Table 1: Formaldehyde content on skin

H ₂ O ₂ level	Formaldehyde level (%)
0.5%	0.23 ± 0.01 ^a
1%	0.12 ± 0.005 ^b
2%	0.11 ± 0.0 ^b

*Different superscript shows the significance different ($P < 0.05$)

Skins with 1% H₂O₂ were tested for free formaldehyde levels and 0.045 mg/kg was the average result (meet the standard on Table 2). Important reductions in the formaldehyde content of formaldehyde resin-treated leathers by the action of adequate scavengers will result in a more sustainable tanning industry not only from the environmental point of view but also from a human health viewpoint, given

the carcinogenic character of formaldehyde. This carcinogenic character fully justifies the

application of the adequate formaldehyde scavengers in industrial processing of leather, textiles and construction materials [5].

Table 2: Free Formaldehyde content standards [6]

Countries/standards	Free formaldehyde content (mg/kg)		
	Articles for babies	Skin contact products	Not contact by skin
China	≤20	≤75	≤300
European Union	≤20	≤75	≤200
America	≤20	≤75	≤300
Japan	≤20	≤75	≤300
Oeko-Tex Standard 100	≤20	≤75	≤300
OKO Tex	≤20	≤75	≤300
SG Mark	≤50	≤75	≤150
ECO-Tex Standard 100		≤75	≤300
Australia		≤100	≤1500

The most dominant reaction between formaldehyde and skin protein is the skin amine group from the amino acid lysine. The reaction between amines and formaldehyde forms a

formation called methylol derivatives [7]. The bond between the skin amine group and the aldehyde as shown in Figure 2.

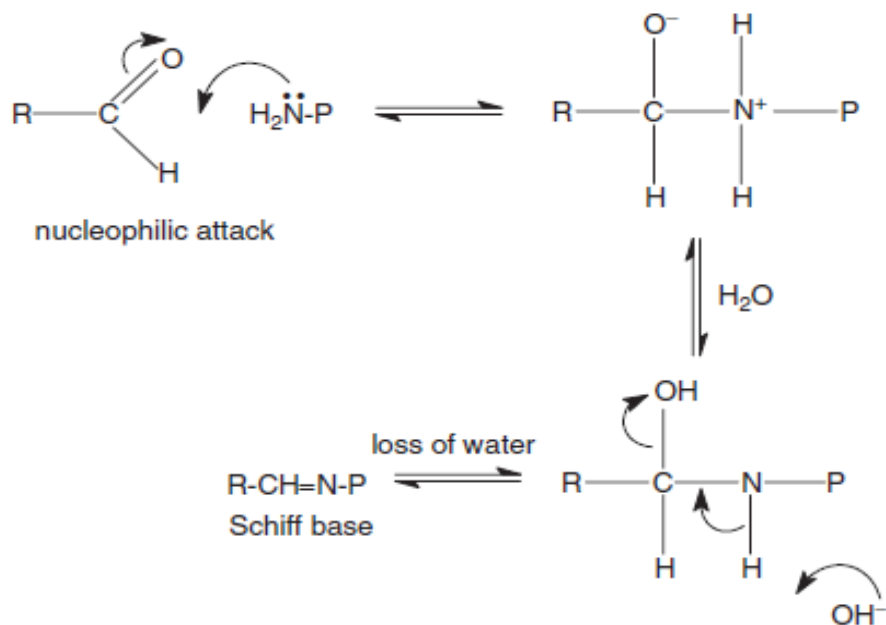


Figure 2. Aldehyde reaction with an amino group of skin proteins (P = protein) [8]

Apart from using peroxide on decrease formaldehyde content, gallic acid can be used [5]. When the presence of formaldehyde in leather is expected, gallic acid is a good option either in the final washing of the leather production process or as an alternative to formic acid as final fixing agent since it causes a marked reduction in the formaldehyde content. In most of the treatments with gallic acid, the formaldehyde content in

treated leathers was below the limit for goods that are in direct contact with skin (65-75 mg/kg).

The values of formaldehyde reduction are somewhat higher due to the greater amount of mimosa extract applied. The change in the formic acid by the gallic acid as fixing agent resulted in a reduction of formaldehyde content that grew from 60% to 85%. This reduction was

even more pronounced if together with the effect of fixing with gallic acid, the action of the mimosa extract in the retanning process was considered. The effect of gallic acid in reducing the formaldehyde content in split leather retanned with melamine formaldehyde resin was more intense and occurred more quickly than that of the mimosa extract, probably due to the greater number of –OH groups amenable to reaction with formaldehyde in the gallic acid offered than in the mimosa extract. Therefore, gallic acid is suitable as formaldehyde scavenger in the leather industry, although further experiments should be carried out to check its effect on fastness properties (mainly to light and temperature) and leather shades [5].

Formalin is a toxic material that is harmful to the environment and health. Formalin can be used as tanning agent because it contains formaldehyde. Formaldehyde is one of the simple aldehyde tanners. Formaldehyde when used as tanning agent can produce white skin (wet white leather).

Formaldehyde has been used as a tanning agent and as a means of hardening proteins for many years. It is a remarkable tanning material that usually has its practical application as an adjunct to some other tanning agent. The predominant reaction between formaldehyde and hide protein is generally accepted to be with the amino acid, lysine. This is a typical amine-

formaldehyde reaction with the formation of the methylol derivatives [7]. The tannage yields leather with shrinkage temperature up to 80°C [8].

Global warming or the issue of “climate change” is pushing for a greener or cleaner industry both for leather, textile and paper processing. Green technology for chrome-free tanning based on D-Lysine GTA has been developed. In the formaldehyde reaction with proteins, the first to be attacked is the amine group in the Lysine position between the polar groups of the peptide. The physicochemical properties of the skin are improved with respect to texture, hydrothermal stability, mechanical strength, resistance to collagenolytic activity, and also organoleptic properties [9]. The amino groups both lysine and hydroxyproline are involved in the glutaraldehyde tanning reaction. It is possible that D-Lysine has improved hydrothermal stability. Increased wrinkle temperature indicates increased stability of wet white skin [9].

The skin which is retouched with formaldehyde resin is then retreated with vegetable polyphenol components, indicating that the formaldehyde content in the skin produced is maintained below 16 mg/kg [3]. States that the formalin content in the skin is reduced by adding grape seed extract to the process of retanning [10].

Table 3: Physical characteristics of goat crust

Treatment	Tear strength (kg/cm)	Softness (mm)
Tanning formaldehyde (without washing)	34.81	4.2
Tanning formaldehyde (washing with peroxide)	29.27	4.27
Chrome tanning	24.52	6.37

Based on Table 3 it can be seen that tanning leather with formalin is able to produce crust leather with higher tear strength than chrome tanning for garment articles. While from the softness level, crust skin tanned using formalin is still low compared to chrome tanning. Tear strength without washing has a higher yield because free formalin is still contained in the skin, so the level of material strength in the skin is stronger than after washing with peroxide. However, the effects produced from the skin without washing formalin are less recommended,

because there are certain standards that must be met by each skin product for tolerance of the formaldehyde content in the skin.

The main advantages of chrome tanning are high speed, low cost, light color, and excellent preservation of the hide protein. Chrome tanning rapidly took its place in the commercial world shortly after its discovery and became the most common method of tanning light leather [7].

Excessive formaldehyde should be removed by washing in order to avoid callouses on the grain. A further disadvantage consists

in the increased water-absorption of leathers treated with formaldehyde. However, a pure white colour of leather and a fine, closed appearance of grain are obtained [11].

In the tanning process using formaldehyde, a cross-linking occurs that forms a covalent bond between the aldehyde group (-CHO) with the NH_2^+ group of the amino acids glycine, proline and hydroxyproline that form bonds with triple helix in skin collagen. However, the bond is lower because in formaldehyde the absorbability of the tanned material is not strong enough compared to the chromium tanning material which has a stronger absorption to form complex bonds [11].

FTIR Analysis

FTIR analysis of the sample is shown in Figure 3. Goat skin has several characteristic

absorption bands. Strong bands at absorption of 1451 cm^{-1} are characteristic of aromatic rings (C-C and C-H), while secondary C-O alcohol vibrations are at 1087 cm^{-1} [12]. The alkyne absorption band C = C is shown as a strong band in the wave region $1500\text{-}1675\text{ cm}^{-1}$ [13]. When viewed from the absorption of infrared radiation, there is no significant change between the absorption bands of the skin before and after washing with peroxide. However, there is a slight difference in the skin sample without the peroxide washing process (0% H_2O_2) where the C=N bond is still detected through absorption bands in the wave number region $1547\text{-}1551\text{ cm}^{-1}$ [12]. While in the process of washing peroxide 0.5%; 1% and 2%, the band size in the C=N bond constricts with increasing peroxide concentration.

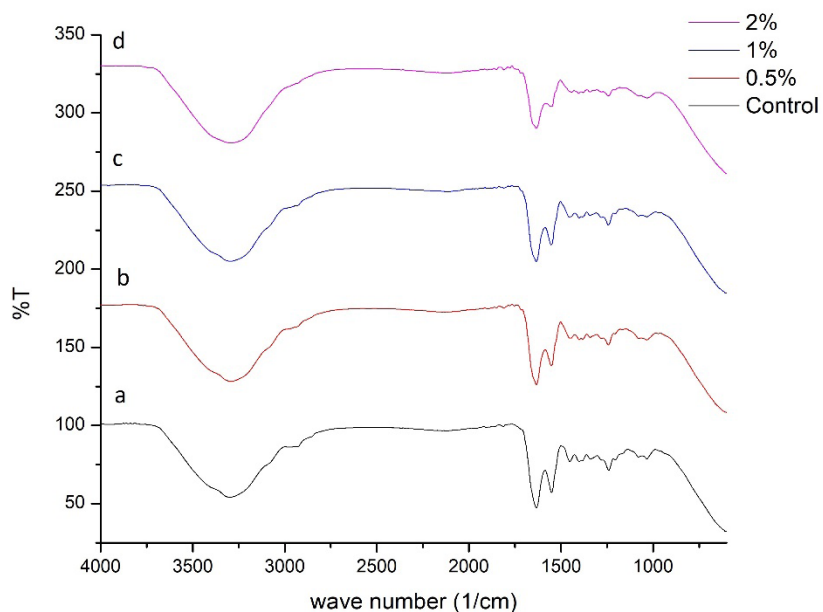


Figure 3. FTIR spectra of goat skin with various H_2O_2 concentrations used in washing process (a) 0%; (b) 0.5%; (c) 1% and (d) 2%

Figure 3 shows the FTIR spectrum of goat skin with various concentrations of peroxide used in the washing process. Strong bands at 1653 cm^{-1} are characteristic of C=O stretching vibrations around $1650\text{-}1900\text{ cm}^{-1}$. Schiff bases are formed due to the reaction between aldehyde bonds and amino groups. The functional group in this compound is the carbonyl group, C=O. The presence of hydrogen atoms makes aldehydes very easily oxidized. Aldehydes can be

easily oxidized using all types of oxidizing agents [14]. Hydrogen peroxide (H_2O_2) is an inorganic chemical that has strong oxidizing properties. One of the advantages of hydrogen peroxide compared to other oxidizing agents is that it is environmentally friendly because it does not leave harmful residues [15].

Goat skin washed with 2% peroxide has the sharpest O-H vibrations. This shows that this sample has the most amount of O-H. These

results illustrate that hydrogen bonds that are bound to amino groups form stable structures. When this occurs, the reactivity of this amino group with formaldehyde can decrease [5]. The hydrogen bond increases for the oxidation of C-OH to C = O, this is known from the change in the O-H band around 2500-3300 cm⁻¹ which is increasingly swooping with the addition of H₂O₂ concentration (Figure 3). Therefore, the optimal concentration of peroxide used is 2%.

CONCLUSIONS

The use of H₂O₂ of 1% can be used to reduce the content of formalin bound in tanned skin using formaldehyde. Tanning with formaldehyde tanning material can produce higher tear strength compared to chrome tanning material.

The use of formaldehyde as a tanning agent must still be considered and further developed for future research. This is because there are still a number of things that remain uncertain regarding environmental regulations, in addition to the formalin tanning material must be considered regarding its usefulness for various types of articles as a substitute for chrome.

REFERENCES

- Anggriyani, E., Nugroho, A.R., Rosiat, N.M., Technology of reducing Cr(VI) on leather processing using mimosa as retanning agent, *Leather and Footwear Journal*, **2019**, 19, 1, 67–72, <https://doi.org/10.24264/lfj.19.1.8>.
- Sun, X., Jin, Y., Lai, S., Pan, J., Du, W., Shi, L., Desirable retanning system for aldehyde-tanned leather to reduce the formaldehyde content and improve the physical-mechanical properties, *J Clean Prod*, **2018**, 175, 199–206, <https://doi.org/10.1016/j.jclepro.2017.12.058>.
- Marsal, A., Cuadros, S., Manich, A.M., Izquierdo, F., Font, J., Reduction of the formaldehyde content in leathers treated with formaldehyde resins by means of plant polyphenols, *J Clean Prod*, **2017**, 148, 518–526, <https://doi.org/10.1016/j.jclepro.2017.02.007>.
- Marsal, A., Cuadros, S., Cuadros, R.M., Font, J., Manich, A.M., Dyestuffs and formaldehyde content in split leather treated with formaldehyde resins, *Dyes Pigm*, **2018**, 158, 50–59, <https://doi.org/10.1016/j.dyepig.2018.05.027>.
- Marsal, A., Cuadros, S., Ollé, L., Bacardit, A., Manich, A.M., Font, J., Formaldehyde scavengers for cleaner production: A case study focused on the leather industry, *J Clean Prod*, **2018**, 186, 45–56, <https://doi.org/10.1016/j.jclepro.2018.03.109>.
- Wang, X., Yan, Z., Liu, X., Qiang, T., Chen, L., Guo, P., Yue, O., An environmental polyurethane retanning agent with the function of reducing free formaldehyde in leather, *J Clean Prod*, **2019**, 207, 679–688, <https://doi.org/10.1016/j.jclepro.2018.10.056>.
- Thorstensen, T., Practical Leather Tehnology, 4rd ed. Florida, New York: Robert E. Keiger Publishing Company Malabar, **1993**.
- Covington, A., Tanning Chemistry: The Science of Leather, Northampton: Royal Society of Chemistry, **2009**.
- Krishnamoorthy, G., Sadulla, S., Sehgal, P.K., Mandal, A.B., Greener approach to leather tanning process: D-Lysine aldehyde as novel tanning agent for chrome-free tanning, *J Clean Prod*, **2013**, 42, 277–286, <https://doi.org/10.1016/j.jclepro.2012.11.004>.
- Bayramoğlu, E.E., Hidden treasure of the nature: PAs. The effects of grape seeds on free formaldehyde of leather, *Ind Crops Prod*, **2013**, 41, 1, 53–56, <https://doi.org/10.1016/j.indcrop.2012.03.040>.
- John, G., Possible Defects in Leather Production, Lampertheim: Europaring 24 D-68623, **1996**.
- Baker, M.J., Trevisan, J., Bassan, P., Bhargava, R., Butler, H.J., Dorling, K.M., Fielden, P.R., Fogarty, S.W., Fullwood, N.J., Heys, K.A., Hughes, C., Lasch, P., Martin-Hirsch, P.L., Obinaju, B., Sockalingum, G.D., Sule-Suso, J., Strong, R.J., Walsh, M.J., Wood, B.R., Gardner, P., Martin, F.L., Using Fourier transform IR spectroscopy to analyze biological materials, *Nat Protoc*, **2014**, 9, 8, 1771–1791, <https://doi.org/10.1038/nprot.2014.110>.
- Canals Parello, T., Morera Prat, J.M., Combalia Cendra, F., Bartoli Soler, E., Application of Infrared Spectroscopy (FTIR and NIR) in Vegetable Tanning Process Control, *J Soc Leath Tech Ch*, **2013**, 97, 93–100.
- Wang, X., Ren, L., Qiang, T., Novel Way of Transformation of Tannery Waste to

- Environmentally Friendly Formaldehyde Scavenger, *Environ Prog Sustain Energy*, **2019**, 28, 2, 285–290, <https://doi.org/10.1002/ep.10329>.
15. Al Zoubi, W., Ko, Y.G., Organometallic complexes of Schiff bases: Recent progress in oxidation catalysis, *J Organomet Chem*, **2016**, 822, 173–188, <https://doi.org/10.1016/j.jorgancem.2016.08.023>.

© 2020 by the author(s). Published by INCDTP-ICPI, Bucharest, RO. This is an open access article distributed under the terms and conditions of the Creative Commons Attribution license (<http://creativecommons.org/licenses/by/4.0/>).

LOAD TRANSFERENCE WITH RUNNING SPEED IN NATURAL REAR-FOOT STRIKE MALE RUNNERS

Ruoyi LI^{1,2}, Hao LIU¹, Xuecan CHEN³, Jitka BADUROVA⁴, Haojun FAN², Luming YANG^{1,2*}

¹National Engineering Laboratory for Clean Technology of Leather Manufacture, Sichuan University, Chengdu, 610065, China

²Key Laboratory of Leather Chemistry and Engineering, Sichuan University, Chengdu, 610065, China

³Fuzhou Customs District P.R. China, Fuzhou, 350000, China

⁴Tomas Bata University, Zlin, 76001, Czech Republic

Received: 16.09.2019

Accepted: 03.04.2020

<https://doi.org/10.24264/lfj.20.2.7>

LOAD TRANSFERENCE WITH RUNNING SPEED IN NATURAL REAR-FOOT STRIKE MALE RUNNERS

ABSTRACT. The purpose of this study was to identify the influence of running speed on plantar pressure, and to use a load transfer algorithm to investigate the load transference in healthy recreational male runners who had a natural rear-foot strike pattern. Totally, 49 healthy males participated in this study, 39 of them (age 22.8 ± 1.8 years, weight 65.6 ± 7.9 kg, height 171.9 ± 4.0 cm) were identified as rear-foot strike runners. Data of pressure parameters, including maximum force, peak pressure, contact area and force-time integral (FTI) was recorded by Pedar-X insole plantar pressure measurement system at 8 different speeds (5, 6, 7, 8, 9, 10, 11, 12 km/h). The results indicated that with the increase of running speed, plantar pressure significantly increased under all foot regions except for the big toe. Faster running speeds resulted in significant lower FTI in all foot regions except for lateral midfoot and heel. Medial metatarsal, central metatarsal, and big toe were the main loading regions for rear-foot strike male runners during running. Load transferred from medial foot to lateral foot in transverse direction, and from toes to metatarsal, midfoot and heel in the longitudinal direction with increasing speeds. As a component of the spring mechanism, the arch played a key role in supporting and transferring loads.

KEY WORDS: running, speed, load transfer, rear-foot strike, plantar pressure

TRANSFERUL DE SARCINĂ ÎN FUNCȚIE DE VITEZA DE ALERGARE ÎN CAZUL ALERGĂTORILOR DE SEX MASCULIN CARE ATING SOLUL CU RETROPICTORUL

REZUMAT. Scopul acestui studiu a fost de a identifica influența vitezei de alergare asupra presiunii plantare și de a utiliza un algoritm de transfer de sarcină pentru a investiga transferul de sarcină la alergătorii amatori sănătoși de sex masculin care au o tendință naturală de a atinge solul cu retropicatorul. În total, 49 de bărbați sănătoși au participat la acest studiu, 39 dintre ei (vârstă $22,8 \pm 1,8$ ani, greutatea $65,6 \pm 7,9$ kg, înălțimea $171,9 \pm 4,0$ cm) au fost identificați ca alergători care ating solul cu retropicatorul. Datele parametrilor de presiune, cuprindând forță maximă, presiunea maximă, zona de contact și integrala forță-timp (FTI) au fost înregistrate de sistemul de măsurare a presiunii plantare Pedar-X la 8 viteze diferite (5, 6, 7, 8, 9, 10, 11, 12 km/h). Rezultatele au indicat că odată cu creșterea vitezei de alergare, presiunea plantară a crescut semnificativ în toate regiunile piciorului, cu excepția degetului mare. Viteza de alergare mai rapidă a condus la o scădere semnificativă a FTI în toate regiunile piciorului, cu excepția zonei laterale și a călcâiului. Principalele regiuni în care s-au înregistrat presiuni mari în cazul alergătorilor de sex masculin care ating solul cu retropicatorul în timpul alergării au fost: zonele mediană și centrală ale metatarsienelor și degetul mare. Sarcina se transferă din zona mediană în zona laterală în direcție transversală, și de la degete la metatarsiene, zona mediană și călcâi în direcție longitudinală odată cu creșterea vitezei. Ca o componentă a mecanismului de arc, boltă plantară a jucat un rol cheie în susținerea și transferul presiunii.

CUVINTE CHEIE: alergare, viteză, transfer de sarcină, atingerea solului cu retropicatorul, presiune plantară

TRANSFERT DE CHARGE EN FONCTION DE LA VITESSE DE COURSE POUR LES COURREURS DU SEXE MASCULIN QUI TOUCHENT LE SOL AVEC L'ARRIÈRE-PIED

RÉSUMÉ. Le but de cette étude était d'identifier l'influence de la vitesse de course sur la pression plantaire et d'utiliser un algorithme de transfert de charge pour étudier le transfert de charge chez des coureurs amateurs du sexe masculin en bonne santé qui ont une tendance naturelle à toucher le sol avec l'arrière-pied. Au total, 49 hommes en bonne santé ont participé à cette étude, 39 d'entre eux (âge $22,8 \pm 1,8$ ans, poids $65,6 \pm 7,9$ kg, taille $171,9 \pm 4,0$ cm) ont été identifiés comme des coureurs qui touchent le sol avec l'arrière-pied. Les données des paramètres de pression, y compris la force maximale, la pression maximale, la zone de contact et l'intégrale force-temps (FTI) ont été enregistrées par le système de mesure de la pression plantaire Pedar-X à 8 vitesses différentes (5, 6, 7, 8, 9, 10, 11, 12 km/h). Les résultats ont indiqué qu'avec l'augmentation de la vitesse de course, la pression plantaire a augmenté de manière significative dans toutes les régions du pied à l'exception du gros orteil. Des vitesses de course plus rapides ont entraîné une baisse significative de la FTI dans toutes les régions du pied, à l'exception du milieu du pied et du talon. Le métatarsien médial, le métatarsien central et le gros orteil étaient les principales régions de chargement des coureurs du sexe masculin qui touchent le sol avec l'arrière-pied pendant la course. La charge est transférée du pied médial au pied latéral dans le sens transversal, et des orteils au métatarsien, au milieu du pied et au talon dans le sens longitudinal à mesure que la vitesse augmente. En tant que composant du mécanisme à ressort, la voûte plantaire a joué un rôle clé dans le soutien et le transfert des pressions.

MOTS CLÉS : course, vitesse, transfert de charge, toucher le sol avec l'arrière-pied, pression plantaire

* Correspondence to: Assoc. Prof. Luming YANG, Key Laboratory of Leather Chemistry and Engineering, Sichuan University, No.24 South Section 1, Yihuan Road, Chengdu, China, 610065, Phone: +86 186 2811 7800, email: ylmll1982@126.com

INTRODUCTION

During the past few decades, running as a recreational activity has become one of the most popular exercises to maintain health. However, running could cause discomfort and injuries in the lower extremity and the foot [1, 2]. A recent meta-analysis revealed that, the reported incidence rate of running-related injury ranged from 2.5 to 33.0 injuries per 1000 hours of running [3]. It can be suggested that the lower limb injuries are associated with excessive high speed running exposure [4, 5]. Furthermore, load distribution plays an essential role for the detection of injuries in the foot [6, 7]. Since running speed effects human biomechanical features, it is necessary to explore how running speed effects human bodies.

The influence of running speed on plantar pressure has been reported in several previous studies. I-Ju Ho *et al.* found that the peak pressure significantly increased except for the medial forefoot and the hallux with the increase of running speed [8]. However, the plantar pressure was compared only in three speeds. Fourchet *et al.* compared the plantar pressure distribution in highly trained adolescent runners at low versus high running velocity [9]. But it is still unclear in the recreational adult male runners. Kernozeck *et al.* reported that all plantar loading variables increased with the exception of contact area when treadmill running speed was increased from 2.24 m/s to 3.13 m/s [10]. Based on the aforementioned studies, it was found that the results of these studies had not reached a consensus. This could be due to the use of many different characteristics, such as the subdivisions of plantar location. An additional important point is that the potentially confounding influence of speed on pressure values was not consistently controlled. One of the influences was the foot-strike pattern. Previous research has revealed three different ways the foot can collide with the ground [11]: heel landing first (rear-foot strike, RFS), ball of the foot landing first (fore-foot strike, FFS) and the heel and ball of the foot land simultaneously (mid-foot strike, MFS). The three ways are different at foot landing, load transference and pressure distribution during running [12, 13], but these differences were not taken into account in the above studies. Since 75–80% of shod endurance

runners were RFS [14], this study chose to focus solely on RFS. Likewise, little attention had been given to the possibility that different shoes used in these studies had effect on plantar pressure distribution in these studies. Unlike other studies, this study concentrated on recreational adult male runners with natural RFS pattern and further used standard shoes. In addition, a wide range of running speeds from 5 km/h to 12 km/h were selected as a supplementary for previous studies.

Old study had indicated to use algorithm and diagram to identify how the load transfer on foot in different situation [15-17]. Bus *et al.* used a load transfer diagram to show how plantar pressure was relieved when using forefoot offloading shoes in diabetic foot [15]. Mingyu Hu *et al.* designed an algorithm to quantify the plantar force transference in children from 2-6 years [16]. In our study, it is the first time a load transfer algorithm is used to explore how the load transfers with the increase of running speed. Moreover, load transfer algorithm was improved in order to better suit this study. Many studies had investigated the influence of running speed on plantar pressure distribution, but how the plantar pressure distribution differences come and how the load transfers with the increase of running speed were still unclearly. The use of this load transfer analysis method can help reach a better understanding of the mechanisms of how the foot structure acts to transfer load in different foot regions.

Therefore, the purpose of this study was to identify the influence of running speed on plantar pressure, and to use a load transfer algorithm to investigate the load transference in healthy recreational male runners who had a natural rear-foot strike pattern. We hypothesized that faster running speed would result in an increase in plantar pressure measurements, and load may transfer along the transverse or longitudinal arch in anterior-posterior and medial-lateral directions.

METHODS

Participants

In total, 49 healthy males (age 22.8 ± 1.7 years, body mass 65.3 ± 7.8 kg, height $172.1 \pm$

3.8 cm), without known neurologic or lower extremity orthopedic pathology participated in this study. They were all right leg dominant recreational runners who ran about one hour per week. Informed consent was obtained from each participant, and the study was approved by the Ethics Committee of Sichuan University. According to Altman and Davis's study [18], participants were defined into rear-foot strike and other foot strike pattern (mid-foot strike and fore-foot strike). 39 males (age 22.8 ± 1.8 years, weight 65.6 ± 7.9 kg, height 171.9 ± 4.0 cm) were identified as rear-foot strike and were focused on in this study. Plantar pressure factors were measured by Novel Pedar-X in-shoe system (Novel, Munich, Germany). Each pressure insole contained 99 capacitive sensors that were calibrated prior to data collection. The insole was flexible so that it could be easily placed into the bottom of the shoe. The sampling rate was set to a frequency of 50 Hz. All the participants were sized and fitted to a pair of standard shoes (Nike Free 5.0, Nike, America) to counter a possible bias of shoe type or shoe construction on the subjects' running style. The shoes size was a US size 8. The shoes were purchased solely for Pedar data collection and had not been used for any other purpose. And the participants were requested to wear the same socks which were provided during the test. The treadmill (King Smith T211&T221, China) consisted of a walking surface of 1220×420 mm and could be set to speeds from 0.0km/h to 16.0km/h accurately. As for Asian recreational male runners, during the pre-test, 5km/h was found to be the lowest speed that participants could jog. Meanwhile, 12 km/h was the highest attainable speed for most participants found among Asian recreational male runners. Therefore, the range of running speed selected in this study was from 5 km/h to 12 km/h.

Procedure

Plantar pressure factors were recorded as participants wearing the same socks and standard shoes ran on the treadmill at 8 different speeds (5, 6, 7, 8, 9, 10, 11, 12 km/h) with zero slope. Data of pressure parameters, including maximum force, peak pressure, contact area and force-time integral (FTI) was recorded by Pedar-X insole plantar pressure measurement system.

Prior to testing, all participants were informed about the procedures. A warmup was instructed that would include regular stretches as well as running at a preferred speed so that participants could familiarize themselves with the treadmill and standard shoes. After the warmup, participants were requested to begin to run on the treadmill in a self-selected speed, allowing their foot strike pattern to be verified from the data collected. Next, treadmill settings were adjusted and data collected at each speed during participants' running process. Participants were allowed one-minute acclimation period before data collection began. Data would be collected for 20 seconds at each speed respectively. A brief rest period was provided (approximately one minute) if the participants needed during the test.

Statistical Analysis

For the analysis of plantar pressure distribution, plantar foot was divided into eight anatomical regions (Figure 1): big toe (BT), toes 2-5 (T2-5), medial metatarsal (MM), central metatarsal (CM), lateral metatarsal (LM), medial midfoot (MMF), lateral midfoot (LMF) and heel (H). Analysis of in-shoe pressure data was done using Novel software. The right foot of each participant was used during statistical analysis [19]. For each runner, the mean plantar pressure parameters of the right foot were calculated based on five successful consecutive steps chosen from 20 seconds of treadmill running data. Statistical analysis was conducted by SPSS17.0. By application of Kolmogorov Smirnov, all data were found to be in normal distribution. A one-Way ANOVA was used to examine the differences in plantar pressure parameters for each region among the different running speeds. The level of $\alpha = 0.05$ ($p \leq 0.05$) was perceived as significant for statistical analyses.

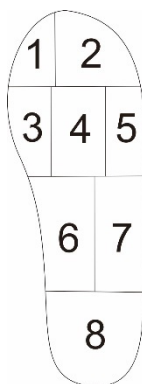


Figure 1. Foot regions

- [1] Big toe
- [2] Toes 2-5
- [3] Medial metatarsal
- [4] Central metatarsal
- [5] Lateral metatarsal
- [6] Medial midfoot
- [7] Lateral metatarsal
- [8] Heel

Load Transfer Algorithm

Plantar load transference has been explored to establish a correlation between the varied parts of the foot structure [16]. A load transfer algorithm was improved to quantify the plantar load transference with the running speeds increasing from 5 km/h to 12 km/h in healthy rear-foot strike male runners (Figure 3). The FTI is a measure of the force impulse or the load applied to the foot in a given region [20]. In this study, inter-regional force transfer was assessed by relative FTI using the load transfer algorithm. Relative FTI was the regional FTI value normalized to total foot FTI. Relative FTI (%) = $100 \times (\text{FTI (foot mask)} / \sum \text{FTI (foot mask)})$. Since the participants may change their gait patterns from jogging to fast running with the increase of running speed, the comparison of regional force impulses among different running speeds allows the calculation of load transfer from a region where load is reduced in one speed to a region where load is increased in comparison with another speed. Furthermore, load transference was divided into two parts, transference in longitudinal (anterior-posterior) direction and transference in transverse (media-lateral) direction, in order to observe the transference respectively. Certain rules for the calculation were formulated, as follows:

Four levels are defined following the anatomical structure along the longitudinal direction: toes (Level 1, BT and T2-5), metatarsal (Level 2, MM, CM and LM), midfoot (Level 3, MMF and LMF) and heel (Level 4, H). The numbers in each foot region are the difference value of relative FTI between the two speeds (Figure 3).

Load transfer calculation starts within level

from high value regions to low value regions. The transference is in transverse (medial-lateral) direction. After the transfer, the values in each region at the same level tend to equal (even in negative values). Load transfer occurs between adjacent anatomical regions first, and then between the further regions. After the transfer, the altered values of relative FTI is exhibited in the red color.

After the within-level transfer, load transfers cross level from high value regions to low value regions. The transference is in longitudinal (anterior-posterior) direction. After the transfer, the values in each region tend to zero. Load transfer occurs between adjacent anatomical regions first, and then between the further regions. After the transfer, the altered values of relative FTI is exhibited in the red color (generally is zero).

RESULTS

Significant differences were found in maximum force, peak pressure, contact area and FTI among different running speeds. The faster running speeds resulted in significant higher values at maximum force and peak pressure under all foot regions except for the big toe (Table 1, Figure 2). Peak pressure was concentrated in MM, CM and BT. Contact area was found significantly increased in T2-5, CM and LM with the increase of running speed (Table 2). With the increase of running speed, significant lower values in FTI were found under all plantar regions except for LMF and H (Table 3). MM, CM and BT were the main loading regions for rear-foot strike male runners during running.

Table 1: Maximum force (N) in different speeds

Regions	5	6	7	8	9	10	11	12	ρ
BT	53.93±21.08	53.48±23.66	53.95±23.07	55.43±23.17	56.78±23.01	58.83±22.26	58.17±20.32	59.13±21.19	0.882
T2-5	49.12±18.68	50.69±18.71	54.62±19.22	59.06±18.68	61.36±20.08	66.36±19.85	67.03±17.91	69.63±20.62	0.000*
MM	165.29±37.57	170.47±38.13	186.33±41.65	193.94±39.66	200.91±38.65	205.78±38.36	210.32±39.88	215.74±40.66	0.000*
CM	220.36±48.08	229.83±48.02	253.16±50.29	267.06±49.49	274.90±51.51	285.48±49.39	292.88±51.55	301.95±52.80	0.000*
LM	97.02±28.00	102.24±26.67	109.67±30.48	116.49±30.84	118.59±31.02	123.63±30.25	126.23±30.73	130.10±31.21	0.000*
MMF	131.13±29.89	137.39±29.69	144.22±28.68	151.69±30.34	157.79±31.35	159.84±30.89	164.88±30.25	167.72±31.23	0.000*
LMF	129.44±34.29	139.40±35.80	140.01±34.40	146.97±35.42	148.91±35.71	152.90±37.37	157.96±37.79	160.44±37.55	0.005*
H	269.53±87.12	314.41±59.13	296.76±89.02	322.95±83.14	341.35±85.13	352.39±97.60	383.08±95.04	391.47±98.18	0.000*

Note: *, $p < 0.05$ Table 2: Contact area (cm^2) in different speeds

Regions	5	6	7	8	9	10	11	12	ρ
BT	4.53±0.27	4.51±0.30	4.57±0.10	4.57±0.10	4.58±0.05	4.59±0.00	4.59±0.00	4.59±0.00	0.153
T2-5	9.48±1.74	9.93±1.28	10.00±1.28	10.21±0.98	10.35±0.79	10.43±0.67	10.34±0.76	10.40±0.79	0.000*
MM	15.72±0.16	15.71±0.23	15.72±0.23	15.75±0.05	15.75±0.05	15.75±0.05	15.76±0.00	15.75±0.05	0.485
CM	23.60±0.27	23.61±0.16	23.65±0.07	23.66±0.00	23.66±0.00	23.66±0.00	23.66±0.00	23.66±0.00	0.035*
LM	15.37±0.71	15.41±0.68	15.52±0.44	15.68±0.20	15.67±0.38	15.72±0.18	15.73±0.16	15.73±0.17	0.000*
MMF	25.07±0.56	25.04±0.75	25.14±0.40	25.17±0.33	25.17±0.38	25.19±0.23	25.21±0.14	25.22±0.05	0.373
LMF	18.90±0.05	18.91±0.00	18.91±0.00	18.91±0.00	18.91±0.00	18.91±0.00	18.91±0.00	18.91±0.00	0.453
H	35.78±6.00	35.75±5.86	35.91±5.04	36.65±3.73	36.88±3.40	36.91±3.54	37.28±3.16	37.39±3.05	0.163

Note: *, $p < 0.05$

Table 3: Force-time integral (N^*s) in different speeds

Regions	speed/(km·h ⁻¹)						ρ
	5	6	7	8	9	10	
BT	15.31±7.44	13.62±6.42	11.82±5.39	10.83±4.80	10.24±4.32	9.85±4.05	9.14±3.58
T2-5	7.68±3.17	7.15±2.64	6.40±2.18	6.13±2.08	5.85±2.23	5.83±2.05	5.54±1.81
MM	15.59±5.70	14.07±4.35	13.50±3.99	12.80±3.64	12.21±3.19	11.78±3.16	11.38±2.98
CM	13.33±3.42	12.43±2.96	12.09±2.66	11.67±2.45	11.19±2.44	10.96±2.26	10.74±2.32
LM	8.63±2.64	8.20±2.55	7.87±2.37	7.66±2.08	7.29±1.98	7.20±1.81	6.99±1.74
MMF	4.51±1.13	4.40±1.01	4.29±0.97	4.24±0.88	4.15±0.88	3.98±0.86	3.96±0.82
LMF	5.95±1.72	5.84±1.80	5.62±1.65	5.57±1.56	5.37±1.51	5.22±1.47	5.17±1.37
H	6.18±2.16	6.09±1.88	5.73±1.76	5.82±1.55	5.78±1.46	5.52±1.56	5.62±1.39

Note: * , $p < 0.05$

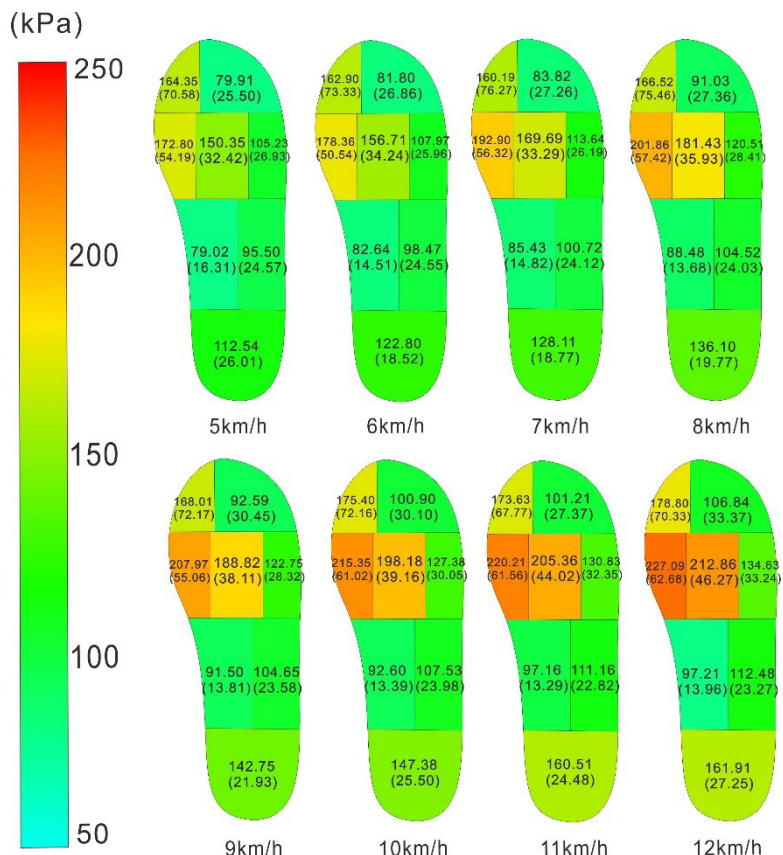


Figure 2. Peak pressure in 5km/h - 12km/h (p value: BT, $p = 0.948$; T2-5, $p < 0.001$; MM, $p < 0.001$; CM, $p < 0.001$; LM, $p < 0.001$; MMF, $p < 0.001$; LMF, $p = 0.022$; H, $p < 0.001$)

Load transferred along the transverse and longitudinal arch in anterior-posterior and media-lateral directions (Figure 3). Force transference was only indicated between the 5 km/h and 8 km/h groups, as well as the 8 km/h and 12 km/h groups, shown in Figure 3. In the pre-test, 5 km/h and 12km/h were found to the lowest speed and highest speed for Asian recreational male runners to keep running. Therefore, 5 km/h and 12 km/h were chosen as typically jogging and fast running condition. Meanwhile, 8 km/h was found to nearest the preferring speed in pre-test. In the post hoc test, we found that when the speed raised up to 8 km/h, some of the plantar regions developed significant lower FTI values comparing with 5 km/h. Therefore, 5 km/h, 8 km/h and 12 km/h were chosen as jogging, normal running and fast running speeds to show the load transference existing with the increase of running speed. Difference values of relative FTI (%) between 5 km/h with 8 km/h, and 8 km/h with 12 km/h were indicated in Table 4. Because FTI significantly decreased in BT, T2-5, MM, CM, LM and MMF, this study would focus on these

regions to find how the load transfer. According to Figure 3, in the transverse direction, load transferred from BT to T2-5, from MM to CM and LM, from MMF to LMF (5 km/h to 8 km/h). In the longitudinal direction, load transferred from level 1 to level 2, level 3 and level 4, that was from toes to metatarsal, midfoot and heel. In other words, load transferred mainly from medial to lateral in transverse direction and from anterior to posterior in longitudinal direction with the increase of running speed.

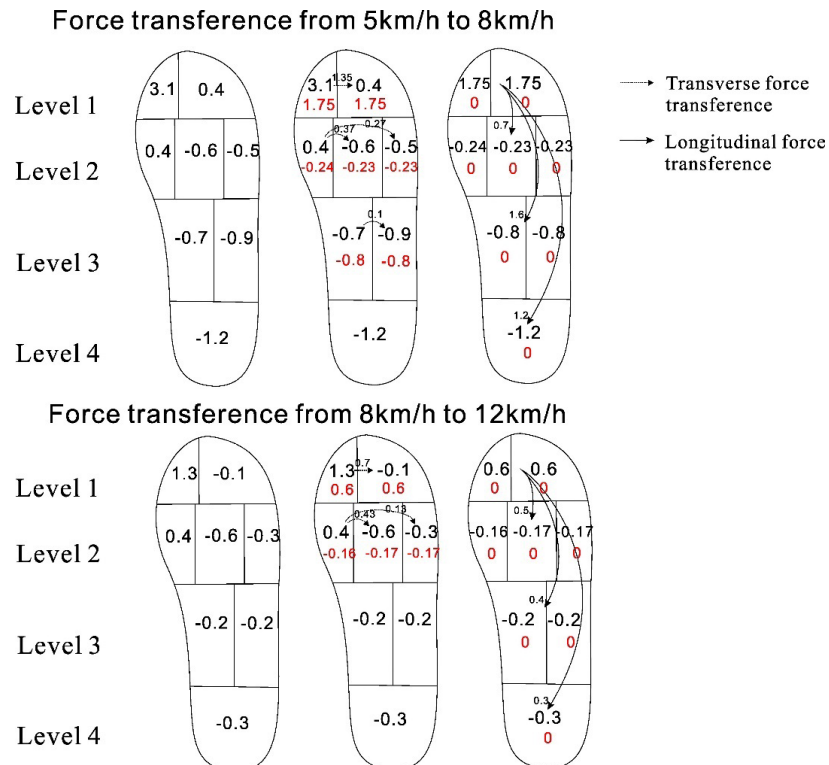


Figure 3. Force transference

Table 4: Relative FTI (%) and the difference value

Foot regions	speed				
	5	8	12	diff.5-8	diff.8-12
BT	19.7	16.6	15.3	3.1	1.3
T2-5	10.0	9.6	9.7	0.4	-0.1
MM	20.0	19.6	19.2	0.4	0.4
CM	17.1	17.7	18.3	-0.6	-0.6
LM	11.2	11.7	12.0	-0.5	-0.3
MMF	5.8	6.5	6.7	-0.7	-0.2
LMF	7.8	8.7	8.9	-0.9	-0.2
H	8.4	9.6	9.99	-1.2	-0.3

DISCUSSION

In this study, the plantar pressure of 39 healthy rear-foot strike male runners was measured and their plantar load transfer were analyzed by a load transfer algorithm. The results showed load transferred along the transverse direction from medial part of the foot to lateral part of the foot, as well as along the longitudinal direction from toes to metatarsal, midfoot and rearfoot. The medial metatarsal, the central metatarsal and the big toe were the main loading regions for rear-foot strike male runners

during running, and medial to lateral, anterior to posterior load transfer were typical. According to the above tracks, the load-transfer mechanism of healthy rear-foot strike Asian male runners was quantified.

With the increase of running speed, the foot had a stronger support to hold the body and generate the propulsion, which could result in higher impact on the foot. While maximum force and peak pressure were generally increased across all regions of the foot with the increase of running speed, it was disproportionately

increased more in the metatarsal area. As the main loading regions of the foot during running, maximum force and peak pressure of MM and CM increased greatly, as an average of 31.1%, 31.4% on MM and 37.0%, 41.6% on CM. In the forefoot, the highest peak pressure was found under MM, which was in accordance with De Cock's work [21]. According to Figure 2, MM, CM and BT demonstrated higher pressure across all of the speeds, which might suggest that these regions had higher risks for stress fracture, especially at high speed running [22]. Running shoes should be designed to provide better protection to the metatarsal in order to avoid the injuries that can occur from excessive impact.

With the increase of running speed, FTI was found significantly decreased under all the plantar regions except for H. It was because that as an influence factor of FTI, the ground contact time decreased. With the increase of running speed, runners showed shorter stride and higher cadence at higher running speed, which indicated that time spent on one gait decreased. Moreover, the actual duration of stance and swing during running gait are variable depending on the running speed. Faster speeds results in decreased support and increased float periods [23], which suggested that the ground contact time on each foot decreased during running gait at higher speed.

Running used a spring mass model in the compliant lower limb in which muscles and tendons sequentially stored and then released energy during the stance phase [24, 25]. As a component of the spring mechanism, the longitudinal arch had an important role as shock absorber for mechanical shock and load during human movement. The longitudinal arch of the human foot compressed and recoiled in response to being cyclically loaded. Foot suffered higher impact with the increase of speed, so the foot arch became flatter for absorbing shocks and made the contact area expanded. This is the reason for increase of contact area. Load transferred along the longitudinal direction from toes to metatarsal, midfoot and heel, which may also suggest that in higher running speed, the spring mechanism become more active to absorb loading forces and produce higher forward propulsion rather than the toes.

To our knowledge, this is the first study to use a load transfer algorithm to analyze the load transfer with the increase of running speed. The load transfer algorithm was also quite different from the old one. In Bus's transfer algorithm [15], load transfer can only occur between adjacent anatomical regions. Because Bus's studies were about how the custom-made insoles or forefoot offloading shoes relief the pressure, it would be more important to explore how the pressure is relieved in one foot region after another region. But in our study, load transfer occurred between adjacent anatomical regions first, and then between the further regions, which could show the origin of the load directly. In Mingyu Hu's study [16], load could only transfer from positive regions to negative ones. But in our study, especially in the within-level transfer, load transferred from high value regions to low value regions, even could transfer from positive region to positive one, and from negative region to negative one. The improved load transfer algorithm was more proper to show the differences of load distribution for this study.

Breine [26] indicated a transition towards a more anterior foot strike pattern in shod runners with increasing speeds from 3.2 m/s (11.5 km/h) to 6.2 m/s (22.3 km/h). In our study, only one participant transferred from rear-foot strike pattern to non-rear-foot strike pattern. The reason might be that the highest speed observed in our study was 12 km/h, but Breine explored higher speed from 3.2 m/s (11.5 km/h) to 6.2 m/s (22.3 km/h) larger than this study. The change of foot strike patterns might occur more frequently in higher speed. Rear-foot strike Asian male shod runners might not change their foot strike patterns when the running speeds are less than 12 km/h.

There are a number of limitations to this study. A potential limitation might be the use of treadmill. Treadmill could control the speed accurately during the test. But it was known that running on the treadmill was associated with a lower magnitude maximum plantar pressure and a lower maximum plantar force in plantar areas [27]. The measurements on the treadmill could be accurately known but it was not equivalent to the measurements overground. Besides,

this study was conducted in healthy Asian recreational male runners with habitual rear-foot strike pattern, and it was unknown if the findings would be replicated in fore-foot strike and mid-foot strike runners or non-Asians.

CONCLUSION

This study demonstrates the influence of running speed on plantar pressure, and show how the load transfer with the increase of running speed in rear-foot strike male runners. With the increase of running speed, maximum force and peak pressure significantly increased under all foot regions except for the big toe. Faster running speeds resulted in significantly lower FTI in all foot regions except for lateral midfoot and heel. MM, CM and BT were the main loading regions for rear-foot strike male runners during running. MM, CM and BT had higher risks for running-related injuries as these regions demonstrated highest pressure across all the speeds, especially at high speed running. Running shoes should be designed to provide better protection to metatarsal to avoid the injury. As a component of the spring mechanism, the arch played a key role in supporting and transferring loads. Load transferred along the longitudinal direction from toes to metatarsal, midfoot and heel, which suggest that in higher running speed, the spring mechanism becomes more active to absorb loading forces and produce higher forward propulsion rather than the toes. Load transferred from medial foot to lateral foot in transverse direction. These findings can improve our understanding of the structure-function relationship of the foot, and reveal the need for special consideration in sports shoes design in order to increase comfort and avoid running-related injury.

Acknowledgments

This work was supported by the National Natural Science Foundation of China [grant numbers: 11502154]. The authors would like to acknowledge all the experimenters for participant recruitment and data collection, and to acknowledge all the participants who made this study possible.

Conflict of Interest

There were no conflicts of interest with other authors or institution for this study.

REFERENCES

- Duhig, S., Shield, A.J., Opar, D., Gabbett, T.J., Ferguson, C., Williams, M., Effect of high-speed running on hamstring strain injury risk, *BrJ Sports Med*, **2016**, 50, 24, 1536-40, <https://doi.org/10.1136/bjsports-2015-095679>.
- Mann, R., Malisoux, L., Urhausen, A., Meijer, K., Theisen, D., Plantar pressure measurements and running-related injury: A systematic review of methods and possible associations, *Gait Posture*, **2016**, 47, 1-9, <https://doi.org/10.1016/j.gaitpost.2016.03.016>.
- Videbaek, S., Bueno, A.M., Nielsen, R.O., Rasmussen, S., Incidence of Running-Related Injuries Per 1000 h of running in Different Types of Runners: A Systematic Review and Meta-Analysis, *Sports Med*, **2015**, 45, 7, 1017-26. <https://doi.org/10.1007/s40279-015-0333-8>.
- Elliott, M.C., Zarins, B., Powell, J.W., Kenyon, C.D., Hamstring muscle strains in professional football players: a 10-year review, *American J Sports Med*, **2011**, 39, 4, 843-50, <https://doi.org/10.1177/0363546510394647>.
- Gabbett, T.J., Ullah, S., Relationship between running loads and soft-tissue injury in elite team sport athletes, *J Strength Cond Res*, **2012**, 26, 4, 953-60, <https://doi.org/10.1519/JSC.0b013e3182302023>.
- Bertelsen, M.L., Hulme, A., Petersen, J., Brund, R.K., Sorensen, H., Finch, C.F., Parner, E.T., Nielsen, R.O., A framework for the etiology of running-related injuries, *Scand J Med Sci Sports*, **2017**, <https://doi.org/10.1111/sms.12883>.
- Rice, H., Nunns, M., House, C., Fallowfield, J., Allsopp, A., Dixon, S., High medial plantar pressures during barefoot running are associated with increased risk of ankle inversion injury in Royal Marine recruits, *Gait*

- Posture*, **2013**, 38, 4, 614-8, <https://doi.org/10.1016/j.gaitpost.2013.02.001>.
8. Ho, I.-J., Hou, Y.-Y., Yang, C.-H., Wu, W.-L., Chen, S.-K., Guo, L.-Y., Comparison of plantar pressure distribution between different speed and incline during treadmill jogging, *J Sport Sci Med*, **2010**, 9, 1, 154-60.
 9. Fourchet, F., Kelly, L., Horobeanu, C., Loepelt, H., Taiar, R., Millet, G.P., Comparison of plantar pressure distribution in adolescent runners at low vs. high running velocity, *Gait Posture*, **2012**, 35, 4, 685-7, <https://doi.org/10.1016/j.gaitpost.2011.12.004>.
 10. Kernozeck, T.W., Zimmer, K.A., Reliability and Running Speed Effects of In-shoe Loading Measurements During Slow Treadmill Running, *Foot Ankle Int*, **2000**, <https://doi.org/10.1177/107110070002100906>.
 11. Lieberman, D.E., Venkadesan, M., Werbel, W.A., Daoud, A.I., D'Andrea, S., Davis, I.S., Mang'Eni, R.O., Pitsiladis, Y., Foot strike patterns and collision forces in habitually barefoot versus shod runners, *Nature*, **2010**, 463, 7280, 531-5, <https://doi.org/10.1038/nature08723>.
 12. Perl, D.P., Daoud, A.I., Lieberman, D.E., Effects of footwear and strike type on running economy, *Med Sci Sports Exerc*, **2012**, 44, 7, 1335-43, <https://doi.org/10.1249/MSS.0b013e318247989e>.
 13. Rooney, B.D., Derrick, T.R., Joint contact loading in forefoot and rearfoot strike patterns during running, *J Biomech*, **2013**, 46, 13, 2201-6, <https://doi.org/10.1016/j.jbiomech.2013.06.022>.
 14. Hasegawa, H., Yamauchi, T., Kraemew, W.J., Foot strike patterns of runners at the 15-km point during an elite-level half marathon, *J Strength Cond Res*, **2007**, 21, 3, 888-93, <https://doi.org/10.1519/00124278-200708000-00040>.
 15. Bus, S.A., van Deursen, R.W., Kanade, R.V., Wissink, M., Manning, E.A., van Baal, J.G., Harding, K.G., Plantar pressure relief in the diabetic foot using forefoot offloading shoes, *Gait Posture*, **2009**, 29, 4, 618-22, <https://doi.org/10.1016/j.gaitpost.2009.01.003>.
 16. Hu, M., Zhou, N., Xu, B., Chen, W., Wu, J., Zhou, J., The mechanism of force transference in feet of children ages two to six, *Gait Posture*, **2017**, 54, 15-9, <https://doi.org/10.1016/j.gaitpost.2017.02.019>.
 17. Li, R., Liu, H., Guo, M., Badurova, J., Yang, L., Fan, H., Differences in loading patterns between fast walking and jogging at the same speed in male adults, *J Leather Sci Eng*, **2020**, 2, 11, <https://doi.org/10.1186/s42825-020-00021-4>.
 18. Altman, A.R., Davis, I.S., A kinematic method for footstrike pattern detection in barefoot and shod runners, *Gait Posture*, **2012**, 35, 2, 298-300, <https://doi.org/10.1016/j.gaitpost.2011.09.104>.
 19. Menz, H.B., Two feet, or one person? Problems associated with statistical analysis of paired data in foot and ankle medicine, *Foot*, **2004**, 14, 1, 2-5, [https://doi.org/10.1016/s0958-2592\(03\)00047-6](https://doi.org/10.1016/s0958-2592(03)00047-6).
 20. Bus, S.A., Ulbrecht, J.S., Cavanagh, P.R., Pressure relief and load redistribution by custom-made insoles in diabetic patients with neuropathy and foot deformity, *Clin Biomech*, **2004**, 19, 6, 629-38, <https://doi.org/10.1016/j.clinbiomech.2004.02.010>.
 21. De Cock, A., Willems, T., Witvrouw, E., Vanrenterghem, J., De Clercq, D., A functional foot type classification with cluster analysis based on plantar pressure distribution during jogging, *Gait Posture*, **2006**, 23, 3, 39-47, <https://doi.org/10.1016/j.gaitpost.2005.04.011>.
 22. Liong, S.Y., Whitehouse, R.W., Lower extremity and pelvic stress fractures in athletes, *Br J Radiol*, **2012**, 85, 1016, 1148-56, <https://doi.org/10.1259/bjr/78510315>.
 23. Lohman, E.B., 3rd, Balan Sackiriyas, K.S., Swen, R.W., A comparison of the spatiotemporal parameters, kinematics, and

- biomechanics between shod, unshod, and minimally supported running as compared to walking, *Phys Ther Sport*, **2011**, 12, 4, 151-63, <https://doi.org/10.1016/j.ptsp.2011.09.004>.
24. Farley, C.T., Houdijk, H.H.P., Van Strien, C., Louie, M., Mechanism of leg stiffness adjustment for hopping on surfaces of different stiffnesses, *J Appl Physiol*, **1998**, 85, 3, 1044-55, <https://doi.org/10.1152/jappl.1998.85.3.1044>.
25. Bramble, D.M., Lieberman, D.E., Endurance running and the evolution of Homo, *Nature*, **2004**, 432, 7015, 345-52, <https://doi.org/10.1038/nature03052>.
26. Breine, B., Malcolm, P., Frederick, E.C., De Clercq, D., Relationship between running speed and initial foot contact patterns, *Med Sci Sports Exerc*, **2014**, 46, 8, 1595-603, <https://doi.org/10.1249/MSS.0000000000000267>.
27. Hong, Y., Wang, L., Li, J.X., Zhou, J.H., Comparison of plantar loads during treadmill and overground running, *J Sci Med Sport*, **2012**, 15, 6, 554-60, <https://doi.org/10.1016/j.jsams.2012.01.004>.

© 2020 by the author(s). Published by INCOTP-ICPI, Bucharest, RO. This is an open access article distributed under the terms and conditions of the Creative Commons Attribution license (<http://creativecommons.org/licenses/by/4.0/>).

ANTIBACTERIAL COMPOUND BASED ON SILICONE RUBBER AND ZnO AND TiO₂ NANOPARTICLES FOR THE FOOD AND PHARMACEUTIC INDUSTRIES. PART I – OBTAINING AND CHARACTERISATION

Mihaela NIȚUICĂ (VÎLSAN)^{1*}, Maria SÖNMEZ¹, Mihai GEORGESCU¹, Maria Daniela STELESCU¹, Laurențiu ALEXANDRESCU¹, Dana GURĂU¹, Carmen CURUȚIU^{2,3}, Lia Maria DITU^{2,3}

¹INCDTP - Division Leather and Footwear Research Institute, 93 Ion Minulescu St., sector 3, Bucharest,

mihaela.nituica@icpi.ro, mihaelavilsan@yahoo.com

²University of Bucharest, Faculty of Biology, 1-3 Portocalelor St., 6th district, 060101, Bucharest, Romania

³Research Institute of University of Bucharest, 36-46 M. Kogalniceanu St., 5th district, 050107, Bucharest, Romania

Received: 27.01.2020

Accepted: 05.06.2020

<https://doi.org/10.24264/lfj.20.2.8>

ANTIBACTERIAL COMPOUND BASED ON SILICONE RUBBER AND ZnO AND TiO₂ NANOPARTICLES FOR THE FOOD AND PHARMACEUTIC INDUSTRIES. PART I – OBTAINING AND CHARACTERISATION

ABSTRACT. Taking into account the progress in science and technology, it has been and is still necessary to develop new innovative and high-performance materials. Globally, obtaining new advanced polymeric structures based on nanopowder-reinforced elastomers, with high-performance properties, offers possibilities for developing new materials and expanding their field of application. At present, polymeric materials occupy a very important place in all areas of human activity, being part more and more of everyday life. The need to develop new materials with high-performance properties led to this paper, which describes the obtaining and characterization of a compound with antibacterial properties based on silicone rubber (silicone elastomer - ELASTOSIL) reinforced with nanoparticles with antifungal, antibacterial and antimicrobial properties (ZnO and TiO₂). The dispersion of nanoparticles in the mass of the elastomeric compound has a decisive role in influencing its antimicrobial and antibacterial sterilization properties. The elastomeric compound based on silicone rubber with antibacterial and antimicrobial properties is obtained by vulcanization, and is characterized from a physical-mechanical, chemical and structural point of view, according to the standards in force. The antibacterial elastomeric compound reinforced with nanoparticles has potential uses in the food and pharmaceutical fields.

KEY WORDS: antibacterial compound, curing, silicone rubber, TiO₂, ZnO

COMPOUND ANTIBACTERIAN PE BAZĂ DE ELASTOMER SILICONIC ȘI NANOPARTICULE DE ZnO ȘI TiO₂, PENTRU DOMENIUL ALIMENTAR ȘI FARMACEUTIC. PARTEA I – OBȚINERE ȘI CARACTERIZARE

REZUMAT. Înăndu-se cont de progresul în știință și tehnologie a fost și este necesară dezvoltarea de noi materiale inovative și performante. La nivel mondial, obținerea de noi structuri polimerice avansate pe bază de elastomeri ranforzați cu nanopulberi, cu proprietăți performante, oferă posibilități de obținere a unor noi materiale și de extindere a domeniului de aplicații ale acestora. În prezent, materialele polimerice ocupă un loc foarte important în toate domeniile activității umane, luând parte din ce în ce mai mult la viața de zi cu zi. Necesitatea dezvoltării de noi materiale cu proprietăți performante a condus la prezenta lucrare, ce descrie obținerea și caracterizarea unui compound cu proprietăți antibacteriene pe bază de cauciuc siliconic (elastomer siliconic - ELASTOSIL) ranforzat cu nanoparticule cu proprietăți antifungice, antibacteriene și antimicrobiene (ZnO și TiO₂). Dispersia nanoparticulelor în masa compoundului elastomeric are rol determinant în influențarea proprietăților de sterilizare antimicrobiană și antibacteriană a acestuia. Compoundul elastomeric pe bază de cauciuc siliconic cu proprietăți antibacteriene și antimicrobiene este obținut prin vulcanizare, urmând a fi caracterizat din punct de vedere fizico-mecanic, chimic și structural, conform standardelor în vigoare. Compoundul elastomeric antibacterian ranforzat cu nanoparticule are potențiale utilizări în domeniul alimentar și farmaceutic.

CUVINTE CHEIE: compound antibacterian, vulcanizare, cauciuc siliconic, TiO₂, ZnO

COMPOSÉ ANTIBACTÉRIEN À BASE D'ÉLASTOMÈRE DE SILICONE ET DE NANOPARTICULES DE ZnO ET TiO₂ POUR LE DOMAIN ALIMENTAIRE ET PHARMACEUTIQUE. PARTIE I - OBTENTION ET CARACTÉRISATION

RÉSUMÉ. Compte tenu des progrès de la science et de la technologie, il a été et est encore nécessaire de développer de nouveaux matériaux innovants et performants. A l'échelle mondiale, l'obtention de nouvelles structures polymériques avancées à base d'élastomères renforcés par des nanopoudres, aux propriétés performantes, offre des possibilités pour le développement de nouveaux matériaux et d'élargissement de leur domaine d'application. Actuellement, les matériaux polymères occupent une place très importante dans tous les domaines de l'activité humaine, participant de plus en plus à la vie quotidienne. La nécessité de développer de nouveaux matériaux aux propriétés performantes a conduit à cet article qui présente l'obtention et la caractérisation d'un composé aux propriétés antibactériennes à base de caoutchouc silicone (élastomère silicone - ELASTOSIL) renforcé de nanoparticules aux propriétés antifongiques, antibactériennes et antimicrobiennes (ZnO et TiO₂). La dispersion des nanoparticules dans la masse du composé élastomère joue un rôle déterminant pour influencer ses propriétés de stérilisation antimicrobienne et antibactérienne. Le composé élastomère à base de caoutchouc silicone aux propriétés antibactériennes et antimicrobiennes est obtenu par vulcanisation, et sera caractérisé d'un point de vue physico-mécanique, chimique et structurel, selon les normes en vigueur. Le composé élastomère antibactérien renforcé de nanoparticules a des utilisations potentielles dans les domaines alimentaire et pharmaceutique.

MOTS CLÉS : composé antibactérien, vulcanisation, caoutchouc silicone, TiO₂, ZnO

* Correspondence to: Mihaela NIȚUICĂ (VÎLSAN), INCDTP - Division Leather and Footwear Research Institute, 93 Ion Minulescu St., sector 3, Bucharest, mihaela.nituica@icpi.ro, mihaelavilsan@yahoo.com

INTRODUCTION

Vulcanization of elastomers (silicone) is a main step that has a major impact on the final properties of the products [1, 2]. Both the quantity and the type of vulcanizing agent, the time, temperature and pressure of vulcanization, are important factors that control the degree of crosslinking, the properties of the finished product, thus leading to obtaining advanced compounds. These advanced materials based on silicone elastomers (silicone rubber), reinforced with nanopowders that have antibacterial, antifungal and antimicrobial properties, contribute to improving product quality, environmental protection and of course human health [3-7]. The dispersion of nanoparticles in the obtained mixture (elastomeric compound) has the decisive role in influencing its antimicrobial and antibacterial sterilization properties [8, 9].

Silicone elastomers - silicone rubber is generally preferred in the food and pharmaceutical fields because it does not contain substances that are not toxicologically acceptable (nitrile, styrene, chlorine, antioxidants and other restricted ingredients), and has characteristics such as high resistance to temperatures from -100°C to above +300°C. Higher temperatures than +300°C are specific to sterilization and therefore silicone elastomers are preferred by the above mentioned fields [10-15].

The aim of this work was to obtain an antibacterial compound based on silicone rubber - Elastosil R701/70-OH, filled with chalk, crosslinked with PD (dicumyl peroxide), stearin as plasticizer and reinforced with two types of nanoparticles - zinc oxide and titanium dioxide, made by mixing on an electric roller between its rollers (the rollers were cooled with water) [16-19]. The obtained antibacterial compound was characterized in terms of physical-mechanical properties (hardness, residual elongation, tear strength), chemically by immersion in various media (three different immersion environments) and by FT-IR spectrometry, all according to standards in force.

EXPERIMENTAL

Materials

The following materials were used to make the antibacterial compound based on siliconic rubber and nanometric particles: (1) Elastosil R701/70-OH – silicone rubber: polydimethylsiloxane with vinyl groups, dynamic viscosity over 9.000.000 mPa*s, in the form of paste, density – 1.32 g/cm³, colour – opaque; (2) stearin, white flakes, moisture - 0.5% max, ash – 0.025 % max; (3) ZnO – zinc oxide microparticles: precipitate 93-95%, in the form of white powder, density – 5.5 g/cm, specific surface – 45-55 m²/g; (4) ZnO – zinc oxide nanoparticles: white powder, 99.99% trace metals basis; (5) TiO₂ - titanium dioxide nanoparticles: white nanopowder, assay ≥ 99.5 % trace metals basis; (6) chalk: CaCO₃ precipitate – white powder, molecular weight 100.09; (7) PD – di(tert-butylperoxyisopropyl) benzene: powder 40% with calcium carbonate and silica – Perkadox 14-40B (1.65 g/cm³ density, 3.8% active oxygen content, pH 7, assay: 39.0-41.0%).

Methods

Preparation of Antibacterial Compound and Characterization Methods

The antibacterial compound based on silicone rubber – Elastosil R701/70-OH, reinforced with nanometric particles TiO₂ and ZnO, filled with chalk - CaCO₃, plasticized with stearin and crosslinked with dicumyl peroxide - PD was developed by electric laboratory roll mill mixing, the rolls were water-cooled. The Elastosil R701/70-OH was plasticized between the rolls for approximately 2.5-3 minutes, then the stearin was added and mixing continued for approximately 2 minutes. After the ZnO microparticle was added and embedded into the mixture until homogenisation, for maximum 2 minutes, the nanoparticles of TiO₂ and ZnO were added, continuing to mix for 3 minutes until the nanometric component was embedded. Mixing continued for 3 minutes while adding the filler - CaCO₃ and the dicumyl peroxide – PD

(last ingredient) was embedded for 2 minutes. The mixture is homogenized on the roll mill for maximum 2 minutes and taken off in the form

of a 3-4 mm thick sheet. The order of adding ingredients was strictly observed, according to Table 1.

Table 1: Formulations of antibacterial compounds based on silicone rubber reinforced with TiO₂ and ZnO nanoparticles

Symbol	MU [g]	CS ₁ (control)	Sample 2	Sample 3	Sample 4
Silicone rubber (Elastosil R701/70-OH)	g	150	150	150	150
Stearin (FLAKES)	g	7.5	7.5	7.5	7.5
Zinc oxide (active powder)	g	6	4.5	3	1.5
Zinc oxide (nanoparticles)	g	-	1.5	3	4.5
Titanium dioxide (nanoparticles)	g	-	1.5	3	4.5
Chalk (CaCO ₃ - powder)	g	15	15	15	15
Dicumyl peroxide (PD– 40% - on silica and CaCO ₃ powder substrate)	g	11.25	11.25	11.25	11.25

The resulting antibacterial compound was subjected to rheological determinations (using a Monsanto rheometer – Figure 1), to establish the optimal curing time in the electrical press.

From the rheological analysis made by comparing the samples it is found that the introduction of nanometric reinforcing agent - ZnO and TiO₂ (with antiseptic, antifungal, antimicrobial role), does not influence the degree of vulcanization of the compound obtained. The samples obtained are similar to each other, compared to the control sample - CS₁. Control sample CS₁ does not contain nanometric reinforcing agent – Figure 2.



Figure 1. Monsanto rheometer used in rheological determination

Sarja:	ML (dNm):	MH (dNm):	ts2 (min):	t50 (min):	t90 (min):
CS1 Martor.rho	5.7	19	1	1.6	2.7
3.rho	6.2	24.4	1.1	2.1	17.8
4.rho	6.3	22.3	0.9	1.7	17.4

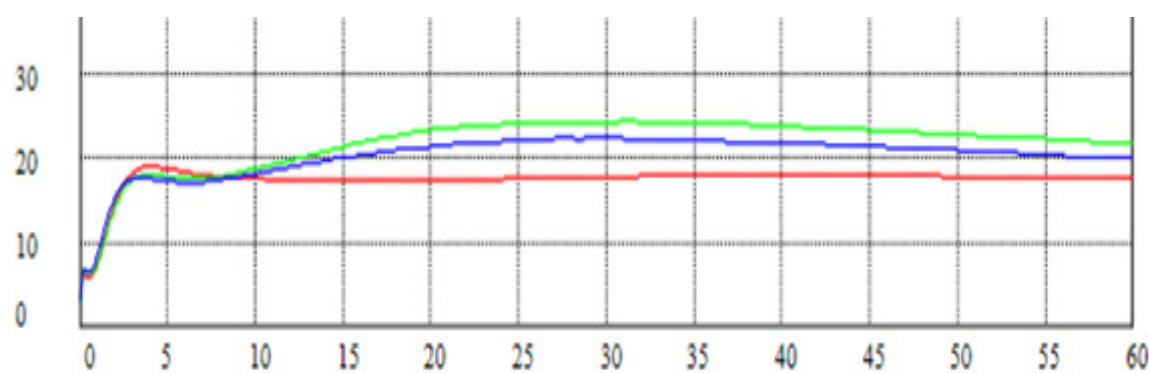


Figure 2. Rheological analysis of samples – CS1 (control), sample 3, sample 4

The specimens were made in an electric press (TP 600) between its plates, by the compression method (by pressing) at the preset parameters: temperature of 170°C, 2 minutes pressing at a pressure of 300 KN, 10 minutes cooling time (Figure 3).

The specimens obtained in the electric press after a stabilization of 24 hours at ambient temperature are then characterized, in compliance with the physical-mechanical standards:

- physically-mechanically (normal state and accelerated aging at 70°C for 168 h,

SR ISO 188-2010): hardness ($^{\circ}\text{ShA}$ -SR ISO 7619: 2011), residual elongation (100% - SR ISO 37-2012), tear strength (N/mm -SR ISO 37-2012);

- chemically (immersion in average media for 24 hours): ISO 1817: 2015, following both the volume variation (ΔV) and the mass variation (ΔM).
- structurally: double beam molecular absorption IR spectrometer in, in the range 4000-600 cm^{-1} , using the Able Jasco 4200 FT-IR device equipped with ATR with diamond crystal.

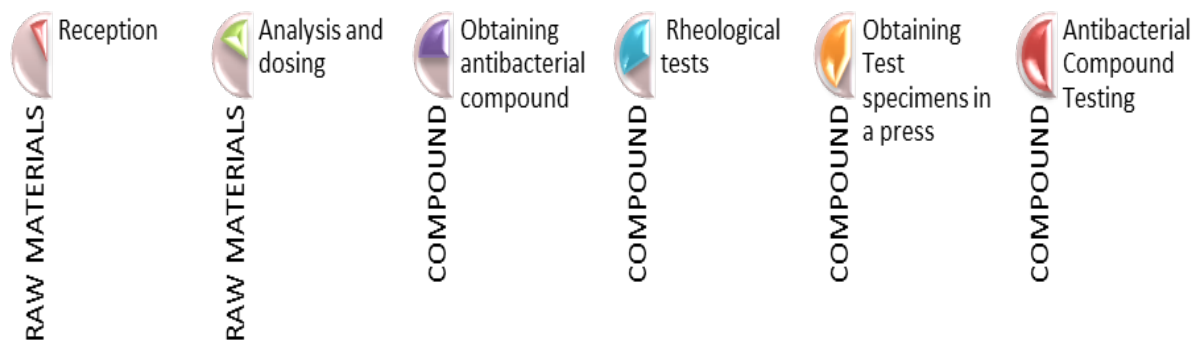


Figure 3. Technological process of obtaining the antibacterial compound reinforced with ZnO and TiO_2 nanoparticles

RESULTS AND DISCUSSIONS

Physical-Mechanical Characterization of Antibacterial Compounds

The antibacterial compounds were tested from a physical-mechanical point of view after

a stabilization for 24 h at room temperature, according to the standards in force (normal state and accelerated aging at 70°C and 168 h).

As a result of the physical-mechanical analysis performed according to Figures 4, 5 and 6, the following are found:

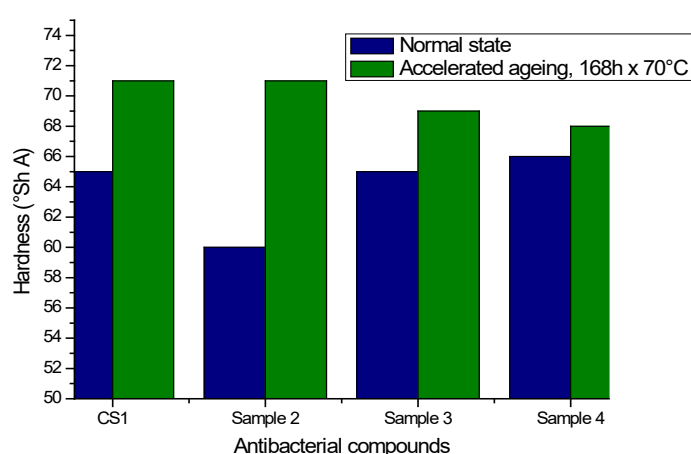


Figure 4. Hardness for antibacterial compounds reinforced with ZnO and TiO_2 nanoparticles

- The **hardness** (Figure 4) of antibacterial compounds based on silicone elastomer in normal state, increases slightly compared to the control sample CS₁. Increasing the amount of nanoparticles (ZnO and TiO₂) added in the mass of the elastomeric compound, it is observed that

the hardness values increase slightly. Due to the loss of plasticizer, the hardness of the samples decreased compared to the control sample, after they were subjected to the accelerated aging process at 70°C for 168h.

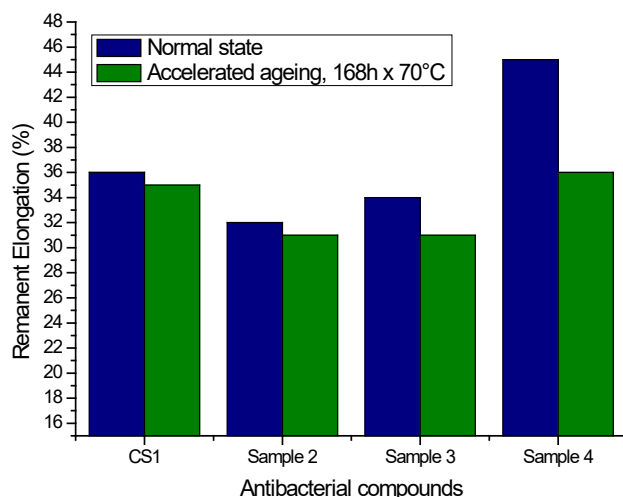


Figure 5. Residual elongation for antibacterial compounds reinforced with ZnO and TiO₂ nanoparticles

- For **residual elongation** (Figure 5), the higher the percentage of reinforcing agent in the form of nanoparticles, the higher the residual elongation, thus demonstrating that the processing parameters are optimal. Similar to hardness, after subjecting the specimens to the

accelerated aging process at 70°C for 168 hours, the values of the residual elongation decrease. Due to the loss of plasticizer, the values decrease by approximately 2.5% compared to the values of the specimens in the normal state.

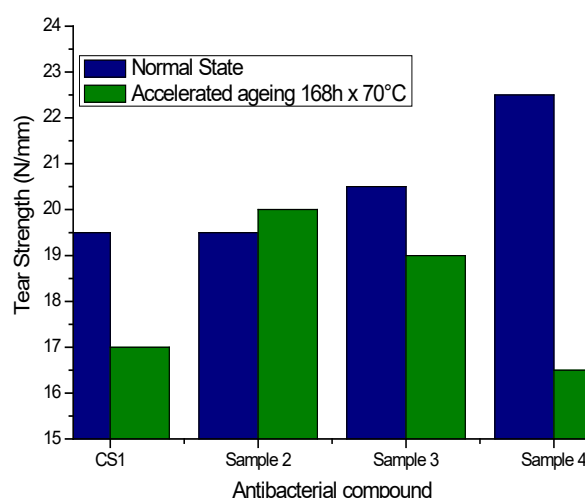


Figure 6. Tear strength for antibacterial compounds reinforced with ZnO and TiO₂ nanoparticles

- Tear strength** (Figure 6) in the normal state increases in proportion to the amount of reinforcing agent added. The values obtained in the normal state are between 19.5-22.5 N/mm, while after subjecting the specimens to the accelerated aging process, the values of tear resistance decrease, presenting values between 16.5 and 20 N/mm.

Chemical Characterization of Antibacterial Compounds

The chemical characterization of antibacterial compounds was performed

by immersing them in various working environments: ethyl alcohol concentration 70%, distilled water and sunflower oil, for 24 hours at room temperature, in dark containers (brown, black), tightly closed (samples are completely covered by the work environment used and are immersed at a relatively equal distance from each other without them coming into contact with each other).

Mass variation – ΔM and volumetric mass – ΔV , after immersion in environments specific to the food, pharmaceutical and food fields are presented in Table 2.

Table 2: Mass variation (ΔM) and volumetric mass (ΔV) of antibacterial compounds reinforced with TiO_2 and ZnO nanoparticles, in various environments

Material	CS_1 (control)		Sample 2		Sample 3		Sample 4	
	ΔM	ΔV	ΔM	ΔV	ΔM	ΔV	ΔM	ΔV
Ethyl alcohol – 70%	-0,75	-1,11	-1,2	-2,72	-1,19	-1,77	-1,34	-1,66
Distilled water	0,16	0,68	0,15	0,38	0,18	0,44	0,72	0,53
Sunflower oil	-1,24	-1,59	-2,23	-3,54	-2,1	-3,26	-1,73	-1,85

The immersion of samples of mixtures based on silicone elastomer reinforced with nanopowders (ZnO and TiO_2) in different specific media, presents the following results:

- in ethyl alcohol, both the mass variation, ΔM , and the volumetric one, ΔV , present negative values, below $\pm 2.8\%$. These values indicate the extraction of substances – stearin and chalk – that take place in this work environment;
- for both ΔM (mass variation) and ΔV (volumetric variation) the values calculated after a 24-hour immersion in distilled water are below 0.8%, which indicates an insignificant swelling of the tested specimens;
- in the vegetable oil environment, the values recorded for the mass and volumetric variation are negative, below $\pm 3.6\%$, indicating, as in the case of specimens immersed in the ethyl alcohol, the extraction of substances such as unreacted crosslinking agent;
- after immersing the samples in the media listed above, it is observed that their surface does not alter, they do not show color change (the color of the

samples being gray) and do not swell, and no cracks or other non-conformities of the specimens are observed on their surface (taking into account that they do not come into contact with each other).

FT-IR Spectrometric Analysis

Samples were tested spectroscopically through FT-IR spectroscopy, using an Able Jasco 4200 FT-IR device coupled with ATR with diamond crystal and sapphire head and all the samples had as reference the spectrum recorded for the principal component – Elastosil R701/70-OH (elastomeric rubber).

The IR frequencies (cm^{-1}) and vibration attributions for the silicone rubber sample – Elastosil R701/70-OH are given in Table 3 and Figure 7.

Table 3: IR frequencies and vibration attributions for the silicone rubber sample

Frequency	Vibration attributions
696	$\nu Si(CH_3)_3$
787.271	$\nu Si(CH_3)$
866.338	$Si(CH_3)_2$ (r)
1007.12	$Si(-CH_3=CH_2)$
1258.78	$\delta SiCH_3$

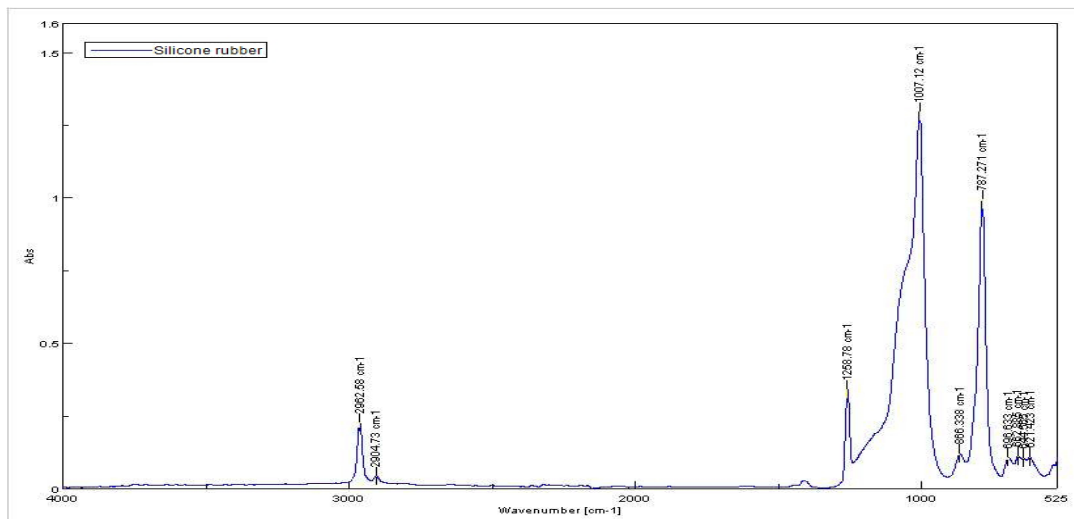


Figure 7. IR spectrum recorded for Elastosil R701/70-OH (silicone rubber)

Control sample, CS₁, has the following IR frequencies (cm⁻¹) and vibration attributions – Table 4, and the IR recorded spectrum – Figure 8.

Table 4: IR frequencies and vibration attributions for the control sample – CS₁

Frequency	Vibration attributions
697.141	ν Si(CH ₃) ₃
786.815	ν Si(CH ₃)
871.667	Si(CH ₃) ₃ + Si(CH ₂) ₂
1006.66	Si(-CH ₃ = CH ₂)
1258.32	δ SiCH ₃
1451.17	ν CH ₃ (CH ₂) ₁₆ -CO- (stearic acid)
2849.31	Si-O-C
3361.32	ν (OH) linked

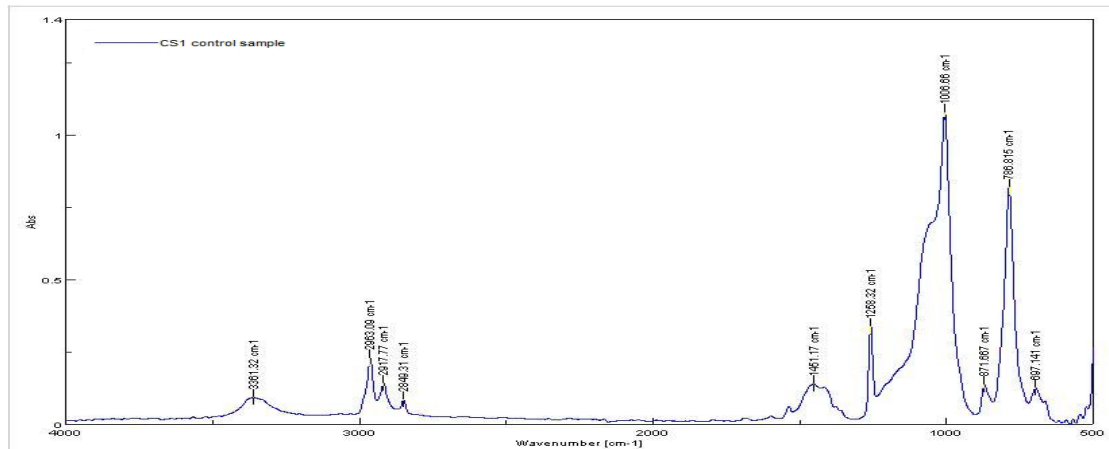


Figure 8. IR spectrum recorded for CS₁ (control sample)

All the samples were tested from the point of view of FT-IR spectroscopy (Figure 9 – A and B) and overlapped spectra confirm the presence of the silicone elastomer Elastosil R701/70-OH by the intensity of the characteristic peaks, this being the main material. The silicone elastomer

– Elastosil R701/70-OH represents the dispersed phase (in the largest quantity), the material in which the other ingredients are incorporated, and from the overlapping spectra, the presence of silicone groups is observed from the intensity of the characteristic peaks.

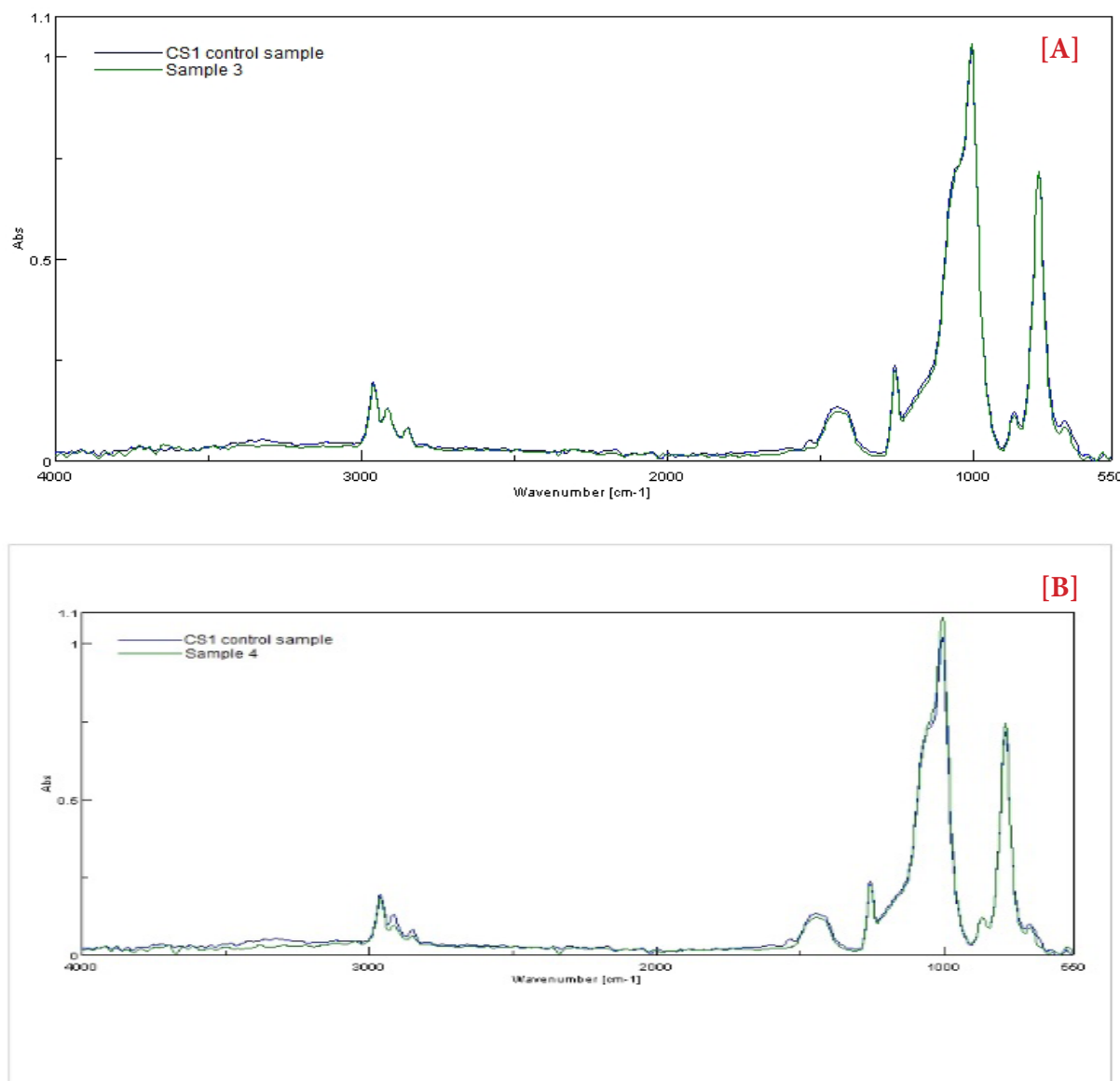


Figure 9. Overlapping spectra recorded for sample 3 [A] and sample 4 [B]

CONCLUSION

The article presents the technology for developing antibacterial compounds based on elastomeric rubber - Elastosil R701/70-OH, reinforced with two types of nanoparticles, ZnO and TiO₂, according to standards in force.

The physical-mechanical characterization after a stabilization for 24 h at room temperature, according to the standards in force, in normal state and after accelerated aging at 70°C and 168 h, confirms the fact that the processing parameters are optimal. After the immersion process, it is observed that the samples do not undergo surface changes, do not show color change and do not swell, and on the surface they

do not show cracks or other non-conformities. FT-IR spectroscopy, by superimposing the spectra of each sample separately with the control sample CS₁, confirms the presence of Elastosil R701/70-OH silicone rubber, by the intensity of its characteristic peaks, this being the material in which the other ingredients are incorporated.

As a result of physical-mechanical, chemical and characteristics of FT-IR frequencies (cm⁻¹) and vibration attributions of antibacterial compounds based on silicone elastomer, we can say that they have potential applications in the food and pharmaceutical field.

Acknowledgements

This research was financed by ANCSI through PN 16-34 01 10/2016 project: "Antibacterial compound based on silicone rubber and ZnO and TiO₂ nanoparticles processed by vulcanization", Sectoral project, No. 3PSI/2019, "Research on risks caused by materials coming into contact with food, per groups of materials. Harmonization with European law" and 6PFE/2018 – PERFORM-TEX-PEL.

REFERENCES

1. Mirici, L.E., Thermoplastic Elastomers, Art. Press & Augusta, Timisoara, **2005**.
2. Volintiru, T., Ivan, Gh., Technological bases of processing elastomers, Technical Press, Bucharest, **1974**.
3. Shi, F., Clayman, R., Louie, M.K., Lin, Y.H., Lin, Y.C., Silicone composition and devices incorporating same, US Patent 8,257,827 B1, 4 September **2012**.
4. Stelescu, M.D., Characteristics of silicone rubber blends, *Leather and Footwear Journal*, **2010**, 10, 3, 51-58.
5. Dobrinescu, A., New types of elastomers for special purposes, Ministry of Light Industry, Centre for Documentation and Technical Publications, Bucharest, **1971**.
6. Hanke, B., Bort, F., Anti-microbial silicone rubber composition and method for making same, US Patent 6,822,034 B2, 23 November **2004**.
7. Zeng, L., Zhang, Y., Rao, Z., Liu, Y., Miao, X., Ma, L., Yan, N., Zeng, X., Zhou, L., Zou, Y., Tong, C., Deng, Z., Study on Thermal Aging Characteristics of HTV Silicone Rubber Sheds of Composite Insulators, IOP Conference Series: Materials Science and Engineering, April **2020**, 782, 022076, <https://doi.org/10.1088/1757-899X/782/2/022076>.
8. Zhou, H., Wang, H., Niu, H., Gestos, A., Wang, X., Lin, T., Fluoroalkyl silane modified silicone rubber/nanoparticle composite: a super durable, robust superhydrophobic fabric coating, *Adv Mater*, **2012**, 24, 2409-2412, <https://doi.org/10.1002/adma.201200184>.
9. Chandra, J., Kuhn, D.M., Mukherjee, P.K., Hoyer, L.L., McCormick, T., Ghannoum, M.A., Biofilm Formation by the Fungal Pathogen *Candida albicans*: Development, Architecture, and Drug Resistance, *J Bacteriol*, **2001**, 183, 18, 5385–5394, PMCID: PMC95423, <https://doi.org/10.1128/JB.183.18.5385-5394.2001>.
10. Byeon, Y., Jeon, Y., Kim, M., Research on AC Tracking Resistance of Silicone Rubber/BN Microcomposites, *Trans Korean Inst Electr Eng*, **2019**, 68, 11, 1389-1395, <https://doi.org/10.5370/KIEE.2019.68.11.1389>.
11. Hwang, S., Ryu, H.J., Kim, Y., So, J.I., Jin, S.H., Baeck, S.H., Shim, S.E., Thermal Stability and Mechanical Properties of Silicone Rubber Composites Filled with Inorganic Fire-proof Fillers and Expandable Materials, *Polym Korea*, **2018**, 42, 3, 354-363, <https://doi.org/10.7317/pk.2018.42.3.354>.
12. Fallahi, D., Mirzadeh, H., Khorasani, M.T., Physical, mechanical, and biocompatibility evaluation of three different types of silicone rubber, *J Appl Polym Sci*, **2003**, 8, 2522–2529, <https://doi.org/10.1002/app.11952>.
13. Hron, P., Slechtova, J., Smetana, K., Dvorankova, B., Lopour, P., Silicone rubber-hydrogel composites as polymeric biomaterials. IX. Composites containing powdery polyacrylamide hydrogel, *Biomaterials*, **1997**, 18, 15, 1069–1073, [https://doi.org/10.1016/S0142-9612\(97\)00039-2](https://doi.org/10.1016/S0142-9612(97)00039-2).
14. Otto, M., Staphylococcal Biofilms, *Curr Top Microbiol Immunol*, **2008**, 322, 207–228, https://doi.org/10.1007/978-3-540-75418-3_10.
15. Mashak, A., *In vitro* drug release from silicone rubber-polyacrylamide composite, *Silicon Chem*, **2008**, 3, 6, 295-301, <https://doi.org/10.1007/s11201-007-9031-1>.
16. Malcolm, K., Woolfson, D., Russell, J., Tallon, P., McAuley, L., Craig, D., Influence of silicone elastomer solubility and diffusivity on the in vitro release of drug from intravaginal rings, *J Control Release*, **2003**, 90, 2, 217–225, [https://doi.org/10.1016/S0168-3659\(03\)00178-0](https://doi.org/10.1016/S0168-3659(03)00178-0).
17. Nituica, M., Sonmez, M., Stelescu, M.D., Gurau, D., Curutiu, C., Ditu, L.M., Polymer nanocomposite based on silicone rubber reinforced with nanoparticles processed by vulcanization, University Politehnica of

- Bucharest, *Sci Bull B Chem Mater Sci*, **2017**, 79, 4, 63-72, ISSN:1454-2331, Accession Number: WOS:000424134600007.
18. Nituica (Vilsan), M., Sonmez, M., Georgecsu, M., Stelescu, M.D., Alexandrescu, L., Gurau, D., Curutiu, C., Ditu, L.M., Antibacterial nanocompound based on silicone rubber. Part II – Biological Characterization, *Leather and Footwear Journal*, **2019**, 19, 4, 227-232, <https://doi.org/10.24264/lfj.19.4.7>.
19. Nituica, M., Alexandrescu, L., Stelescu, M.D., Sonmez, M., Georgescu, M., Antibacterial polymer composite based on silicone elastomer and ZnO and TiO₂ nanoparticles, Patent no. 132483, **2019**.

© 2020 by the author(s). Published by INCOTP-ICPI, Bucharest, RO. This is an open access article distributed under the terms and conditions of the Creative Commons Attribution license (<http://creativecommons.org/licenses/by/4.0/>).

MULTICRITERIA COMPROMISE OPTIMIZATION FOR LEATHER AND FUR SKIN MATERIALS TANNING TECHNOLOGY

Halyna YEFIMCHUK^{1*}, Vladyslava SKIDAN², Mariya NAZARCHUK³, Eduard SELEZNOV¹, Anzhelika YANOVETS¹

¹Lutsk National Technical University, Lvivska Str., build.75, Lutsk, Ukraine, 43018, email: gefimchuk@gmail.com

²Kyiv National University of Technology and Design, Nemyrovych-Danchenko Str., build.2, Kyiv, Ukraine, 01011

³Lesya Ukrainka Eastern European National University, Voli Prosp., build.13, Lutsk, Ukraine, 43025

Received: 15.02.2020

Accepted: 10.06.2020

<https://doi.org/10.24264/ljf.20.2.9>

MULTICRITERIA COMPROMISE OPTIMIZATION FOR LEATHER AND FUR SKIN MATERIALS TANNING TECHNOLOGY

ABSTRACT. The work is devoted to the study of the influence of electro-activated aqueous solutions on the technological cycle of leather and fur skin materials production and footwear made of them. The influence of electro-activated aqueous solutions on the physicochemical transformations of the structure of skin tissue collagen is exemplified by rabbit fur skins used for shoe production. The spectral characteristics of changes in the structure and chemical composition of dermal collagen are determined and optimal modes of tanning process of leather and fur skin materials based on multicriteria compromise optimization are determined.

KEY WORDS: electro-activated aqueous solutions, anolyte, catholyte, leather and fur skin materials, footwear

OPTIMIZARE MULTICRITERIALĂ A TEHNOLOGIILOR DE TĂBĂCIRE A PIEILOR ȘI BLĂNURIILOR PRIN GĂSIREA UNEI SOLUȚII DE COMPROMIS
REZUMAT. Lucrarea este dedicată studierii influenței soluțiilor apoase activate electrochimic asupra ciclului tehnologic al producției de piele și blană pentru încăltăminte. Influența soluțiilor apoase activate electrochimic asupra transformărilor fizico-chimice ale structurii colagenului din țesutul pielii este exemplificată prin piei cu blană de iepure utilizate pentru producerea încăltămintei. S-au determinat caracteristicile spectrale ale modificărilor în structura și compoziția chimică a colagenului din stratul dermic sunt determinate, precum și metodele optime de tăbăcire a pielei și blănii pe baza optimizării multicriteriale prin găsirea unei soluții de compromis.

CUVINTE CHEIE: soluții apoase activate electrochimic, anolit, catolit, piele și blană, încăltăminte

OPTIMISATION MULTICRITÈRES DES TECHNOLOGIES DE TANNAGE DU CUIR ET DE LA FOURRURE VISANT À TROUVER UN COMPROMIS
RÉSUMÉ. Le travail est consacré à l'étude de l'influence des solutions aqueuses électro-activées sur le cycle technologique de la production du cuir et de la fourrure pour la production de chaussures. L'influence des solutions aqueuses électro-activées sur les transformations physicochimiques de la structure du collagène des tissus cutanés est illustrée par les fourrures de lapin utilisées pour la production de chaussures. On a déterminé les caractéristiques spectrales des changements dans la structure et la composition chimique du collagène dermique et les modes optimaux de processus de tannage des cuirs et des fourrures basés sur l'optimisation multicritère visant à trouver un compromis.

MOTS CLÉS : solutions aqueuses électro-activées, anolyte, catholyte, cuir et fourrure, chaussures

INTRODUCTION

Technologies that provide the manufacture of leather and fur skin materials simply the retention of beneficial properties of both the skin tissues and its hair-covering, and ensure permanency of these materials during continuous exploitation of products made of them. The most toilful and time-consuming processes in the leather and fur skin manufacturing cycle are preparatory and tanning stages. These processes are carried out with significant water consumption, while water is acting as a solvent for chemical reagents, and their utilization requires significant costs in the future [1].

The most promising solution to the problem of reducing water consumption and material

consumption of fur production are methods that activate chemical reagents in water such as usage of electric current. The effect of the latter is widely studied by a number of scientists [2, 3], but the nature and action mechanism of the water being treated by electricity has not been sufficiently studied yet.

Liquid processes in the production of leather and fur skin materials are fully associated with the presence in the water solution of electrolytes formed in the result of the dissociation of ions of chemical formations in the protein structure, hydrolysis of bonds, the carriers of which are structural elements of the protein, as well as relatively free ions. At the same time, ions introduced with water as a solvent

* Correspondence to: Halyna YEFIMCHUK, Lutsk National Technical University, Lvivska Str., build.75, Lutsk, Ukraine, 43018, email: gefimchuk@gmail.com.

of chemical components, in particular $\text{Na}^+ + \text{Cl}^-$ ions, are involved. Natural (tap) and distilled water has minimal electrical conductivity in its structure, and electro-activated water (anolyte and catholyte) has 2-3 times greater electrical conductivity, that indicates that the conductivity in these solutions is provided not only by $\text{Na}^+ + \text{Cl}^-$ but also by ions formed by the excess of mobile ions with a positive or negative charge that may be carried by groups with water molecules.

One of the most common forms of polymeric material study is their physical and mechanical testing, as their physical and mechanical properties are widely used in light industry to evaluate the quality of fully processed products. Studies of the relaxation and deformation characteristics of materials are of considerable scientific and practical interest. The results of such experiments allow to record simultaneously during one experiment the following kinetic curves [4]: the curve of development and relaxation and deformation in the sample, changes in its linear dimensions and hygroscopicity.

It is known [5] that objects with complex curvilinear surface shape (foot, shoe pad, shoe upper parts) are of the greatest complexity for design, because anatomical structure of the foot and the properties of the leather and fur skin materials from which the footwear is made must be taken into account in order to ensure their proper quality. However, in the conditions of production of leather and fur skin materials, most often according to the existing technological schemes and instructions it is not possible to determine the optimal combination of technological factors by which in particular case it is possible to achieve the maximum approximation to the required properties of the prefabricated leather component at the minimum cost of chemical materials.

Solving the problems of optimization and mathematical modeling of complex technological systems is characterized by significant particular characteristics due to the narrow application orientation of the obtained solutions, sometimes by the lack of sufficient information about the mechanisms occurring inside the system. At the same time the solution of such problems leads to the random nature of the change of optimality criteria and some factors with a considerable

number of quality indicators (optimization criteria) and as well as to factors that are taken into account in optimization and modeling [6].

The applied methodology for solving these problem classes provides various recommendations for the nature of this study. According to the classical, i.e. theoretical and analytical approach [7], it is recommended to obtain a mathematical model and then, using it, to find the optimal conditions.

EXPERIMENTAL

Materials and Methods

Rabbit skins that differ in the way they had been made were selected as the object of the study. Thus, for the manufacture of skins at all stages of the technological cycle electro-activated aqueous media was used. Skins, tanned by the standard technology were used to control the initial performance indicators of the dermis and to compare them.

The change in the structure and chemical composition of the rabbit dermis collagen was evaluated by the results of IR spectroscopy (Bruker TENSOR spectrometer) within the spectral range of 4000-400 cm^{-1} . The test specimens were prepared in the form of a tablet which contained potassium bromine (KBr) with a sample of ground tissue 0.5-1 mg. The IR spectra of the studied materials were described on the basis of reference data [8-10].

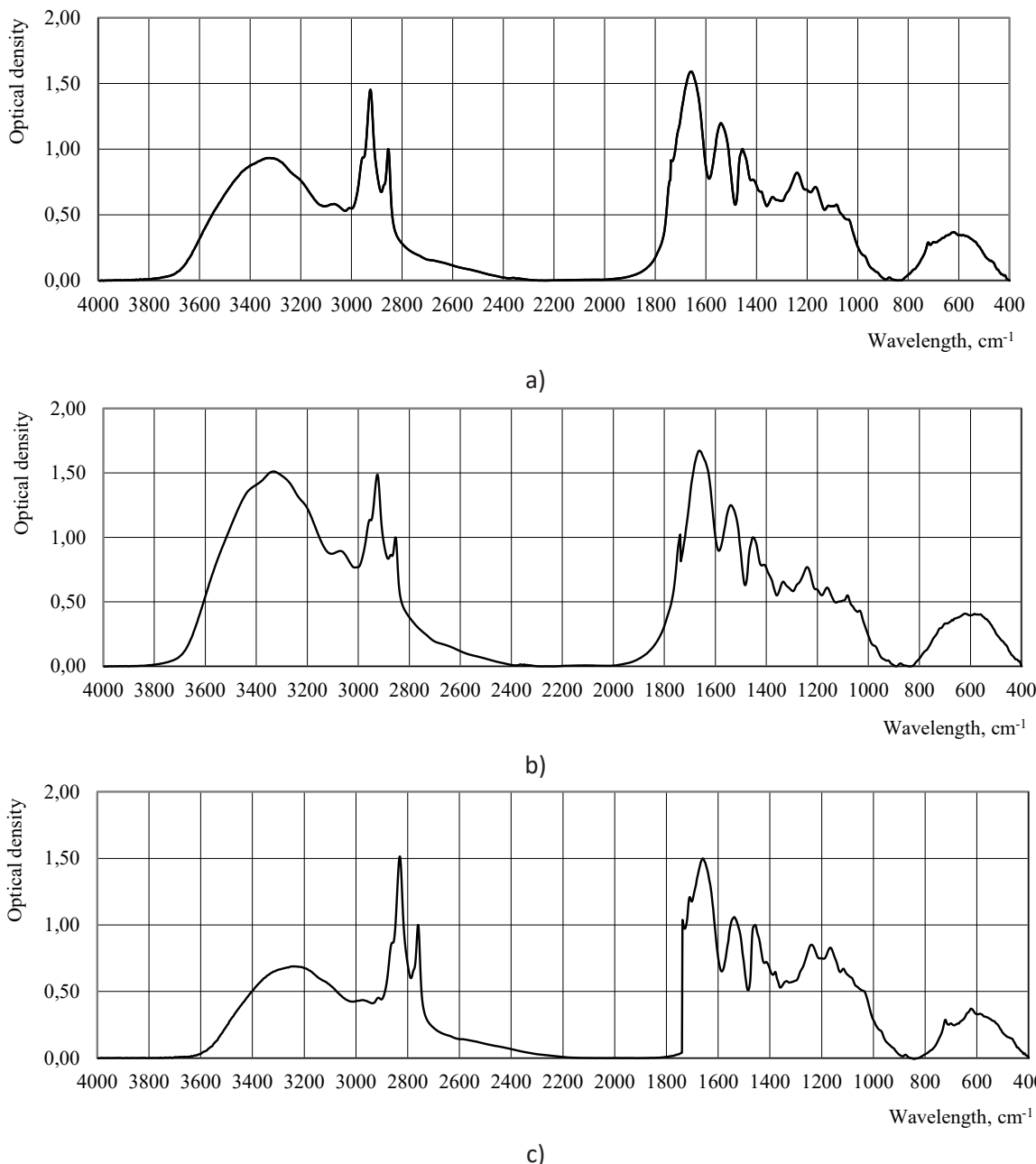
The IR spectra of rabbit skin tissue in the range of 3800-2600 cm^{-1} and 1800-400 cm^{-1} were studied. The nature of the interaction of the studied systems was evaluated by the disappearance, displacement and intensity change of the corresponding characteristics of bandwidths. The bandwidths in the IR spectra of the initial materials and the products of their interaction were assigned according to the bandwidths of the characteristic bonds of C – C atoms group and CH_2 .

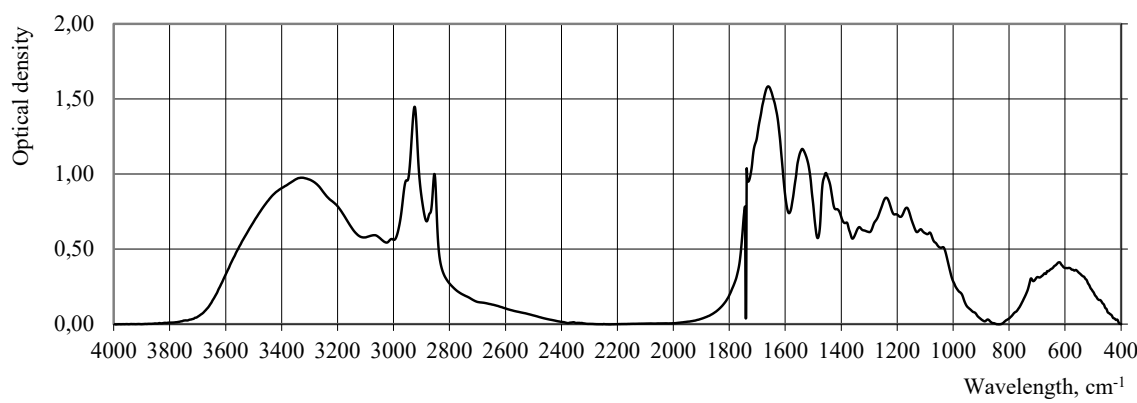
The influence of the electrical conductivity of water on the basic chemical parameters of rabbit fur skin was evaluated by the content of fat in the skin tissue, its welding temperature and the indicator of the formation of dermal volume in samples that were tanned using the appropriate technologies [11].

RESULTS AND DISCUSSIONS

To make a quantitative study of changes in protein functional groups and skin-forming components within certain characteristic waves, the optical density was determined using the baseline method [8]. The bands of 2854 cm^{-1} and 1454 cm^{-1} were selected as the internal standard

due to the valence vibrations of the methylene groups - CH_2 and carbon chain C-C groups (Fig. 1). Characteristic wave frequencies for the collagen dermis of rabbit skin tissue that relate to the characteristic wave frequencies of certain functional groups or their interactions were taken into account.





d)

Figure 1. Experiment spectrum where the following substance was used in the technological processes: a – water formed in the result of passage of current on a negative electrode (anolyte); b – water formed in the result of passage of current on a positive electrode (catholyte); c – distilled water; d – technical water

Tables 1, 2 show the oscillation frequencies of characteristic groups that change in the skin tissue during the manufacturing cycle of fur

production. In all cases the content of neutral salts per NaCl was the same and was equal to 0.2 g/l.

Table 1: Optical density of skin tissue samples IR spectra in the range 3800-2600 cm⁻¹

Water source	Electrical conductivity, $\mu\text{S}/\text{cm}$	Optical density at wave frequency					
		3410 cm^{-1}	3325 cm^{-1}	3246 cm^{-1}	3070 cm^{-1}	2926 cm^{-1}	2855 cm^{-1}
Near anion electrode (anolyte)	2800	0,86	0,932	1,02	0,582	1,45	1,00
Near cationic electrode (catholyte)	1270	1,390	1,51	1,35	0,89	1,49	1,00
Distilled water	710	0,481	0,641	0,689	0,489	0,71	0,87
Technical water	750	0,894	0,975	0,867	0,59	1,45	1,00

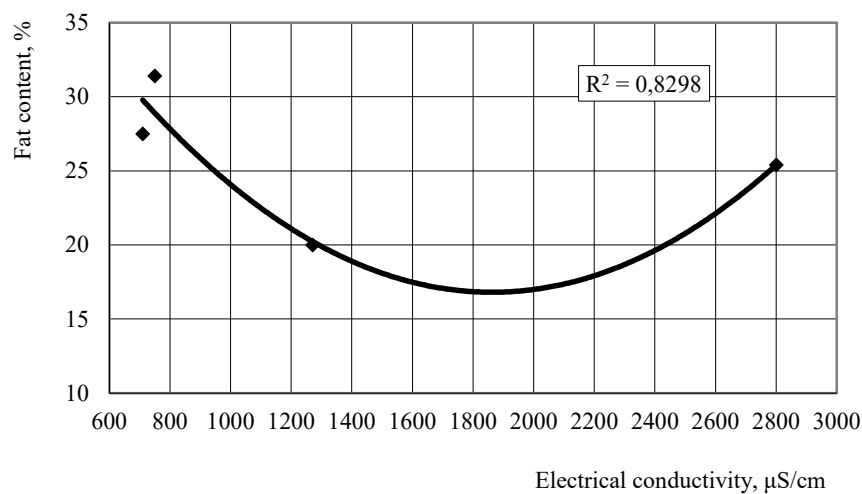
Table 2: Optical density of samples IR spectra in the range of 1800-400 cm⁻¹

Water source	Electrical conductivity, $\mu\text{S}/\text{cm}$	Optical density at wave frequency									
		1663 cm^{-1}	1539 cm^{-1}	1410 cm^{-1}	1335 cm^{-1}	1240 cm^{-1}	1166 cm^{-1}	1084 cm^{-1}	1036 cm^{-1}	633 cm^{-1}	
Near anion electrode (anolyte)	2800	1,59	1,19	0,76	0,63	0,82	0,71	0,57	0,46	0,36	
Near cationic electrode (catholyte)	1270	1,67	1,25	0,78	0,65	0,76	0,61	0,58	0,43	0,40	
Distilled water	710	1,50	1,06	0,71	0,57	0,85	0,82	0,60	0,50	0,37	
Technical water	750	1,58	1,17	0,75	0,64	0,84	0,77	0,61	0,51	0,41	

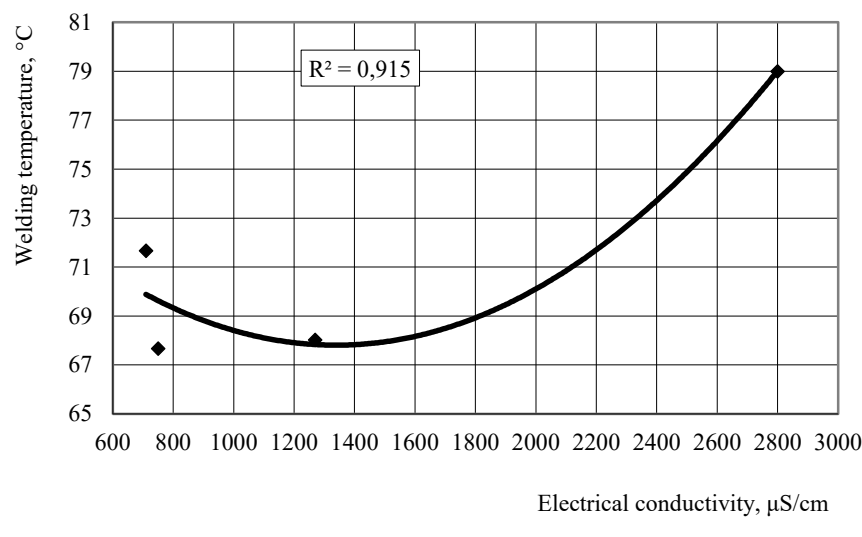
Based on the obtained data it can be stated that water of different origin affects the spectra of rabbit skin tissue differently in the range of the spectra of 3800-2600 cm⁻¹ and 1800-400 cm⁻¹. These spectra are characteristic for dermis collagen tanned with basic chromium salts. Specific features of the spectrum include the appearance of 1663 cm⁻¹ wavelength which is inherent to the valence oscillation C = O of medium intensity, and wave of 1036 cm⁻¹ which is inherent to the deformation oscillation C – O – C of medium intensity, which corresponds directly to the aldehyde group and the product of its interaction with the carbon chain, resulting in the emergence of heat-resistant bonds. The

appearance of thermo-resistant bonds of the dermis with chromium salt can be estimated by changing the optical density at a wavelength of 1084 cm⁻¹.

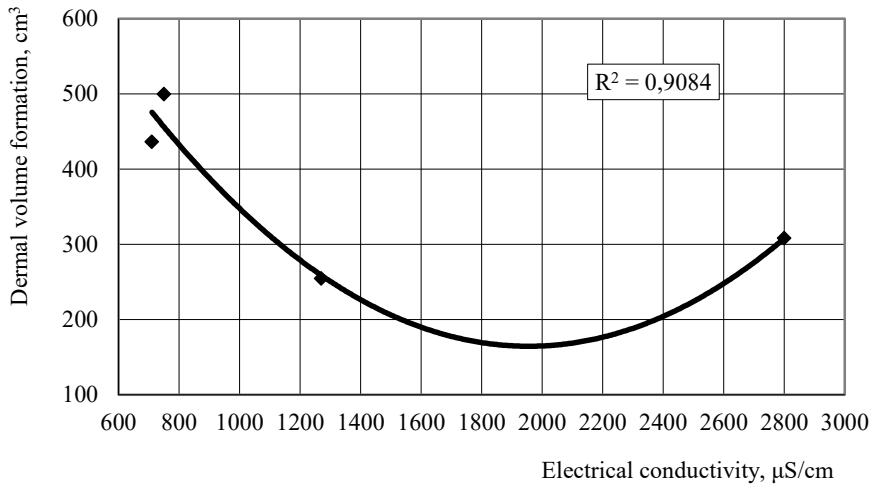
The study results proved that the technological processes of production of leather and fur skin materials, such as wetting, pickling (using technical and distilled water), tanning, greasing and drying are significantly influenced by the general characteristics of water, that can be reduced to its electrical conductivity (Tables 1-2), and the main indicators of the finished product (Fig. 2) with of the square values of the correlation ratio R greater than 0.8.



a)



b)

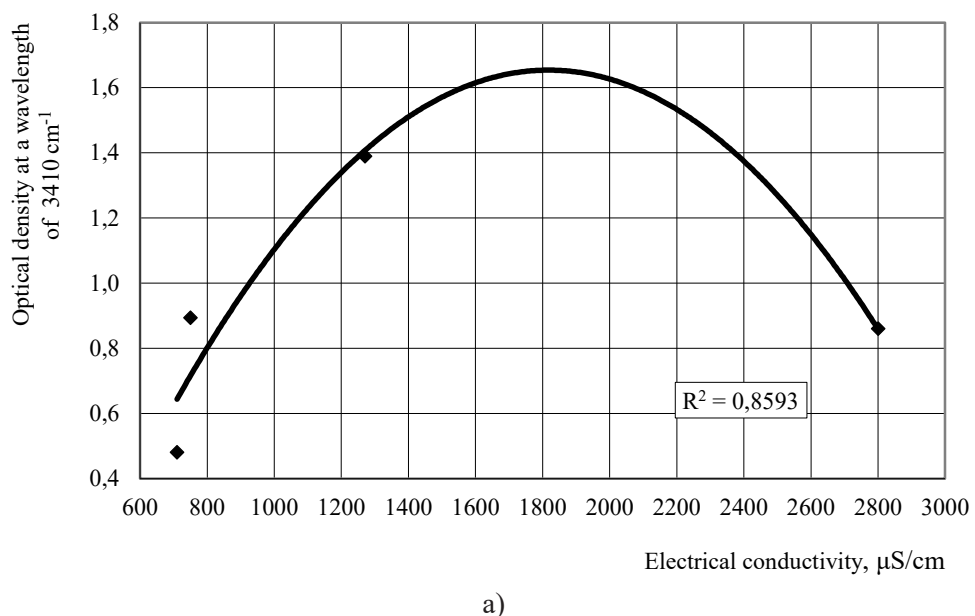


c)

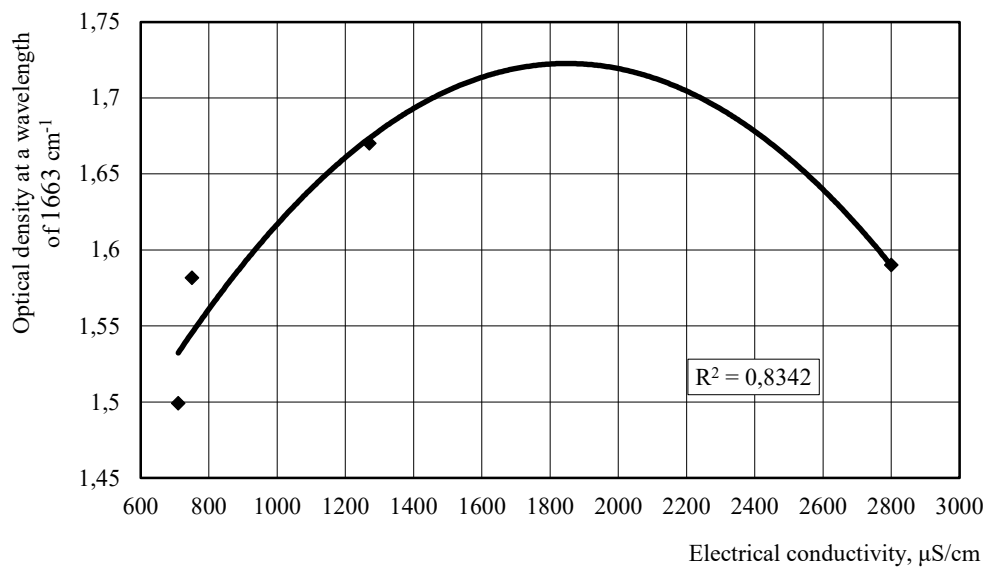
Figure 2. Water electrical conductivity effect on:
a) skin tissue fat content; b) welding temperature;
c) dermal volume formation

Using water with different electrical conductivity as a solvent, it was discovered that it significantly affects the degree of the polar part of both soluble substances and directly hydrophobic and hydrophilic balance inside the dermis. This leads to different interactions of the functional groups both in solution itself and between the water-soluble compounds and the active groups that are present in the dermis. The result of this interaction is a change in the analytic characteristics of the skin tissue and

the index of the dermis volume formation. The positive charge of amino groups can be stated on the basis of the existence of characteristic waves with length of 3410 cm^{-1} and 1663 cm^{-1} especially in acidic environment during pickling (Fig. 3). With a certain electrical conductivity, the maximum value of the optical density can be observed. Increasing and decreasing leads to a deviation in the downward direction of the optical density when the wave oscillation frequency is of 3410 cm^{-1} and 1663 cm^{-1} .



a)



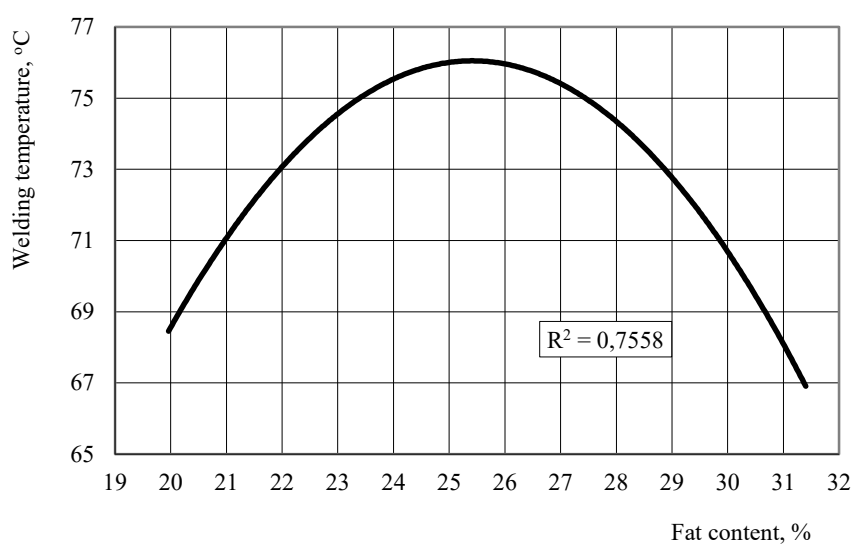
b)

Figure 3. Water electrical conductivity effect on optical density at the wave spectrum: a) 3410 cm^{-1} ; b) 1663 cm^{-1}

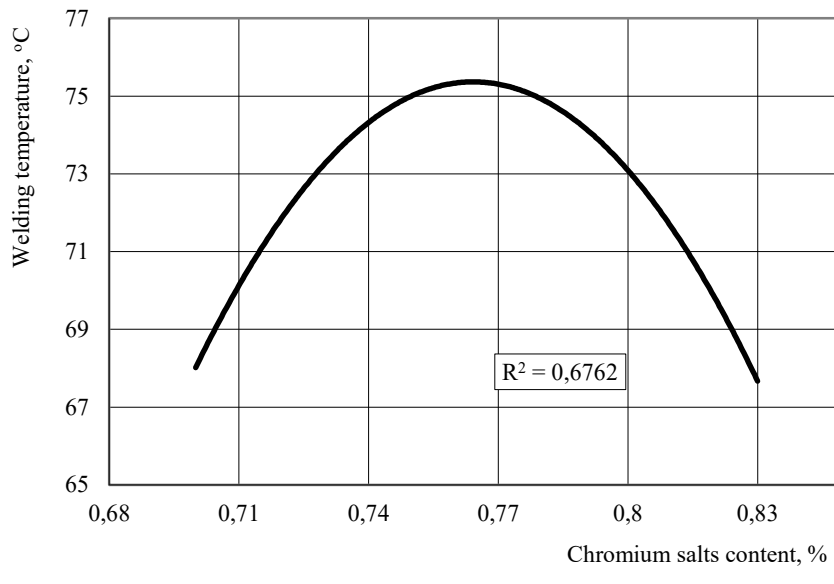
Wavelengths of 3410 cm^{-1} and 1663 cm^{-1} are associated with the formation of hydrogen bonds, a great number of which significantly affects the dermal collagen welding temperature. The essence of these connections means that after breaking in one place, they are re-formed in another place, that provides to some extent the possibility of deformation and fixing of the residual deformation.

A distinctive feature of the process of forming heat-resistant bonds in the dermis is

the result of several, at first glance, opposite reactions. First of all, the normal formation of heat-resistant bonds is due to the carboxyl group being included in the chromium complex. And the interaction of the fat molecule with the chromium complexes prevents the further formation of a heat-resistant bridge. Thus, the thermal resistance of the skin tissue decreases (Fig. 4).



a)



b)

Figure 4. Relationship between dermal welding temperature and: a) the fat content; b) the content of chromium salts

However, this interpretation does not explain why the properties of the skin are restored during a short period of time after welding. This phenomenon is observed when the skin is being tanned with aldehyde compounds. The appearance of C-O-C groups with a wavelength

of 1084 cm^{-1} (Fig. 5) in the structure of the derma is a consequence of the interaction of dialdehyde compounds with protein. The aldehyde groups appear due to the presence of a large number of oxidants or reducing agents in the catholyte and anolyte in the system respectively.

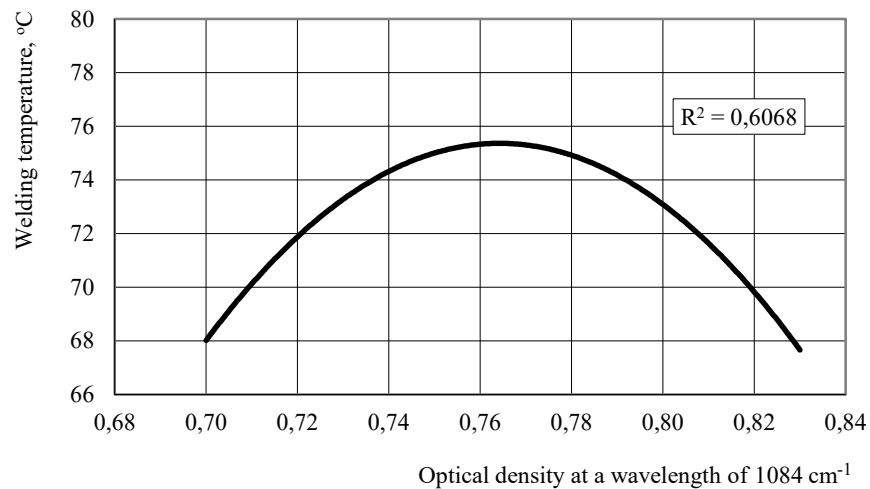


Figure 5. Relationship between dermal welding temperature and optical density wavelength 1084 cm^{-1}

The wavelength of 1663 cm^{-1} corresponds to the carbonyl groups, that is conditioned by their presence in proteins and fatty substances in the form of triglycerides. Meanwhile, this wave is characteristic for the fluctuations of the N-H protein groups, that can be manifested as a result of the transformation of the general restructuring of the protein structure in the

spectrum (Fig. 6). The imprint of the restructuring (deformation under load) on the vibrations of the groups N – H and C = O, that corresponds to the model of change in the deformation of the tensile under load and after its removal allows us to confirm the correctness of the physical model to the full extent [11].

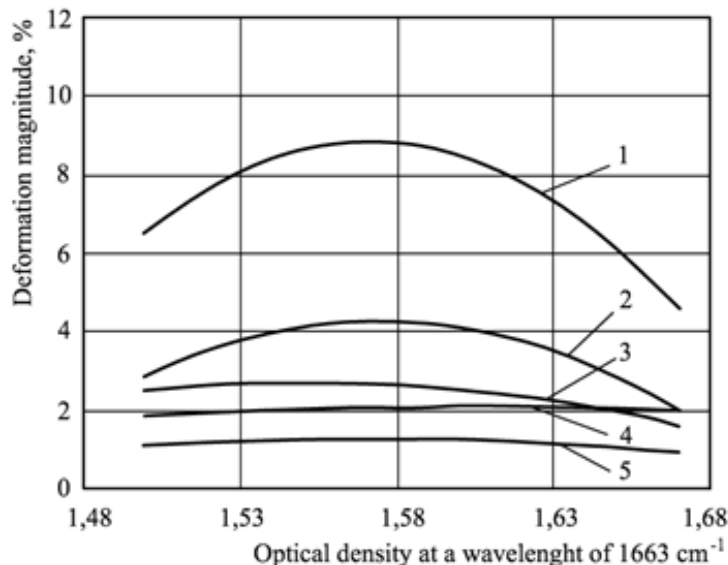


Figure 6. Relationship between the carbonyl group in the peptide bond and deformation components, %: 1 - total deformation, $R^2=0,8883$; 2 - plastic deformation, $R^2 = 0,5975$;
3 – plastic deformation, $R^2 = 0,8196$; 4 - instantaneous deformation, $R^2 = 0,1341$;
5 - elastic deformation, $R^2 = 0,7061$

Negative OH⁻ groups that are a part of the complex chromium sphere are dominated in catholyte, can result in the formation of neutral or negative charge tanner particles. The latter is most likely when using catholyte during tanning. Therefore, the negatively charged chromium molecule interacts with the positively charged NH²⁺ amino group, that results in the partial neutralization of the negatively charged chromium complex, freeing the coordination center in the chromium to interact with other groups having the ability of entering the complex sphere of chromium atoms. It is possible to form heat-resistant bonds in both cases that provide the effect of tanning (welding temperature increase). In the presence of trivalent chromium in a highly saturated with oxygen (in the form of OH⁻ ions medium), the processes of oxidation of

hydrocarbons with the formation of aldehydes are possible, which form heat-resistant bonds, that are destroyed at a temperature in the aqueous medium above 65°C, and at a lower temperature below the specified level they are being restored. The appearance of such bonds is evidenced by the presence of C-O-C groups at wave frequencies of 1166 cm⁻¹, 1036 cm⁻¹ and 1084 cm⁻¹, that are the result of the interaction of dialdehyde compounds with the protein. The wave frequency of 1036 cm⁻¹ can be partially attributed to the OH alcohol group (Fig. 7). Bearing in mind that the OH and C-O-C groups have a high affinity for the formation of complex compounds, it can be deduced that this effect (restoration of the sample after welding during cooling) causes the restoration of heat-resistant samples.

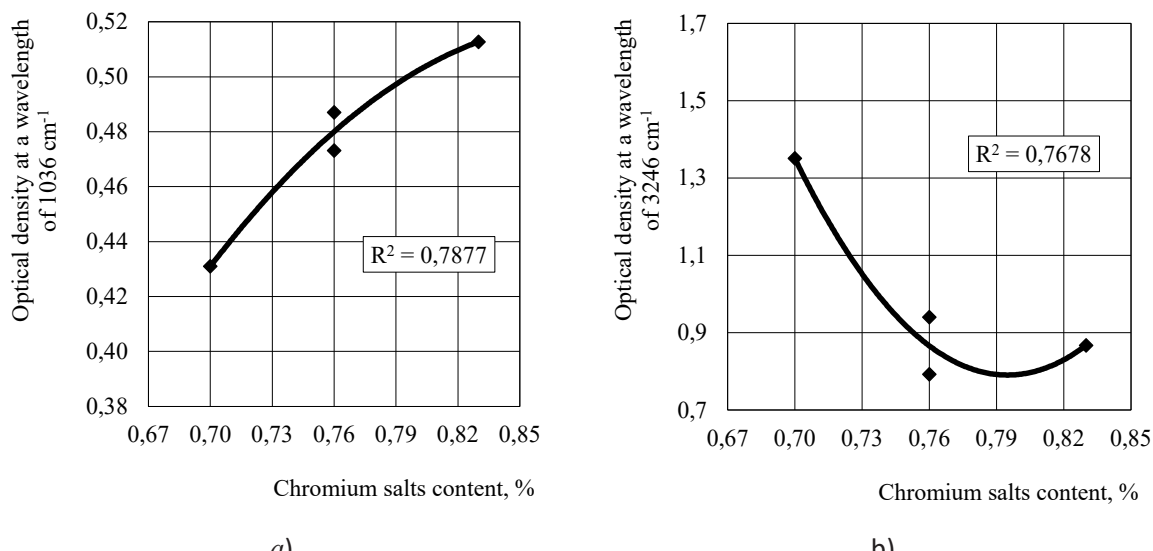


Figure 7. Relationship between the content of chromium salts in the skin derma and optical density at a wavelength of: a) 1036 cm^{-1} ; b) 3246 cm^{-1}

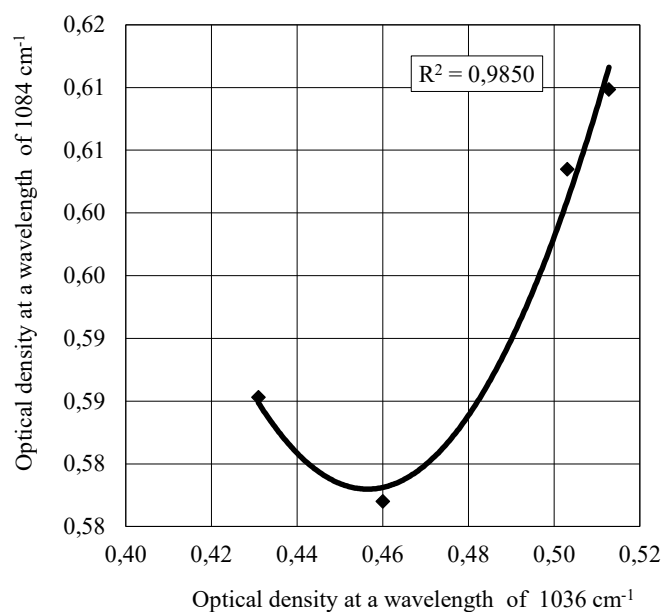


Figure 8. Relationship between optical density at 1084 cm^{-1} and 1036 cm^{-1} spectrum waves

The practical solution to the optimization problem is done almost approximate due to a large number of factors that are responsible for the results of manufacturing products and their quality. The methodology of multicriteria compromise optimization was used to final solution of the technology optimization problem. This methodology is used when there are more than two quality criteria according to which compromise optimization is performed [6].

Performing multicriteria compromise optimization requires finding a target function that looks like:

$$\gamma_{\text{tar},r} = \sqrt{\sum_{j=1}^m (1 - D_{jr})^2 \cdot W_j^2}, \quad (1)$$

where $\gamma_{\text{tar},r}$ - is the value of the generalized

objective function for the r-th experiment experience, which in the case of finding the optimum tends to 0 ($\gamma_{tar,r} \rightarrow 0$) and is a value of

the proximity of this point to the hypothetical optimal value in coded form which is equal to 1;

D_j - reduced to the interval 0 ... 1 the value

of the j-th response (quality criterion) in the r-th experiment experience, depending on the target quality selected for a specific criterion this value is calculated by different formulas;

W_j - weight of j-th quality criterion (response);

practically equals to $\frac{1}{\sum m}$;

m - the number of quality response criteria.

To find a generalized criterion for the quality of leather and fur skin materials an array of data was created which consists of analytical indicators and indicators characterizing the porous structure and deformation properties. The results of the calculation are shown in Table 3.

Table 3: Basic data to calculate the objective response function

Group	Fat content, %	Chromium salts content, %	Derma volume formation, cm ³	Derma collagen welding temperature, °C	Macropores volume	$V_{mac} \times 10^5$, kg/m ³	Micropores volume	$V_{mic} \times 10^5$, kg/m ³	Total pore volume	$V_{tot} \times 10^5$, kg/m ³	Components of deformation, %				Overall objective response function γ
											Elastic (spring-type) ε_{sp}	Plastic ε_{pl}	Full ε_{full}	Elastic ε_{el}	Instant ε_0
Anolyte	25,4	0,76	308,1	76	81,55	38,37	137,05	2,9	5,3	9,6	1,4	4,6	0,09		
Catholyte	20	0,70	254,5	67	34,51	34,46	96,39	1,4	2,9	5,4	1,1	1,9	0,21		
Distillate	27,5	0,76	435,9	68	30,62	35,96	91,93	1,5	2,7	5,2	0,9	2,3	0,16		
Technical water	31,4	0,83	499,6	66	29,92	34,13	92,21	1,7	1,9	4,6	0,9	1,9	0,26		

As it is seen from the Table 3, the smallest value of the generalized quality criterion γ (0.09) is observed in the anolyte treatment method which corresponds to the point of the factor space closest to the hypothetically optimal one.

There is a generalized dependence between the objective function, which

characterizes the porous structure of the skin tissue, its analytical parameters (fat content, chromium oxide, volume formation, derma welding temperature), deformation characteristics and electrical conductivity values of the water that was used (Fig. 9).

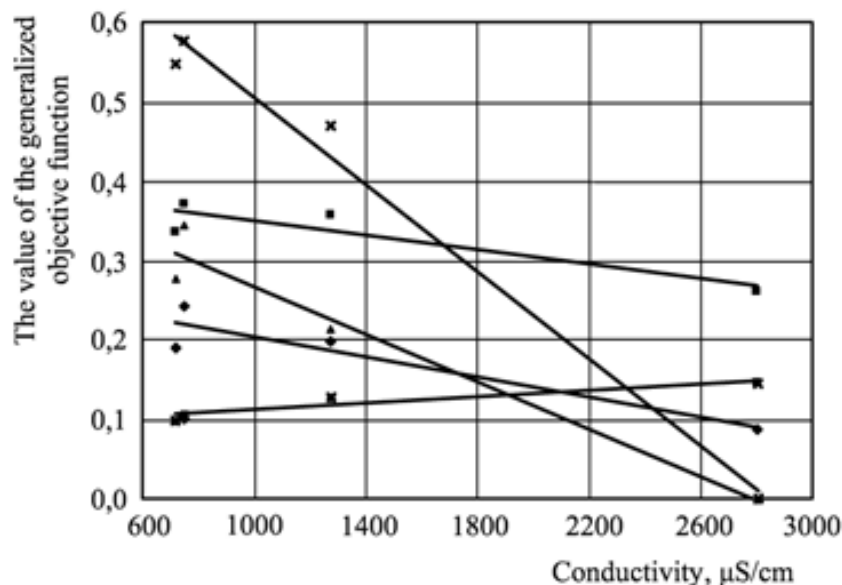


Figure 9. Effect of electrical conductivity on a generalized objective function, which is characterized by: 1 - porous structure of skin tissue ($R^2 = 0,9298$); 2 - analytical indicators of skin tissue ($R^2 = 0,0927$); 3 - spectral characteristics ($R^2 = 0,9205$); 4 - deformation characteristics ($R^2 = 0,5613$); 5 - generalized set of indicators inherent to rabbit skin ($R^2 = 0,6480$)

The spectral characteristics do not define the quality of the material, but mainly reflect the presence of functional groups that affect the parameters that characterize the quality of the finished skin. The deviation of the generalized objective function, which characterizes the spectral and analytical characteristics of rabbit skin tissue, is not significant; that is why this optimization is not taken into account.

The porosity characteristics (curve 1) and the deformation characteristics (curve 4) of skin tissue made on the basis of technologies involving the use of electro-activated water (anolyte with an electrical conductivity of 2800 $\mu\text{S}/\text{cm}$, catholyte with a catalyst of 2800 $\mu\text{S}/\text{cm}$) are most significantly influenced by the value of the generalized objective function (Fig. 15)

with electrical conductivity of 1270 $\mu\text{S}/\text{cm}$) and not activated water (with electrical conductivity of 710-750 $\mu\text{S}/\text{cm}$). When searching for the optimum, the smallest values of the generalized objective function correspond to the anolyte.

The most significant contribution to the disclosure of the essence of transformations in the skin tissue derma in the process of its manufacture is made by its spectral characteristics and porosity characteristics.

The presence of C-O-C groups (Fig. 10), which arise from the interaction of electro-activated water with the protein and the formation of aldehydes in the protein structure, which are subsequently transformed into simple heat-resistant ether bonds, has the influence on the overall objective function of the spectrum.

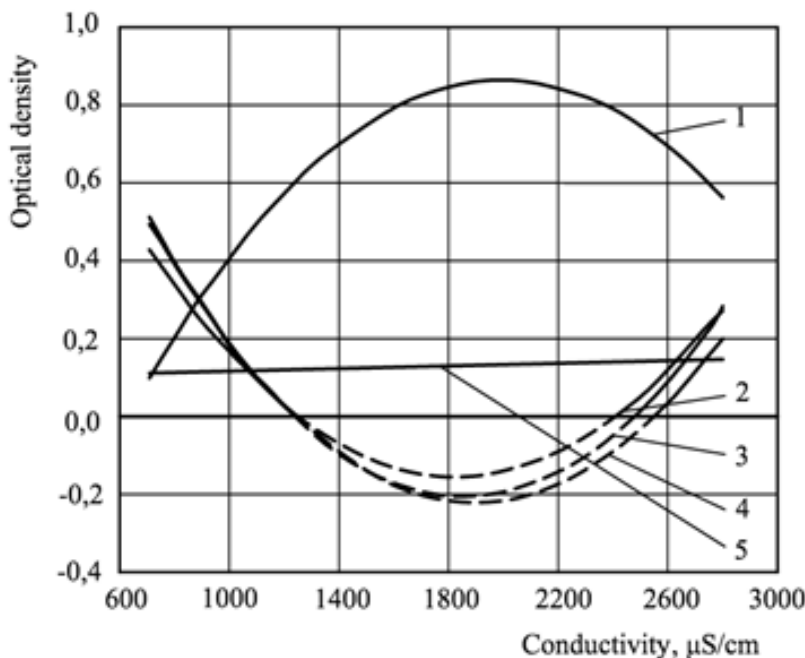


Figure 10. Effect of electrical conductivity on the optical density of the spectrum waves, characteristic for the groups: 1 - C-O-C ($R^2 = 0.9937$); 2 - N-H ($R^2 = 0.9059$); 3 - C-H ($R^2 = 0.7564$); 4 - COO- ($R^2 = 0.6402$); 5 - generalized objective function ($R^2 = 0.9205$)

The obtained optical density values (Fig. 10), which are lower than 0 (curves 2–4), are extrapolated. They are not taken into account in the analysis because they are imaginary. Optical density limits at conductivity values up to 1260 $\mu\text{S}/\text{cm}$ and greater than 2400 $\mu\text{S}/\text{cm}$ are significant.

CONCLUSIONS

The treatment of leather and fur skin materials with electro-activated water in the technological cycle of their production significantly affects the quantitative indicators that objectively characterize the quality of the skin tissue (skin fat content, dermal welding temperature) and participate in the formation of skin structure (volume formation indicator), and also contributes to the elastic and plastic properties of the skin that must be taken into account when making footwear from materials with predicted properties.

The most probable reactions of the rabbit skin tissue using water with different conductivity characteristics when natural salt is present (industrial water), distilled water when table salt is present, and distilled water in the presence

of table salt formed on the cathode and anode (catholyte and anolyte) are considered. The latter have shown their specificity in influencing the technological processes of fur skin production from rabbit skins. The properties of the finished skins depend entirely on the content of the components that may be the carriers of the electric charge.

The specificity of electro-activated water is that in the process of its manufacture in the anolyte an excess of electrons is observed, and in the catholyte, on the contrary, their lack is observed. This leads to the formation of compounds that have a reactive activity, that means that they interact with each other and with other active groups of collagen, which provides the appearance of cross-links in the irrigated derma that largely resistant to temperature as well as changing elastic and plastic properties of skin tissue. Thus, advanced technology can be used in industry as an effective method of leather and fur skin materials with specific properties tanning that can be predicted at the stage of their manufacture.

REFERENCES

1. Chowdhury, M., Mostafa, M.G., Biswas, T.K., Saha, A.K., Treatment of leather industrial effluents by filtration and coagulation processes, *Water Resour Ind*, **2013**, 3, 11-22, <https://doi.org/10.1016/j.wri.2013.05.002>.
2. Bordun, I., Ptashnyk, N., Chernovol, H., Investigation of the change of transmission spectra of electrochemically activated water during the relaxation process (in Ukrainian), Bulletin of Lviv University, Physics Series, Lviv, Ivan Franko National University of Lviv, **2010**, vol. 45, 100-106.
3. Danylkovich, A.G., Lishchuk, V.I., Romaniuk, O.O., Use of electrochemically activated aqueous solutions in the manufacture of fur materials, *SpringerPlus*, **2016**, 5, 1, 214-224, <https://doi.org/10.1186/s40064-016-1784-6>.
4. Lutsyk, R.V., Mentkovskii, Y.L., Kholod, V.P., The relationship of deformation-relaxation and heat and mass transfer processes (in Russian), Vyshcha Shkola Publishing House, 183 p., **1992**.
5. Skidan, V., Nadopta, T., Mytelska, O., Yefimchuk, H., Stetsiuk, I., Yanovets, A., Method of sketch profiling with spline curves for footwear design, *Leather and Footwear Journal*, **2019**, 19, 2, 113-122, <https://doi.org/10.24264/lfj.19.2.3>.
6. Horbachov, A.A., Kerner, S.M., Andrieieva, O.A., Orlova, O.D., Fundamentals of the creation of modern technologies of skin and fur production (in Ukrainian), K: KNUTD, 190 p., **2007**.
7. Vinarsky M.S., Lurie, M.V., Experiment planning in technological researches (in Russian), K: Tekhnika, 168 p., **1975**.
8. Bellamy, L., Infrared molecules spectra (in Russian): Translated from English, M: Foreign Literature, 444 p., **1957**.
9. Bulanin, M.O., Molecular Interaction Spectroscopy (in Russian), L: Leningrad State University, 192 p., **1970**.
10. Chirgadze, Y.N., Infrared spectra and structure of polypeptides and proteins (in Russian), M: Nauka, 136 p., **1965**.
11. Zlotenko, B.M., Savchenko, H.V., Matvienko, O.A., Use of electro-activated aqueous media in footwear production (in Ukrainian): Research Monograph, K: Kafedra, 144 p., **2012**.

© 2020 by the author(s). Published by INCOTP-ICPI, Bucharest, RO. This is an open access article distributed under the terms and conditions of the Creative Commons Attribution license (<http://creativecommons.org/licenses/by/4.0/>).

CHARACTERIZATION OF NEW AND ARTIFICIALLY AGED PARCHMENTS

Lucreția MIU^{1*}, Elena BADEA^{1,2}, Claudiu ȘENDREA¹

¹INCDTP – Division: Leather and Footwear Research Institute, 93 Ion Minulescu st., 030215 Bucharest, Romania,

lucretia.miu@icpi.ro

²Department of Chemistry, Faculty of Sciences, University of Craiova, Calea București 107 I, 200585 Craiova, Romania

Received: 25.07.2019

Accepted: 10.06.2020

<https://doi.org/10.24264/lfj.20.2.10>

CHARACTERIZATION OF NEW AND ARTIFICIALLY AGED PARCHMENTS

ABSTRACT. This study aims to characterize new and artificially aged parchments. Parchment samples of calf, sheep, goat and pig were exposed to artificial ageing at 70°C in 3 cycles: first cycle for 7 days, second cycle for 14 days and 21 days for the 3rd cycle. Thus, a treatment temperature of 70°C was selected to avoid sudden structural changes and rapid collagen denaturation. To evaluate the deterioration degree of parchments, the samples exposed to the first cycle were subjected to physical-mechanical, chemical tests and shrinkage temperature while the samples exposed to the second and 3rd cycle to physical-mechanical test. Depending on the ageing cycles significant changes were reported. The accelerated ageing of parchments degraded the physical-mechanical properties and lowered the shrinkage temperature. The behavior of sheep and goat parchment samples to accelerated ageing suggests a rather high deterioration in the hydrothermal stability.

KEYWORDS: physical-mechanical properties, shrinkage temperature, parchment, collagen, accelerated ageing

CARACTERIZAREA PERGAMENTELOR NOI ȘI ÎMBĂTRÂNITE ARTIFICIAL

REZUMAT. Acest studiu își propune să caracterizeze pergamentele noi și îmbătrânește artificial. Probe de pergament de vițel, oaie, capră și porc au fost expuse la îmbătrânire artificială la 70°C în 3 cicluri: primul ciclu timp de 7 zile, al doilea ciclu timp de 14 zile și 21 de zile pentru al 3-lea ciclu. A fost selectată astfel o temperatură de tratare de 70°C pentru a evita schimbările brusătoare structurale și denaturarea rapidă a colagenului. Pentru a evalua gradul de deteriorare a pergamentelor probele expuse la primul ciclu de îmbătrânire au fost testate prin analize fizico-mecanice, chimice și temperatură de contractie, iar probele expuse la ciclurile II și III la analize fizico-mecanice. În funcție de ciclurile de îmbătrânire au fost raportate modificări semnificative. Îmbătrânirea accelerată a pergamentelor a produs degradări ale proprietăților fizico-mecanice și ale temperaturii de contractie. Comportamentul probelor de pergament de ovine și caprine la îmbătrânirea accelerată sugerează o deteriorare destul de mare a stabilității hidrotermice.

CUVINTE CHEIE: proprietăți fizico-mecanice, temperatură de contractie, pergament, colagen, îmbătrânire accelerată

CARACTÉRISATION DES PARCHEMINS NOUVEAUX ET ÂGÉS ARTIFICIELLEMENT

RÉSUMÉ. Cette étude vise à caractériser les parchemins nouveaux et artificiellement âgés. Des échantillons de parchemin de veau, mouton, chèvre et porc ont été exposés au vieillissement artificiel à 70°C en 3 cycles : premier cycle pendant 7 jours, deuxième cycle pendant 14 jours et 21 jours pour le 3^e cycle. Ainsi on a choisi une température de traitement de 70°C pour éviter les changements structurels soudains et dénaturation rapide du collagène. Des tests physico-mécaniques, chimiques et de température de retrait ont été utilisés pour évaluer le degré de détérioration des parchemins. Selon les cycles de vieillissement, des changements importants ont été signalés. Le vieillissement accéléré des parchemins a provoqué des dégradations des propriétés physico-mécaniques et de la température de retrait. Le comportement des échantillons de parchemins de mouton et de chèvre au vieillissement accéléré suggère une détérioration assez élevée de la stabilité hydrothermale.

MOTS CLÉS : propriétés physico-mécaniques, température de retrait, parchemin, collagène, vieillissement accéléré

* Correspondence to: Lucreția MIU, INCDTP – Division: Leather and Footwear Research Institute, 93 Ion Minulescu st., 030215 Bucharest, Romania, lucretia.miu@icpi.ro

INTRODUCTION

Used for writing purposes, parchment is a very stable biomaterial, but it has a major drawback: it degrades with time. One of the oldest materials of cultural interest, parchment can survive for long periods of time if proper conditions are maintained. A fascinating discovery in 1947, in the caves of Qumram, dating from the beginning of 250 B.C. up to 68 A.D., has revealed one of the oldest preserved parchment manuscripts (Dead Sea Scrolls) [1]. These artefacts are a unique and non-renewable resource whose protection requires a thorough knowledge about the materials, their deterioration processes and the factors that cause them.

Studies on the damage of parchment have highlighted that their deterioration is due to environmental factors (temperature, humidity, light, pollution), biological factors (bacteria, fungi, rodents, insects) and chemical factors (acids, bases, oxygen, ozone, ultraviolet radiation) [2]. These factors cause numerous structural changes that must be understood scientifically to achieve appropriate restoration-conservation treatment with compatible materials.

Throughout the centuries, the manufacturing technologies of parchment have varied. The pre-medieval parchment was lightly tanned with vegetable matter and in the medieval period alkaline limestone baths were used [1, 3]. Although parchment manufacturing technologies have been modernized, they are based on medieval recipes using alkaline lime solutions [4-6]. Due to the number of components introduced in the fabrication process, parchment is subjected during production to changes in the structure of collagen. The hierarchical structure of the collagen (molecules, fibrils, fibers) in parchment determines the mechanical properties of resistance. Parchments are complex systems consisting of collagen where added solids and liquids are dispersed or dissolved in the substrate. These solids and liquids interact with each other in different processing stages.

Frequently handling the parchments by everyday use can result in mechanical damage. The processes of physical-chemical deterioration of the parchment structure have so far been little studied. In this study we aim to characterize new and artificially aged parchments by physical-

mechanical, chemical tests and shrinkage temperature.

EXPERIMENTAL

For this study, parchment was prepared using technology inspired from ancient recipes at the Leather and Footwear Research Institute (ICPI) of the National Research and Development Institute for Textiles and Leather (INCDTP), Bucharest. In the current technological process of parchment manufacturing, skins preserved by salting [1, 4, 5, 7] were used. The first stage of skin processing, soaking, is done with clean water of about 22°C. After soaking and fleshing the liming operation is performed, 6-8% Ca(OH)₂, whose main objective is the removal of the epidermis and hair. The skins are treated with a solution of lime for 3-4 days. The mechanical or manual fleshing is done before the second liming operation of about 2-3 days, 3-4% Ca(OH)₂. Then, deliming and washing operations are performed and at the end the skin is stretched over a wooden frame and left to dry [8, 9].

The samples were cut with the help of a press knife 110 mm long and 30 mm wide for the elongation at a load of 10 N/mm² and elongation at break, 80 mm long and 40 mm wide for the tensile strength, 120 mm long and 30 mm wide for the tear strength and for the dimensional stability the specimens were cut 80 mm long and 60 mm wide, 50 mm long and 40 mm wide and square with the side of 40 mm.

The parchment samples underwent artificial ageing treatments by heating at fixed temperature. Parchment samples of calf (C), sheep (S), goat (G) and pig (P) were exposed to artificial ageing at 70°C in 3 cycles: first cycle for 7 days, second cycle for 14 days and 21 days for the 3rd cycle. Thus, a treatment temperature of 70°C was selected to avoid sudden structural changes and rapid collagen denaturation [10, 11]. To evaluate the deterioration degree of parchments, the samples exposed to the first cycle were subjected to physical-mechanical, chemical tests and shrinkage temperature, while the samples exposed to the second and 3rd cycle to physical-mechanical test.

Physical-chemical characteristics of new and artificially aged parchment samples (Table 1 and Table 2) were determined according to standardised methods for obtaining moisture,

extractable substances, combined fat substances, total fat substances, total ash, total nitrogen, ammoniacal nitrogen, protein nitrogen and pH [12-16].

Shrinkage activity was evaluated by the SR EN ISO 3380: 2003 method. The method is useful in cases where the shrinkage temperature is below 100°C and it is used as a means of quality control in different stages of the technological process of manufacturing parchment. At INCOTP-ICPI, determination of the shrinkage temperature is performed with the Giuliani IG/TG equipment. The 50 mm long and 3 mm wide specimen is perforated and attached to the support hook. Before determining the shrinkage temperature, the specimen is conditioned by immersion in water for a few minutes for saturation. This will rehydrate the sample and facilitate the perforation by the two hooks. Then,

it is immersed in the vessel filled with water. The vessel is then heated slowly at 2°C/min, and the shrinkage temperature is visually determined by an operator, this being identified with the moment when the specimen is contracted.

The samples of parchments were also subjected to standardized physical-mechanical tests [17], before and after artificial ageing.

RESULTS AND DISCUSSION

Chemical Characteristics

The chemical characteristics fall within the limits imposed. After artificial ageing (7 days at 70°C) only humidity shows losses of 10 ± 2%. The other characteristics have no significant variations (Table 1 and Table 2).

Table 1: Physical-chemical characteristics of untreated parchments

No.	Characteristics	MU	Sample code/Values			
			Goat	Calf	Sheep	Pig
1	Moisture	%	17.33	17.56	18.24	18.51
2	Extractable substances	%	5.61	0.61	2.23	0.20
3	Combined fat substances	%	1.66	0.70	3.30	0.72
4	Total fat substances	%	7.27	1.31	5.53	1.02
5	Total Ash	%	2.20	3.87	1.98	9.42
6	Total Nitrogen	%	18.52	17.90	17.43	15.18
7	Ammoniacal Nitrogen	%	0.22	0.13	0.10	-
8	Protein Nitrogen	%	18.30	17.77	17.32	15.18
9	pH	%	6.2	6.3	6.2	6.8

Table 2: Physical-chemical characteristics of artificially aged parchments

No.	Characteristics	MU	Sample code/Values			
			Goat	Calf	Sheep	Pig
1	Moisture	%	15.40	16.50	16.40	16.50
2	Extractable substances	%	5.61	0.61	2.23	0.2
3	Combined fat substances	%	1.66	0.70	3.30	0.72
4	Total fat substances	%	7.27	1.31	5.53	1.02
5	Total Ash	%	2.20	3.87	1.98	9.42
6	Total Nitrogen	%	18.52	17.90	17.43	15.18
7	Ammoniacal Nitrogen	%	0.22	0.13	0.10	-
8	Protein Nitrogen	%	18.30	17.77	17.32	15.18
9	pH	%	6.2	6.3	6.2	6.8

Effect of Accelerated Ageing on Thermal Stability

Shrinkage temperature is a standard feature of leather and parchment. When collagen fibers are heated in water, they contract in length at a specific temperature [6, 18-20], which depends on the strength or quality of the leather and the degree of its deterioration.

Collagen fiber contraction represents the macroscopic manifestation of the process of thermal denaturation of collagen molecules, a process that results in the collapse of the structure of the triple helix, whose integrity is essential for maintaining the mechanical, structural, physical-chemical and functional properties of the collagen materials.

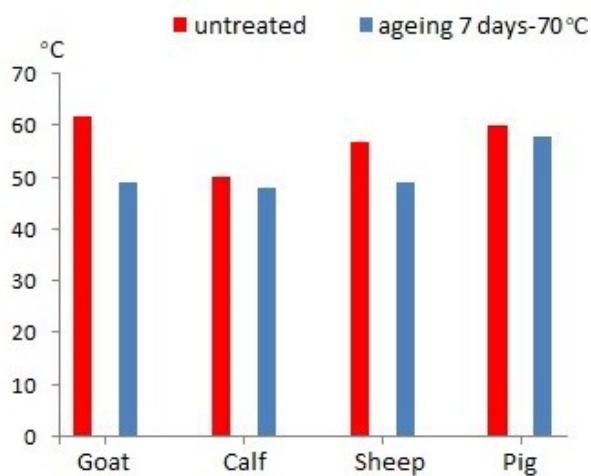


Figure 1. Variation of shrinkage temperature before and after accelerated ageing treatment

In Figure 1 we can see a comparison of shrinkage temperature among parchment samples before and after accelerated ageing treatment at 70°C for 7 days.

Shrinkage temperatures showed a rather good hydrothermal stability for the untreated parchment samples; shrinkage temperature differs depending on the characteristics of the skin of the animal species (goat, calf, sheep and pig).

The shrinkage temperature decreases by 3-4 to 15-20% in the artificially aged samples

compared to the control samples. From Figure 1 we can observe in the case of calf and pig parchment samples a better withstand to the destabilizing effects, with only 2°C decrease. The sheep and goat samples were the least resistant to the ageing treatment, with a decrease of 8 to 13°C.

Physical-Mechanical Tests

The parchment sample were analysed from the physical-mechanical point of view, before and after artificial ageing (Table 3).

Table 3: Physical-mechanical characteristics of the goat parchment - sample G, for the untreated sample and after the accelerated ageing cycles (cycle I, cycle II, cycle III)

Characteristics Treatment	Thickness mm	Elongation %		Tensile strength N/mm ²	Tear strength N/mm	Dimensional stability (shrinkage) %		
		at a load of 10N/mm ²	at break			Length	Width	Surface
Sample G untreated	a - 0.25	10	26	61.7	33.3			
	b - 0.24	8	24	53.3	44.4			
	average	9	25	57.5	38.8			

Parchment G exposed to artificial ageing									
Ageing	a - 0.21	6	28	51.2	45.4	2.8	2.2	4.9	0
7 days – 70°C	b - 0.22	4	28	54.8	40.9	2.3	1.7	4.0	0
cycle I	average	5	28	53.0	43.1	2.5	1.9	4.4	0
Ageing	a - 0.25	6	30	87.2	43.5	3.2	3.0	6.0	0
14 days – 70°C	b - 0.30	8	32	83.3	37.5	3.2	2.2	5.3	0
cycle II	average	7	31	85.2	40.5	3.2	2.6	5.6	0
Ageing	a - 0.26	8	36	51.2	37.5	4.1	4.2	8.1	0
21 days – 70°C	b - 0.25	8	30	46.8	28.6	3.8	3.3	7.0	0
cycle III	average	8	33	49.0	33.0	3.9	3.7	7.5	0

From Table 3 it can be observed that the applied oxidizing ageing cycles lead to the following physical-mechanical changes:

- The elongation at a load of 10 N/mm² decreases by 56% after the first cycle, increases by 40% in the second cycle compared to the first cycle, increases by 14% in the third cycle compared to second cycle and in the third cycle it is close to the value of the untreated sample;

- The elongation at break remains almost constant over the three cycles;

- Tensile strength decreases by 8% in cycle I as compared to control sample, in cycle II it increases by 38% as compared to cycle I, and in cycle III it decreases by 42% as compared to cycle II and by 15% as compared to control sample;

- The tear strength increases by 10% in cycle I compared to the control sample, in cycle II it decreases by 6% compared to cycle I, and in cycle III it reaches the value of the control sample;

- The decrease of the surface of the parchments after each cycle of thermal ageing is progressive.

These characteristics fall within the limits imposed by standards.

The analysis of the results shown in Table 3 has allowed the evaluation of the degradation state of the parchments. The results of the ageing behaviour showed that the ageing treatment at 70°C, in several cycles, produced a degradation of the physical mechanical properties of resistance that materialized also by lowering the shrinkage temperature by 2-10°C. This allowed us to select the parchment variants which showed the smallest dimensional change after artificial ageing (an essential requirement for the parchment used in the museum field, which ensures a stable behaviour, preventing the formation of tensions that lead to damage).

The calf parchment was characterized in the same way (Table 4).

Table 4: Physical-mechanical characteristics of the calf parchment - sample C, for the untreated sample and after the accelerated ageing cycles (cycle I, cycle II, cycle III)

Characteristics Treatment	Thickness mm	Elongation %		Tensile strength N/mm ²	Tear strength N/mm	Dimensional stability (shrinkage) %		
		at a load of 10N/mm ²	at break			Length	Width	Surface
Sample C untreated	a - 0.44	6	32	117.3	52.1			
	b - 0.44	14	32	104.2	54.9			
	average	10	32	110.7	53.5			
Parchment C exposed to artificial ageing								
Ageing 7 days – 70°C cycle I	a - 0.49	6	30	90.9	32.2	3.2	3.4	6.6
	b - 0.45	6	32	109.3	23.3	3.6	4.2	7.7
	average	6	31	100.1	27.7	3.4	3.8	7.1
Ageing 14 days – 70°C cycle II	a - 0.60	6	28	99.1	38.6	3.9	4.8	8.4
	b - 0.54	8	32	130.6	48.4	3.9	4.3	7.9
	average	7	30	101.1	43.5	3.9	4.5	8.1

Ageing 21 days – 70°C cycle III	a -0.62 b- 0.58 average	8 6 7	28 30 29	113.5 92.7 103.1	66.2 33.3 49.7	4.2 4.2 4.2	4.8 4.3 4.5	8.8 8.4 8.6	7.6 9.7 8.6
---------------------------------------	-------------------------------	-------------	----------------	------------------------	----------------------	-------------------	-------------------	-------------------	-------------------

From Table 4 it can be observed that the thermal ageing cycles applied to sample C lead to the following changes in physical-mechanical resistance:

- The elongation at a load of 10 N/mm² decreases by 40% after cycle I then remains constant in cycles II and III;

- The elongation at break remains constant during the three cycles of ageing;

- The tensile strength remains constant during the three ageing cycles;

- The tear strength decreases by 48% after cycle I, increases by 36% in cycle II compared to cycle I, and in cycle III it increases by 12.5% compared to cycle II, and approaches the value of the control sample;

- Dimensional stability gradually decreases in cycles I, II and III.

The characteristics of the sheep parchment are presented in Table 5.

Table 5: Physical-mechanical characteristics of the sheep parchment - sample S, for the untreated sample and after the accelerated ageing cycles (cycle I, cycle II, cycle III)

Characteristics Treatment	Thickness mm	Elongation % at a load of 10N/ mm ²	at break	Tensile strength N/mm ²	Tear strength N/mm	Dimensional stability (shrinkage) %			
						Length	Width	Surface	Thickness
Sample S untreated	a - 0.56 b - 0.44 average	6 8 7	24 28 26	40.6 41.1 40.8	13.2 21.6 17.4				
Parchment S exposed to artificial ageing									
Ageing 7 days – 70°C cycle I	a - 0.40 b - 0.38 average	6 6 6	22 20 21	39.5 34.7 37.1	13.0 7.5 10.2	1.9 2.5 2.2	2 2 2	4.0 4.8 4.4	0 2.9 -
Ageing 14 days – 70°C cycle II	a - 0.32 b - 0.53 average	8 8 8	30 28 29	40.2 35.0 37.6	12.8 16.7 14.7	3.2 3.8 3.5	3.7 2.9 3.3	6.8 6.7 6.7	3.1 2.9 3.0
Ageing 21 days – 70°C cycle III	a - 0.50 b - 0.37 average	10 12 11	28 26 27	29.5 29.1 29.3	9.2 7.3 8.2	3.2 3.8 3.5	3.7 2.9 3.3	6.8 6.7 6.7	3.1 0 -

From Table 5 it can be observed that the applied thermal ageing cycles lead to the following changes in physical-mechanical resistance:

- The elongation at a load of 10 N/mm² after cycle I is the same as the control sample, in cycle II it increases by 25% compared to cycle I; in cycle III it increases by 27% compared to cycle II and by 45% compared to cycle I;

- The elongation at break decreases by 19% in cycle I compared to the control sample, increases in cycle II by 28% compared to cycle I, and in cycle III is constant compared to cycle II;

- The tensile strength decreases by 9% in cycle I compared to untreated sample, in cycle II

it increases, it is maintaining the same value as in cycle I, and then in cycle III it decreases by 22% compared to cycles I and II;

- Tear strength decreases by 41% in cycle I compared to the control sample; in cycle II it increases by 31% compared to cycle I, and in cycle III it decreases by 56% compared to cycle II;

- Dimensional stability indicates a surface change after cycle I of 4.4%, which increases in cycle II and cycle III, at 6.7%.

The physical-mechanical characteristics of the pig parchment are presented in Table 6.

Table 6: Physical-mechanical characteristics of the pig parchment - sample P, for the untreated sample and after the accelerated ageing cycles (cycle I, cycle II, cycle III)

Characteristics Treatment	Thickness mm	Elongation % at a load of 10 N/ mm ²	at break	Tensile strength N/mm ²	Tear strength N/mm	Dimensional stability (shrinkage) %			
						Length	Width	Surface	Thickness
Sample P untreated	a - 0.75	6	26	62.3	59.0				
	b - 0.96	8	28	54.7	43.5				
	average	7	27	58.5	51.2				
Parchment P exposed to artificial ageing									
Ageing 7 days – 70°C cycle I	a - 0.86	6	28	68.7	48.8	4.3	5.0	9.2	3.6
	b - 0.86	8	36	69.3	43.8	4.8	4.6	9.3	0
	average	7	32	69.0	46.3	4.5	4.8	9.2	-
Ageing 14 days – 70°C cycle II	a - 0.57	6	30	51.4	36.4	5.4	5.5	10.5	5.3
	b - 0.85	6	20	57.4	68.1	5.4	5.4	10.4	3.8
	average	6	25	54.4	52.2	5.4	5.4	10.4	4.5
Ageing 21 days – 70°C cycle III	a - 1.04	18	24	63.4	62.6	5.4	5.5	10.5	8.9
	b - 0.92	6	30	73.4	57.3	5.4	5.2	10.2	3.8
	average	12	27	68.4	60	5.4	5.3	10.3	6.3

From Table 6 it can be observed that the applied thermal ageing cycles lead to the following changes of physical-mechanical resistance:

- The elongation at a load of 10 N/mm² after cycle I remains constant compared to the control sample, and in cycle III it increases by 41.6% compared to the control;
- The elongation at break after cycle I has a slight increase of 15.2% compared to the control sample (initially), and in cycle II and III it remains constant;
- The tensile strength in cycle I and III increases compared to the control by 15% and remains constant in cycle III;
- The tear strength remains almost constant comparing the values of the specimens with the same thickness;
- The modification of the surface of the parchments is important after cycle I of ageing and remains at the same value after cycles II and III.

CONCLUSION

In order to simulate a natural ageing process, we investigated the influence/behaviour of accelerated ageing treatments on parchment samples and evaluated the effects generated. We have exposed new parchments of different animal species i.e., goat, calf, sheep

and pig to artificial ageing at 70°C in 3 cycles: first cycle for 7 days, second cycle for 14 days and 21 days for the 3rd cycle.

The results of the ageing behaviour showed that the ageing treatment at 70°C, in several cycles, caused a degradation of the physical mechanical properties of resistance that materialized also by lowering the shrinkage temperature. As the ageing cycle increases, there was a tendency in the values of the physical-mechanical parameters to decrease.

The accelerated ageing treatments affected the shrinkage temperature of the parchment samples. The hydrothermal stability is most affected in sheep and goat parchment samples, it drastically decreased by 15-20% compared to the untreated samples.

Therefore, it can be stated that the physical-mechanical tests and shrinkage temperature are parameters that can indicate the evolution of the thermal destabilization processes in the collagen matrix.

Acknowledgements

This work was supported by a grant of the Romanian Ministry of Research and Innovation (now Ministry of Education and Research), CCCDI - UEFISCDI, project number PN-III-P1-1.2-PCCDI-2017-0878/ no. 55PCCDI/2018, IMPLEMENT, within PNCDI IsII.

REFERENCES

1. Larsen, R., Microanalysis of Parchment, Archetype Publications, London, England, **2002**.
2. Miu, L., Giurginca, M., Gaidău, C., Bratulescu, V., Meghea, A., Albu, L., Iftimie, N., Bocu, V., Budrigeac, P., Igna, A., Leather and Parchment Heritage Objects, vol. 1: Investigating Deterioration of Heritage Objects (in Romanian), CERTEX Press, Bucharest, **2004**.
3. Fuchs, R., The History and Biology of Parchment, *Gazette*, **2004**, 67, 13.
4. Gullick, M., From parchmenter to scribe: some observations on the manufacture and preparation of medieval parchment based upon a review of the literary evidence, Pergament: Geschichte, Struktur, Restaurierung, Herstellung / Hrsg. von Peter Rück, **1991**, 145-157.
5. Ryder, M.L., The biology and history of parchment, Pergament: Geschichte, Struktur, Restaurierung, Herstellung / Hrsg. von Peter Rück, **1991**, 25-33.
6. Axelsson, K.M., Larsen, R., Sommer, D.V.P., Dimensional studies of specific microscopic fibre structures in deteriorated parchment before and during shrinkage, *J Cult Herit*, **2012**, 13, 2, 128-136, <https://doi.org/10.1016/j.culher.2011.08.001>.
7. Dumitrescu, G., Badea, E., Parchment... a Story, the Unseen Face of Parchment Documents Issued by the Royal Chancellery in the Time of Stephen the Great (in Romanian), Excelența prin cultura, Bucharest, **2015**.
8. Reed, R., The Nature and Making of Parchment, The Elmete Press, **1975**.
9. Miu, L., Medieval Documents on Parchments (in Romanian), CERTEX Press, **2007**.
10. Fessas, D., Signorelli, M., Schiraldi, A., Kennedy, C.J., Wess, T.J., Hassel, B., Nielsen, K., Thermal analysis on parchments I: DSC and TGA combined approach for heat damage assessment, *Thermochim Acta*, **2006**, 447, 1, 30-35, <https://doi.org/10.1016/j.tca.2006.04.007>.
11. Jeyapalina, S., Geoffrey, E., Attenburrow, E., Covington, A.D., Dynamic mechanical thermal analysis (DMTA) of leather Part 1: Effect of tanning agent on the glass transition temperature of collagen, *J Am Leather Chem As*, **2007**, 91, 6, 236-242.
12. SR EN ISO 4684:2006.
13. SR EN ISO 4048:2008.
14. SR ISO 5397:1996.
15. SR EN ISO 4047:2002.
16. SR EN ISO 4045:2008.
17. SR ISO 3376:2012.
18. Larsen, R., Poulsen, D.V., Vest, M., The Hydrothermal Stability (Shrinkage Activity) of Parchment Measured by the Micro Hot Table Method (MHT), Microanalysis of Parchment, **2002**, 55-62.
19. Balfe, M.P., Humphreys, F.E., The shrinkage temperature of collagen and leather, and the effects of heat and moisture on leather, Progress in Leather Science: 1920- 1945 London: British Leather Manufacturers Research Association, **1947**, 415-425.
20. Holst Rasmussen, L., Larsen, R., A simple micro-method for the determination of the shrinkage temperature of leathers, parchments and skins, *Zeitschrift für Kunsttechnologie und Konservierung*, **2002**, 16, 2, 252-256.

© 2020 by the author(s). Published by INCDTP-ICPI, Bucharest, RO. This is an open access article distributed under the terms and conditions of the Creative Commons Attribution license (<http://creativecommons.org/licenses/by/4.0/>).

EUROPEAN RESEARCH AREA

COTANCE NEWSLETTERS

Starting with January 2019, the COTANCE Council will issue a monthly ***COTANCE Newsletter*** with the purpose of **promoting an improved image of leather** to relevant decision makers and domestic stakeholders including Members of the European and National Parliament, Governmental authorities, Ministerial officers, Customers of the leather industry, Brands, Retail chains, Relevant NGOs, Designers, etc. The monthly newsletters present topics that tell the truth about a controversial aspect or a fact that is not well known by the general public to bring about a better understanding of leather and the European leather industry, as well as a positive predisposition to legislate in favor of the leather industry. The newsletters are available in seven languages at <https://www.euroleather.com/index.php/newsletter>, and were also published in the 2019 issues as well as the first 2020 issue of Leather and Footwear Journal. Newsletters 4 and 5 are given below.

NEWS 4/2020

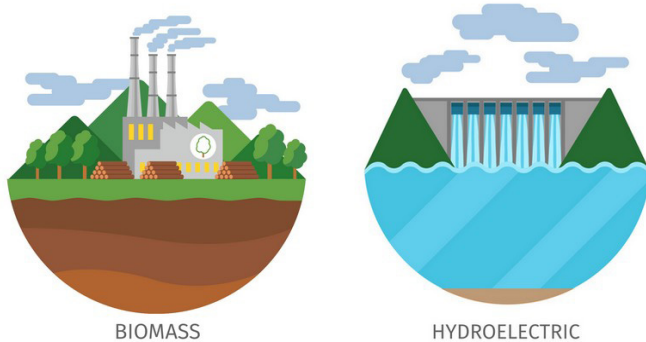


Fossil-free power in all Swedish Tanneries



Products cannot be made without the use of energy. This includes the production of leather.

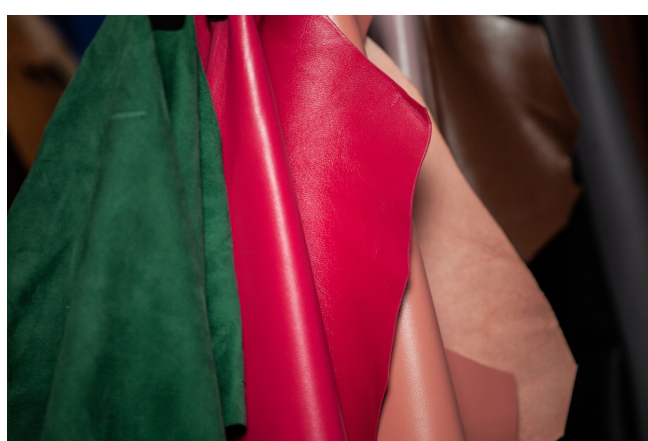
Twenty five years ahead of the target date set by the Swedish Parliament to make the country climate neutral, all Swedish tanneries have replaced fossil-based energy supplies with greener alternatives.



Sweden's aim of zero net greenhouse gas emissions, calls for all energy production to be fossil fuel-free by 2045, and Sweden's tanners were quick to act. The country's leather industry used different approaches to reach this important goal depending on whether the company was producing its own energy or purchasing energy from external suppliers. The solution: either bio-based energy sources or hydrothermal energy.

The fundamental difference between energy supply from fossil fuels and from biomass is that burning fossil fuels releases carbon that has been locked up in the ground for millions of years, while burning biomass emits carbon that is part of the biogenic carbon cycle (simply returning to the atmosphere, the carbon absorbed by plants as they grew).

- As early as 2012, one Swedish tannery replaced the use of oil for heating, with electricity from hydropower.
- Another turned to purchasing both their heat energy and electricity from an external supplier, generated using wood chips from the local area.
- Similarly, as a third example, a tannery started using biofuel-based steam for heating and electricity from exclusively renewable and fossil-free sources.
- The fourth and last Swedish tanner replaced its oil-based heater with a heater using biobased pellets, reducing its CO₂ emissions by 450 tonnes/year.



Swedish tanneries use exclusively green power from renewable and fossil-free sources. In addition, all have implemented energy saving measures.

Sweden is a good example that illustrates how European tanneries act proactively to implement environmentally friendly measures.

edited by



in collaboration with

Svenska Garveriidkareföreningen

NEWS 5/2020



An experiment in bargain hunting



“Leather jackets for less than 70€, handbags and leather shoes at low discount prices”

The fact that such online deals are so abundant suggests that they must be a “good deal”, for the suppliers at least.

Our test buyers from the Association of the German Leather Industry (VDL) gave one such deal a try.

In a few clicks, they landed on www.whoinns.com and found a leather jacket they liked. The price was down from 140€ to under 70€, and with the product description (“medium-length hooded solid fashion autumn leather jacket”) and picture. this made it very tempting.

The lack of contact information and the negative ratings of the online platform were concerning, but how many consumers actually check such sources before buying? Probably not that many. With a few clicks, the jacket was ordered with an estimated delivery time of 15 to 20 days.





Tracking down Internet fraudsters

Three weeks later and nothing had arrived! Our test buyers enquired but were asked to wait a little longer. Five weeks after the purchase, they enquired again and received an answer... in Chinese. After six weeks, they said 'STOP!' and asked the credit card company to refund the money; a buyer has 30 days to recover the cost of a purchase if the item is not delivered. After seven weeks, a plastic bag arrived from China. The declared customs value said \$17, below the threshold for customs controls.

So, what was in the bag? A jacket definitely, but certainly not a leather one. The label inside stated '100% PVC' and visually, this jacket looked like a cheap product, **very different from the image shown on the website.**

A complaint to the police about this deceptive commercial practice was met with only a shrug. At least the credit card company gave the money back.

All's well that ends well? Not so fast...

Caution, health risk!

The jacket was then tested for compliance with EU law. The results showed that it contained a high concentration of Bis(2-ethylhexyl) phthalate, also known as DEHP, a plasticiser banned from general use under EU law, as well as carcinogenic Polyaromatic Hydrocarbons (PAHs) and other critical substances which, when disposed of, can harm the environment.



Consumers and authorities should act

Our bargain hunt has shown that consumers should always beware tempting offers from untrustworthy platforms, and **always check the reliability of Internet suppliers.**

COTANCE and its member associations advocate for greater transparency and **better rules for descriptions of leather products.** We are committed to increasing consumer awareness of high-quality genuine leather and that for the real thing, there are simply no serious offers below a certain price level.

edited by



in collaboration with



News Release from the IULTCS

16 June 2020

ERRETRE and Leather Naturally Support the IULTCS Young Leather Scientist Grant Programme 2021

The Executive Committee of the IULTCS is pleased to announce the 2021 grants to be awarded to three young scientists, under the age of 35, for research projects in the categories: Leather Research, Machinery / Equipment and Sustainability to be conducted at a recognized institution in 2021.

Italy based leather technology provider and machinery manufacturer, ERRETRE S.p.a., confirmed support of the 2021 YLSG programme of IULTCS in the category Machinery/Equipment. The grant is to encourage young leather students and scientists to run a leather research project in the areas of development of machines for leather processing, automation, chemical/physical analysis and environmental equipment. Mr Adriano Peruzzi from Erretre remarks: "Our company supports leather education and we strongly believe our sector needs young motivated people to implement innovation and face the challenges the industry is face during the coming years. Erretre is again proud to award one young scientist for the work on a remarkable research project on Machinery/Equipment and for the contribution to the leather industry."



Prof. Mike Redwood

"Leather Naturally is proud to sponsor the Professor Mike Redwood Sustainability/Environment grant for another two years" said Egbert Dikkers, Chairperson. "With Leather Naturally's focus on providing education to designers, brands and consumers, it was a logical step to sponsor this award and honour our founder Professor Mike Redwood." Who is quoted as saying: "I wrote my first sustainability report in 1993 and those companies who have embraced the subject positively since then have all benefited from the solid science-based foundation it establishes when fighting competitive materials on environmental grounds. To pursue sustainability as an ongoing objective stimulates the leather industry to be dynamic and innovative. I am immensely honoured to be named in this grant and hope that it will allow candidates to feel free to challenge the industry with creative and unexpected ideas".

2021 will be the seventh year of the grant, and IULTCS will provide the monetary sponsorship for a single sum of €1,500 grant to Basic Research; ERRETRE will sponsor the €1,000 grant for Machinery / Equipment and Leather Naturally the €1,000 sponsorship for the Professor Mike Redwood grant on Sustainability/Environmental.

Michael Meyer, Chairman of the International Union of Research Commission (IUR) of IULTCS and Research Director at Freiberg (Germany) based FILK Leather Institute expressing his appreciation of the engagement: "We very much value the contribution of ERRETRE and Leather Naturally to our



Adriano Peruzzi, Erretre

YLSG programme. It is a vital instrument to encourage young leather scientists to acquire awareness and become more connected to the established research community of our industry. We have seen the programme growing stronger over the past years. Last year's edition brought up numerous, ambitious applications to step forward with innovative ideas and sustainable technologies."

Application submission for the 2021 YLSG programme will open in September and Luis Zugno, President of IULTCS, asks young research talents of the industry to file courageous project ideas.

Details of the eligibility requirements are available on the IULTCS website (<http://www.iultcs.org/research-iur.php>).

The IULTCS requests that readers of this announcement forward the information to those institutions and individuals who could benefit from the award.

INSTRUCTIONS FOR AUTHORS

Publication Ethics and Malpractice Statement

Revista de Pielarie Incaltaminte publishes peer-reviewed articles. It is necessary to agree upon. The Publication Ethics and Malpractice Statement for *Revista de Pielarie Incaltaminte*, based on COPE's Best Practice Guidelines for Journal Editors, clearly outlines standards of expected ethical behavior for all parties involved in the act of publishing (the author, the journal editor(s), the peer reviewer and the publisher) and is available on the journal's website,
<http://www.revistapielarieincaltaminte.ro>.

Open Access Statement

Revista de Pielarie Incaltaminte is a peer reviewed, open access journal. All articles published open access will be immediately and permanently free for everyone to read, download, copy and distribute, under the provisions of a Creative Commons Attribution (CC BY) which lets others distribute and copy the article, create extracts, abstracts, and other revised versions, adaptations or derivative works of or from an article (such as a translation), include in a collective work (such as an anthology), text or data mine the article, even for commercial purposes, as long as they credit the author(s), do not represent the author as endorsing their adaptation of the article, and do not modify the article in such a way as to damage the author's honor or reputation.

Open Access Publication Fee

Revista de Pielarie Incaltaminte requires article processing charges of 100 EURO per article, for accepted manuscripts, payable by the author to cover the costs associated with publication. There are no submission charges.

Author Rights

The copyright for all articles published in *Revista de Pielarie Incaltaminte* shall remain the property of the author(s). The copyright on the layout and final design of the articles published in *Revista de Pielarie Incaltaminte* belongs to INC DTP – Division: Leather and Footwear Research Institute and cannot be used in other publications.

Presentation of Papers

The scientific papers should be presented for publishing in English only. The text of the article should be clear and precise, as short as possible to make it understandable. As a rule, the paper should not exceed fifteen pages, including figures, drawings and tables. The paper should be divided into heads and chapters in a logical sequence. Manuscripts must meet high scientific and technical standards. All manuscripts must be typewritten using MS Office facilities, single spaced on white A4 standard paper (210x297 mm) in 11-point Times New Roman (TNR) font.

Paper Format

Title. Title (Centered, 12 pt. TNR font) should be short and informative. It should describe the contents fully but concisely without the use of abbreviations.

Authors. The complete, unabbreviated names should be given (Centered, 10 pt. TNR font), along with the affiliation (institution), city, country and email address (Centered, 9 pt. TNR font). The author to whom the correspondence should be addressed should be indicated, as well as email and full postal address.

Abstract: A short abstract in a single paragraph of no more than 200-250 words must accompany each manuscript (8 pt. TNR font). The abstract should briefly describe the content and results of the paper and should not contain any references.

Keywords. Authors should give 3-5 keywords.

Text

Introduction. Should include the aims of the study and results from previous notable studies.

Materials and Methods. Experimental methods should be described clearly and briefly.

Results and Discussions. This section may be separated into two parts. Unnecessary repetition should be avoided.

Conclusions. The general results of the research are discussed in this section.

Acknowledgements. Should be as short as possible.

References. Must be numbered in the paper, and listed in the order in which they appear.

Diagrams, Figures and Photographs should be constructed so as to be easy to understand and should be named "Figures"; their titles should be given below the Figure itself. The figures should be placed immediately near (after or before) the reference that is being made to them in the text. Figures should be referred to by numbers, and not by the expressions "below" or "above". The number of figures should be kept to minimum (maximum 10 figures per paper).

Tables. Should be numbered consecutively throughout the paper. Their titles must be centered at the top of the tables (12 pt. TNR font). The tables text should be 9 pt. TNR font. Their dimensions should correspond to the format of the Journal page. Tables will hold only the horizontal lines defining the row heading and the final table line. The tables should be placed immediately near (after or before) the reference that is being made to them in the text. Tables should be referred to by numbers, and not by the expressions "below" or "above". The measure units (expressed in International Measuring Systems) must be explicitly presented.

Formulas, Equations and Chemical Reactions should be numbered by Arabic numbers in round brackets, in order of appearance, and should be centered. The literal part of formulas should be in Italics. Formulas should be referred to by Arabic numbers in round brackets.

Nomenclature. Should be adequate and consistent throughout the paper, should conform as much as possible to the rules for Chemistry nomenclature. It is preferable to use the name of the substances instead of the chemical formulas in the text.

References should be numbered consecutively throughout the paper in order of citation in square brackets; the references should list recent literature also. Footnotes are not allowed. If the cited literature is in other language than English, the English translation of the title should be provided, followed by the original language in round brackets. Example: Handbook of Chemical Engineer (in Romanian), vol. 2, Technical Press, Bucharest, 1951, 87.

We strongly recommend that authors cite references using DOIs where possible. DOIs are persistent links to an object/entity and can be used to cite and link to any article existing online, even if full citation information is not yet available. DOIs should always be displayed as full links. Example: Onem, E., Cin, G., Alankus, A., Pehlivan, H., Mutlu, M.M., Utilization of Chestnut Shell Wastes as a Dyeing Agent for Leather Industry, *Revista de Pielarie Incaltaminte (Leather and Footwear Journal)*, 2016, 16, 4, 257-264, <https://doi.org/10.24264/rjf.16.4.1>.

Citation of Journal Articles: all authors' names (surname, name initials), abbreviated journal title, year, volume number, issue number, full page reference, e.g.: Helissey, P., Giorgi-Renault, S., Renault, J., *Chem Pharm Bull*, 1989, 37, 9, 2413-2425.

In case the reference is not cited in original, the author(s) should also list the original paper that has been consulted.

Citation of Books: authors' full name and name (initials), title of the book, issue number in Arabic numbers, publishing house, editors' names (if present), city where the book has been published, year of publication, the page(s) containing the text that has been cited.

Citation of Patents: all authors' names (surname, name initials), or company's name, country and patent number, date of issuance.

Paper template is available for download on the journal's website, <http://www.revistapielarieincaltaminte.ro>.

Manuscript Submission

Manuscripts should be submitted in electronic format by email to the following address:

Dana GURĂU, Editor-in-chief

INC DTP - Leather and Footwear Research Institute (ICPI)

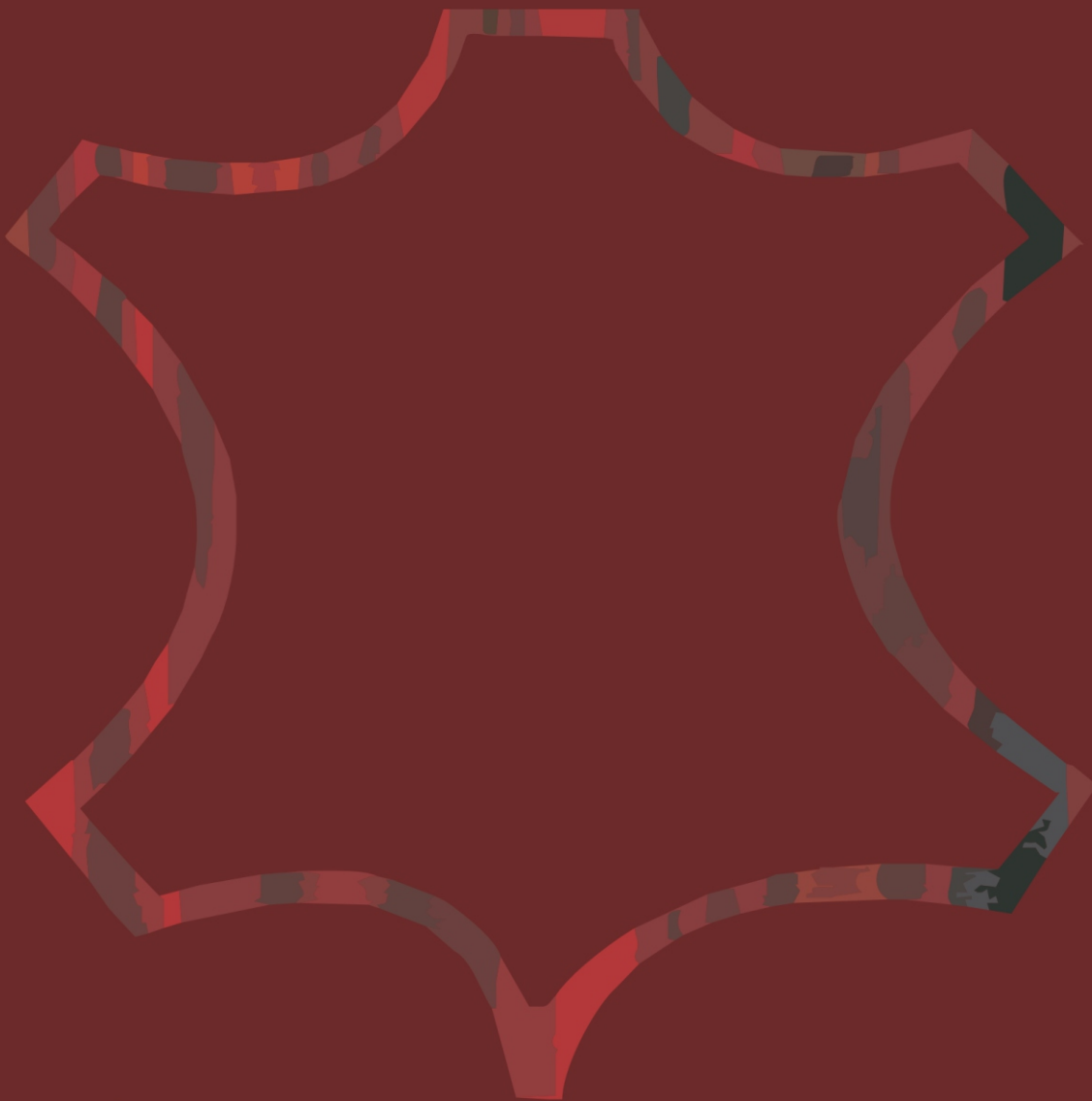
93 Ion Minulescu St., code 030215, Bucharest, Romania

Phone: +4021-323.50.60; Fax: +4021-323.52.80.

E-mail: jlfjournal@gmail.com



INCDTP - SUCURSALA INSTITUTUL DE CERCETĂRI PIELĂRIE ÎNCĂLȚĂMINTE



LUCRARE EDITATĂ CU SPRIJINUL MINISTERULUI EDUCAȚIEI ȘI CERCETĂRII